N° d'ordre : **Année : 2015**

REPUBLIQUE ALGERIENNE DEMOCRATIQUE ET POPULAIRE

Ministère de l'enseignement supérieur
et de la recherche scientifique
UNIVERSITE DJILLALI LIABES DE SIDI BEL ABBES
Faculté de Technologie
Département d'électronique

Laboratoire de Télécommunications et de Traitement Numérique du Signal

THESE

POUR L'OBTENTION DU DIPLÔME DE DOCTORAT

EN ÉLECTRONIQUE

DOCTORAT EN SCIENCES

Option : Signal et Télécommunications

Présentée et soutenue par : **Mr. BOUDAA Ahmed**.

Thème

HYBRID MULTIPLEXING APPROACH OF MIMO MULTI USER SYSTEMS

Thèse soutenue le

Devant le jury composé de :

Président :	Prof. Mr. Naoum Rafah	UDL-SBA
Directeur de thèse :	Prof. Mr. Bouziani Merahi	U-El Baiedh
Examinateur 1 :	Prof. Mr. Bassou Abdesselem	U-Bechar
Examinateur 2 :	MCA. Mr. Bouazza Boubakeur Seddik	U-Saida

Annee Universitaire 2014-2015

Acknowledgement

In the name of Allah the most Compassionate and the most Merciful, who has favored me with countless blessings.

I would like to express my high gratitude to my advisor, Pr. M. BOUZIANI who helped me in all the way to this end. His encouragement has had a crucial value in my work. I had the great pleasure of working with them. Under their supervision, they gave me the chance to work independently and be creative.

I am deeply grateful to Pr. Rafah Naoum, Bassou Abdesselem and Dr. Bouazza Boubakeur Seddik for accepting to be on my thesis committee.

My special thanks is to Pr. Bassou Abdesselem for his comments and views were very insightful and helpful.

I would also like to thank all of the ex CFTE workers of Laboratory research such helpful and best friends for shaping me to the mentality I have today which is getting vital in the carrier I am facing.

Abstract

In this work, we exploit the SVD assisted Multiuser Transmitter (MUT) and Multiuser Detector (MUD) technique, using the Downlink (DL) pre-processing transmitter and DL post-processing receiver matrices with the combination of the MIMO OFDM space Time block code (STBC). And also propose the pre-coded DL transmission scheme, were both proposed schemes take advantage of the channel state information (CSI) of all users at the base station (BS), but only of the mobile station (MS) owns, CSI, to decompose the MU MIMO channels into parallel single input single output (SISO), these two proposed schemes are compared to the vertical Bell layered space time (V-BLAST) detector combined with STBC OFDM (V-BLAST STBC OFDM). Our simulation result on hybrid approach show that the performance of the proposed scheme with DL Zero Forcing (ZF) transmitter outperforms the V-BLAST STBC OFDM and the pre-coded DL schemes with ZF receiver, respectively, in frequency selective fading channels. So this hybrid approach, exploit the time, space and frequency diversity.

Table of Contents

Chapter III*: *The Basic principles of OFDM

Lists of Tables

List of Figures

List of Abbreviations

AWGN Additive White Gaussian Noise

BER Bit Error Rate

BLAST Bell Lab Layered Space Time

BS Base Station

BF Beamforming

BLAST Bell Labs Layered Space Time

CSI Channel State Information

CDMA Code Division Multiplexing Access

CP Cyclique Prefix

D-BLAST Diagonal BLAST

DOF Degree of freedom

DFT Discrete Fourier Transformer

DD Delayed Diversity

DS Direct Spread Code Division Multiplexing Access

EM eigenmode

EGC Equal Gain Combining

FD Frequency Diversity

FDD Frequency Division Multiplexing

FDM Frequency Division Multiplexing

FDMA Frequency Division Multiple Access

FFT Fast Fourier Transformer

FH Frequency Hopping

FM Frequency Modulation

GI Guard Interval

H-BLAST Horizontal Bell Labs Layered Space Time

IAI Inter Antenna Interference

ICI Inter Carrier Interference

IDFT Inverse Discrete Fourier Transformer

IFFT Inverse Fast Fourier Transformer

ISI Inter Symbol Interference

LOS Line Of Sight

LST Layered Space Time

MAI multiple access interference

MC Multi Carrier

MIMO Multiple Input Multiple Output

MISO Multiple Input Single Output

ML Maximum Likelihood

MMSE Minimum Mean Square Error

MMSE-SIC Minimum Mean Square Error with Successive Interference Cancellation

MRC Maximum Ratio Combing

MPSK M Phase Shift Keying

MS Mobile Station

MUD Multi User Detection

OFDM Orthogonal Frequency Division Multiplexing

OSTBC Orthogonal Space Time Block Codes

OSIC Ordered Successive Interference Cancellation

PD polarization Diversity

PN Pseudo Noise

RD Receive Diversity

RMS Root Mean Square

SDMA Space Division Multiple Access

SC Selection Combining

SD Spatial Diversity

SF Space Frequency

SIC Successive Interference Cancellation

SIMO Single Input Multiple Output

SISO Single Input Single Output

SM Spatial Multiplexing

SNR Signal to Noise Ratio

SS spread spectrum

ST Space Time

STBC Space Time Block Code

STC Space Time Code

STCM Space Trellis Coded Modulation

STTC Space Time Trellis Code

SNIR Signal to Noise plus Interference Ratio

SVD Singular Value Decomposition

TDMA Time Division Multiple Access

TH Time Hoping

TD Transmit Diversity

UE User Equipment

V-BLAST Vertical Bell Labs Layered Space Time

V-BLAST Vertical BLAST

WLAN Wireless Local Area Network

ZF Zero Forcing

ZF-SIC Zero Forcing with Successive Interference Cancellation

Notations:

C^N: Vector space of complex vectors of length *N*.

s : Scalar complex.

S : Vector complex

I_{Mt} : $Mt \times Mt$ identity matrix

0_{Mt} : $Mt \times Mt$ null matrix

X^T : Transpose matrix

X^*: Conjugate matrix

$\otimes$: Circular convolution

$(.)^{\mathrm{H}}$: Hermitian matrix (transpose and conjugate matrix)

exp : Exponential map.

J_0: Bessel function.

p_e : Error probability

$CN(u, \sigma_n^2)$: Circularly symmetric, complex Gaussian random variable of mean u and covariance σ_n^2.

$rank(X)$: The rank of matrix X

$tr(.)$: The trace operation

||.||: Euclidean norm

$diag(.)$: The diagonal of a matrix

$E[.]$: The mathematical expectation

$|.|$: The absolute value

F : FFT matrix

Main Symboles:

f: The frequency

h_{ji}: The tap of the channel between antennas j and i.

L: Number of path between the antenna j and i.

H: Channel matrix

i: The transmit antenna index

j: The receive antenna index

k: The frequency index

t: The time

n : Time index

M: The symbol constellation size

Mt: The number of transmit antennas.

Nr: The number of receive antennas

y, r: The vectors observation

$s_t^{(i)}$: The symbol constellation transmitted at time index t from antenna i.

S : The transmitted symbol vector

T: The symbol period.

w_f: The angular frequency

σ_n^2: The noise variance

τ_{max}: Maximal delay spread of the channel

v : The speed of move

c : The speed of light

λ : The wavelength

d_{tr} : The distance of transmitted wave

d_{rw} : The distance of reflected wave

Δ_{φ} : The phase difference

G_{STC} : The Matrix code

P: The pre-processing matrix

Introduction

Emergent services, with the increasing demand in system capacity and high data rate services for the future wireless communication systems, especially in the downlink systems, many attempts in finding techniques to provide higher system capacity and data rate services have been done. Among these, orthogonal frequency division multiplexing (OFDM) based multiple input multiple output (MIMO) systems is the most promising technique to satisfy the demand for the future wireless communication due to the fact that MIMO-OFDM systems can provide spatial diversity and combat multipath environment [1,2,3]. In wireless communications, exploiting the spatial dimension using antenna arrays at the transmitter and/or receiver can increase both the reliability and data rate of a transmission. More recently, researchers have investigated using such a MIMO system to service multiple users. MIMO schemes are known to provide two main types of gains: spatial multiplexing gain and diversity gain. Spatial multiplexing gain describes the higher data rates that can be obtained using the spatial sub-channels created by the MIMO channel. An example of a pure multiplexing scheme is the vertical Bell laboratories layered space-time (V-BLAST) [4]. On the other hand, pure diversity schemes, like space time block codes (STBC) [5, 6], are concerned with diversity gain.

Space Division Multiple Access (SDMA) constitutes an attractive MIMO sub-class, which is capable of achieving a high user capacity by supporting a multiplicity of subscribers within the same frequency bandwidth [7]. In MIMO aided multiuser systems, both the uplink (UL) and downlink (DL) transmissions experience multiuser interference (MUI), also referred to as multiple access interference (MAI), as well as inter antenna interference (IAI).

A particularly promising candidate for next-generation fixed and mobile wireless systems is the combination of MIMO technology with OFDM, known as MIMO-OFDM schemes. In practice, OFDM could be used in combination with space time coding, which can be performed in a MIMO system, to increase the diversity gain and/or to enhance the system capacity over time variant and frequency selective channels [8, 9, 10, 11]. Otherwise, the performance of wireless communications is also primarily limited by MAI in multiuser applications. And it has been demonstrated that the downlink performance of wireless communication systems can be significantly improved by properly designed STBC. In this context, the STBC-OFDM system may be one of most promising system configurations that can be adopted for next generation mobile systems.

Orthogonal STBC [12] constitutes an attractive low complexity technique designed for attaining spatial diversity, when communicating over Rayleigh fading channels. Alamouti's remarkable orthogonal transmission structure [13] can be applied in space time (ST), to exploit the spatial, temporal, diversities or space frequency (SF) domain, to exploit the spatial and frequency diversities available in frequency selective MIMO channels in OFDM systems, as it is shown in [14] and [15], to exploit the spatial, time and frequency diversities and to obtain higher signal quality. Both ST and SF have proven to be an effective technique in enhancing the error performance and increasing the capacity of wireless channels [16, 17, 18, 19].

In MIMO-OFDM, the orthogonal designs can be applied as STBC-OFDM or SFBC-OFDM. In STBC-OFDM, the symbols are transmitted over the same sub-carriers by using two or more adjacent OFDM symbols. On the other hand, in SFBC-OFDM, the symbols are combined using an orthogonal matrix through the neighboring sub-carriers in the same OFDM symbol. In both cases, it is generally assumed that the channel coefficients are constant over neighboring sub-carriers or OFDM symbols in the orthogonal code structure. STBC-OFDM and SFBC-OFDM can be used to increase the resultant Signal to Noise Ratio (SNR) at the receiver, thus, increasing the coverage area in a cellular system.

Diversity techniques can be used to obtain reliable transmission systems or beamforming (BF), it is shown that the transmit beamforming offers the best performance but requires high rate feedback channel, and can be used to increase the signal strength towards a particular user, thus reducing interference to others [20]. When the wireless channels between transmit and receive antennas are correlated to each other, then transmit diversity scheme is not expected to perform well, i.e. if independent fading among the antenna signals cannot be achieved, BF is preferred over transmit diversity [21].

Finally, another type exploits the knowledge of channel at the transmitter. It decomposes the channel coefficient matrix using Singular Value Decomposition (SVD) [22] to obtain the largest Eigen, and uses these decomposed unitary matrices as pre and post filters at the transmitter and the receiver to achieve near capacity [22, 23, 24]. If multiple transmit antennas are employed in combination with single or multiple receive antennas per user MIMO, the spatial domain can be exploited by means of SDMA, i.e. users sharing the same time frequency resource are then spatially separated by orthogonal or semi-orthogonal beamforming techniques [25]. In some sense, eigen beamforming is an optimal space time

processing scheme. However, it requires SVD on every sub-carrier. The receiver not only needs to feedback the largest Eigen, but also the corresponding eigen-vectors.

The efficient design of the downlink transmitter is of paramount importance for the sake of achieving a high throughput. The effects of MUI may be mitigated by employing spatio temporal pre-processing at the transmitter. Consequently, the downlink receiver's complexity may be reduced with the advent of transmit pre-processing at the base station, a technique, which is also often referred as Multi-User Transmission (MUT) [26]. To obtain this, it is important to find schemes that are able to reduce the effects of fading and explore new type of diversity, as well as to reduce Inter-Path Interference (IPI) and MAI. In the case of frequency selective fading, it can be observed that different symbols suffer from interference from each other, whose effect is usually known as Inter symbol Interference (ISI), which tends to increase with the used bandwidth.

If the Channel Impulse Response (CIR) information associated to different MS is available at the BS, the use of pre-processing schemes at the transmitter, BS allows simpler MS receiver implementations (and, eventually better performances). By reducing the signal processing requirements at the MS, we can reduce the battery drainage and decrease the terminal cost, key aspects in the MS design. Therefore, the complexity costs can be shared by all MS and should be transferred into the BTS, and the mobile units (mobile station: Ms) must be inexpensive and low power.

In an effort to reduce the receiver complexity of the MS, substantial research efforts have been devoted to pre-processing the signal at the base station before transmission. These systems include the Maximum Ratio Combining (MRC) transmit scheme [27, 28], the Zero-Forcing (ZF) transmit scheme [29, 30, 31] and the pre-coding scheme [32, 33]. These signal pre-processing schemes assume the knowledge of the channel at the receiver, which is generated with the aid of channel estimation or by utilizing a feedback link from the transmitter.

In this thesis, SVD based SDMA MUDs designed for DL MUT is investigated. When using combined SVD-based pre-processing and post-processing and assuming that the (CIRs) of all users are perfectly known both at the MUT and MUD at the instant of transmission and reception, respectively, then the effect of both the MAI as well known MUI and IAI can perfectly be eliminated in both the UL and DL, since all signal links are uniquely and unambiguously identified by their CIRs.

Thesis outlines

Chapter 1 provides a brief introduction to wireless communications and MIMO transmissions. The main characteristics of radio channel propagation are described: the time selectivity, the frequency selectivity and the space selectivity. The radio propagation effects such as path loss, frequency selective fading, Doppler spread and multi-path delay spread. The performance of any wireless communication system is highly dependent on the propagation channel, and so a detailed knowledge of radio propagation is important for optimization of wireless communications. Two widely used fading models are presented: the Rayleigh and Rician fading models. The capacity of the MIMO wireless channel in Rayleigh fading is discussed in the case of transmit diversity and receive diversity with and no channel state information.

In chapter 2, we will provide an introduction of diversity techniques for fading channel, the definition of diversity gain: time diversity, frequency diversity, space diversity and polarization diversity. Then we provide an introduction of the space time code, first background information and basic principle in MIMO-STBC is given, describing a remarkable block code. The Alamouti scheme as a base stone of this theory is clearly interpreted. The simple mathematical formula in matrix form for general structure of Alamouti scheme with one and two receive antenna configuration is developed, followed by the encoding and the decoding process. Second, an introduction about spatial multiplexing or MIMO-BLAST as a mean to increase spectral efficiency or in the other words increasing the data rate of wireless system is given. The pure example the Bell Labs Layered Space Time (BLAST), we introduces the BLAST schemes and describing the Diagonal BLAST (D-BLAST) and the vertical BLAST (V-BLAST) architecture. Then the main steps detection process of the V-BLAST architecture. In addition’s, the V-BLAST capacity calculation.

Chapter 3, provides an introduction to OFDM in general and present a Principle basic concept of OFDM systems, and outlines some of the problems associated with it. This chapter describes what OFDM is, and how it can be generated and received. It also looks at why OFDM is a robust modulation scheme and some of its advantages over single carrier modulation schemes. The association of MIMO and OFDM system is discussed and modeled. At the end the combination of STBC OFDM, describing the coding and the decoding process in space time coding STBC-OFDM or space frequency coding SFBC-OFDM. Mathematical expression in time-domain and frequency domain for data transmission and reception in a

very simple and understandable form is developed. Some applications field for MIMO OFDM is given and discussed.

Chapter 4, an overview of Multi User system (MU), a brief definition of multiple access technique: TDMA, FDMA, CDMA. The concept of MU detection technique for interference canceller is discussed. Follow by the association of the MIMO and MU systems. The comparison between single and MU systems, with single and multiple antennas user's equipments. This Chapter presents a method for exploiting the effects of multi-path propagation in multiuser OFDM applications in order to improve the spectral efficiency of the system and so an understanding of radio propagation characteristics is needed before different forms of multi user OFDM. The hybrid MU schemes using V-BLAST detection is described. The simulation results over frequency selective fading channel is given under multiuser environment and discussed.

In chapter 5, we present the combination of the SVD technique with the MU STBC OFDM. Then we exploit the knowledge of the channel state information at the transmitter and the receiver side, and describing the SVD assisted MU transmitter and MU detector. This chapter investigates the feasibility of such techniques and the possible advantages such as increased capacity, improved quality of service (QoS), and a significant reduction of SNR. We first investigate the performance of the proposed Zeros Forcing receiver detection technique based on SVD under multiuser environment. Second we investigate the performance of the proposed Zeros Forcing transmitter under multiuser environment. And then examine properties and performance of the proposed schemes under various channel conditions. Simulation results is given and discussed at the end.

In chapter 6, results discussion is provided, which summarizes the major results obtained in this thesis, and presents the performance comparison of the different hybrid MU detection technique.

Finally, we provide a thesis conclusion and future works.

CHAPTER I

Wireless Channel Characteristics

1.1 Propagation characteristic of Radio channel

Wireless communication suffers from inherent channel impairments which arise from the physical propagation environment and which can severely degrade system performance. As shown in Figure 1.1. In a real environment radio waves from mobile devices travel through the air, the surrounding objects, such as mountains, buildings, trees and houses, cause reflection, diffraction and scattering of the transmitted signal. Due to these effects, the transmitted electromagnetic waves travels along different paths of varying lengths and therefore have different amplitudes, phases, delays and angles of arrival. At the receiver, the destructive interaction between these wave components causes multi-path fading, and the power of the waves decreases as the distance between the transmitter and receiver increases. The movement of objects in the channel or that of the receiver causes an apparent shift in the carrier frequency. A reliable communication system tries to overcome or take advantage of these channel perturbations.

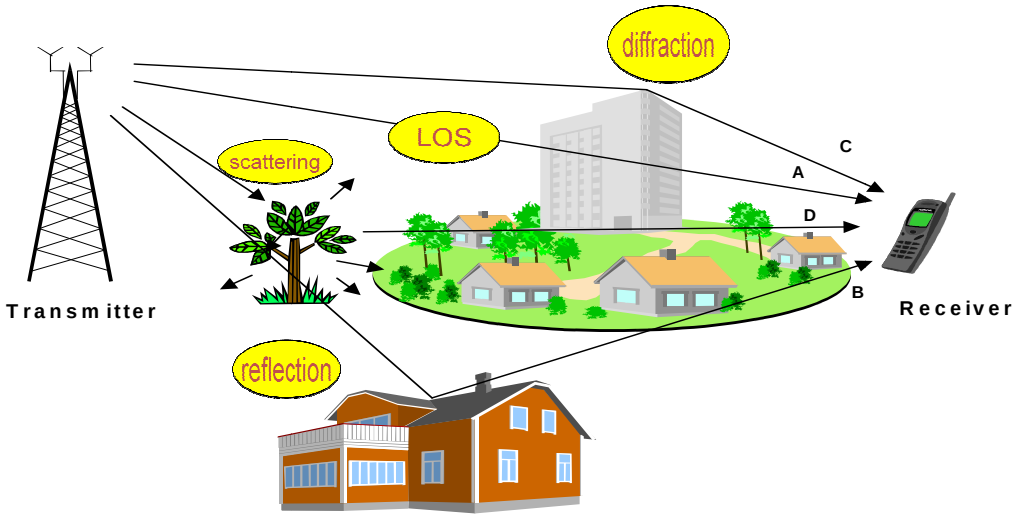

Figure 1.1: The mobile radio channel [34]

Typically, propagation models are classified into two categories.

Propagation models that predict the mean signal strength at a given distance from the transmitter are called large scale propagation models, since they characterize signal strength over large transmitter-receiver distances (usually a few kilometers). On the other hand, small scale or fading models are used to characterize the rapid fluctuations of the received signal strength over very short distances or short time durations, where the received power sometimes varies as much as 30 to 40 dB when the receiver moves only a fraction of a

wavelength. The statistical characteristics of fading channels are determined by many factors, such as multiple path propagation, the relative speed of the transmitter and receiver, the speeds of surrounding objects, and the transmission bandwidth of the signal.

The mobile radio channel may be modeled as a linear filter with a time varying impulse response, where the time variation is due to motion of the transmitter, receiver or scatterers. The filtering nature of the channel is caused by the summation of amplitudes and delays of the multiple arriving waves at any instant of time. A discrete model for a channel with *L* taps can be expressed as

$$y(n) = \sum_{l=0}^{L-1} h(n,l)x(n-\tau_l) + z(n) \qquad (1.1)$$

where $x(n)$ is the transmitted signal, $y(n)$ is the received signal, $h(n,l)$ is the response at time n of the time-varying channel if an impulse is sent at time $n-\tau_l$ and $z(n)$is the noise .

Two common parameters associated with fading channels are the coherence bandwidth which is the range of frequencies over which two frequency components have a strong potential of amplitude correlation and the coherence time which refers to the time rate of change of the channel characteristics [35, 36]. Multi-path propagation delays in a fading channel can cause time dispersion.

1.1.1 Time Selectivity

Wireless channels vary with time because the transmitter or the receiver moves or their environment changes. When the transmitter and the receiver are both static, the channel slowly changes because cars and people move, the wind makes leafs quiver, etc. The modifications of the propagation environment impact the channel on a larger time scale than the moving of the transmitter or the receiver [35]. The faster the transmitter/receiver moves, the faster the channel changes.

The first Doppler shift, D_1, amounts to $-f\frac{v}{c}$ while the second one, D_2 amounts to $f\frac{v}{c}$,where v is the speed of move, and c is the speed of light. The difference between both Doppler shifts is called the Doppler spread of the channel.

$$D_s = D_2 - D_1 \qquad (1.2)$$

In fact it is a sinusoid at frequency f with an envelope whose amplitude varies at frequency

$$f\frac{v}{c} = \frac{D_s}{2} \tag{1.3}$$

the time between a peak and a valley of this envelope is equal to $\frac{1}{2D_s}$. To characterize the time varying nature of the channels often we used the coherence time, T_{coh} which is related to the Doppler shift given by [35]:

$$T_{coh} = \frac{1}{2D_s} \tag{1.4}$$

The channel coherence time is related to the root mean square (RMS) bandwidth f_{RMS} of the Doppler power spectrum as [35]

$$T_{coh} \approx \frac{1}{f_{RMS}} \tag{1.5}$$

And from other author is given by [36]:

$$T_{coh} \approx \frac{9}{16\,\pi\, f_{max}} \tag{1.6}$$

Where f_{max} is the maximum Doppler shift given by $f_{max} = \frac{v}{\lambda}$.

The coherence time T_{coh} is the time difference at which the magnitude or envelope correlation coefficient between two signals at the same frequency falls below 0.5. In other words it can be assumed that the two signal components separated in time by T_{coh} will undergo independent attenuations.

If the coherence time is large compared to the symbol duration, T_s is much smaller than the channel coherence time, $T_s < T_{coh}$, signal experiences slow or time non-selective fading. The channel can be assumed to be static over several symbols; we may also say that the channel is quasi static, which is referred as slow fading. When the channel changes more quickly $T_s > T_{coh}$, we say that the channel experiences fast fading and that it is time selective or frequency dispersive.

Since the channel coherence time can be approximated by taking the inverse of the Doppler spread, it relates to the degree of mobility in the propagation environment. In particular, although there may be some motion of the scatterers, the fixed wireless channel has negligible Doppler spread, or equivalently a large coherence time, and is therefore a slow fading channel. In the context of mobile communications, since the symbol period is also the inverse of the signal bandwidth or symbol rate, fast fading arises in cases where the bandwidth is

smaller than the Doppler spread of the channel, i.e., when the symbol rate is low and the mobile unit is moving rapidly.

As the data rate increases and/or the mobile unit's mobility decreases, the channel becomes more slowly fading. Also note that the maximum Doppler shift is proportional to the carrier frequency. Thus time selectivity also becomes a more important consideration as transmission frequencies increase [37].

1.1.2 Frequency Selectivity

The channel strength varies with the position of the receive antenna. It also varies with the wave frequency because the propagation delays of the direct and reflected waves are different. The multi-path structure of a channel is quantified by its delay spread or by its RMS value. The delay spread of the channel, which is the difference between propagation delays, is denoted by T_d is given [35]:

$$T_d = \frac{2\, d_{rw}}{c} \tag{1.7}$$

If f changes by $\frac{c}{4\, d_{rw}}$, the channel changes significantly; we move from a peak of the received power to a valley, this quantity is called the coherence bandwidth. Time domain parameters for multi-path fading such as RMS delay spread are derived from the power delay profile. Coherence bandwidth B_{coh} is inversely proportional to the RMS delay spread, which characterizes the channel in the frequency domain [38].

$$B_{coh} = \frac{1}{2\, T_d} \tag{1.8}$$

And from other author is given by [36]:

$$B_{coh} = \frac{1}{50\, \tau_{RMS}} \tag{1.9}$$

Where, τ_{RMS} is the RMS delay spread.

The coherence bandwidth B_{coh} captures the analogous notion for two signals of different frequencies transmitted at the same time. A signal experiences flat or frequency non-selective fading if its bandwidth W_B is much smaller than the channel coherence bandwidth $W_B <$ *Bcoh*, and frequency selective fading if *WB>Bcoh*.

In narrowband systems, the bandwidth of the transmitted signal is smaller than the channel's coherence bandwidth and multi-path delay spread (maximum excess delay*)* τ_{max} is smaller

than a symbol period $\tau_{max} < T_s$. The channel is called frequency non-selective channel or a flat fading channel.

In wideband systems, by contrast, the multi-path delay spread is larger than the symbol duration $\tau_{max} > T_s$, The channel is time dispersive or frequency selective fading. In such cases, the spectrum of the channel varies over the signaling bandwidth, which leads to inter-symbol interference between transmitted signals. The baseband representation of the received signal $y(t)$ is then

$$y(t) = h(t)x(\mathrm{t} - \tau) + n(\mathrm{t}) \qquad (1.11)$$

Where $x(\mathrm{t})$ and $n(\mathrm{t})$ respectively denote the transmitted signal and the noise, τ is the propagation delay, and $h(t)$ denotes the channel which may depend on the time t. When $T_s \leq T_d$, the channel is a frequency-selective fading channel. Its baseband representation is made up of several taps $h(t, l)$:

$$y(t) = \sum_{l=0}^{L-1} h(t, l)x(\mathrm{t} - \tau_l) + n(\mathrm{t}) \qquad (1.12)$$

Where L denotes the number of distinguishable channel taps and τ_l is the propagation delay associated to channel tap $h(t, l)$ may denoted by h_l.

1.1.3 Space Selectivity

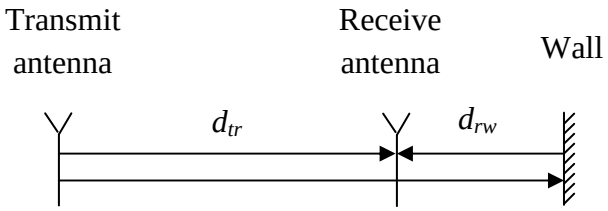

Figure 1.2: The reflector scheme

When using multi elements antennas arrays, the coherence distance represents the minimum distance in space separating two antenna elements such that they experience independent fading. In Figure 1.2, illustrates the multi-path fading phenomenon. It shows that the channel strength may quickly vary with the position of the receive antenna. The direct and the reflected waves, both of frequency f, add constructively or destructively. It depends on their phase difference Δ_φ given by [35].

$$\Delta_{\varphi} = \frac{w_f\ (d_{tr} + 2d_{rw})}{c} + \pi\ -\ \frac{w_f d_{tr}}{c}\ =\ \frac{2w_f d_{rw}}{c}\ +\ \pi \qquad (1.13)$$

Both waves add constructively when the phase difference is an even multiple of π. The electric field is then strong, even stronger than in the free space case. However, both waves add destructively when the phase difference is an odd multiple of π . The received signal is then weak. This phenomenon is called signal fading.

This distance clearly depends on the wavelength ¸ of the transmitted signal, as the phases of higher frequency signals are more sensitive to small distance changes than those of low frequency signals. Thus antenna separations and coherence distances are typically expressed in terms of wavelengths of the carrier signal [35]. Using the wavelength $\lambda = \frac{c}{f} = \frac{2\pi c}{w_f}$ instead of the angular frequency, (1.13) can be rewritten as

$$\Delta_{\varphi} = \frac{4\ \pi d_{rw}}{\lambda} + \pi \qquad (1.14)$$

The distance between a valley and a peak of the received power is λ/4. This distance is called the coherence distance d_{coh}. It means that the channel changes a lot when the distance between the receive antenna and the wall d_{rw} varies by λ/4. Also d_{coh} depends on the presence of scatterers in the vicinity of the antenna array, and generally falls somewhere between, $\frac{\lambda}{4}$ and 12λ [37]. In a rich scattering environment, where many scatterers are approximately uniformly distributed over $[0, 2\pi]$ around the receive array, the envelope correlation between two signals seen at antennas separated by $d_{coh} > \lambda/4$ is less than 0.5 [37]. Thus, given this angle spread and antenna separation, the channel exhibits independent or spatially selective fading.

1.1.4 Attenuation

Attenuation is the loss of average received signal power. Factors responsible for attenuation are the distance between the transmitter and receiver, the obstacles in between, their physical properties, etc. Attenuation due to distance increases exponentially, and, in addition to this, the presence of very large obstacles such as buildings, hills, etc causes another type of attenuation known as log normal shadowing. Statistically, the attenuation is considered as a random variable having a well known distribution.

A common formula used to model attenuation given by [36]:

$$PL(d)[dB] = \overline{PL}(d_0) + 10\,\alpha \log\left(\frac{d}{d_0}\right) + X_\sigma \qquad (1.15)$$

Where, X_σ is a zero mean Gaussian distributed random variable (in *dB*) with standard deviation σ (also in *dB*) and accounts for the log normal shadowing effect. The path loss at any arbitrary distance d is statistically described relative to the close in reference point d_0, the path loss exponent α, and the standard deviation σ. The exponent α can have values from 1.6 (in indoor line of sight) up to 6 (in highly built up cities).

1.1.5 The Doppler Effect

When there is relative movement between the transmitter and receiver scatterers. The carrier frequency, as perceived by the receiver, gets changed by some amount; this leads to frequency spreading of the transmitted signal, called Doppler spreading, which causes signal fading to vary with time. Here spread is used to denote the fact that a pure tone of frequency f_c in Hertz spreads across a finite bandwidth $f_c \mp f_d$. The amount of frequency shift depends on the relative speed, the direction of movement and the frequency of the carrier. The Maximum Doppler shift of the received signal is denoted by f_d and given by [36].

$$f_d = \frac{v}{\lambda} \times \cos\theta \qquad (1.16)$$

Where v is the relative speed, between the transmitter and receiver, θ is the angle between the direction of motion and the wave propagation, and $\lambda = \frac{c}{f_c}$ is the carrier wavelength.

A Doppler shift can be negative as well as positive, meaning an apparent decrease or increase in frequency, respectively. However, most often the maximum absolute value is considered and normalized with respect to the symbol rate and denoted by $F_d T$.

$$F_d T = \frac{|f_d|}{f_{sym}} \qquad (1.17)$$

Where f_{sym} is the symbol rate. A typical office environment has $F_d T$ value of about 2^{-3}.

The time autocorrelation of the flat fading channel $h(t)$ is approximated by Jakes' model [38].

$$R(\tau) = E[h(t)\ h(t+\tau)^*] = J_0(2\pi f_d \tau) \qquad (1.18)$$

Where $J_0(.)$ is the zeroth order modifed Bessel function of the first kind. Its Fourier transform is the Doppler power spectrum.

1.1.6 Fading

The result of multi-path and the Doppler shift is fading. Fading is the rapid variation in signal strength over a short distance or time interval where the large scale attenuation is constant. A fade can be flat or frequency selective depending on the multi-path structure of the channel, and slow or fast depending on the Doppler effect.

Flat fading occurs when the bandwidth of the signal is less than the coherence bandwidth. This type of fading is common, and some communication systems are designed specifically to operate in very narrow bandwidth mode. If the signal bandwidth is wider than the coherence bandwidth then different frequencies undergo independent fading and the result is ISI. How rapidly the channel changes as compared to the signal variation determine whether the fading is slow or fast. The Doppler effect is the reason for this type of fading as any movement of the receiver or any object in the channel produces a Doppler shift. The symbol period of the transmitted signal has to be shorter than the coherence time for a slow fading channel. A channel can be either flat or frequency selective and either slow or fast fading.

1.1.7 Rayleigh and Ricean Distribution

The Rayleigh distribution is commonly used to describe the statistical time varying nature of the received envelope of a flat fading signal, or the envelope of an individual multipath component. The amplitude of two quadrature Gaussian signals follows the Rayleigh distribution whereas the phase follows a uniform distribution. A very common fading model is the Rayleigh fading. A complex channel tap h_l that experiences Rayleigh fading is a circularly symmetric complex Gaussian random variable $h_l \sim N_c(0, \sigma_l^2)$.

Whose variance is σ_l^2. This model is called Rayleigh fading because the tap amplitude is Rayleigh distributed. As for the tap phase, it is uniformly distributed between 0 and 2π. The Rayleigh fading model assumes that there are a large number of statistically independent reflected paths that contribute to this tap. Rayleigh fading corresponds to a non line of sight (NLOS) situation. The probability distribution function (PDF) of a Rayleigh distribution is given by [38]:

$$P(r) = \begin{cases} \frac{r}{\sigma^2} exp\left(\frac{-r^2}{2\sigma^2}\right), & 0 \le r \le \infty \\ 0, & r < 0 \end{cases} \tag{1.19}$$

Where $2\sigma^2$ is the mean power of the multi-path signal. If there is a direct (Line of Sight :LOS) path wave, also called the specular path, such in an indoor environment where the chance of a line of sight path is high, the signal envelope is no longer Rayleigh and the distribution of the signal is Ricean the fading follows a Ricean distribution with PDF [36, 38]:

$$P(r) = \begin{cases} \frac{r}{\sigma^2} exp \frac{-(r^2 + A^2)}{2\sigma^2} I_0\left(\frac{Ar}{\sigma^2}\right), & A \geq 0, r \geq 0 \\ 0, & r < 0 \end{cases} \quad (1.20)$$

Where A is the peak amplitude of the dominant path and $I_0(.)$ is the modified Bessel function of the first kind and order zero. Figure 1.3, shows the PDFs of Rayleigh and Ricean distributions

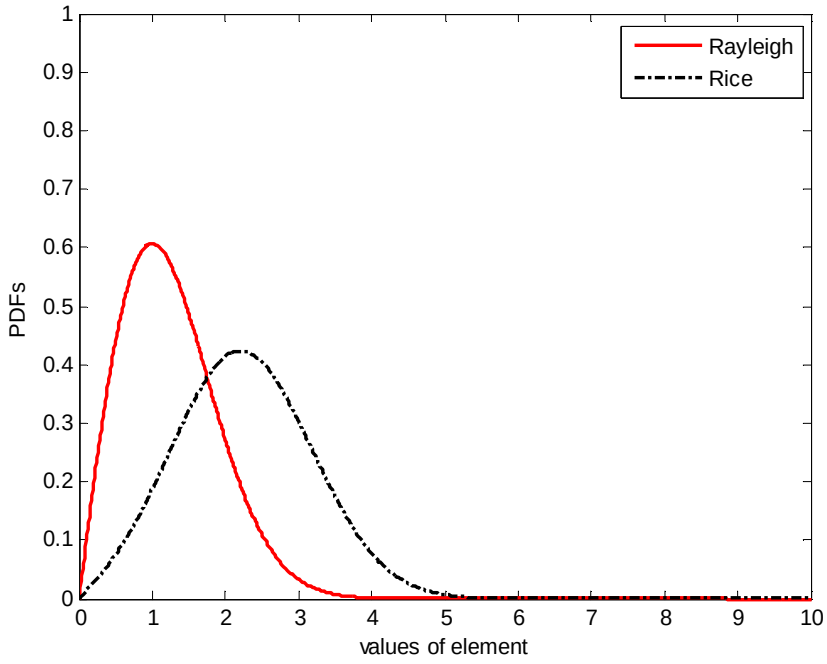

Figure 1.3: PDFs of Rayleigh and Ricean distributions

In a typical land mobile radio channel, it is often assumed that there is no direct line of sight (LOS) wave and the receiver obtains only reflected waves. Since the fading is a superposition of a large number of independent scattered components [38].

1.2 Channel Capacity

The channel capacity *C* is defined as a mutual information, its represents the maximum data rate that can be supported by the channel under arbitrarily small probability of error rate. A common representation of the channel capacity is within a unit bandwidth of the channel and can be expressed in bps/Hz. This representation is also known as spectral (Bandwidth) efficiency and can be derived as:

1.2.1 SISO Capacity without CSI in the Transmitter

When the receiver knows the channel at each time instant, the system is equivalent to AWGN channel conditioned on h.

$$C_{SISO} = E_h\{log_2(1 + SNR|h|^2)\}\ bits/s/Hz \quad (1.22)$$

Where $E_h\{.\}$ is the expectation operator with respect to the channel coefficient h, which is a complex Gaussian random variable with zero mean and a variance of 0.5 per dimension, and SNR is the average signal to noise ratio for each receiving antenna. This is often termed ergodic capacity. For a given h, there is only one way to increase the capacity of the SISO channel and that is by increasing SNR. Also, the capacity increases logarithmically with increasing SNR.

1.2.2 MISO Capacity without CSI in the Transmitter

The capacity of multiple input single output (MISO) channels (Transmit Diversity Systems) As shown in Figure 1.4. The Capacity of a MISO system using transmits diversity only with Mt transmits and one receive antenna, without CSI in the transmitter with total transmit power P_T and power $\frac{P_T}{Mt}$ per antenna can be written as:

$$C_{MISO} = E_h\left\{log_2\left(1 + \frac{SNR}{Mt}\sum_{i=1}^{M_t}|h_i|^2\right)\right\}\ \ bits/s/Hz \quad (1.23)$$

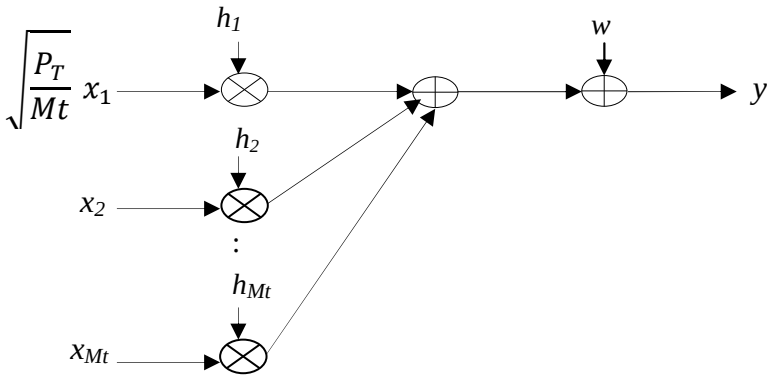

Figure 1.4: Transmit diversity systems

Received signals should combine as with maximum ratio combining MRC.

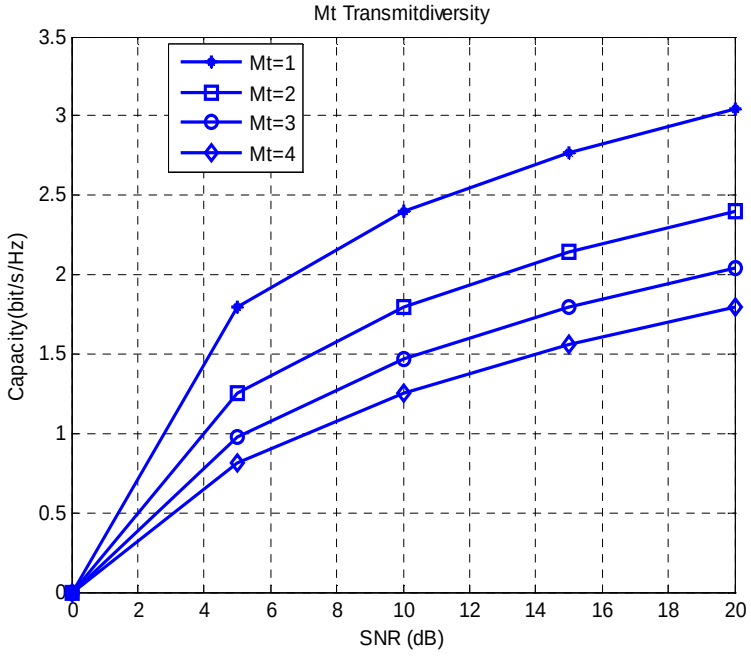

Figure 1.5: Capacity of transmit diversity for different values SNR

But Figure 1.5 shows that for transmit diversity or Multiple Input Single Output (MISO) system, the capacity doesn't increase that much as the number of transmits antennas increase. The maximum capacity that can be achieved in transmit diversity is that of AWGN's channel capacity. This is also implied in the capacity expression of MISO systems.

1.2.3 SIMO Capacity without CSI in the Transmitter

For a Single Input Multiple Output (SIMO) channel (receive diversity systems) with one transmit and Nr receive antennas as shown in Figure.1.6.

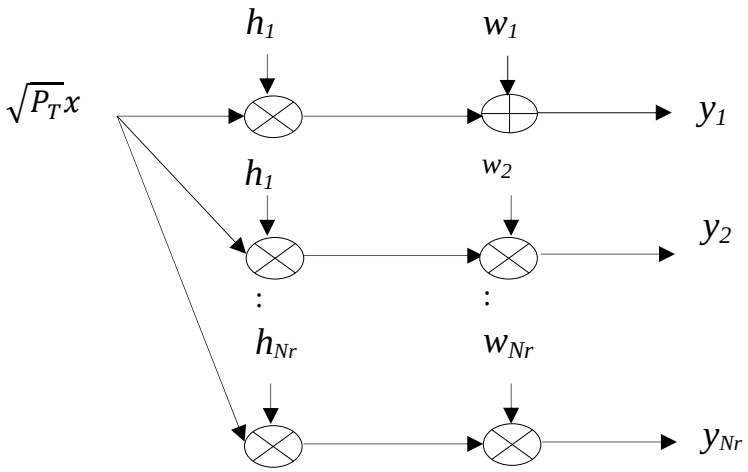

Figure 1.6: Receive diversity systems

The above capacity corresponds to maximum ratio combining of the received signals.

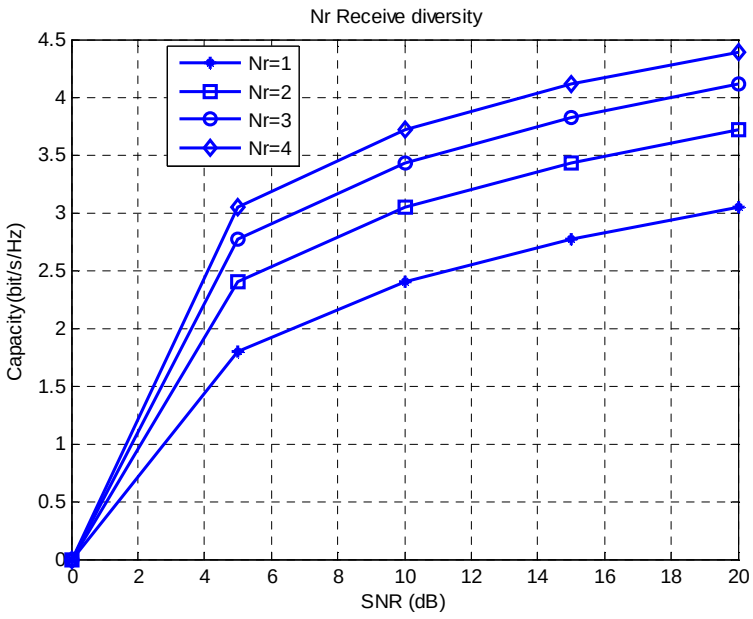

Figure 1.7: Capacity of receive diversity for different values SNR

From the Figure 1.7, we can see that for receive diversity or single input multiple output (SIMO) system, the channel capacity increases almost logarithmically with the number of receive antennas for a given signal to noise ratio. This is in agreement with the channel capacity expression for SIMO system which is given by:

$$C_{SIMO} = E_h \left\{ log_2 \left(1 + SNR \sum_{i=1}^{N_r} |h_i|^2 \right) \right\} bits/s/Hz \quad (1.24)$$

Where *C* is the normalized capacity with the channel bandwidth. Expression (1.24) shows that increasing the number of receive antennas result in increasing the array gain through the summation, which in turn is related to the capacity logarithmically.

1.3 MIMO Capacity

1.3.1 MIMO without CSI in the Transmitter

For Mt transmit antennas and N_r receive antennas, the MIMO flat fading channel capacity can be expressed as:

$$C_{MIMO} = \begin{cases} E_H \left\{ log_2 (det(I_{Nr} + \frac{SNR}{Mt} HH^H)) \right\} & bps/Hz, Nr < Mt \\ E_H \left\{ log_2 (det(I_{Nr} + \frac{SNR}{Mt} H^H H)) \right\} & bps/Hz, Nr \geq Mt \end{cases} \quad (1.25)$$

Unlike Figure 1.6 and 1.7, Figure 1.8 shows that there exists almost a linear increase in capacity with the number of transmit and receive antennas in MIMO system.

Figure 1.8 shows, an analysis of the capacity of the system having multiple transmitters and receivers. The capacity of a MIMO system has been plotted against SNR (dB). This provides a fundamental limit on the data throughput in MIMO systems. From the Figure 1.8, it is clear that with increase in the number of antennas at the both sides capacity increases linearly i.e. with $Mt = 4$ and $Nr = 4$ we have achieved highest capacity in MIMO systems. It is also worth mentioning that when we have $Mt = 2$ and $Nr = 3$ the result is almost the same with $Mt = 3$ and $Nr = 2$ which shows that the increasing number of antennas at either side of the MIMO system will have same effect in raising the capacity [39, 40].

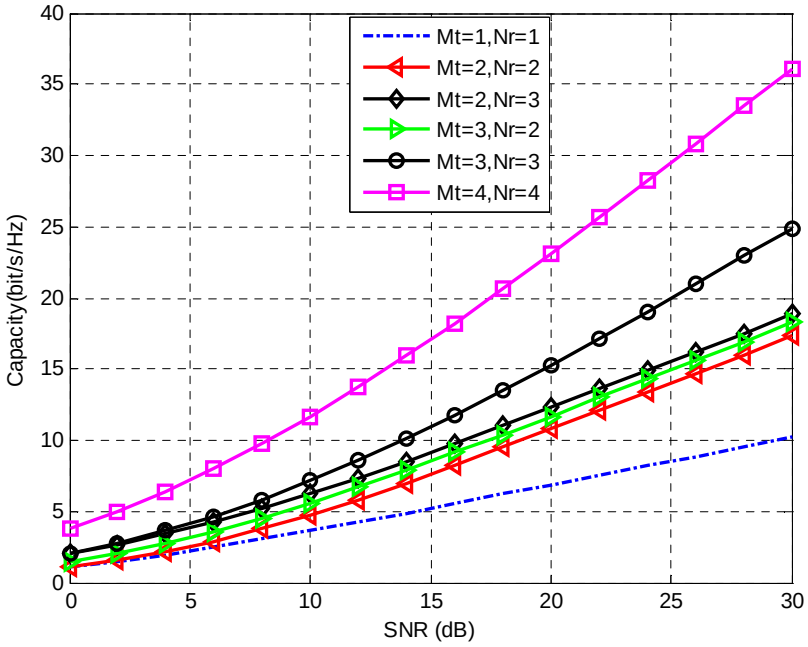

Figure 1.8: MIMO Capacities

1.3.2 MIMO with CSI in the Transmitter

All the analysis shows that it is advantageous to transmit signals through different sub-channels with reduced power to enhance the capacity rather than sending the total power through a single channel.

It is interesting to express the channel capacity in terms of the eigen-values of HH^H as illustrated in [41]. The rank of H is defined as the number of linear independent columns or rows and it is equal to the number of nonzero eigen-values of H^H :

$$rank(H) = rank(HH^H) = r_H \leq min(Nr\,, Mt)$$

Using singular value decomposition (SVD), the channel matrix H can be decomposed as:

$$H = UDV^H \qquad (1.26)$$

Where D is an $Nr \times Mt$ diagonal matrix having the singular values on its diagonal. U is an $Nr \times Nr$ unitary matrix that spans the column space of H and V is an $Mt \times Mt$ unitary matrix that spans the row space of H.

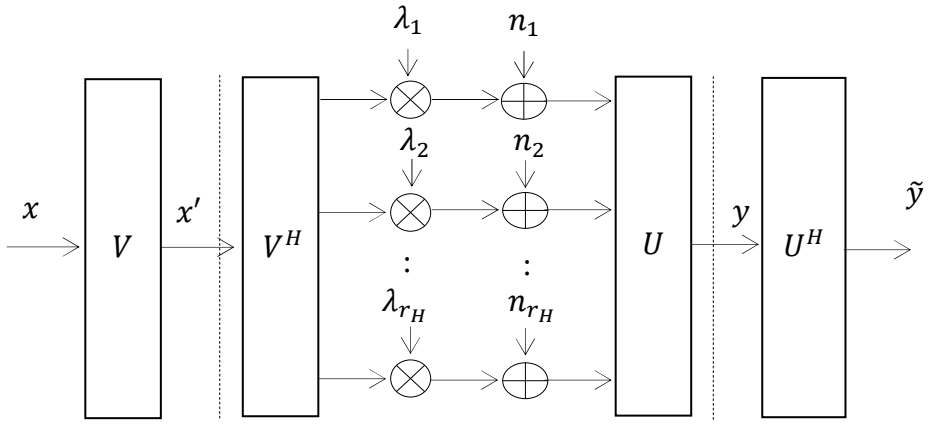

Figure 1.9: Converting the MIMO channel into a parallel channel by SVD

The singular values are non-negative real numbers and defined as the square roots of the eigen-values of HH^H. Thus, the diagonal matrix D is equal to $diag\left(\sqrt{\lambda_1}, \sqrt{\lambda_2}, .., \sqrt{\lambda_{r_H}}, 0 \dots, 0\right)$ where r_H is the rank of H and λ_{r_H} is the ${r_H}^{th}$ eigen-value of HH^H.

The received samples at time t on the Nr receive antennas, shown in Figure.1.9, can be written as:

$$y = Hx + n \tag{1.27}$$

Where x is the $Mt \times 1$ transmitted vector, and n is the $Nr \times 1$ additive white Gaussian noise (AWGN) vector.

Decomposing H and applying a unitary transformation to (1.27) results in:

$$y = UDV^H x + n\, U^H$$

$$y = DV^H x + U^H n$$

$$\tilde{y} = D\tilde{x} + \tilde{n} \tag{1.28}$$

Since U and V are unitary matrices, the statistics of y, x and n are preserved. Thus, the MIMO communication channel is equivalent to r_H parallel SISO channels. The ${r_H}^{th}$ channel has a power of λ_{r_H}.

In the decomposed parallel model as shown in Figure 1.9, independent data are sent across each of the independent parallel channels so extension of the SISO capacity to the parallel decomposed MIMO channel is as simple as just adding the capacity of these r_H independent and scalar channels. If we have r_H independent parallel channel then the total capacity is the sum of all the r_H capacity's is given by [42]:

$$C = \sum_{i=1}^{r_H} c_i \tag{1.29}$$

By using the parallel Gaussian channel capacity formula with uniform power distribution, the MIMO flat fading capacity is written as:

$$C_{MIMO} = \sum_{i=1}^{r_H} E_{\lambda_i}\left[log_2\left(1 + \frac{SNR}{Mt}\,\lambda_i\right)\right] bps/Hz \tag{1.30}$$

In this scheme there is a linear increase in channel capacity with the minimum number of transmit Mt and receive Nr antennas. i.e. the spectral efficiency grows linearly with number of parallel Mt and Nr antennas at a fixed power.

It is clear that the capacity increases linearly with increasing r_H where, $r_H = min(Nr, Mt)$.

Representing the capacity of MIMO channels in terms of the singular values of the channel matrix H clearly shows the effect of spatially correlated or rank deficient MIMO channels on the capacity. Correlated MIMO channels have lower rank than independent channels. Therefore, they have a lower number of non-zero singular values resulting in reduced channel capacity.

1.4 Conclusion

In chapter 1, the propagation characteristic of radio channel was studied, and show that the system performance highly degraded by the fading effect which arise from the physical propagation environments. Furthermore, the use of the diversity gain Corresponds to the mitigation of the effect of multi-path fading and improve the reliability of transmission which increase the coverage area and QoS, by means of transmitting or receiving over multiple antennas at which the fading is sufficiently de-correlated.

The capacity of MIMO channels was studied and it is implied that this capacity is optimally achieved if the number of transmit and receive antennas are equal. The channel capacity can be greatly increased by using multiple transmit and receive antennas, which is usually called MIMO systems. The linear increasing in MIMO channel capacity with the minimum number of transmits Mt and receives Nr antennas. i.e. the spectral efficiency grows linearly with number of parallel Mt and Nr antennas at a fixed power. It is clear that the capacity increases linearly with increasing of the rank r_H, which indicates the number of spatial degrees of freedom (DOF) where, $r_H = min(Nr, Mt)$ rather than logarithmically.

CHAPTER II

SPACE TIME CODE

2.1 Diversity Techniques for Fading Channels

In order to meet the demands on higher data rates, better quality and availability from an ever increasing number of wireless sub-scribers. The characteristics of wireless channel impose fundamental limitations on the performance of wireless communication systems. The wireless channel can be investigated by composing it into two parts, i.e., large scale (long term) impairments including path loss, shadowing and small scale (short term) impairment which is commonly referred as fading. The former component is used to predict the average signal power at the receiver side and the transmission coverage area. The latter is due to the multi-path propagation which causes random fluctuations in the received signal level and affects the instantaneous signal to noise ratio (SNR).

For a typical mobile wireless channel in urban areas where there is no line of sight propagation and the number of scatters is considerably large, the application of central limit theory indicates that the complex fading channel coefficient has two Quadrature components which are zero mean Gaussian random processes. As a result, the amplitude of the fading envelope follows a Rayleigh distribution. In terms of error rate performance, Rayleigh fading converts the exponential dependency of the bit error probability on the SNR for the classical AWGN channel into an approximately inverse linear one, resulting in a large SNR penalty. New techniques in signal processing and coding, need to be developped and implemented. To achieve high data rate communication, the system has to overcome problems such as additive noise and channel fading. One way is to make several replicas of the signal available to the receiver with the hope that at least some of them are not severely attenuated. This technique is called diversity [43].

A common approach to mitigate the degrading effects of fading is the use of diversity techniques. Diversity improves transmission performance by making use of more than one independently faded version of the transmitted signal. If several replicas of the signals are transmitted over multiple channels that exhibit independent fading with comparable strengths, the probability that all the independently faded signal components experience deep fading simultaneously is significantly reduced.

There are various approaches to extract diversity from the wireless channel. The most common methods of diversity techniques include time diversity, frequency diversity and space diversity [35, 39, 43].

2.1.1 Time Diversity

In time diversity the same information symbol is repeatedly transmitted at different time slots with the hope that they will suffer independent fading and the receiver will combine them properly, where the separation between the successive time slots equals or exceeds the coherence time of the channel. If the channel is time varying, each copy will experience different channel conditions and this results in the reception of multiple, independently faded copies of the transmitted signal at the receiver, thereby providing for diversity. This time separation is obtained by time interleaving the sequence of bits or symbols. Since this time interleaving results in decoding delay, this technique is effective for delay insensitive applications such as data transmission or fast fading channels where the channels coherence time is small. For slow fading channels, the large interleaving distance can lead to significant delay which is untolerable for delay sensitive applications such as voice. In addition, time diversity results in some data rate lose as the same message is sent in different time periods which could have been used for new message. Due to the redundancy introduced in the time domain, time diversity results in a loss in bandwidth efficiency.

2.1.2 Frequency Diversity

In frequency diversity, replicas of the same message are transmitted in different frequency slots that are separated enough to ensure independent fading. The frequency separation between these slots should at least be equal to the coherence bandwidth of the channel, where the coherence bandwidth is small compared to the bandwidth of the signal which is the frequency band in which the fading statistics is correlated. Frequency diversity has usually been provided by spread spectrum such as direct sequence spread spectrum (DSSS) and frequency hopping (FH). More recently, frequency diversity can also be provided by multi-carrier modulation methods, such as OFDM. Similar to time diversity, frequency diversity induces a loss in bandwidth efficiency due to the redundancy introduced in the frequency domain.

2.1.3 Spatial Diversity

Space diversity is also called antenna diversity and it is an effective method for combating multi-path fading. Is the diversity technique that does not require any additional bandwidth and does not introduce much decoding delay [39]. It is typically implemented using multiple antennas or antenna arrays arranged together in space for transmission and/or reception. The multiple antennas are separated by a sufficient distance at least equal to the coherence

distance of the channel. Coherence distance is a distance over which the channel fading statistics is correlated to allow the signal replicas to undergo independent fading. Depending on the antenna height, propagation environment and frequency, the channel's coherence distance vary. Through the number of paths that are created due to these multiple antennas, the same information signal can be sent such that each message from the respective antenna sees different fading statistics. This is because in a rich scattering environment the chance of a line of sight path is low, and most paths are reflected or diffracted from obstacles. Usually antenna diversity is used only at the base station because multiple antennas on the portable unit pose a design challenge and do not justify the cost.

Unlike time and frequency diversity, space diversity does not result in a loss of bandwidth efficiency, which makes it very attractive for high data rate wireless communications. Depending on whether multiple antennas are used for transmission or reception, space diversity can be classified into two categories: receive diversity and transmit diversity.

Receive Diversity: has been widely used in the uplink of cellular communication systems, with multiple antennas at the base station to pick up independent copies of the transmitted signal. Receive diversity is characterized by the number of independent fading branches or paths. These paths are also known as the diversity order and are equal to the number of receive antennas. The replicas of the transmitted signals are properly combined to increase the overall receive SNR and mitigate fading. There are many possible combining methods, including selection combining, switching combining, maximum ratio combining and equal gain combining [44].

Transmit Diversity: which uses multiple antennas at the transmitter, has received less attention than receive diversity. Transmit diversity often requires more signal processing at both the transmitter and the receiver. Because it is generally harder for the transmitter to obtain information about the channel, transmit diversity schemes are often more complex than receive diversity. But with the advent of space time coding schemes, it became possible to implement transmit diversity without knowledge of the channel. In recent years, one new approach to space diversity has emerged which deploys multiple antennas at both the transmitter and the receiver, leading to the so-called MIMO systems.

2.1.4 Polarization Diversity

Electromagnetic waves have vertical and horizontal polarizations that also show decorrelation [36-40]. In this technique multiple versions of signal are transmitted and received. It is used to minimize the effects of selective fading of the horizontal and vertical components of a radio signal. Where the required antenna spacing for space diversity is not feasible, polarization diversity is used as an alternative as the same antenna can be used for different polarizations. However, it is not possible to have more than 2-way polarization diversity.

2.2 Space Time code

Space time coding (STC) combines modulation, channel coding and antenna diversity. The main purpose of space time codes is to combat the multi-path fading phenomenon of wireless channel by using multiple transmit and receive antennas [45]. Each pair of transmit and receive antennas provides a signal path from the transmitter to the receiver. In STC, the signal is coded across both spatial and time domains to introduce correlation between signals transmitted from various antennas at various time periods. The signal copy is not only transmitted from another antenna but also at another time. This delayed transmission is called Delayed Diversity [46]. Space Time Codes combine spatial and temporal signal copies. By doing this, both the data rate and the performance can be significantly improved without sacrificing bandwidth. By sending signals that carry the same information through different paths, multiple independently faded replicas of the data symbol can be obtained at the receiver end; hence, more reliable reception is achieved.

Let us define some common terminologies in space time coding:

- Full rank code is a STC that has full rank. It has full transmit diversity, and is also called a full diversity code.
- Full rate code is the one that achieves the maximum rate, which is equal to b bps/Hz, where the code symbols are drawn from a constellation set M of size 2^b. In general, STC's offer diversity gain and coding gains to the system.

Two approaches exist for STC. Space Time Trellis Codes (STTC) and Space Time Block Codes (STBC) aim at achieving high diversity gains. The first one is an extension of the trellis coded modulation [47], (STCM Space Trellis Coded Modulation) [48], and the second one is based on block codes [5] (STBC Space Time Block Code). The STTC approach introduces a time and spatial correlation into the signal so it provides a diversity gain at the receiver and a

coding gain over the uncoded signal. But the decoding complexity of STTC is much higher compared to that of the STBC. The STBC uses the block encoder to achieve diversity and orthogonalization of the channels [12]. The orthogonal channel allows for a simpler implementation of the receivers.

Although many designs of STBC exist, additional properties such as the orthogonality of matrix code allow improved performance and easy decoding at the receiver. Such properties are realized by the so-called Alamouti space time code [13], explained later in this chapter. The total diversity order which can be realized in the Nr to Mt MIMO channel is $Mt \times Nr$ when entries of the MIMO channel matrix are statistically uncorrelated. While STC techniques improve the reliability of reception, there are other MIMO techniques that increase the rate of communication for a fixed reliability level by increasing the degrees of freedom (DOF) available for communication [49].

2.2.1 Space Time Block Codes

In STBC, the data stream to be transmitted is encoded in blocks which are distributed among spaced antennas and across time. This distribution of transmitted symbols over multiple transmits antennas and different time slots can be represented in the form of a matrix as shown below.

$$time\ slots \downarrow \begin{bmatrix} S_{1,1} & S_{1,2} & \dots & S_{1,Mt} \\ S_{1,1} & S_{1,1} & \dots & S_{2,Mt} \\ \vdots & \vdots & \vdots & \vdots \\ S_{n_T,1} & S_{n_T,2} & \dots & S_{n_T,Mt} \end{bmatrix} \quad (2.1)$$

$$\rightarrow antennas$$

Mt is the number of transmit antennas and n_T is the number of time slots. Each row represents a time slot and each column represents one antenna's transmissions over time. While it is necessary to have multiple transmit antennas, it is not necessary to have multiple receive antennas, although to do so improves performance.

2.2.2 The Alamouti code

A simple (STBC) scheme is the famous Alamouti code [13]. As shown in Figure 2.1, the Alamouti scheme is designed for two transmit antennas. In Alamouti encoding scheme, during any given transmission period two signals are transmitted simultaneously from two transmit antennas. The orthogonal structure of the transmitted signal decouples the two

symbols sent at the same time and the maximum likelihood detection of the 2-D structure is greatly simplified.

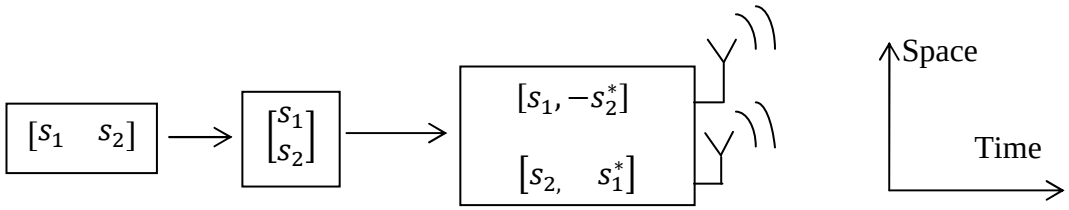

Figure 2.1: The Alamouti Space Time Block Code for 2 Tx antennas

The encoder takes two modulated symbols $s_1$and s_2 at a time. The transmit matrix *C* is given by equation (2.2).

$$C = [c(t) \;\; c(t+T)]$$

$$C = \begin{bmatrix} s_1 & -s_2^* \\ s_2 & s_1^* \end{bmatrix} \qquad (2.2)$$

Where s^* *is* complex conjugate of s. During the first transmission period, two signals, $s_1$and s_2 are transmitted simultaneously from antenna one and antenna two, respectively. In the second transmission period, signal $-s_2^*$ is transmitted from transmit antenna one and signal s_1^* from transmit antenna two. It is clear that the encoding is done in both space and time domain. The transmit sequence from antennas one and two is showed by S^1 and S^2, respectively.

$$S^1 = [S_1, -S_2^*]$$
$$S^2 = [S_2, \quad S_1^*] \qquad (2.4)$$

The encoder outputs are thus transmitted in two consecutive transmission periods where the column of the code matrix indicates symbols transmitted simultaneously and the rows indicate symbols transmitted from respective antennas. It is clear that the encoding is done in both time and space domains. Since N_s symbols are transmitted during L_t time slots, the rate (*Rs*) of STBC is:

$$R_s = \frac{N_s}{L_t} \frac{symbols}{time\ slot} \qquad (2.5)$$

The above matrix is orthogonal; the code belongs to a special subclass of STBCs known as Orthogonal Space Time Block Codes (OSTBC) [12].

The code matrices of OSTBCs satisfy the following constraint.

$$C^H C = D = (|s_1|^2 + |s_2|^2)\, I_2 \tag{2.6}$$

Where is a diagonal matrix.

$$C^H C = \begin{bmatrix} |s_1|^2 + |s_2|^2 & 0 \\ 0 & |s_1|^2 + |s_2|^2 \end{bmatrix} \tag{2.7}$$

2.2.3 Alamouti Scheme 2×1 Space Time Code

Alamouti proposed a method of signaling that exploits transmit diversity. He showed that the same diversity benefit can be obtained when using transmit diversity as when using receive diversity. Furthermore, the system with two transmit antennas and one receive antenna can perform as well in the presence of multi-path as a system with one transmit antenna and two receive antennas. The key to Alamouti's scheme, referred to as the Alamouti 2x1 STC. Figure 2.2, shows the Alamouti's scheme system with two transmit antennas and one receive antenna.

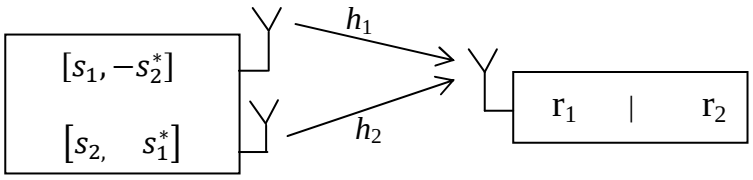

Figure 2.2: Alamouti transmit diversity scheme

Assuming a flat fading channel and denoting the two channel coefficients h_1 and h_2, the received vector r is formed by stacking two consecutive data samples $r = [r_1\ r_2]^T$ in time. The received signal can be represented by a matrix form as

$$r = G\ C + n \tag{2.8}$$

We define the received signal vector $r = [r_1\ r_2]^T$, the code symbol vector $C = [c_1\ c_2]^T$, the noise vector $n = [n_1\ n_2]^T$. Where the channel matrix is defined as $G = [h_1\ h_2]^T$.
The signals received at time t and $t + T$ are respectively:

$$r_1 = h_1 s_1 + h_2 s_2 + n_1 \tag{2.9}$$

$$r_2 = -h_1 s_2^* + h_2 s_1^* + n_2 \tag{2.10}$$

Where $h_1$and h_2 are the fading channel coefficient gains, and n_1 and n_2 are zero-mean complex Gaussian noise.

The received signal at time t and $t+T$can be written as

$$\begin{bmatrix} r_1 \\ r_2 \end{bmatrix} = \begin{bmatrix} s_1 & -s_2^* \\ s_2 & s_1^* \end{bmatrix} \begin{bmatrix} h_1 \\ h_2 \end{bmatrix} + \begin{bmatrix} n_1 \\ n_2 \end{bmatrix} \quad (2.11)$$

Where $h_1 = |h_1|\, e^{j\varphi_1}$ and $h_2 = |h_2|\, e^{j\varphi_2}$ are complex channel responses for antennas 1 and 2, respectively, and $|h_i|$ and φ_i, are the amplitude gain and phase shift for the path, and n_1 and n_2 complex noises at times *t* and *t* +*T*. The signal vector can be rewritten as, or in short notation

$$y = HS + n' \quad (2.12)$$

$$\begin{bmatrix} r_1 \\ r_2^* \end{bmatrix} = \begin{bmatrix} h_1 & h_2 \\ h_2^* & -h_1^* \end{bmatrix} \begin{bmatrix} s_1 \\ s_2 \end{bmatrix} + \begin{bmatrix} n_1 \\ n_2^* \end{bmatrix} \quad (2.13)$$

Where $y = [r_1\ r_2^*]^T$, the symbol vector $S = [s_1\ s_2]^T$, the noise vector $n = [n_1\ n_2^*]^T$. Where the equivalent channel matrix is defined as

$$H = \begin{bmatrix} h_1 & h_2 \\ h_2^* & -h_1^* \end{bmatrix} \quad (2.14)$$

2.2.4 Maximum Ratio Combining and Decoding 2×1 Schemes

Assuming perfect channel knowledge at the receiver, vector y is multiplied by the Hermitian transpose channel matrix, which because of its orthogonality results into:

$H^H H = HH^H = h^2 I_2$

Where the 2×2 identity matrix I_2as well as the gain of the channel $h^2 = |h_1|^2 + |h_2|^2$ was introduced, indicating a two times diversity for the reception of both symbols. Note that each matrix element h_i is assumed to be a complex Gaussian random variable with unit variance. Therefore, the decoded signal can be obtained as

$$\tilde{S} = \begin{bmatrix} \tilde{s}_1 \\ \tilde{s}_2 \end{bmatrix} = H_{es}^H HS + H_{es}^H\, n' \quad (2.15)$$

With $E[n'\, n'^H] = \sigma_n^2 I_2$

$$\tilde{S} = \begin{bmatrix} h_1^* & h_2 \\ h_2^* & -h_1 \end{bmatrix} \begin{bmatrix} r_1 \\ r_2^* \end{bmatrix} \quad (2.16)$$

In the above equation, if the channel estimation is perfect, that is, $H_{es} = H$, then we have

$$\tilde{S} = (|h_1|^2 + |h_2|^2)S + n_{\tilde{S}} \quad (2.17)$$

With

$$E\left[n_{\tilde{S}}\, n_{\tilde{S}}^H\right] = (|h_1|^2 + |h_2|^2)\sigma_n^2 I_2 \quad (2.18)$$

$$\tilde{s}_1 = h_1^* r_1 + h_2 r_2^*$$

$$= [s_1(|h_1|^2 + |h_2|^2) + (h_1^* n_1 + h_2 n_2^*)] \quad (2.19)$$

$$\tilde{s}_2 = h_2^* r_1 - h_1 r_2^*$$

$$= [s_2(|h_1|^2 + |h_2|^2) + (h_2^* n_1 - h_1 n_2^*)] \quad (2.20)$$

The soft output data can be detected independently. There is a straightforward way to evaluate the above expression for Nr receives antennas.

Despite the fact that both antennas send signals simultaneously, we observe that the interference has been totally removed in (2.19) and (2.20). The only assumption is that the receiver has perfect knowledge of the channel gains. On the contrary, the transmitter does not need knowledge of the channel gains with this scheme. These combined signals $\tilde{s}_1$ and $\tilde{s}_2$ are then sent to the maximum likelihood decoder (see Appendix A).

2.2.5 ML Decision

As the signal $\tilde{s}_1$ depends only on $s_1$and $\tilde{s}_2$ only on s_2, we can decide on s_1 and s_2 by applying the maximum likelihood rule on $\tilde{s}_1$ and $\tilde{s}_2$ separately. These combined signals are sent to a maximum likelihood decoder which for each transmitted symbol $s_i, i = 1,2,$ selects a symbol $\hat{s}_i$ from the M-ary signal set such that, $d^2(\tilde{s}_i, \hat{s}_i)$ is minimum, where $d^2(\tilde{s}_i, \hat{s}_i)$ is the Euclidean distance between the two symbols. $\hat{s}_i$ is the estimate of the transmitted symbol s_i. Thus the ML decoding rule of equation (2.17) can be separated in to two independent decoding rules

$$\hat{s}_1 = min_{s_1 \in S} \left[\left((|h_1|^2 + |h_2|^2) - 1 \right) |s_1|^2 + d^2(\tilde{s}_1, \hat{s}_1) \right] \quad (2.21)$$

$$\hat{s}_2 = min_{s_2 \in S} \left[\left((|h_1|^2 + |h_2|^2) - 1 \right) |s_2|^2 + d^2(\tilde{s}_2, \hat{s}_2) \right] \quad (2.22)$$

For MPSK modulation, all the symbols in the constellation set M have equal energy, hence the ML decoding rule then becomes

$$s_1 = min_{s_1 \in S} d^2(\tilde{s}_1, s_1) \quad (2.23)$$

$$s_2 = min_{s_2 \in S} d^2(\tilde{s}_2, s_2) \quad (2.24)$$

The complexity of the decoder is linearly proportional to the number of antennas and the transmission rate.

2.2.6 Zero Forcing Method

The transmitted symbols can be computed by the ZF approach

$$\hat{S} = [H^H H]^{-1} H^H y = \frac{1}{h^2} H^H y \quad (2.25)$$

Which gives equivalent results to the ML solution due to the diagonal structure of the HH^H, however, with less receiver complexity. This can be further elaborated on:

$$\hat{S} = S + [H^H H]^{-1} H^H n \quad (2.26)$$

Revealing the noise filtering. The noise variance for the two symbols is given by

$$\sigma_n^2 \, trace([H^H H]^{-1}) = \frac{2\sigma_n^2}{h^2} \quad (2.27)$$

Using complex valued modulation, only for the two antenna scheme such an improvement is possible.

2.2.7 Alamouti Scheme 2×2 Space Time Code

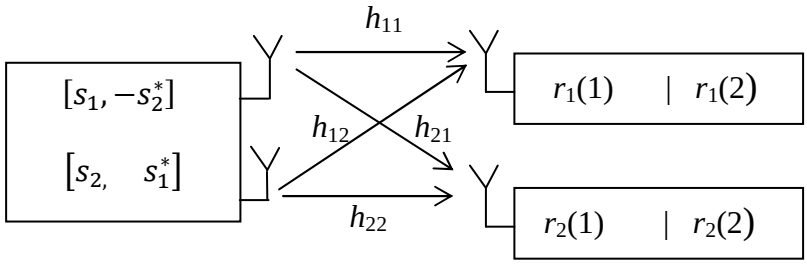

Figure 2.3: Alamouti transmit and receive diversity 2×2 STBC

The block diagram of the Alamouti's scheme 2x2 STC, with transmit and receive diversity is shown in Figure 2.3, the fading channel coefficients from the transmit antennas i to the receive antennas j is denoted by $h_{ji}(t)$.

Let's assume that two receive antennas are used at the receiver and also assume that the fading coefficients are constant across two consecutive symbol transmission periods, means that channel is quasi static within transmission block. Hence following equation (2.28), (2.29), (2.30) and (2.31) for every single channel coefficients at time interval *T* can be written. Where $|h_{ji}|$ and φ_p, are the amplitude gain and phase shift for the path, and *T* is the symbol duration.

$$h_{11}(t) = h_{11}(t+T) = h_{11} = |h_{11}| \, e^{j\varphi_0} \quad (2.28)$$

$$h_{12}(t) = h_{12}(t+T) = h_{12} = |h_{12}| \, e^{j\varphi_1} \quad (2.29)$$

$$h_{21}(t) = h_{21}(t+T) = h_{21} = |h_{21}| \, e^{j\varphi_2} \quad (2.30)$$

$$h_{22}(t) = h_{22}(t+T) = h_{22} = |h_{22}| \, e^{j\varphi_3} \quad (2.31)$$

Then the received signals over the two symbol interval at times 0 and T for a 2×2 MIMO system is given by

$$r_1(t) = r_1(0) = h_{11}s_1 + h_{12}s_2 + n_{11} \quad (2.32)$$

$$r_2(t) = r_2(0) = h_{21}s_1 + h_{22}s_2 + n_{21} \quad (2.33)$$

$$r_1(t+T) = r_1(T) = -h_{11}s_2^* + h_{12}s_1^* + n_{12} \quad (2.34)$$

$$r_2(t+T) = r_2(T) = -h_{21}s_2^* + h_{22}s_1^* + n_{22} \quad (2.35)$$

These are the signals that are received by each of the antennas at the receiver across the two time periods. Where $r_j(t)$ represents the output from the *j-th* antenna at time instance t and n_{ji} is zero mean complex Gaussian noise. Using Equations 2.3 and 2.4, the received matrix in a 2x2 system can be written as

$$\begin{bmatrix} r_1(0) & r_1(T) \\ r_2(0) & r_2(T) \end{bmatrix} = \begin{bmatrix} h_{11} & h_{12} \\ h_{21} & h_{22} \end{bmatrix} \begin{bmatrix} s_1 & -s_2^* \\ s_2 & s_1^* \end{bmatrix} + \begin{bmatrix} n_1(0) & n_1(T) \\ n_2(0) & n_2(T) \end{bmatrix} \quad (2.36)$$

Due to the orthogonal design, decoding of STBC is easily implemented in two steps. The first is decoupling the received vectors over the whole observation time into estimates of the transmitted symbols using maximum ratio combining (MRC). After that, maximum likelihood detection of the estimated symbols is performed separately. To illustrate the decoding algorithm, let us consider the 2×2 STBC system. We can rewrite (2.36) as:

$$\begin{bmatrix} r_1(0) \\ r_2(0) \\ r_1^*(T) \\ r_2^*(T) \end{bmatrix} = \begin{bmatrix} h_{11} & h_{12} \\ h_{21} & h_{22} \\ h_{12}^* & -h_{11}^* \\ h_{22}^* & -h_{21}^* \end{bmatrix} \begin{bmatrix} s_1 \\ s_2 \end{bmatrix} + \begin{bmatrix} n_1(0) \\ n_2(0) \\ n_1^*(T) \\ n_2^*(T) \end{bmatrix} \quad (2.37)$$

$$y = H\,S + v \quad (2.38)$$

Where, $y = [r_1(0), r_2(0), r_1^*(T), r_2^*(T)]^T$, are the received signals, and $S = [s_1\ s_2]^T$ is the transmitted symbol vector.

and $H = \begin{bmatrix} h_{11} & h_{12} \\ h_{21} & h_{22} \\ h_{12}^* & -h_{11}^* \\ h_{22}^* & -h_{21}^* \end{bmatrix}$ is the equivalent channel matrix response of the 2x2 STBC system.

And $v = [n_1(0), n_2(0), n_1^*(T), n_2^*(T)]^T$, is the Gaussian noise vector.

2.2.8 Maximum Ratio Combining and Decoding

If the channel fading attenuations h_i can be perfectly recovered at the receiver, if the channel estimation is perfect, that is $H_{es} = H$, the receiver will use them as the channel state information (CSI) in the decoder. Since H_{es} is orthogonal, the transmitted symbols could be easily estimated by decoupling the received signals after multiplying y by H_{es}. This corresponds to MRC and results in maximizing SNR of the estimated symbols.

The transmitted symbols s_1 and s_2 can be estimated by first combining the received signals according to the following equations:

$$\tilde{S} = H_{es}^H\, y = H_{es}^H H\, S + H_{es}^H\, v \tag{2.39}$$

The resulting channel matrix H is orthogonal, i.e.

$$H_{es}^H H = \begin{bmatrix} |h_{11}|^2 + |h_{12}|^2 + |h_{21}|^2 + |h_{22}|^2 & 0 \\ 0 & |h_{11}|^2 + |h_{12}|^2 + |h_{21}|^2 + |h_{22}|^2 \end{bmatrix} \tag{2.40}$$

$$\tilde{s}_1 = h_{11}^* r_1(0) + h_{12} r_1(T)^* + h_{21}^* r_2(0) + h_{22} r_2(T)^* \tag{2.41}$$

$$\tilde{s}_2 = h_{12}^* r_1(0) - h_{11} r_1(T)^* + h_{22}^* r_2(0) - h_{21} r_2(T)^* \tag{2.42}$$

And then using a standard Maximum Likelihood (ML) detector to attempt to recover $s_1$and s_2 from $\tilde{s}_1$and $\tilde{s}_1$. This is the decoupled ML detection that is common to all OSTBCs. By substituting the values of $r_1(0), r_1(T)$, $r_2(0)$ and $r_2(T)$ from equations (2.32), (2.33), (2.34) and (2.35) into equations (2.41) and (2.42) to obtain the following. Substituting the equations we have

$$\tilde{s}_1 = (|h_{11}|^2 + |h_{12}|^2 + |h_{21}|^2 + |h_{22}|^2)s_1 + e1 \tag{2.43}$$

$$\tilde{s}_2 = (|h_{11}|^2 + |h_{12}|^2 + |h_{21}|^2 + |h_{22}|^2)s_2 + e2 \tag{2.44}$$

Where

$$e1 = h_{11}^* n_1(0) + h_{12} n_1(T)^* + h_{21}^* n_2(0) + h_{22} n_2(T)^* \tag{2.45}$$

$$e2 = -h_{11} n_1(T)^* + h_{12}^* n_1(0) - h_{21} n_2(T)^* + h_{22}^* n_2(0) \tag{2.46}$$

As can be seen, the decision statistics for $\tilde{s}_i, i = 1,2$, is a function of only s_i, thus the ML decoding rule of equation (2.43) and (2.44) can be separated in to two independent decoding rules

$$\hat{s}_1 = min_{s_1 \in S}\left[\left((|h_{11}|^2 + |h_{12}|^2 + |h_{21}|^2 + |h_{22}|^2) - 1\right)|s_1|^2 + d^2(\tilde{s}_1, \hat{s}_1)\right] \tag{2.47}$$

$$\hat{s}_2 = min_{s_2 \in S}\left[\left((|h_{11}|^2 + |h_{12}|^2 + |h_{21}|^2 + |h_{22}|^2) - 1\right)|s_2|^2 + d^2(\tilde{s}_2, \hat{s}_2)\right] \tag{2.48}$$

For MPSK modulation, all the symbols in the constellation set M have equal energy, hence the ML decoding rule then becomes

$$s_1 = min_{s_1 \in S}\, d^2\,(\tilde{s}_1, s_1) \tag{2.49}$$

$$s_2 = min_{s_2 \in S}\, d^2\,(\tilde{s}_2, s_2) \tag{2.50}$$

Equations (2.47) and (2.48) show that when the received signals are combined according to equations (2.41) and (2.42) the transmitted symbols are combined coherently and weighted by a positive factor, i.e. $|h_{11}|^2 + |h_{12}|^2 + |h_{21}|^2 + |h_{22}|^2$. The noise samples however, get combined in an incoherent manner. This is how the Alamouti scheme is able to achieve an improvement in performance over SISO systems (see Appendix A).

The transmitted symbols can be computed by the ZF approach, according to [50]

$$\hat{S} = [H_{es}^H H_{es}]^{-1} H_{es}^H = \frac{1}{h^2} H_{es}^H\, y \tag{2.51}$$

Where $h^2 = |h_{11}|^2 + |h_{12}|^2 + |h_{21}|^2 + |h_{22}|^2$

Which gives equivalent results to the ML solution due to the diagonal structure of the HH^H, however, with less receiver complexity. This can be further elaborated on:

$$\hat{S} = S + [H_{es}^H H_{es}]^{-1} H_{es}^H\, v \tag{2.52}$$

Where

$$\hat{S} = [\hat{s}_1 \;\; \hat{s}_2]^T \tag{2.53}$$

The ML solution can then be found by inverting the channel matrix derived in (2.37). Note that it is not usually the case that the optimal ML estimate can be obtained using linear techniques. Since the constructed channel matrix is a scaled unitary matrix, i.e., $\det(H)\, H^{-1} = H^+$ (+: Pseudo inverse matrix), the ML, Zero Forcing and MMSE solutions are all equivalent [37].

2.3 Spatial Multiplexing

STC is used to combat fading. However, fading can also be exploited to increase the data rate. Essentially, if the path gains between individual transmit and receive antenna pairs fade independently, the channel matrix is well conditioned with high probability, in which case multiple parallel spatial channels are created. By transmitting independent information streams in parallel through the spatial channels, the data rate will be increased. This effect is also called spatial multiplexing (SM). Hence, the concept of SM is different from STC method, which permits to efficiently introduce a space time correlation among transmitted

signals to improve information protection and increase diversity gain. Unlike spatial diversity, the main objective in this scheme is to increase the throughput of communication channel [51]. SM methods uses multiple antennas at the transmitter and the receiver and send independent data streams over the individual transmit antennas. In conjunction with a rich scattering environment, within the same frequency band to provide a linearly increasing of capacity gain in the number of antennas [39].

The data streams are separated by an interference cancellation type of algorithm. With SM schemes, the overall data rate can be increased significantly (it is proportional to the number of transmit antennas) while maintaining the spectral occupation. A well known example of an SM scheme is the Bell Labs Layered Space Time (BLAST) scheme. In this chapter, we shall focus on early and well known high rate MIMO architecture, known as the Bell Labs Layered Space Time system.

2.3.1 Bell Labs Layered Space Time Architecture

One of the earliest communication systems that were proposed to take advantage of the promising capacity of MIMO channels is the BLAST architecture. It achieves high spectral efficiencies by spatially multiplexing coded or uncoded symbols over the MIMO fading channel. Mt symbols are transmitted through Mt antennas. Each receive antenna receives a superposition of Mt faded symbols.

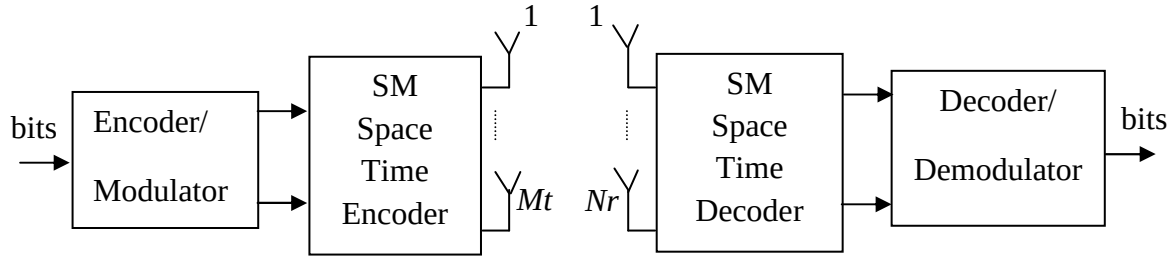

Figure 2.4: Block diagram of SM system

BLAST system is shown in Figure 2.4. A single data stream is de-multiplexed into Mt sub-streams, and each sub-stream is then encoded into symbols and fed to its respective transmitter. Because streams of independent data are transmitted over different antennas, thus maximizing the average data rate over the MIMO system. There are three well known algorithms in SM namely D-BLAST, V-BLAST and H-BLAST. The more popular one is V-BLAST transmission which has optimum tradeoff between performance efficiency and computational complexity.

More practical decoding architectures were proposed in the literature. They can be classified under two categories: D-BLAST and V-BLAST. The diagonally layered space time architecture D-BLAST architecture was originally proposed by Foschini in 1996 [52]. The target application was for fixed and low mobility wireless networks, such as WLAN.

The D-BLAST uses multiple antennas at both the transmitter and receiver, and a codec architecture that disperses the coded blocks across the diagonals in space time. In a rich Rayleigh scattering environment, this codec structure has capacity that increases linearly with the number of antenna elements, up to 90% of the Shannon theoretical capacity limit. However, D-BLAST suffers from high implementation complexity, and a simplified coding technique, vertical BLAST or V-BLAST, is proposed in [4, 51]. The essential difference between D-BLAST and V-BLAST lies in their respective transmission coding processes.

In D-BLAST, temporal redundancy is introduced between the sub-streams by dispersing the code blocks along the space time diagonals. In V-BLAST, however, the encoding process is simply a de-multiplexing operation. The inter sub-stream block coding technique is what leads to D-BLAST's higher spectral efficiency. For a large number of antennas, D-BLAST can offer at most 30% increase in capacity over V-BLAST. The receiver processing for V-BLAST is much simplified over D-BLAST, however, since the nulling and cancellation detection algorithm does not extend across the temporal domain.

2.3.2 D-BLAST Architecture

The single data stream is encoded, modulated and de-multiplexed in to Mt branches by a STC encoder and transmitted by each of the Mt transmit antennas as shown in Figure 2.5. The mapping of symbols to each of the transmit antenna can be done in to two common schemes: D-BLAST and V-BLAST.

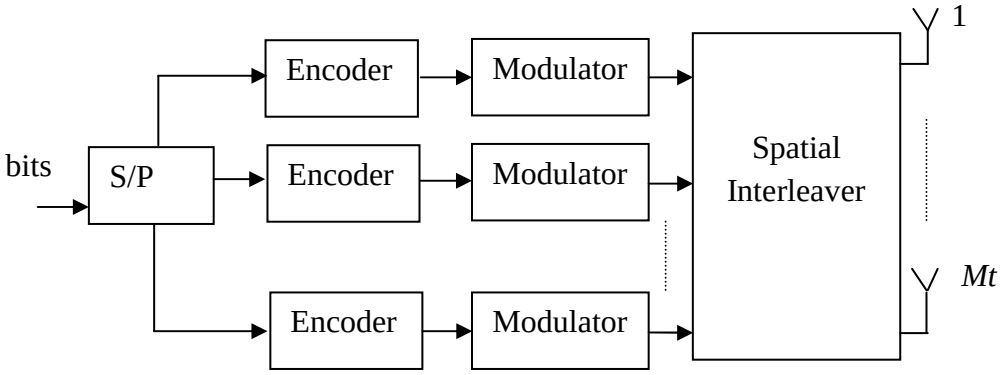

Figure 2.5: Block diagram of layers D-BLAST

In D-BLAST architecture the modulated symbol of each encoder is distributed among the Mt transmit antennas along the diagonal of the transmission array. For a three by three antenna array this encoding process is shown below.

$$\begin{bmatrix} x_1^1 & x_2^1 & x_3^1 & \cdots \\ x_1^2 & x_2^2 & x_3^2 & \cdots \\ x_1^3 & x_2^3 & x_3^3 & \cdots \end{bmatrix} \Rightarrow \begin{bmatrix} x_1^1 & x_2^1 & x_3^1 & x_4^1 & \cdots & \cdots \\ 0 & x_1^2 & x_2^2 & x_3^2 & x_4^2 & \cdots \\ 0 & 0 & x_1^3 & x_2^3 & x_3^3 & x_4^3 \end{bmatrix}$$

$$\Rightarrow \begin{bmatrix} x_1^1 & x_1^2 & x_1^3 & x_1^4 & \cdots \\ 0 & x_2^1 & x_2^2 & x_2^3 & \cdots \\ 0 & 0 & x_3^1 & x_3^2 & \cdots \end{bmatrix} \qquad (2.54)$$

Where x_t^i is the symbol transmitted from antenna i at time t. In the first transmission matrix, the output of each modulator is supposed to be mapped to each of the respective transmit antennas. But in D-BLAST architecture the lower rows are padded with zeros that introduce delays as is shown in the second transmission matrix. Finally the symbols in the first diagonal are transmitted from antenna one, symbols in the second diagonal are transmitted from antenna two and so on. So, the rows of the last transmission matrix indicate symbols transmitted from the respective antennas. As we can see from this last transmission matrix, in the first transmitting time slot only the first antenna will transmit and at the second transmitting time slot only antenna one and two will transmit and antenna 3 will start transmitting at the third time slot. The diagonal layering introduces space diversity and thus achieves a better performance even though there is some rate loss since the portion of the transmission matrix on the left is padded with zeros. The added complexity in D-BLAST architecture makes its initial implementation somewhat difficult and led to V-BLAST architecture.

2.3.3 V-BLAST Architecture

The V-BLAST system model or known such as SM with Mt transmitted antenna and Nr received antenna. This system includes two parts: The transmitted part and the received part.
The V-BLAST architecture breaks the input data stream, $S = [s_1\ s_2\ s_3 \ldots s_M]^T$, into Mt sub-streams, each sub-stream is then encoded into constellation symbols and fed to its respective transmitter. And each of them is subsequently modulated by an *M*-level modulation (MQAM or MPSK) and then de-multiplexed in to Mt sub-streams and transmitted simultaneously on the individual antennas, i.e. the encoding process is simply a de-multiplexing operation, no inter sub-stream coding or interleaving of any kind is used, the system is shown in Figure 2.6.

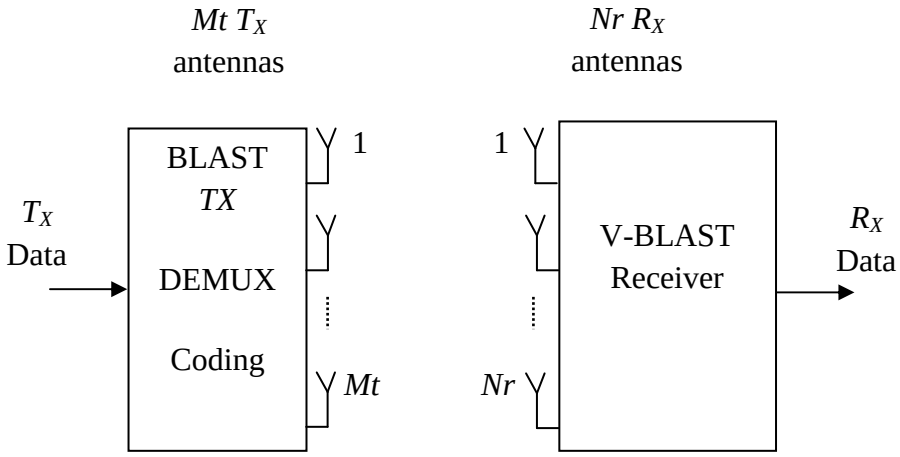

Figure 2.6: V-BLAST system model

Assume that time is synchronous and transmit power is standardized the same for each transmit antenna. The signal processing chain related to an individual sub-stream is referred to as a layer. As shown in Figure. 2.7, the modulated symbols are arranged into a transmission matrix, denoted by X, which consists of Mt rows and N columns, where N is the transmission block length. The t-th column of the transmission matrix, denoted by x_t:

$$x_t = (x_t^1\ x_t^2\ \dots\ x_t^{Mt})^T, \qquad t = 1,2,\dots\dots,N \tag{2.55}$$

At a given time t, the transmitter sends the t-th column from the transmission matrix, one symbol from each antenna. That is, a transmission matrix entry x_t^i is transmitted from antenna i at time t, $i = 1,\dots\dots,Mt$. The vertical architecture above transmit sequence the columns of transmission matrix at space time. If without inter-coding then each symbol is only transmitted one time. Therefore, the time elements of code are lost and only attain the space diversity. Hence, this model is also known such as spatial multiplexing.

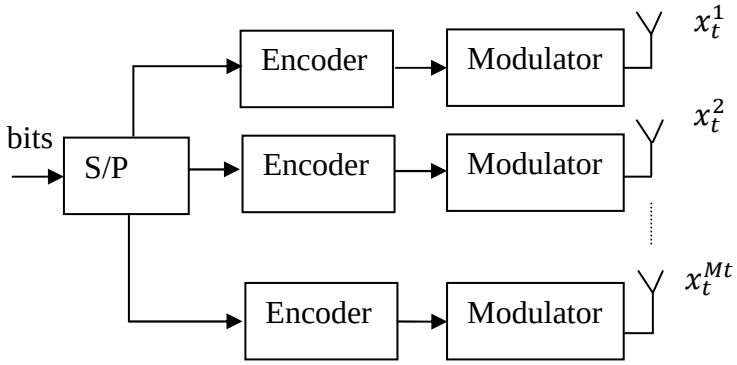

Figure 2.7: The detail scheme of the transmitter

We only interest in V-BLAST system without inter-coding and detect the receive signal at each time. For example, in a system with three transmit antennas, the transmission matrix *X* is given by

$$X = \begin{bmatrix} x_1^1 & x_2^1 & x_3^1 & \cdots \\ x_1^2 & x_2^2 & x_3^2 & \cdots \\ x_1^3 & x_2^3 & x_3^3 & \cdots \end{bmatrix} \quad (2.56)$$

Where the first row is symbols transmitted from antenna one and the second row is symbols transmitted from the second antenna and so on. Had the number of transmit antenna be greater than three, the number of rows of the transmission matrix which is equal to the number of transmit antennas would be greater than three. Columns of the transmission matrix indicate symbols transmitted at time instants t, $t + 1$ etc. (Unlike the transmission matrix of (2.2), four different symbols are transmitted in two symbol periods and hence added rate of transmission).

Receive antennas $Nr - 1$ receives signals radiated from all transmit antennas, hence the need arise to remove the mixing operation of the channel. The signals transmitted are assumed to propagate through a rich scattering environment which causes the signals on different paths to interfere with each other upon reception at the receiver.

This interference is represented by the following matrix operation

$$y = Hx + n \quad (2.57)$$

where y is an Nr component column matrix of the received signals across Nr receive antennas, x is the *t-th* column in the transmission matrix X and n is an Nr component column matrix of the AWGN noise signals at the receive antennas, where the noise variance per receive dimension is denoted by σ_n^2 and mean by 0.

2.3.4 V-BLAST Detector

The V-BLAST detector decodes the sub-streams using a sequence of nulling and cancellation steps. An estimate of the strongest transmitted signal is obtained by nulling out all the weaker transmit signals using the ZF criterion or MMSE criterion [53, 54, 55], then subtract this strongest signal from the received signal, proceed to decode the strongest signal of the remaining transmitted signals, and so on. We will mention the algorithm for detection at receive of V-BLAST system model below. The detection process consists of two main operations [56]:

1- Interference suppression (nulling): the suppression operation nulls out interference by projecting the received vector onto the null subspace (perpendicular subspace) of the subspace spanned by the interfering signals. After that, normal detection of the first symbol is performed.

2- Interference cancellation (sub-traction): the contribution of the detected symbol is subtracted from the received vector.

The interference suppression and cancellation are serially repeated until all symbols are detected as shown in Figure 2.8.

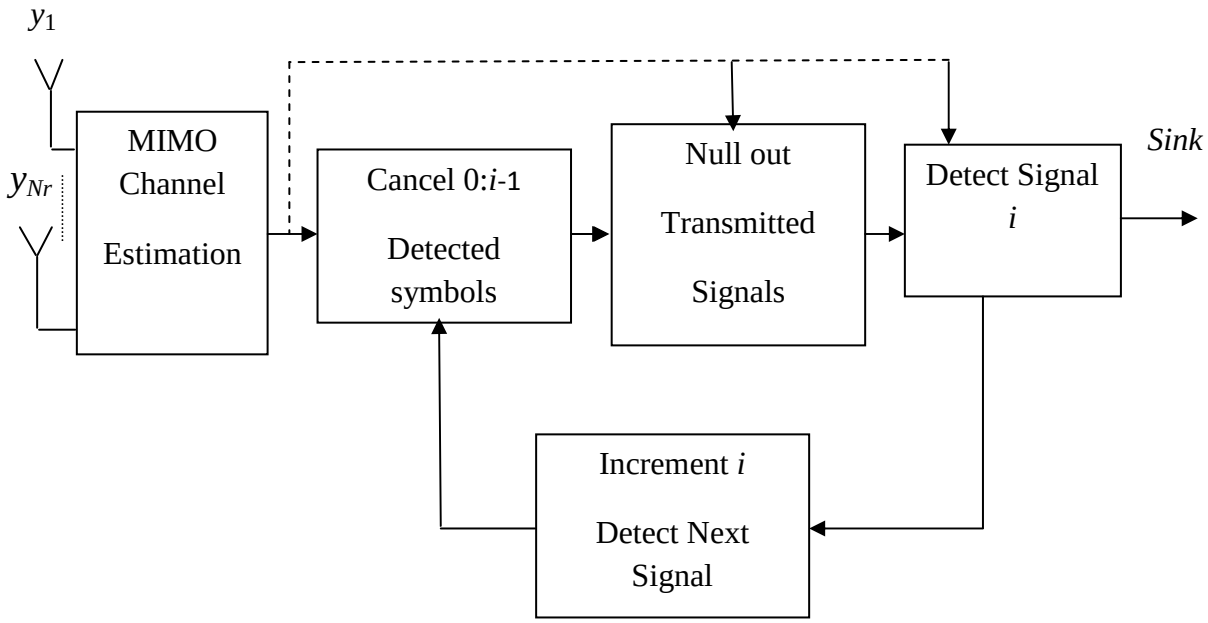

Figure 2.8: Block diagram of a BLAST receiver: Serial interference suppression and cancellation algorithm

BLAST detection algorithm combines linear (interference suppression) and nonlinear (serial cancellation) algorithms [54]. This is similar to the de-correlating decision feedback multiuser detection algorithm. A drawback of BLAST algorithms is the propagation of decision errors. Also, the interference nulling operation requires that the number of receive antennas be greater than or equal to the number of transmit antennas [53, 54]. As it is usually considered for V-BLAST MIMO schemes, the current scheme, is equipped with Mt transmit and Nr receive antennas, with $Nr \geq Mt$.

Furthermore, due to the interference suppression, early detected symbols benefit from lower receives diversity than later ones. Thus, the algorithm results in unequal diversity advantage for each symbol.

The detection algorithm of a conventional V-BLAST system consists of a linear nulling and Successive Interference Cancellation (SIC) process to estimate the Mt transmitted symbols from the received signal. The signal with the highest Signal to Noise plus Interference Ratio (SNIR) is first detected using a linear nulling process such as ZF or MMSE. The detected symbol is regenerated, and the corresponding signal portion is subtracted from the received signal. This cancellation process results in a modified received signal, with fewer interfering signal components left. This process is repeated, until all Mt symbols are detected.

2.3.4.1 Detection Process

The detection process of the V-BLAST system involves the estimation of x given y and H, of the received signal given by the equation (2.57). The t elements of the transmit vector x_t are constellation symbols which are assumed to be uncorrelated. We also assume that the channel matrix H is full rank. It is shown later that the second assumption is very crucial to the operation of the V-BLAST system. The receiver knows the received vector y and has an estimation of H. The detection process is then a multiuser detection type process. The process involves two steps [36]:

• Slicing (and then decoding) a symbol while nulling the others.

• Cancelling the effect of each new decoded symbol from the rest.

2.3.4.2 Linear Detection

The Diagram for general linear detection is showed in Figure 2.9.

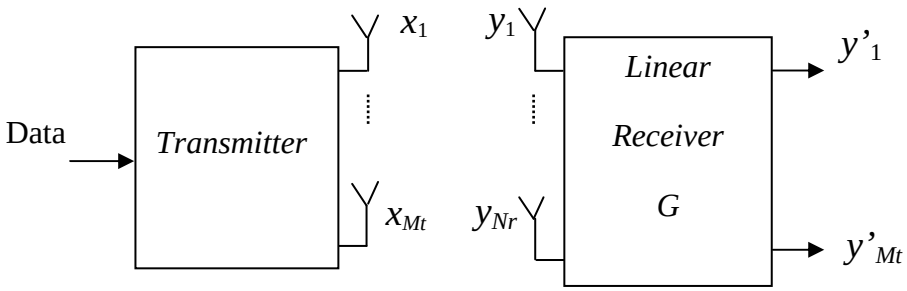

Figure 2.9: Block diagram for general linear detection receiver

The received vector of equation (2.57) $y = [y_1, y_2, \ldots, y_{Nr}]^T$, is Nr by one column matrix received signal from Nr receive antenna and y depend on each system. Where x_i is the symbol transmitted from the *i*-th antenna and h_i is the *i*-th column of Nr by Mt transition matrix H.

2.3.4.3 Linear Detection Base on ZF

To perform the un-mixing operation the received signal is multiplied by matrix G, Linear detection base on ZF criterion then x is evaluated follow the equation below

$$\tilde{x} \quad = G\, y = H^{+} y = (H^{H} H)^{-1} H^{H} \tag{2.58}$$

Where H^{+} is Moore-Penrose pseudo-inverse matrix form:

$$G = H^{+} = (H^{H} H)^{-1} H^{H} \tag{2.59}$$

And $H^{H}$is the Hermitian matrix form.

Then, $\tilde{x}$ is quantized follow the type of modulation at the transmission.

2.3.4.4 Linear detection base on MMSE

Linear detection base on MMSE criterion is the same ZF detection, except x is evaluated follow the equation below

$$\tilde{x} = Gy \tag{2.60}$$

With $G = (H^{H} H + \sigma^{2} I_{Nr})^{-1} H^{H}$

The $\tilde{x}$ is quantized the same with ZF.

2.3.4.5 Non Linear Detector

The operation of mitigating the interference with linear signal processing is normally referred to as nulling [4, 36, 52, 53]. However, a superior performance can be reached when a non-linear spatial processing approach is used. A common non-linear detector is based on interference cancellation (IC), wherein the contribution of the detected symbols to the received signal is reconstructed and subtracted. Assuming correct decisions, the resulting signal is free from the interference of the detected symbols, yielding better estimates of the remaining symbols. One particularly successful IC algorithm is called SIC. The important problem of SIC detection find the optimal order to obtain BER better. Assume that K_0 is the optimal order, SIC detection implement with four steps below [54]:

- Delete the detected symbol
- Cancellation
- Evaluation
- Optimal order

2.3.5.1 Nulling

Let consider the received signal at time *t* of equation (2.57), hence the received vector can be also be written in another form as:

$$y = x_1 h_1 + x_2 h_2 + \cdots + x_{Mt} h_{Mt} + n \tag{2.61}$$

Here x_i is the transmitted symbol from the *i*-th transmit antenna, and h_i is the *i*-th column of the transition matrix. Nulling is performed by linearly weighting the received symbols to satisfy the ZF or MMSE performance criterion.

The *i*-th ZF nulling vector w_i is defined as the unique minimum norm vector .The ZF nulling vector w_i is chosen to satisfy:

$$w_i^T h_j = \begin{cases} 0 & for\ i \neq j \\ 1 & for\ i = j \end{cases} \tag{2.62}$$

Where $()^T$ denotes transpose vector.

Orthogonal to the sub-space spanned by the contributions to y_i due to the symbols not yet estimated and cancelled and is given by the *i*-th row of H. Then, the decision statistic for the *i*-th symbol is

$$\tilde{x}_i = w_i^T y_i$$

$$= x_1 w_i^T h_1 + x_2 w_i^T h_2 + \cdots + x_i w_i^T h_i \ldots . + x_t w_i^T h_t + w_i^T n$$

$$= 0 + 0 + \cdots + x_i + \cdots . + 0 + \tilde{n}_i \tag{2.63}$$

A soft or hard decision now can be made on $\tilde{x}_i$ to estimate the transmitted symbol

$$\hat{x}_i = Q(\tilde{x}_i) \tag{2.64}$$

Where $Q(\,)$ is the soft/hard decision function.

In SIC, the layers are detected sequentially. Initially, the received signal y goes through a linear detector for layer 1, whose output is used to produce a hard estimate of the symbols at this layer $\hat{x}_1$. Denoting the received vector y by y_1, if the nulling vector is w_1, the 'first' symbol is

$$\tilde{x}_1 = w_1^T y_1 \tag{2.65}$$

Then the decision statistic for $\tilde{x}_1$ is

$$\hat{x}_1 = Q(\tilde{x}_1) \tag{2.66}$$

2.3.5.2 Interference Canceller

The effect of symbols already detected can be subtracted from the symbols yet to be detected. This improves the overall performance when the order of detection is chosen carefully.

After the suppression by the nulling vector w_1 , and if $\hat{x}_1 = Q(\tilde{x}_1)$ is the estimate of x_1 after the decision (soft or hard), then the interference due to $\hat{x}_1$ on the other symbols can be subtracted by taking

$$y_2 = y_1 - \hat{x}_1 h_1 \tag{2.67}$$

The hard decision on $\tilde{x}_1$ will result in the symbol x_1. The effect of x_1 on other symbols yet to be detected is removed (canceled) through the operation. Then, the contribution of layer 1 to the received signal is estimated and cancelled, generating the signal y_2.

Assuming $\hat{x}_1 = x_1$, i.e., the decision taken was correct. The next symbol is then detected by finding w_2 and then making a decision on $w_2^T y_2$ and so on. The 'second' symbol is

$$\tilde{x}_2 = w_2^T y_2 \tag{2.68}$$

After finding w_2, x_2 can be decoded in similar way using y_2 as a received signal and the process continues till the last symbol. The process of SIC detection is depicted in Figure 2.10.

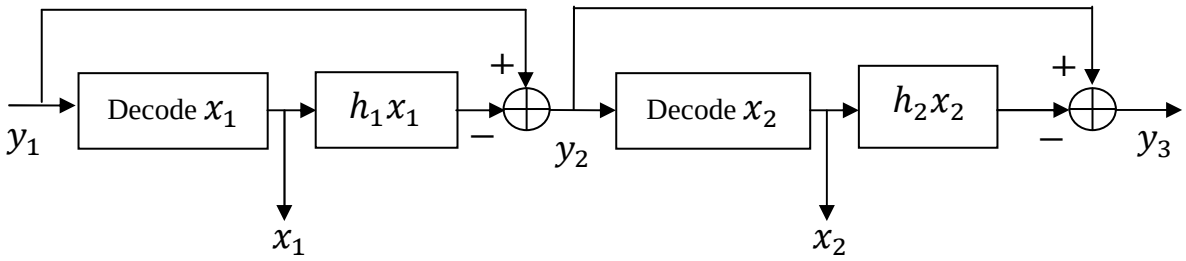

Figure 2.10: Block diagram of SIC detection of V-BLAST

The performance of this successive cancellation and detection scheme depends on the decision taken on each stage, as any wrong decision is propagated through all the later stages.

The process is then repeated. In general, at the *i*-th layer, the signal y_i , hopefully free from the interference of layers $j < i$, goes through a linear detector that tries to mitigate the interference from layers $j > i$. A hard estimate of the symbol at this layer $\hat{x}_i$, is then produced, based on the output of this linear detector. Then, the contribution of this layer to the received signal y_i, is estimated and cancelled.

This procedure yields a modified received signal given by

$$y_{i+1} = y_i - \hat{x}_i h_i \tag{2.69}$$

Where h_i is the *i*-th column of the matrix channel *H* corresponding to the channel gains associated to layer i, and $\hat{x}_i h_i$ represents the estimated interference from the *i*-th layer. The result is that y_{i+1} is free from the interference coming from layers $\{1, \ldots, i\}$. This signal is then fed into the linear detector for the (i+1)-th layer. This technique is also known as nulling and cancelling algorithm [57].

The performance of SIC can be improved if the layers are detected in an appropriate order [36, 51], resulting in ordered successive interference cancellation (OSIC). Indeed, one of the disadvantages of SIC is that the signal associated with the first detection layer may exhibit a lower received SNR than that of the other layers. This may increase the probability of detection errors, which can propagate through the serial detection process, degrading performance of the overall receiver. This problem can be mitigated if the layers are ordered by decreasing SNR, so that the first layer to be detected is that with the higher SNR. The effect of this error propagation can be minimized by proper ordering of the detection process. I.e. first recover a symbol corresponding to a signal with high SNR in such a way that the probability of committing an error in its detection is minimized. Subtract the effect of this symbol from the received signal and then recover the symbol corresponding to a signal with the next higher SNR and keep on till the end. Sometimes this approach is called best first cancellation [39].

Due to the nulling and cancelling processing of the IC algorithm in the SIC approach, the layers coming after the first one take advantage of the cancelling algorithm and this is translated into a higher diversity order for the next detected layers and the performance of the whole receiver.

2.3.5.3 Optimal Detection Order

To minimize error propagation the strongest symbols are detected first. This is known to be the optimal detection order. A simple optimal ordering is based on the post detection *SNR* of each sub-stream. The *SNR* for the i^{th} detected symbol of vector y is given by [36].

$$\rho_i = \frac{E\{|x_i|^2\}}{\sigma_n^2(\|w_i\|^2)} \tag{2.70}$$

Where σ_n^2 is the noise power and $E\{\}$ denotes the expectation.

The optimal detection order is determined by choosing the row of G with minimum euclidean norm (to maximize the SNR), where G is defined in (2.59), (2.60). The row index is obtained from (2.71).

$$ind = arg\{min_i \|(G)_i\|^2\} \quad (2.71)$$

As $\left\|w_i^T h_i\right\|^2 = \|w_i\|^2 \|h_i\|^2$, from (2.62) it is seen that a smaller $\|w_i\|^2$ value requires the corresponding h_i have higher 2 norm. So the SNR in (2.67) for the *i*-th sub-stream is proportional to the norm of the *i*-th column of H Thus, the optimal detection order is in decreasing order of the 2 norm of the columns of H.

2.3.5.4 Computing the ZF Nulling Vector

The vector w_i in (2.72) is unique and is the *i*-th row of the pseudo-inverse of H

$$w_i^T = \langle H^+ \rangle_i \quad (2.72)$$

Where $\langle .^+ \rangle_i$ denotes the *i*-th row and (+) denotes the pseudo-inverse.

With the successive cancellation and decoding, w_i^T is chosen as the *i*-th row of pseudo-inverse of H whose 1 to $i-1$ columns are set to zero. This is due to the fact that at the *i*-th stage the vector w_i has to be orthogonal only to h_j for $j = 1, \dots, Mt$.

With optimal ordering, if $\{ind_1, ind_2, \dots\dots, ind_{Mt}\}$ denotes the optimal order, at the *ind*-th stage the ZF nulling vector w_{k_i} is

$$w_{k_i}^T = \langle H_{k_{i-1}}^+ \rangle_{k_i} \quad (2.73)$$

Where $H_{k_{i-1}}^+$ denotes the matrix obtained from H by zeroing the columns $\{k_1, k_2, \dots\dots, k_{i-1}\}$

Using the MMSE criterion, the nulling vector w_i^T is the *i*-th row of the matrix

$$G = \left(H^H H + \frac{1}{\rho} I\right)^{-1} H^H \quad (2.74)$$

Where ρ is the SNR. For successive decoding and optimal ordering based on G, the matrix G should be computed on each step from the partially zeroed H as in (2.73). The MMSE criterion always results in better SNR and thus a better performance. But the disadvantages are that the SNR has to be known at the receiver and matrix inverse needs to be computed.

2.3.5.5 Detection Algorithm

Is given by [54]

initialisation

1. $i \leftarrow 1$
2. $G_1 = H^+$
3. $k_1 = min\left\|\langle G_1\rangle_j\right\|^2$

iteration

1. $w_{k_i}^T = \langle G_i\rangle_{k_i}$
2. $d_{k_i} = w_{k_i}^T\, y_i$
3. $\hat{x}_{k_i} = Q\left(d_{k_i}\right)$
4. $y_{i+1} = y_i - \hat{x}_{k_i} H_{k_i}$
5. $G_{i+1} = H_{k_i}^+$
6. $ind_{i+1} = min_{j\notin\{ind_1, ind_2, \ldots, ind_i\}}\left\|\langle G_{i+1}\rangle_j\right\|^2$
1. $i \leftarrow i + 1$

Note that in step 3 (and 6) $ind_i = min_j\left\|\langle G_i\rangle_j\right\|^2$ is the optimal detection order and $(G_i)_j$ is j column of G_i, which used to pick the strongest symbol.

This is the due to the reason that the row j of G, which has the minimum norm, corresponds to the j-th column of H which will have the maximum norm.

2.3.6 V-BLAST Capacity

The above discussion leads to a general transceiver architecture that can achieve the channel capacity and is called V-BLAST. The V-BLAST structure is shown in Figure 2.11. In V-BLAST the independent data streams are multiplexed via the unitary matrix Q which can be dependent on H or not. The i-th data stream is allocated a power p_{ri} while $p_{r1} + p_{r2} + \cdots + p_{rMt} = Pr$; where Pr is the total power constraint.

There are different versions of V-BLAST which differ in receiver architecture but all of them share the same transmitter structure.

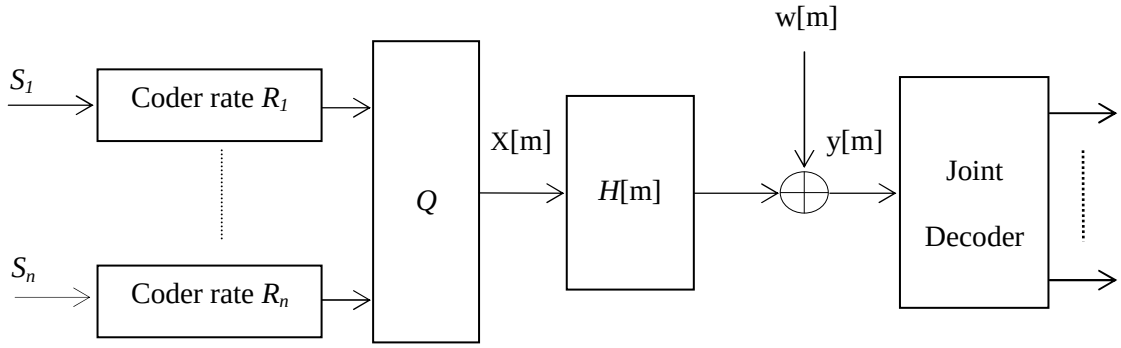

Figure 2.11: The V-BLAST Architecture transceiver

The two mentioned circumstances are two special cases of V-BLAST and can be summarized as follows:

2.3.6.1 Capacity with Perfect channel information at the transmitter

If the channel information (CSI) is available at the transmitter, the multiplexing coordinate system is defined by the matrix $Q = V$; where V is derived from section (1.3.2) by using the singular decomposition of H where $H = UDV^H$, and the powers are given by waterfilling allocation method. The channel capacity will be given by

$$C \approx \sum_{i=1}^{m} log_2\left(1 + \frac{P_i^* \lambda_i}{N_0}\right) bits/s/Hz \qquad (2.74)$$

2.3.6.2 Capacity with no Channel Information at the Transmitter

When the channel information CSI is not available at the transmitter, the multiplexing coordinate system is defined by unitary matrix $Q = I_{Mt}$, independent data streams with equal power are sent on the different transmit antennas. The channel capacity will be given by

$$C = \log_2 \det\left(I_{Nr} + \frac{SNR}{Mt}\, H\, H^H\right) bits/s/Hz \qquad (2.75)$$

So far we have considered the deterministic MIMO channel whereas wireless channels characteristically experience fading which results in a random channel gain matrix H.

2.3.6.3 Capacity with Perfect Channel Knowledge at the Receiver

Consider the V-BLAST architecture, each realization of the fading channel can be treated as a deterministic channel and has a maximum information rate given by equation (2.76). By coding over many coherence time intervals of the channel, the rate of reliable communication of the fast fading channel can be obtained by the ensemble average of the information rate over the elements of channel matrix H. The capacity which is also called ergodic capacity is given by [41].

$$C = \max_{ind_x} E\left[\log_2 \det\left(I_{Nr} + \frac{1}{N_0} H\ ind_x H^H\right)\right] \quad (2.76)$$

Here, the optimal ind_x depends on the statistics of the channel not on each channel realization since they are not known at the transmitter.

In a richly scattered environment, i.e. the elements of H are i.i.d. $N_c(0,1)$ and we have the Rayleigh fading model, the optimal covariance matrix is simply

$$K_x = \left(\frac{P}{Mt}\right) I_{Nr} \quad (2.77)$$

Using the singular decomposition of *H* and (2.76) the resulting capacity is

$$C = E\left[\log_2 \det\left(I_{Nr} + \frac{SNR}{Mt} H\ H^H\right)\right]$$

$$= \sum_{i=1}^{m} E\left[log_2\left(1 + \frac{SNR}{Mt}\ \lambda_i\right)\right] \quad (2.78)$$

In order to observe the performance gains, we analyze the high SNR and low SNR regimes separately.

$$C \approx m\ log\frac{SNR}{Nr} + \sum_{i=1}^{m} E[log_2\lambda_i] \quad (2.79)$$

For all *i* and $m = min(Mt, Nr)$. Note that the capacity at high SNR scales linearly with m. Hence, the larger the number of antenna arrays, both at transmitter and receiver, the larger the capacity.

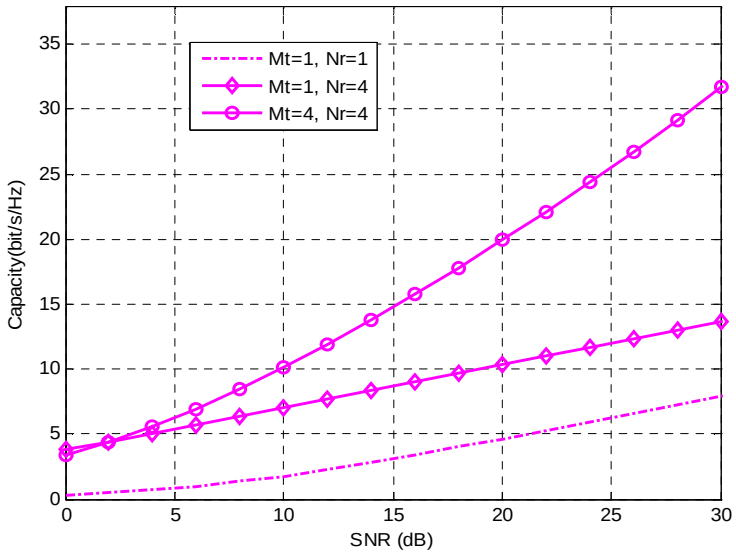

(*a*)

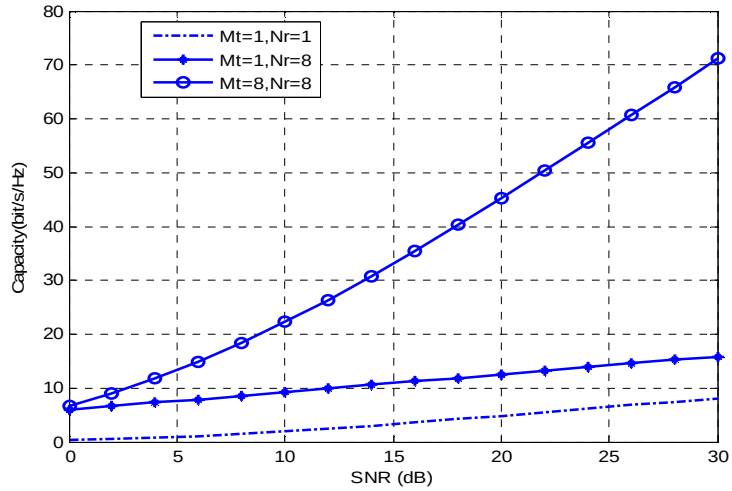

(*b*)

Figure 2.12: Capacity of an i.i.d. Rayleigh fading channel

This is shown in Figure 2.12. At low SNR regime, using the approximation $log_2(1+x) \approx log_2 e$ for small x in (2.78), we get

$$C = \sum_{i=1}^{m} E\left[log_2\left(1 + \frac{SNR}{Mt}\,\lambda_i\right)\right] \approx \sum_{i=1}^{m} \frac{SNR}{Mt} E[\lambda_i]\, log_2 e$$

$$= \frac{SNR}{Mt} E\left[Tr[HH^H]\right] log_2 e = \frac{SNR}{Mt} E\left[\sum_{i,j} |h_{ij}{}^2|\right] log_2 e$$

$$= Nr\ SNR \log_2 e \qquad (2.80)$$

It is interesting to observe here that the capacity does not depend on Mt. There is no multiplexing gain at low SNR, but there is a power gain that scales with Nr. We can conclude that at low SNR without any channel knowledge, multiple antennas at the transmitter are not useful.

Table 2.1, provides comparisons among V-BLAST, D-BLAST and Alamouti codes in terms of spectral efficiency, error probability and implementation complexity.

Scheme	Spectral Efficiency	P_e	Implementation Complexity
V-BLAST	HIGH	HIGH	LOW
D-BLAST	MODERATE	MODERATE	HIGH
ALAMOUTI	LOW	LOW	LOW

Table 2.1: V-BLAST, D-BLAST and Alamout's code Comparison

2.4 Conclusion

This chapter focused on the space time coding which benefits from the space time diversity of the MIMO channel, The main purpose of Space Time Codes is to combat the multi-path fading phenomenon of wireless channel by using multiple transmit and receive antennas and improve the reliability of reception. Space Time Block Coding (STBC) and Spatial multiplexing (SM) are promise approaches that exploit the MIMO channel to provide higher data rates and diversity gains, with no sacrifice in bandwidth.

First, the STBC was studied in flat fading channel, and has been demonstrated to be a powerful diversity technique to combat channel fading in wireless communication. The STBC uses the block encoder to achieve diversity and orthogonalisation of the channels. In particular the investigating of the Alamouti code, which offers very simple encoding/decoding and is particularly suitable for future wireless systems.

Second, the SM corresponds to the multiplicative factor by which the spectral efficiency is increased by a given scheme. A well-known example of an SM scheme is the Bell Labs Layered Space Time (BLAST) scheme. Space time layered architectures offer a big increase in capacity, promising a linear growth with the size of the antenna array under some circumstances. The more popular one is V-BLAST transmission which has optimum tradeoff between performance efficiency and computational complexity. However, suffer from error propagation and exploit the receiver diversity than transmit antenna diversity.

CHAPTER III

The Basic principles of OFDM

3.1 OFDM Systems

3.1.1 Evolution of OFDM

In classical data systems in which more data rate was sought by exploiting the frequency domain, parallel transmissions where achieved by dividing the total signal frequency band into N_c non overlapping frequency sub-channels. This technique is referred to as FDM (Frequency Division Multiplexing) [3, 58], has been used for a long time to carry more than one signal over a telephone line. FDM divides the channel bandwidth into sub-channels or sub-carrier is modulated with a separate symbol and then the N_c sub-channel are frequency multiplexed, and transmits multiple relatively low rate signals by carrying each signal on a separate carrier frequency.

A simple example of FDM is the use of different frequencies for each FM (Frequency Modulation) radio station. All stations transmit at the same time but do not interfere with each other because they transmit using different carrier frequencies. Additionally they are bandwidth limited and are spaced sufficiently far apart in frequency so that their transmitted signals do not overlap in the frequency domain. At the receiver, each signal is individually received by using a frequency tune able band pass filter to selectively remove all the signals except for the station of interest. This filtered signal can then be demodulated to recover the original transmitted information. Spectral overlap is avoided by putting enough guard space between adjacent sub-channels. In this way, inter carrier interference (ICI) is eliminated. Typically with FDM the transmission signals need to have a large frequency guard band between channels to prevent interference. This lowers the overall spectral efficiency.

This technique, however, leads to a very inefficient use of the available spectrum. A more efficient use bandwidth can be obtained with parallel transmissions if the spectra of the individual sub-channels are permitted to partly overlap. This requires that specific orthognality constraints are imposed to facilitate separation of the sub-channels at the receiver. Figure 3.1, shows the general structure of multi carrier system. The data stream $S(i)$ is converted to parallel data stream, which are modulated onto separated sub-channels. The resulting signals are summed and transmitted. At the receiver, the different sub-channels are down converted to parallel baseband signals, demodulated, and then concatenated to serial data stream.

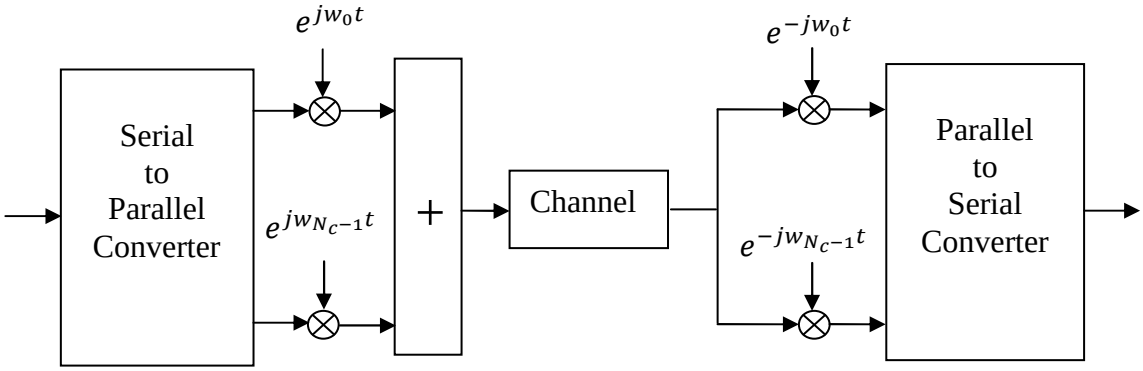

Figure 3.1: Basic structure of a multi carrier system

3.1.2 Principles of OFDM Systems

In order to solve the bandwidth efficiency problem, orthogonal frequency division multiplexing (OFDM) was proposed, where the different carriers are orthogonal to each other. However with OFDM the orthogonal packing of the sub-carriers greatly reduces this guard band, improving the spectral efficiency. With OFDM, it is possible to have overlapping sub-channels in the frequency domain, thus increasing the transmission rate. The basic functions are represented in Figure 3.2. This carrier spacing provides optimal spectral effiency.

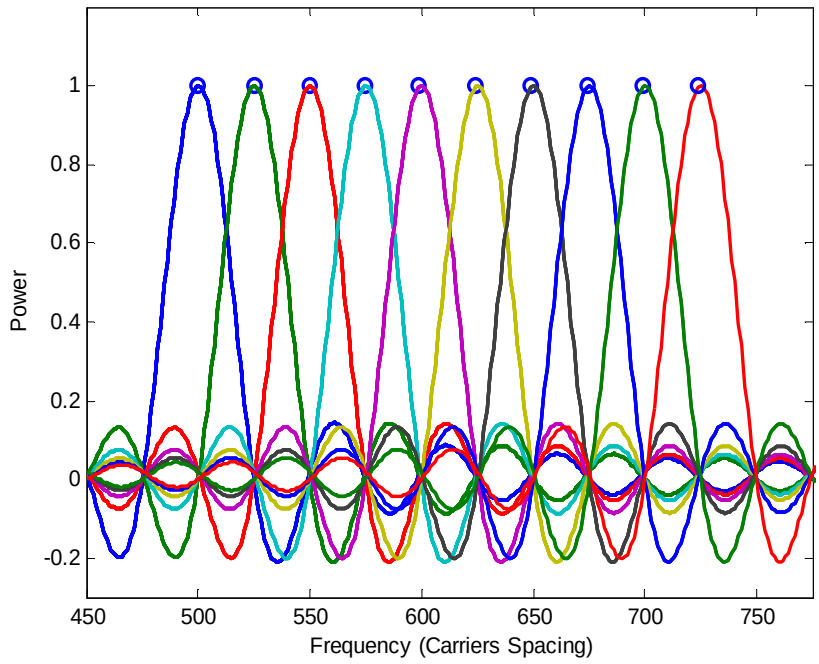

Figure 3.2: Frequency response of the sub-carriers in a 10 tone OFDM signal

OFDM is a bandwidth efficient, multi-carrier transmission technique that is tolerant to channel disturbances such as multi-path fading. OFDM combat the frequency selective fading of the channel effectively by dividing it into multiple flat fading sub-channels. The system's operational principle is that the original bandwidth is divided in a high number of narrow sub-bands, in which the mobile channel can be considered non dispersive. These OFDM systems often also termed as FDM or multi-tone systems while OFDM transmission over mobile communications channels can alleviate the problem of multi-path propagation.

The basic principle of OFDM is to split a higher rate data stream into a number of lower rate streams which are modulated on a separate sub-carrier, and transmitted simultaneously over a number of sub-carriers. Since the symbol duration increases for lower rate parallel sub-carriers, the relative amount of time dispersion caused by multi-path delay spread is decreased, making OFDM efficient in wireless propagation scenarios.

By lowering the rate of the stream, the symbol duration is increased so that it is longer compared to the delay spread of the time dispersive channel. Another way of looking at it is that by lowering the rate of the stream, the bandwidth of the sub-carrier is squeezed so that it is small compared with the coherence bandwidth of the channel, thereby making the individual sub-carriers experience flat fading, which requires simple equalization techniques [59, 60]. Hence no channel equalizer is required and instead of implementing a bank of sub-channel modems they can be conveniently implemented by the help of a single Fast Fourier Transformer (FFT). At the same time, ISI is eliminated almost completely by introducing a guard time in every OFDM symbol. In the guard time, the OFDM symbol is cyclically extended to avoid inter carrier interference (ICI). Thus OFDM effectually converts a frequency selective fading channel into a set of parallel flat fading channels. Lowering the rate of the sub-streams can be compensated for by selecting a set of orthogonal sub-carriers whose spectra overlap, but at the same time do not interfere with each other, thereby avoiding inter-channel interference [61, 62].

The orthogonality allows simultaneous transmission on a lot of sub-carriers in a tight frequency space without interfering with each other. Robustness in multi-path propagation environments is important for broadband wireless communication systems and thus OFDM is considered as a promising transmission scheme for its ability to deal with high delay spread channels. Today, OFDM has grown to be the most popular communication system in high speed communications [1, 2, 19, 63].

3.1.3 Orthogonality

Signals are orthogonal if they are mutually independent of each other. The Orthogonality is a property that allows multiple information signals to be transmitted perfectly over a common channel and detected, without interference. Loss of orthogonality results in blurring between these information signals and degradation in communications. Many common multiplexing schemes are inherently orthogonal. Time Division Multiplexing (TDM) allows transmission of multiple information signals over a single channel by assigning unique time slots to each separate information signal. During each time slot only the signal from a single source is transmitted preventing any interference between the multiple information sources. Because of this TDM is orthogonal in nature. In the frequency domain most FDM systems are orthogonal as each of the separate transmission signals are well spaced out in frequency preventing interference. Although these methods are orthogonal the term OFDM has been reserved for a special form of FDM. The sub-carriers in an OFDM signal are spaced as close as is theoretically possible while maintain orthogonality between them. OFDM achieves orthogonality in the frequency domain by allocating each of the separate information signals onto different sub-carriers. OFDM signals are made up from a sum of sinusoids, with each corresponding to a sub-carrier. The baseband frequency of each sub-carrier is chosen to be an integer multiple of the inverse of the symbol time, resulting in all sub-carriers having an integer number of cycles per symbol. As a consequence the sub-carriers are orthogonal to each other.

3.1.4 Frequency Domain Orthogonality

OFDM maximizes spectral efficiency by overlapping sub-carrier spectra while maintaining orthogonality between sub-carriers. This implies a spacing of $1/T_u$ between each sub-carrier frequency as defined in equation (3.1)

$$f_k = f_0 + \frac{k}{T_u} \quad k = 0,1,\dots,N-1 \tag{3.1}$$

Are the *N* sub-carriers which are separated by a distance of the reciprocal of the useful symbol time $T_u = T_s - T_G$, and T_s is the total symbol time.

Where T_u is the sub-carrier symbol duration. We define in equation (3.2) and (3.3) a basis of elementary signals to describe the sub-carrier symbols.

$$\psi(n) = g_k(t - nT_u) \quad n = (-\infty, \infty) \tag{3.2}$$

$$g_k(t) = \begin{cases} e^{j2\pi f_k t}, & 0 \le t < T_u \\ 0, & otherwise \end{cases} \quad (3.3)$$

The elementary signals satisfy the orthogonality condition in equation (3.4)

$$\int_{-\infty}^{\infty} \psi_k(n)\, \psi_{k'}^*(n')dt = \begin{cases} T_u, & n = n', k = k' \\ 0, & otherwise \end{cases} \quad (3.4)$$

Where (*) denotes scalar complex conjugate.

This is a result of the symbol time corresponding to the inverse of the carrier spacing. This symbol time corresponds to the inverse of the sub-carrier spacing of $1/T_{FFT}\, Hz$. The orthogonality between sub-carriers can also be demonstrated in another way. According to (3.1), each OFDM symbol contains sub-carrier signals that are non-zero over an T_u interval. Hence, the spectrum of a OFDM signal is a convolution of a group of Dirac pulses located at the sub-carrier frequencies with the spectrum of a square pulse that is one for a T_u second period and zero otherwise. This rectangular waveform in the time domain results in a *sinc* frequency response in the frequency domain. In the frequency domain each OFDM sub-carrier has a *sinc*, $sin\,(x)/x$, frequency response, as shown in Figure 3.2, The *sinc* shape has a narrow main lobe, with many side lobes that decay slowly with the magnitude of the frequency difference away from the centre. Each carrier has a peak at the centre frequency and nulls evenly spaced with a frequency gap equal to the carrier spacing. The amplitude spectrum of the square pulse is equal to $sinc(\pi f T_u)$, which has zeros for all frequencies f that are an integer multiple of $1/T_u$.

The orthogonal nature of the transmission is a result of the peak of each sub-carrier corresponding to the nulls of all other sub-carriers. The power spectrum of sub-carriers is shown in Figure 3.3 where the *sinc* spectra of individual sub-carriers are overlapped. At the maximum of each sub-carrier spectrum, all other sub-carrier spectra are zero. Because an OFDM receiver essentially calculates the spectrum values at those points that correspond to the maxima of individual sub-carriers, it can demodulate each sub-carrier free from any interference from the rest sub-carriers.

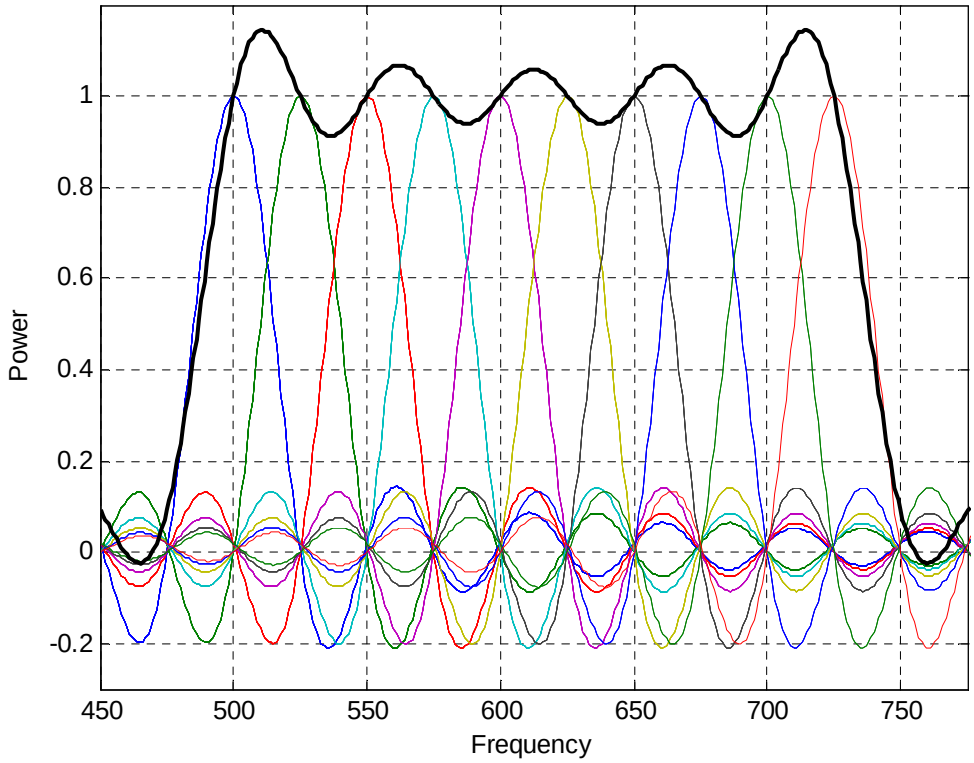

Figure 3.3: An OFDM signal with overlapped spectra

3.1.5 Spectrum efficiency η for single carrier vs. OFDM

We assume R is data rate of each sub-carrier, bandwidth defined from null to null, N sub-carriers. The spectrum efficiency η for single carrier and OFDM symbol can be defined as follows [64]:

The spectrum efficiency for single carrier is given by:

$$\eta = \frac{R}{2f_0} \tag{3.5}$$

For OFDM symbol is given by:

$$\eta = \frac{NR}{(N+1)f_0} \tag{3.6}$$

When OFDM symbol has an infinite number of sub-carriers, the spectrum efficiency can be expressed as:

$$N \longrightarrow \infty; \eta \longrightarrow \frac{R}{f_0} \tag{3.7}$$

3.1.6 Multi path Distortion

The reason that the information transmitted on the sub-carrier can be separated at the receiver is the orthogonality relation giving OFDM, its name. By using an Inverse Discrete Fourier Transform (IDFT) for modulation, the spacing of the sub-channel is implicitly chosen in such a way that, at the frequencies where the received signals are evaluated (at peaks of the *sinc* functions in Figure 3.2), all other signals are zeros. In order for this orthogonality to be preserved, the following must be true:

1. The receiver and the transmitter must be accurately synchronized. This means they both must have exactly the same modulation frequency and the same time scale for transmission.
2. The analogue components', part of transmitter and receiver, must be very high quality.
3. There should be no multi path channel.

In OFDM the system bandwidth is broken up into N_c sub-carriers, resulting in a symbol rate that is N_c times lower than the single carrier transmission. This low symbol rate makes OFDM naturally resistant to effects of ISI caused by multi-path propagation. Unfortunately, multi-path distortion is almost unavoidable in radio communication system.

Multi-path propagation is caused by the radio transmission signal reflecting of objects in the propagation environment, such as walls, buildings, mountains, etc. These multiple signals arrive at the receiver at different times due to the transmission distances being different. In an OFDM system, the channel has a finite impulse response. We note τ_{max} the maximum delay of all reflected paths of the OFDM transmitted signal. This spreads the symbol boundaries causing energy leakage between them, and, thus, the received signal is affected. The truncated sub-channel sinusoids are delayed by different amounts (i.e. channel delays), the distortion is mainly concentrated at the on off transmissions of these waveforms.

In an OFDM signal the amplitude and phase of the sub-carrier must remain constant over the period of the symbol in order for the sub-carriers to maintain the orthogonality. If they are not constant it means that the spectral shape of the sub-carriers will not have the correct *sinc* shape, and thus the nulls will not be at the correct frequencies, resulting in ICI. At the symbol boundary the amplitude and phase change suddenly to the new value required for the next data symbol. Hence, a guard space (in frequency), and a guard time by means of cyclic prefix (CP), chosen longer than the maximal delay spread. However**,** the length of the OFDM

symbol cannot be increased indefinitely. Hence, a guard interval, or a CP of time duration, T_G or G, samples is inserted in front of the OFDM symbol.

The length of this CP should be ideally greater than or equal to the maximum delay spread of the channel. As long as the CP has a duration greater than τ_{max}, it would maintain orthogonality between the sub-carriers and eliminate most interference among channels. (i.e, ICI and between adjacent transmission blocks (i.e., ISI) at a cost of a rate loss and power loss by a factor proportional to $G/(N+G)$.

3.1.7 Guard Period

Cyclic prefix is a crucial feature of OFDM to combat the effect of multi-path. The CP, in general, is chosen equal to the last part of the OFDM symbol and, therefore, often is referred to as cyclic extension. The effect of ISI on an OFDM signal can be further improved by the addition of a guard period (Guard interval: GI) to the start of each symbol. This guard period is a cyclic copy that extends the length of the symbol waveform.

Each sub-carrier, in the data section of the symbol, (i.e. the OFDM symbol with no CP) has an integer number of cycles. Because of these placing copies of the symbol end to end results in a continuous signal, with no discontinuities at the joins. Thus by copying the end of a symbol and appending this to the start results in a longer symbol time. Figure 3.4 shows the insertion of a guard period.

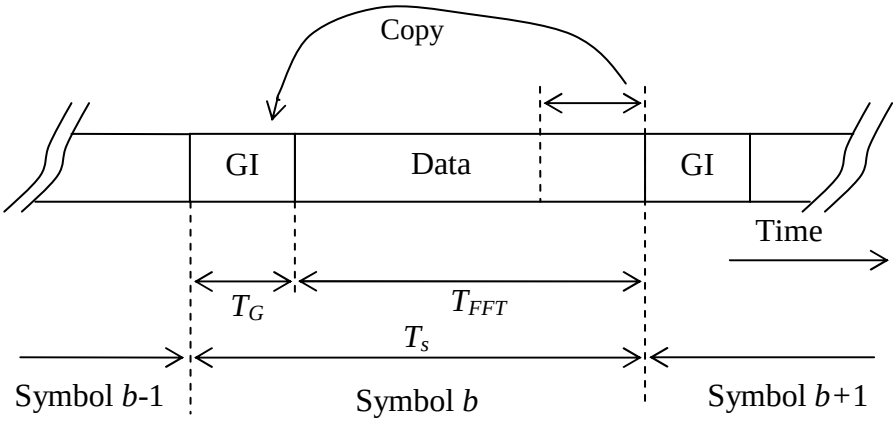

Figure 3.4: Addition of a Guard period to an OFDM signal

The total length of the symbol is $T_s = T_G + T_{FFT}$, where T_s is the total length of the symbol in samples, T_G is the length of the guard period in samples, and T_{FFT} is the size of the IFFT used to generate the OFDM signal.

In addition to protecting the OFDM from ISI, the guard period also provides protection against time offset errors in the receiver as shown in Figure 3.5. However, in order to preserve the orthogonality property, that the guard period is longer than the delay spread of the radio channels. As shown below, once the above condition is satisfied, there is no ISI since the previous symbol will only have effect over samples within $[0, \tau_{max}]$. And it is clear that the orthogonality is maintained so that there is no ICI.

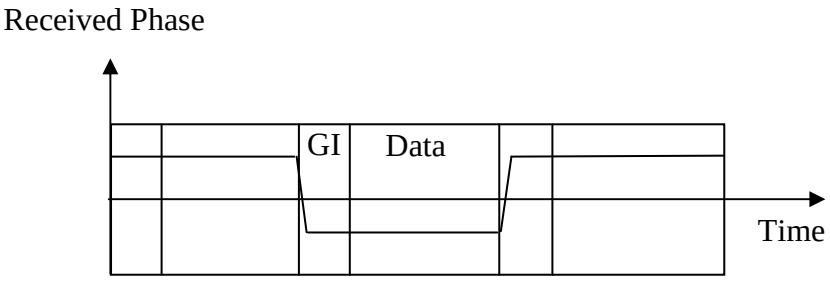

Figure 3.5. (*a*): Function of the guard period for protecting against ISI, in Propagation environment with no multi-path

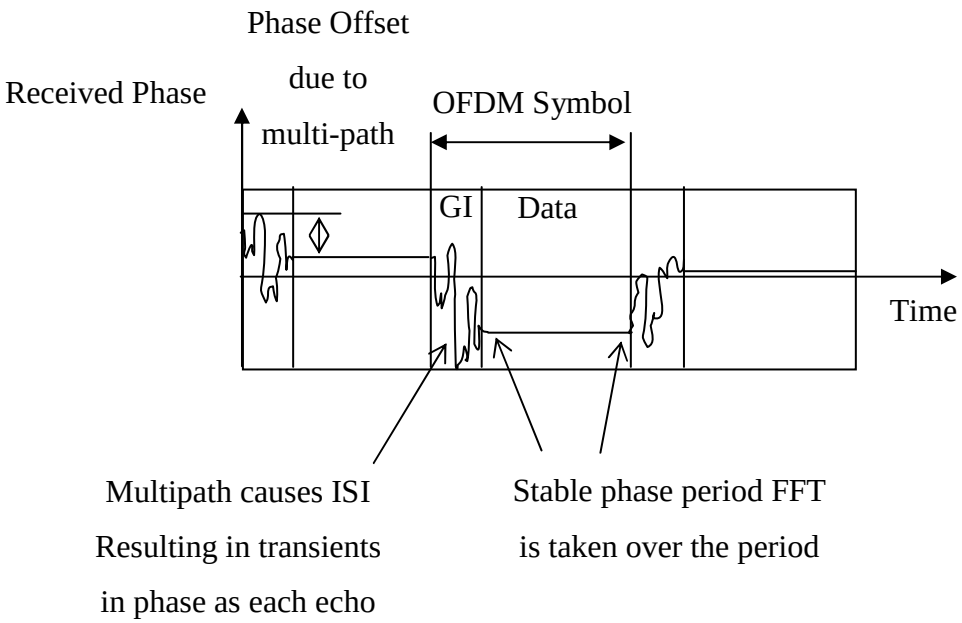

Figure 3.5. (*b*): Function of the Guard period for protecting against ISI, in propagation environment with multi-path .

To avoid out of band radiation the on off transitions must be smoothened. This can be implemented by, e.g., windowing each OFDM symbol by a raise cosine window. Figure 3.6 depicts schematically the implementation of windowing in OFDM symbol.

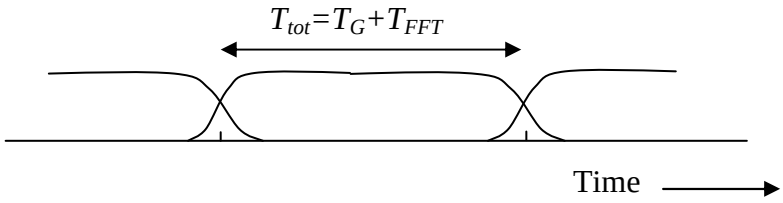

Figure 3.6: The principle of windowing

The validity of windowing each OFDM symbol by a raised cosine window can be explained by looking to the shapes of the sub-carriers sinusoids after the multi-path fading channel. An OFDM receiver uses only a part of this signal to calculate the FFT. This part should be chosen such that in this FFT interval with a length of T_{FFT} seconds, which at the Nyquist rate equals $N_c T_s$ seconds, every sub-carrier has an integer number of cycles, which ensures orthogonality. In the multi-path fading channel, the receiver input signal will be a sum of delayed and scaled replicas of the transmitted sub-carriers, Figure 3.6. Note that a sum of scaled and delayed sinusoid is a gain a sinusoid. So, as long as the larger than the maximal channel delay we can choose the window for applying the FFT such that there will still be an integer number of cycles within this FFT interval for each multi-path component keeping the reflections of previous symbols out and preserving the orthogonality.

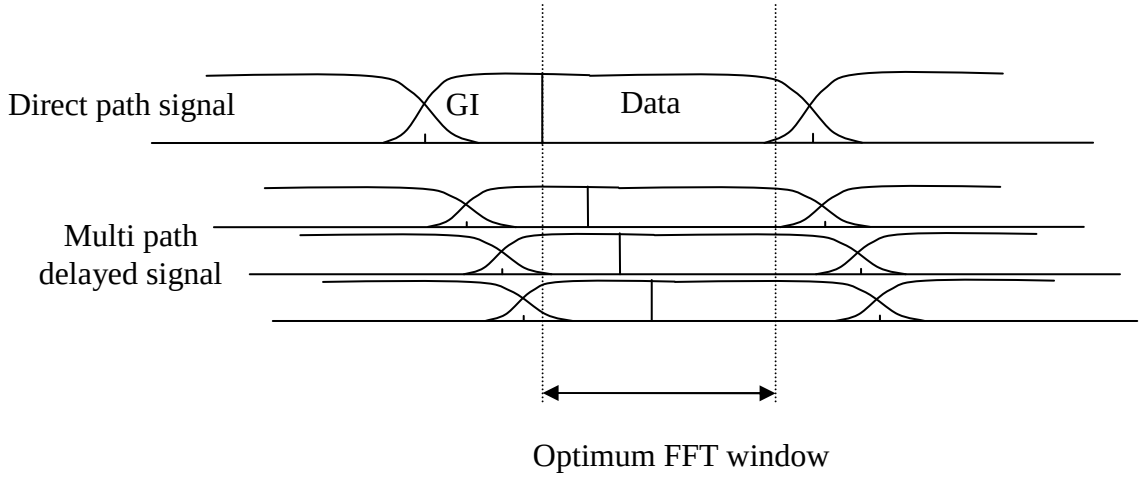

Figure 3.7: An OFDM symbol with cyclic prefix

So, thank to the guard interval and windowing, the wideband multi-path fading is experienced in OFDM as set of narrowband fading sub-carriers without ICI and ISI. The only remaining effect of multi-path is a random phase and amplitude per sub-carrier. This effect can be minimized by correcting the sub-carriers of the received signal with reference amplitudes and phases, i.e., channel estimates, per sub-carrier, which can be obtained during a training phase. The sub-carriers in deep fades still are a problem but in order to deal with these weak sub-carriers that have a large probability to be detected erroneously, forward error correction across the sub-carriers can be applied.

3.1.8 OFDM Transceiver

The transmitter section as shown in Figure 3.8.(*a*), converts digital data to be transmitted, into a mapping of sub-carrier amplitude and phase. The system maps the input bits into complex valued symbols $X(k)$ in the modulation block, which determines the constellation scheme of each sub-carrier. Data to be transmitted is typically in the form of a serial data stream. So a serial to parallel conversion stage is needed to convert the input serial stream to the data to be transmitted in each OFDM symbol. In an OFDM system, the data are modulated onto different sub-carriers and sent in blocks. It then transforms this spectral representation of the data into the time domain using an IDFT. The IFFT performs the same operations as an IDFT, except that it is much more computationally efficiency, and so is used in all practical systems.

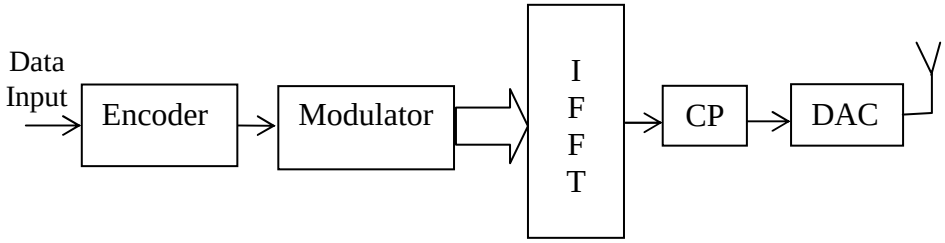

(*a*).Transmitter structure

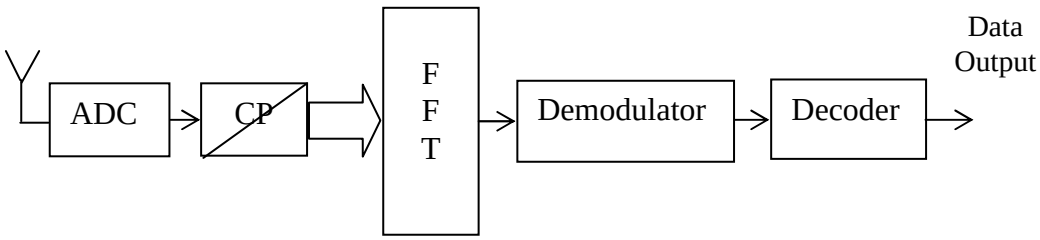

(*b*).Receiver structure

Figure 3.8: Block diagram of an OFDM system.

Figure 3.9 shows the IFFT section of the OFDM transmitter. In the frequency domain, before applying the IFFT, each of the discrete samples of the IFFT corresponds to an individual sub-carrier. Most of the sub-carriers are modulated with data. The IFFT block modulates $X(k)$ onto N orthogonal sub-carriers, a cyclic prefix is added to the multiplexed output of the IFFT before it is transmitted through a fading channel as shown in Figure 3.8.(a), the cyclic extension is chosen to be longer than the impulse response to avoid inter block interference and preserve orthogonality of the sub-channels.

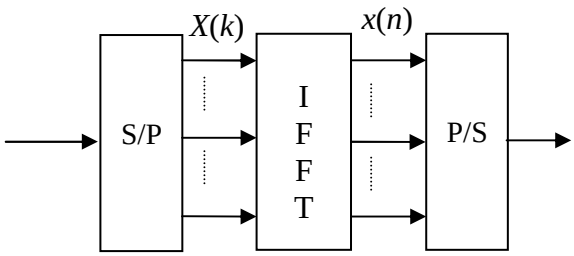

Figure 3.9: OFDM generation, IFFT stage

Therefore, we assume the channel to have finite impulse response (FIR). For simple notation, we denotes $N_c = N = N_{FFT}$.

Suppose the data set to be transmitted is

$$X_k(b) = [x_1(b), x_2(b), \dots\dots\dots, x_N(b)]^T \qquad (3.8)$$

Where N is the total number of sub-carriers. And b is the number of the OFDM block sub-carriers. The discrete time representation of OFDM symbols, where $t = nT$ and select $f_0 = 1/NT$ of the signal after IFFT is:

$$S(t = nT) = S(n) = \frac{1}{\sqrt{N}} \sum_{n=0}^{N-1} X_k \exp\left(\frac{j2\pi nk}{N}\right), \qquad n = 0 \dots\dots\dots N-1 \qquad (3.9)$$

Where $S(b) = [s_1(b), s_2(b), \dots, s_N(b)]^T$ is the time domain of the b^{th} OFDM block.

We can rewrite the equation () by using matrix representation, the resulting N point time domain signal is given by

$$S(n) = F^H X_k \qquad (3.10)$$

Where F is $(N \times N)$ FFT matrix of the (m, n) is given by

$$F_{m,n} = \frac{1}{\sqrt{N}} \exp\left(-j2\pi \frac{(m-1)(n-1)}{N}\right), \qquad (n, m = 0 \dots\dots\dots N-1) \qquad (3.11)$$

So F^H represent $(N \times N)$ IFFT matrix.

The cyclic prefix T_G (guard interval) is inserted to maintain the orthogonality between signals at different sub-carriers and consecutive OFDM blocks. Hence the total duration of an OFDM block is $T_s = T_{FFT} + T_G$. Where $T_{FFT} = 1/\Delta f$ is the IFFT/FFT period, and $\Delta f = B/N$ is the sub-carrier spacing, B is the total bandwidth, and N is the total number of sub-carriers. With the insertion of CP, the received signal is complete free of ISI during $0 < t < T_{FFT}$, if the maximum delay of the channel impulse response is less than T_G. A cyclic prefix is then added to the multiplexed output of IFFT. The obtained signal is then converted to a time continuous analog signal before it is transmitted through the selective fading channel.

The receiver structure, as shown in Figure 3.8. (*b*), performs the reverse operation of the transmitter, mixing the RF (Radio frequency) signal to base band for processing, then using a Fast Fourier Transform (FFT) to analyze the signal in the frequency domain. The amplitude and phase of the sub-carriers is then picked out and converted back to digital data. Thus, at the receiver, the signals at different sub-carriers can be separated by FFT of the received signal after the part during the guard interval is discarded. The data is recovered by performing FFT on the received signal $y(n)$.

$$Y_k = \frac{1}{\sqrt{N}} \sum_{n=0}^{N-1} y(n) \exp\left(-\frac{j2\pi nk}{N}\right), \qquad k = 0 \dots \dots \dots N-1 \tag{3.12}$$

We can rewrite the equation (3.12) by using matrix representation, the resulting frequency domain signal is given by

$$Y_k = F\, y(n) \tag{3.13}$$

When the orthogonality is satisfied, i.e.[64]

$$\sum_{n=0}^{N-1} \exp\left(-\frac{j2\pi nk}{N}\right) \exp\left(\frac{j2\pi nk'}{N}\right) = \delta(k-k') \tag{3.14}$$

A N point FFT only requires $Nlog(N)$ multiplications, which is much more computationally efficient than an equivalent system with equalizer in time domain [58].

The insertion of cyclic prefix converts the linear convolution of the channel impulse response with the transmitted signal to cyclic convolution. Therefore, assuming the channel response stays constant during each OFDM block, the channel frequency response for the *k*-th sub-carrier during the OFDM block is

$$H(k) = \sum_{l=0}^{L-1} h_l \exp(-j2\pi k \Delta f \tau_l) \tag{3.15}$$

The channel frequency response over the *k*-th sub-carrier is given by where $k = 1,2, \ldots, N$. And τ_l and h_l are the delay and complex amplitude matrix of the lth path between transmitters and receivers respectively. Δf is the sub-carrier separation in the frequency domain. From above expressions the sub-carrier waveforms are now given by

$$s(n) = \frac{1}{\sqrt{N}} \sum_{k=0}^{N-1} X(k) \exp\left(\frac{j2\pi nk}{N}\right) \qquad k = 0,1, \ldots N-1 \tag{3.16}$$

The idea behind this is to convert the linear convolution (between signal and channel response) to a circular convolution as shown in Figure 3.10. In this way, the FFT of circularly convolved signals is equivalent to a multiplication in the frequency domain [58]. However, in order to preserve the orthogonality property, τ_{max} should not exceed the duration of the time guard interval. As shown below, once the above condition is satisfied, there is no ISI since the previous symbol will only have effect over samples within $[0, \tau_{max}]$. And it is clear that orthogonality is maintained so that there is no ICI.

Figure 3.10: Linear to circular convolution conversion

$$\begin{aligned} r(n) &= s(n) \otimes h(n) + e(n) \quad k = 0,1, \ldots, N-1 \\ Y(k) &= DFT\big(y(n)\big) = DFT(IDFT\big(X(k)\big) \otimes h(n) + e(n)) \\ Y(k) &= X(k).DFT\big(h(n)\big) + DFT\big(e(n)\big) \\ &= X(k).H(k) + E(k) \end{aligned} \tag{3.17}$$

Where $\otimes$ denotes circular convolution and $E(k) = DFT\big(e(n)\big)$. Another advantage with the cyclic prefix is that it serves as a guard between consecutive OFDM frames. This is similar to adding guard bits, which means that the problem with inter frame interference also will disappear.

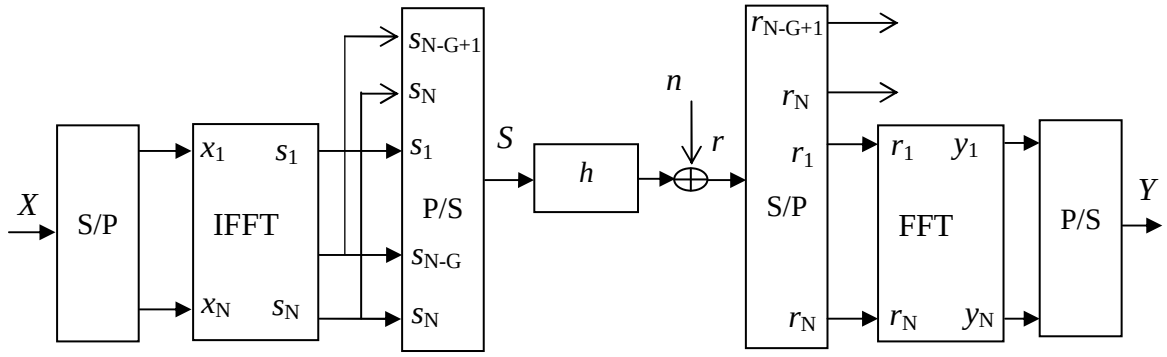

Figure 3.11: OFDM Modulation and Demodulation

At the transmitter side after the serial to parallel conversion and applying the IFFT operation, the CP is added as shown in Figure 3.11, it should be greater than the delay spread of the channel, the symbol vector to be transmitted can be expressed as:

$$\begin{aligned}\bar{s}(b) &= [\bar{s}_1(b) \dots . \bar{s}_N(b)\bar{s}_{N+1}(b) \dots \bar{s}_{N+G}(b)]^T \\ &= [s_{N-G+1}(b) \dots s_N(b)s_1(b) \dots s_N(b)]^T \end{aligned} \quad (3.18)$$

We assume that the frequency selective Rayleigh fading channel is constant during each OFDM block (quasi-static, i.e., the fading coefficients are constant over the transmission of one packet), and vary from block to another, and the noise be neglected. The received signal can be written as follows:

$$\begin{bmatrix} \bar{r}_1(b) \\ \bar{r}_2(b) \\ \vdots \\ \vdots \\ \bar{r}_{N+G}(b) \end{bmatrix} = \begin{bmatrix} h_{L-1} & \cdots & h_0 & 0 & \cdots & \cdots & \vdots \\ 0 & h_{L-1} & \cdots & h_0 & \ddots & \cdots & \vdots \\ \vdots & \ddots & \ddots & \ddots & \ddots & \ddots & \vdots \\ \vdots & \ddots & \ddots & \ddots & \ddots & \ddots & 0 \\ \vdots & \cdots & \cdots & 0 & h_{L-1} & \cdots & h_0 \end{bmatrix} \cdot \begin{bmatrix} \bar{s}_{N-G-L+1}(b-1) \\ \vdots \\ \bar{s}_{N+G}(b-1) \\ \bar{s}_1(b) \\ \vdots \\ \bar{s}_{N+G}(b) \end{bmatrix} \quad (3.19)$$

At the receiver side the CP is removed as shown in Figure 3.11, and the signal vector r can be expressed as:

$$r(b) = \begin{bmatrix} r_1(b) \\ \vdots \\ \vdots \\ \vdots \\ r_N(b) \end{bmatrix} = \begin{bmatrix} \bar{r}_{G+1}(b) \\ \vdots \\ \vdots \\ \vdots \\ \bar{r}_{N+G}(b) \end{bmatrix}$$

$$= \begin{bmatrix} h_{L-1} & \cdots & h_0 & 0 & \cdots & \cdots & \vdots \\ 0 & h_{L-1} & \cdots & h_0 & \ddots & \cdots & \vdots \\ \vdots & \ddots & \ddots & \ddots & \ddots & \ddots & \vdots \\ \vdots & \ddots & \ddots & \ddots & \ddots & \ddots & 0 \\ \vdots & \cdots & \cdots & 0 & h_{L-1} & \cdots & h_0 \end{bmatrix} . \begin{bmatrix} \bar{s}_{G-L+1}(b-1) \\ \vdots \\ \vdots \\ \vdots \\ \vdots \\ \bar{s}_{N+G}(b) \end{bmatrix} \quad (3.20)$$

We can rewrite $r(b)$ by using the cyclic character of $\bar{s}(b)$, as follows:

$$r(b) = \begin{bmatrix} h_0 & 0 & \cdots & 0 & 0 & h_{L-1} & \cdots & h_1 \\ h_1 & h_0 & 0 & \ldots & 0 & 0 & \ddots & \vdots \\ \vdots & h_1 & h_0 & 0 & \cdots & 0 & 0 & h_{L-1} \\ h_{L-1} & \vdots & h_1 & \ddots & h_0 & \ldots & 0 & 0 \\ 0 & h_{L-1} & \vdots & \ddots & \ddots & 0 & \cdots & 0 \\ \vdots & 0 & h_{L-1} & \vdots & \ddots & \ddots & 0 & \vdots \\ 0 & \vdots & \vdots & \ddots & \vdots & \ddots & \ddots & 0 \\ 0 & 0 & 0 & 0 & h_{L-1} & \ldots & h_1 & h_0 \end{bmatrix} . \begin{bmatrix} s_1(b) \\ \vdots \\ \vdots \\ \vdots \\ \vdots \\ \vdots \\ \vdots \\ s_N(b) \end{bmatrix} \quad (3.21)$$

The received signal can be expressed as follows:

$$r(b) = H\, S(b) \quad (3.22)$$

According to the guard intervals properties, the channel matrix is circular, we can perform the FFT of $r(b)$, the frequency signal domain $Y(b)$ can be expressed as:

$$Y(b) = F.H.F^H.X(b) \quad (3.23)$$

The matrix $F.H.F^H$ is the frequency channel expression, where the circular matrices are diagonal in the frequency domain.

$$Y(b) = \begin{bmatrix} \widetilde{H}_1 & 0 & \cdots & 0 \\ 0 & \ddots & \ddots & \vdots \\ \vdots & \ddots & \ddots & 0 \\ 0 & \cdots & 0 & \widetilde{H}_N \end{bmatrix} . X(b) \quad (3.24)$$

Where $\widetilde{H}_k$ are the channel frequency responses given by:

$$\widetilde{H}_k = \sum_{l=0}^{L-1} h_l \exp\left(-j2\pi lk/N\right) \quad (3.25)$$

We can write the frequency received signal, for *k*-th sub-carrier and *b*-th symbol block as:

$$Y_k(b) = \widetilde{H}_k . x_k(b) + n_k(b) \quad (3.26)$$

Where n_k is the AWGN noise vector with variance σ_n^2, where $n_k \sim (0, \sigma_n^2)$.

3.2 MIMO OFDM

Future wireless systems require high data rates. Conventional systems are limited by ISI due to frequency selectivity of the wireless channel. By sending information in parallel with larger symbol durations, OFDM systems avoid the ISI significantly. OFDM is a multi-carrier transmission scheme that is well recognized for its potential for attaining high rate transmission over frequency selective channels. OFDM is thus a promising candidate for mobile broadband wireless and has already been adopted in many high rate wireless communications standards such as DAB/DVB-T, 802.11 WLAN, 802.16 WMAN etc. SM have been used providing a data rate increase. The system includes de-multiplexing and multiplexing units (no coding) with the effect that the information stream is split into multiple parallel systems, which are independently encoded and transmitted simultaneously from the multiple antennas, the data rate can be further increased via the exploitation of the MIMO technique.

MIMO technology can be used to improve further OFDM systems in terms of spectrum efficiency/capacity, link reliability and coverage. Given an arbitrary wireless communication system, we consider a link for which the transmitter and the receiver are equipped with multiple antenna elements. The basic idea of MIMO is that the signals on the transmit antennas and the receive antennas are combined in such a way that the QOS (bit error ratio - BER) or the capacity (bits per second - *bps*) will be improved. We will focus on spatial multiplexing systems, that offer a linear (in the number of transmit-receive (T_X-R_X) antenna pairs or $min\,(Mt, Nr)$) increase in the capacity for the same bandwidth and with no additional power expenditure. MIMO offers additional parallel channels in spatial domain to boost the data rate [42]. The combination of MIMO and OFDM, Hence, MIMO OFDM is a promising combination for the high data requirement of future wireless systems [1, 2, 8, 18, 63].

3.2.1 MIMO OFDM Transceiver

For a MIMO OFDM system with Mt transmit and Nr receive antennas, as shown in Figure 3.12. (*a*) and (*b*), we show the transmitter and receiver structure of the MIMO OFDM system. The information bits are modulated with a selected constellation. The modulation symbols will then go through the MIMO block and be mapped to different spatial streams. After that, the data on each spatial stream are OFDM modulated and transmitted the frequency selective channel. In other words, the duplication is repeated in the next OFDM symbol rather than the next sub-carrier frequency. The operations of the OFDM modulation and demodulation are shown in Figure 3.12.

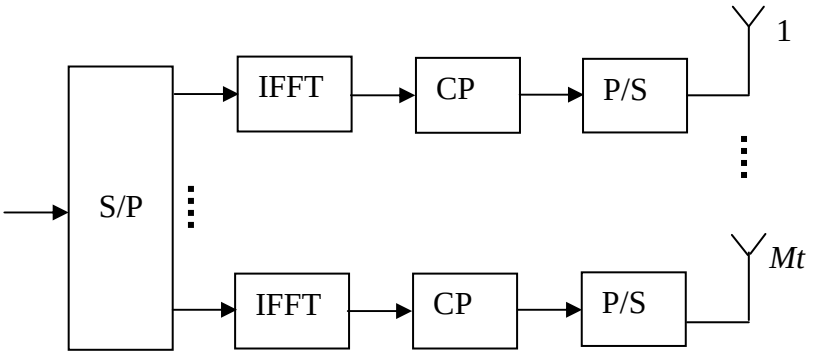

(*a*). Transmitter structure

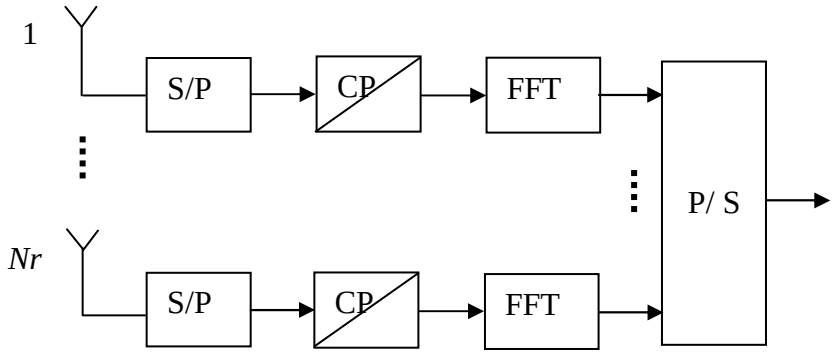

(b).Receiver structure

Figure 3.12: System diagram of a MIMO OFDM with Mt transmit and Nr receive antennas.

Each spatial stream goes through a serial to parallel (S/P) conversion and the IFFT block to convert the frequency domain signals into time domain. The time domain signal then goes through the parallel to serial (P/S) conversion and is appended with a CP. The length of the CP has to be longer than the delay spread of the multi-path channel in order to preserve the orthogonality among the sub-carriers of an OFDM symbol. At the receiver, a reverse process is implemented, i.e. the CP is removed after the timing synchronization is achieved, and FFT operation is performed to convert the time domain signals into frequency domain. The MIMO detection is then carried out in the frequency domain for each sub-carrier.

The MIMO OFDM system breaks the modulated symbols $X(k)$ and de-multiplexed into Mt sub-streams, with N time period sub-carrier of OFDM symbols. Denotes X_i symbol vector $N \times 1$, corresponding N sub-carriers to be transmitted from antenna $i, i = 1, .., Mt$.

Let be the modulated data matrix $Mt \times N$:

$$X = [X_1^T, X_2^T, \dots\dots, X_{Mt}^T]^T \tag{3.27}$$

Each sub-stream goes through an OFDM modulator and performing the IFFT operation at each transmit antenna to make Mt OFDM symbols, the CP is inserted to each OFDM symbol to avoid ISI due to channel delay spread. The transmitted time domain is given by:

$$s_i = F^H X_i \tag{3.28}$$

$$x_i = [s_i(G - L + 1) \dots . s_i(N) s_i(1) \dots .. s_i(N)] \tag{3.29}$$

At the receiver, the received signal at the *j*-th receive antenna is the superposition of all Mt transmitted OFDM blocks going through channel plus noise.

$$r_j = \sqrt{\frac{Es}{Mt}} \sum_{i=1}^{Mt} \tilde{h}_{j,i}\ x_i + n_j \qquad j = 1, \dots .., Nr \tag{3.30}$$

The equation (4.7) in expanded form can be represented by following matrix form:

$$\begin{bmatrix} r_1^j \\ r_2^j \\ . \\ . \\ : \\ . \\ r_{N+T_G}^j \end{bmatrix} = \sum_{i=1}^{Mt} \left[\begin{bmatrix} h_0^{ji} & 0 & \cdots & & & & & \\ h_1^{ji} & h_0^{ji} & 0 & 0 & 0 & 0 & 0 & 0 \\ \vdots & h_1^{ji} & h_0^{ji} & \dots & 0 & 0 & 0 & 0 \\ h_{L-1}^{ji} & \vdots & h_1^{ji} & 0 & \cdots & \cdots & \cdots & \vdots \\ 0 & h_{L-1}^{ji} & \vdots & \ddots & 0 & \cdots & \cdots & \vdots \\ \vdots & 0 & h_{L-1}^{ji} & \ddots & \ddots & 0 & \cdots & \vdots \\ 0 & \vdots & \vdots & \ddots & \vdots & \ddots & \ddots & 0 \\ 0 & 0 & 0 & 0 & h_{L-1}^{ji} & \cdots & h_1^{ji} & h_0^{ji} \end{bmatrix} . \begin{bmatrix} x_1^i \\ x_2^i \\ . \\ . \\ : \\ . \\ x_{N+G}^i \end{bmatrix} \right] + \begin{bmatrix} n_1^j \\ n_2^j \\ . \\ . \\ : \\ . \\ n_{N+G}^j \end{bmatrix} \tag{3.31}$$

We can rewrite the received vector r_j by using the cyclic character of s_i, as follows:

$$r_j = \sqrt{\frac{Es}{Mt}} \sum_{i=1}^{Mt} h_c^{j,i}\ s_i + n_j \qquad j = 1, \ldots\ldots, Nr \tag{3.32}$$

$$\begin{bmatrix} r_1^j \\ r_2^j \\ . \\ . \\ : \\ . \\ r_N^j \end{bmatrix} = \sum_{i=1}^{Mt} \begin{bmatrix} h_0 & 0 & \cdots & 0 & 0 & h_{L-1} & \cdots & h_1 \\ h_1 & h_0 & 0 & \ldots & 0 & 0 & \ddots & \vdots \\ \vdots & h_1 & h_0 & 0 & \cdots & 0 & 0 & h_{L-1} \\ h_{L-1} & \vdots & h_1 & \ddots & h_0 & \cdots & 0 & 0 \\ 0 & h_{L-1} & \vdots & \ddots & \ddots & 0 & \cdots & 0 \\ \vdots & 0 & h_{L-1} & \vdots & \ddots & \ddots & 0 & \vdots \\ 0 & \vdots & \vdots & \ddots & \vdots & \ddots & \ddots & 0 \\ 0 & 0 & 0 & 0 & h_{L-1} & \ldots & h_1 & h_0 \end{bmatrix} \begin{bmatrix} s_1^i \\ s_2^i \\ . \\ . \\ : \\ . \\ s_N^i \end{bmatrix} + \begin{bmatrix} n_1^j \\ n_2^j \\ . \\ . \\ : \\ . \\ n_N^j \end{bmatrix} \tag{3.33}$$

The circular matrix $N \times N$, satisfy:

$$h_c^{j,i} = F^H\ \Omega_{j,i}\ F \tag{3.34}$$

$$\Omega_{j,i} = diag\left(H_{j,i}(1), H_{j,i}(2), \ldots . H_{j,i}(N)\right) \tag{3.35}$$

The channel frequency domain is given by:

$$H_{j,i}(k) = \sum_{l=0}^{L-1} h_{(j,i)}(l)\ e^{-j\,2\,\pi\frac{kl}{N}} \tag{3.36}$$

We can rewrite the equation (3.33) as follows:

$$r_j = \sqrt{\frac{Es}{Mt}} \sum_{i=1}^{Mt} F^H\ \Omega_{j,i}\ F \quad s_i + n_j \qquad j = 1, \ldots\ldots, Nr \tag{3.37}$$

After removing CP and FFT transformation by OFDM demodulator, the received signal in frequency domain at each receive antenna j can be represented by equation (3.37).

$$\begin{aligned} y_j\ &=\ F\ r_j \\ &= \sqrt{\frac{Es}{Mt}} \sum_{i=1}^{Mt} F\ F^H\ \Omega_{j,i}\ \ F\ s_i + F\ n_j \qquad j = 1, \ldots\ldots, Nr \\ &= \sqrt{\frac{Es}{Mt}} \sum_{i=1}^{Mt} F\ F^H\ \Omega_{j,i}\ F\ \ F^H\ X_i + F\ n_j \qquad j = 1, \ldots\ldots, Nr \\ &= \sqrt{\frac{Es}{Mt}} \sum_{i=1}^{Mt} \Omega_{j,i}\ \ X_i + v_j \end{aligned} \tag{3.37}$$

Since F is an orthogonal matrix, and the matrices $\Omega_{j,i}$ are diagonal, we can write the k-th component of y_j as follows:

$$y_j(k) = \sqrt{\frac{Es}{Mt}} \sum_{i=1}^{Mt} H_{j,i}(k)\ X_i(k) + v_j(k) \quad k = 1, \ldots\ldots, N \tag{3.38}$$

$$y_j(k) = \sqrt{\frac{Es}{Mt}}\, \bar{H}_j(k) X_i(k) + v_j(k) \quad k = 1, \ldots\ldots, N \tag{3.39}$$

Where $X_i(k)$ is the Mt transmitted symbols, at the k-th sub-carrier. And $\bar{H}_j(k)$ are the channel coefficient gains at the k-th sub-carrier.

$$X_i(k) = [X_1(k), X_2(k), \ldots\ldots, X_{Mt}(k)]^T \tag{3.40}$$

$$\bar{H}_j(k) = \left[h_{j,1}(k), h_{j,2}(k), \ldots\ldots, h_{j,Mt}(k)\right] \tag{3.41}$$

The resulting of the Nr receive signal vector, can be represented by the following model:

$$\begin{bmatrix} y_1(k) \\ \vdots \\ y_{Nr}(k) \end{bmatrix} = \sqrt{\frac{Es}{Mt}} \begin{bmatrix} \bar{H}_1(k) \\ \vdots \\ \bar{H}_{Nr}(k) \end{bmatrix} X_i(k) + \begin{bmatrix} v_1(k) \\ \vdots \\ v_{Nr}(k) \end{bmatrix} \tag{3.42}$$

$$y(k) = \sqrt{\frac{Es}{Mt}}\, \bar{H}(k) X_i(k) + v(k) \quad k = 1, \ldots\ldots, N \tag{3.43}$$

From the equation (3.43), the frequency selective MIMO channel is decoupled into N parallel flat fading channels. We consider all the N tone sub-carrier; the all received signal can be express as:

$$y = \sqrt{\frac{Es}{Mt}}\, \bar{H} X_i + w \tag{3.44}$$

$$\bar{H} = \begin{bmatrix} \bar{H}(0) & 0 & \cdots & 0 \\ 0 & \bar{H}(1) & \cdots & \vdots \\ \vdots & \vdots & \ddots & 0 \\ 0 & \cdots & 0 & \bar{H}(N) \end{bmatrix} \tag{3.45}$$

If the frequency selective Rayleigh fading channel is constant during each OFDM block (quasi-static, i.e., the fading coefficients are constant over the transmission of an OFDM symbol), then

$$\bar{H}(1) = \bar{H}(2) = \cdots = \bar{H}(N) = H \tag{3.46}$$

The overall received signal can be written as:

$$Y = \sqrt{\frac{Es}{Mt}}\, HX + W \tag{3.47}$$

3.2.2 Capacity Calculations

Considering the channel that is unknown at the transmitter and perfectly known at the receiver, the open loop capacity of MIMO OFDM channel is the mean over all frequency subcarriers defined in [10, 66]. For large number of random channels, the mean and outage capacity can be calculated using (3.48) given by.

$$C = \frac{1}{N_c}\sum_{k=1}^{N_c} log_2\left(I_{Nr} + \frac{SNR}{Mt} H_k H_k^H\right) \qquad (3.48)$$

Where $SNR = Es/2\sigma_n^2$ and H_k is the $Nr \times Mt$ channel matrix at the *k*-th sub-carrier block index.

3.3 MIMO STBC OFDM Schemes

Recent researches results have shown that the adverse effects of the wireless propagation environment can be significantly reduced by employing multiple transmit and receive antennas, resulting in MIMO communication systems.

Traditional space time codes were designed to extract spatial diversity from a flat fading MIMO channel, and are not generally effective at extracting the additional frequency diversity of a frequency selective fading channel. Combining MIMO systems with OFDM modulation, MIMO-OFDM systems have been proposed, and two coding approaches have been suggested for such systems: Space frequency (SF) coding [10,17,67,68], to exploit the spatial and frequency diversities, and space time (ST) coding [11,69,70,71], to exploit the spatial, temporal, diversities available in frequency selective MIMO channels. Both ST and SF have proven to be effective techniques in enhancing the error performance and increasing the capacity of wireless channels.

In multi-path MIMO channels, the maximum achievable diversity order is the product of the number of transmit and receive antennas and the number of resolvable propagation paths (i.e., the number of nonzero channel taps) [63,72]. To achieve this full diversity requires that the information symbols be carefully spread over the tones as well as over the transmitting antennas. One advantage in using SFBC instead of STBC is that, in SFBC, the coding is done across the sub-carriers inside one OFDM symbol duration, while STBC applies the coding across a number of OFDM symbols equal to number of transmit antennas, thus, an inherent processing delay is unavoidable in STBC.

3.3.1 Space Time Block Code OFDM

The encoding of each user data is done by STBC-OFDM encoder [9]. The *q*-th user's continuous input signal blocks $1 \times N$ of length $S1^q$ and $S2^q$ will be encoded as two consecutive transmitting OFDM symbol blocks. Space time block encoder takes each pair of input vectors together and applies the Alamouti scheme on them. The length of each vector is N, which is the number of OFDM sub-carriers. For each pair of two successive data symbol vectors, if $S1$ is the first block data symbol vector and $S2$ is the second block vector, which are the frequency domain symbols, they are defined as

$$S1 = [S(1)\ S(2)\ S(3) \dots \dots \dots \dots S(N)] \quad (3.49)$$

$$S2 = [S(N+1)\ \ S(N+2) \dots S(2N)] \quad (3.50)$$

For the first transmitter, $S1$ is transmitted during the first time slot followed by $-S2^*$ in the second time slot. For the second transmitter, $S2$ is transmitted first followed by $S1^*$. The equivalent space time block code transmission matrix is given by

$$G_{STBC} = \begin{bmatrix} S1 & -S2^* \\ S2 & S1^* \end{bmatrix} \quad (3.51)$$

Therefore, entries of the transmission matrix are the OFDM symbol vectors $S1$, $S2$, and their complex conjugates.

3.3.1.1 STBC user with Single receive antenna case

We assume that the channel responses are constant during the two time slots. Let $r^1(k)$ and $r^2(k)$ represent the demodulated symbols at single receive user's antenna, after the OFDM demodulator, on the *k*-th sub-carrier at the first and second time slot, respectively. $r^1(k)$ and $r^2(k)$, $k = 1,2, \dots, N$,can be represented as

$$r^1(k) \ = H_{11}(k)\, S1(k) + H_{12}(k)\, S2(k) + n^1(k) \quad (3.52)$$

$$r^2(k) = -H_{11}(k)\, S2^*(k) + H_{12}(k)\, S1^*(k) + n^2(k) \quad (3.53)$$

Assuming that ideal Channel State Information (CSI) is available at the receiver, the decision variables are constructed by combining $r^1(k)$, $r^2(k)$, and the channel frequency response, we get

$$\hat{S}1(k) = (|H_{11}|^2 + |H_{12}|^2\ )\, S1(k) + \ H_{11}{}^*(k)\, n^1(k) + H_{12}(k)\, n^{2^*}(k) \quad (3.54)$$

$$\hat{S}2(k) = (|H_{11}|^2 + |H_{12}|^2\ )\, S2(k) + \ H_{12}{}^*(k) n^1(k) - H_{11}(k)\, n^{2^*}(k)) \quad (3.55)$$

Which are then sent to the maximum likelihood decoder, to decide the most probable sent vectors $S1$ and $S2$.

3.3.1.2 STBC User with Two receive antenna case

We assume that the channel responses are constant during the two time slots. Let $r_1^1(k), r_1^2(k)$ and $r_2^1(k), r_2^2(k)$, represent the demodulated symbols, after the OFDM demodulator, on the *k*-th sub-carrier at the first and second time slot, respectively, at receive antenna 1 and 2 .The received signal $r_1^1(k), r_1^2(k)$ and $r_2^1(k)$, $r_2^2(k)$, $k = 1,2, \dots, N$,can be represented as

$$r_1^1(k) = H_{11}(k)\, S1(k) + H_{12}(k)\, S2(k) + n_1^1(k) \quad (3.56)$$

$$r_1^{2^*}(k) = -H_{11}{}^*(k)\, S2(k) + H_{12}{}^*(k)\, S1(k) + n_1^{2^*}(k) \quad (3.57)$$

$$r_2^1(k) = H_{21}(k)\, S1(k) + H_{22}(k)\, S2(k) + n_2^1(k) \quad (3.58)$$

$$r_2^{2^*}(k) = -H_{21}{}^*(k)\, S2(k) + H_{22}(k)\, S1(k) + n_2^{2^*}(k) \quad (3.59)$$

Assuming that ideal Channel State Information (CSI) is available at the receiver, the decision variables are constructed by combining $r_1^1(k), r_1^2(k)$, $r_2^1(k), r_2^2(k)$, and the channel frequency response we get.

$$\begin{aligned}\hat{S}1(k) = {} & (|H_{11}|^2 + |H_{12}|^2 + |H_{21}|^2 + |H_{22}|^2)S1(k) \\ & + (H_{11}{}^*(k) n_1^1(k) + H_{21}(k) n_2^1(k) \\ & + H_{12}(k) n_1^{2^*}(k) + H_{22}(k)\, n_2^{2^*}(k)) \end{aligned} \quad (3.60)$$

$$\begin{aligned}\hat{S}2(k) = {} & (|H_{11}|^2 + |H_{12}|^2 + |H_{21}|^2 + |H_{22}|^2)S2(k) \\ & + H_{12}(k)\, n_1^1(k) - H_{11}(k)\, n_1^{2^*}(k) \\ & - H_{21}(k)\, n_2^{2^*}(k) + H_{22}(k)\, n_2^1(k) \end{aligned} \quad (3.61)$$

Which are then sent to the maximum likelihood decoder, to decide the most probable sent vectors $S1$ and $S2$. For more detail of encoding and decoding of STBC-OFDM, for more detail (see Appendix B).

3.3.2 Space Frequency Block Code OFDM

Now we describe the encoding and decoding process using space frequency block coded OFDM (SFBC-OFDM) proposed in [73].

In SFBC-OFDM, the data symbol vector for q-th user is defined as $S^q = [S(1)S(2) \dots S(N)]$, where N is the number of OFDM sub-carrier.

The symbol vector is coded into two length $1 \times N$ vectors, S_1 and S_2 by the space frequency encoder block as:

$$S_1 = [S(1) \ -S^*(2) \dots \dots S(N-1) \ -S^*(N)] \quad (3.62)$$

$$S_2 = [S(2) \quad S^*(1) \dots . . S(N) \quad S^*(N-1)] \quad (3.63)$$

(*) denote the conjugate of symbol S .

S_1 is transmitted from the first antenna transmitter, while S_2 is transmitted simultaneously from the second antenna transmitter. The operations of the space frequency encoder and decoder can be best described in terms of even and odd component vectors. According to the operation of the SFBC encoder described in [10, 67], the symbol vector S is divided into the even component S^e and the odd component S^o.

Let S^e and S^o be two length $N/2$ vectors denoting the even and odd component vectors of S. Therefore,

$$S^o = [S(1) \ S(3) \dots \ S(N-3) \ S(N-1)] \quad (3.64)$$

$$S^e = [S(2) \ S(4) \dots \dots \dots \ S(N-2) \ S(N)] \quad (3.65)$$

Similarly, ${S_1}^e$, ${S_1}^o$, ${S_2}^e$, and ${S_2}^o$ denote the even and odd component vectors of S_1 and S_2, respectively. Then the output of the SFBC encoder can be expressed in terms of the even and odd component vectors as:

Equations (3.64) and (3.65) can then be expressed in terms of the even and odd component vectors as

$$\begin{cases} {S_1}^e = -S^{e*} \\ {S_2}^e = S^{o*} \end{cases} \qquad \begin{cases} {S_1}^o = S^o \\ {S_2}^o = S^e \end{cases} \quad (3.66)$$

3.3.2.1 SFBC User with Single receives antenna case

Let $r(k)$ represents the demodulated symbol, after the OFDM demodulator, on the *k*-th sub-carrier, $k = 1,2, \dots, N$

$$r(k) = H_{11}(k)\ S_1(k) + H_{12}(k)\, S_2(k) + n(k) \quad (3.67)$$

Where $H_{ji}(k)$ is the channel frequency response from transmit antenna i to receive antenna j, on the *k*-th sub-carrier. Let $r^e(k)$ and $r^o(k)$, $k = 1,2, \dots, N/2$, represent the even and odd components of $r(k)$. Thus, $r^e(k)$ and $r^o(k)$, can be represented as:

$$r^o(k) = H_{11}^o(k)\, S_1^o(k) + H_{12}^o(k)\, S_2^o(k) + n^o(k) \quad (3.68)$$

$$r^e(k) = H_{11}^e(k)\, S_1^e(k) + H_{12}^e(k)\, S_2^e(k) + n^e(k) \quad (3.69)$$

Where $n^e(k)$ and $n^o(k)$ represent the even and odd components, respectively, of the demodulated noise vector. Substituting equations (3.66) into equations (3.68) and (3.69), we get

$$r^o(k) = H_{11}^o(k)\, S^o(k) + H_{12}^o(k)\ S^e(k) + n^o(k) \quad (3.70)$$

$$r^e(k) = -H_{11}^e(k)\, S^{e*}(k) + H_{12}^e(k)\, S^{o*}(k) + n^e(k) \quad (3.71)$$

From equations (3.70) and (3.71), we conclude that SFBC-OFDM can be represented by the transmission matrix for adjacent OFDM sub-carrier.

$$G_{SFBC} = \begin{bmatrix} S^o & -S^{e*} \\ S^e & S^{o*} \end{bmatrix} \quad (3.72)$$

Assuming that ideal channel state information is available at the receiver, the decision variables are constructed by combining $r^e(k)$, $r^o(k)$ and the channel frequency response, and the complex channel gains between adjacent sub-carriers are approximately constant, such as

$H_{11}^o(k) = H_{11}^e(k) = H_{11} \qquad H_{12}^o(k) = H_{12}^e(k) = H_{12}$

Therefore, we get

$$\hat{S}^o(k) = (|H_{11}^o|^2 + |H_{12}^e|^2)S^o(k) + H_{11}^{o\,*}(k)n^o(k) + H_{12}^e(k)\, n^{e*}(k) \quad (3.73)$$

$$\hat{S}^e(k) = (|H_{11}^o|^2 + |H_{12}^o|^2)\, S^e(k) + H_{12}^{o\,*}(k)n^o(k) - H_{11}^e(k)n^{e*}(k) \quad (3.74)$$

Where $\hat{S}^e(k)$ and $\hat{S}^o(k)$, $k = 1,2, \dots, N/2$ are combined together to construct $\hat{S}(k)$, $k = 1,2, \dots, N$. $\hat{S}(k)$, is sent to the maximum likelihood decoder, to decide the most probable sent vectors S.

3.3.2.2 SFBC User with Two receives antenna case

Let $r_1(k)$, $r_2(k)$ represents the demodulated symbol, after the OFDM demodulator, on the *k*-th sub-carrier, $k = 1,2, \dots, N$ at receive antenna 1 and 2.

$$r_1(k) = H_{11}(k)\ S_1(k) + H_{12}(k)\ S_2(k) + n_1(k) \quad (3.75)$$

$$r_2(k) = H_{21}(k)\ S_1(k) + H_{22}(k)\ S_2(k) + n_2(k) \quad (3.76)$$

Where $H_{ji}(k)$) is the channel frequency response from transmit antenna j to receive antenna i, on the *k*-th sub-carrier. Let $r_1^e(k)$, $r_1^o(k)$ and $r_2^e(k)$, $r_2^o(k)$, $k = 1,2, \dots, N/2$, represent the even and odd components of $r_1(k)$, $r_2(k)$ respectively. Thus, $r_1^e(k)$, $r_1^o(k)$ and $r_2^e(k)$ $r_2^o(k)$, can be represented as:

$$r_1^e(k) = H_{11}^e(k)\ S_1^e(k) + H_{12}^e(k)\ S_2^e(k) + n_1^e(k) \quad (3.77)$$

$$r_1^o(k) = H_{11}^o(k)\ S_1^o(k) + H_{12}^o(k)\ S_2^o(k) + n_1^o(k) \quad (3.78)$$

$$r_2^e(k) = H_{21}^e(k)\ S_1^e(k) + H_{22}^e(k)\ S_2^e(k) + n_2^e(k) \quad (3.79)$$

$$r_2^o(k) = H_{21}^o(k)\ S_1^o(k) + H_{22}^o(k)\ S_2^o(k) + n_2^o(k) \quad (3.80)$$

Where $n_1^e(k)$, $n_1^o(k)$ and $n_2^e(k)$, $n_2^o(k)$ represent the even and odd components, respectively, of the demodulated noise vector.

Substituting equation (3.66) into equations (3.77),(3.78) and (3.79), (3.80) we get

$$r_1^e(k) = -H_{11}^e(k)\ S^{e*}(k) + H_{12}^e(k)\ S^{o*}(k) + n_1^e(k) \quad (3.81)$$

$$r_1^o(k) = H_{11}^o(k)\ S^o(k) + H_{12}^o(k)\ S^e(k) + n_1^o(k) \quad (3.82)$$

$$r_2^e(k) = -H_{21}^e(k)\ S^{e*}(k) + H_{22}^e(k)\ S^{o*}(k) + n_2^e(k) \quad (3.83)$$

$$r_2^o(k) = H_{21}^o(k)\ S^o(k) + H_{22}^o(k)\ S^e(k) + n_2^o(k) \quad (3.84)$$

Assuming that ideal channel state information is available at the receiver, the decision variables are constructed by combining $r_1^e(k), r_1^o(k), r_2^e(k), r_2^o(k)$ and the channel frequency response, and the complex channel gains between adjacent sub-carriers are approximately constant, such as

$$H_{11}^e(k) = H_{11}^o(k)\ ,\ H_{12}^e(k) = H_{12}^o(k)\ ,\ \ H_{21}^e(k) = H_{21}^o(k)\ ,\ \ H_{22}^e(k) = H_{22}^o(k)$$

$$\hat{S}^o(k) = (|H_{11}^o|^2 + |H_{12}^e|^2 + |H_{21}^o|^2 + |H_{22}^e|^2\ )\ S^o(k) + H_{12}^e(k)\ n_1^{e*}(k) + H_{11}^{o\ *}(k)\ n_1^o(k) + H_{22}^e(k)\ n_2^{e*}(k) + H_{21}^{o\ *}(k) n_2^o(k) \quad (3.85)$$

$$\hat{S}^e(k) = (\ |H_{11}^e|^2 + |H_{12}^o|^2 + |H_{21}^e|^2 + |H_{22}^o|^2\ ) S^e(k) - H_{11}^e(k)\ n_1^{e*}(k) - H_{21}^e(k) n_2^{e*}(k) + H_{12}^{o\ *}(k) n_1^o(k) + H_{22}^{o\ *}(k) n_2^o(k) \quad (3.86)$$

Were $\hat{S}^e(k)$ and $\hat{S}^o(k)$, $k = 1,2,\dots,N/2$ are combined together to construct $\hat{S}(k), k = 1,2,\dots,N$. $\hat{S}(k)$, is sent to the maximum likelihood decoder, to decide the most probable sent vectors S. For more detail of encoding and decoding SFBC-OFDM, for more detail see Appendix B.

That is why we denote this scheme by space frequency, as each transmitted symbol is encoded on two consecutive sub-carriers, instead of two consecutive OFDM frames as in STBC-OFDM. In SFBC-OFDM, the encoding is done over one OFDM frame.

3.4 MIMO and OFDM Applications

MIMO is applicable to all kinds of wireless communication technologies. However, the combination of MIMO and OFDM has the following advantages. OFDM is adapted for multi-path propagation in wireless systems. The length of the OFDM frames is determined by the GI. This Guard Interval restricts the maximum path delay and therefore the expansion of the network area. MIMO also uses the multi-path propagation.

OFDM is a wideband system with many narrowband sub-carriers. The mathematical MIMO channel model is based on a narrow band non-frequency selective channel. The latter is supported by OFDM as well. Fading effects in wideband systems normally occur only at particular frequencies and interfere with few sub-carriers. The data is spread over all carriers, so that only a small amount of bits get lost, and these can be repaired by a forward error correction (FEC). OFDM provides a robust multi-path system suitable for MIMO. At the same time OFDM provides high spectral efficiency and a degree of freedom in spreading the time dimension of Space Time Block Codes over several sub-carriers. This results in a stronger system.

3.5 MIMO Standards

Table 3.1, gives an overview of all current MIMO standards and their technologies [74]. It is clear to see, that with the exception of 3GPP Release 7, all standards work with OFDM. The advantages of OFDM can obviously be linked to MIMO.

Standard	Technology
WLAN 802.11n	OFDM
WIMAX 802.16-2004	OFDM/OFDMA
WIMAX 802.16e	OFDMA
3GPP Release 7	WCDMA
3GPP Release 8 (LTE)	OFDMA
802.20	OFDM
802.22	OFDM

Table 3.1: MIMO Standards and the corresponding technology

3.6 Conclusion

In this chapter, we introduced a unified view on OFDM technique. First the FDM evolution and the basic principles of the OFDM system is explained with introducing its signal model, and the orthogonality concept .Thus OFDM effectually converts a frequency selective fading channel into a set of parallel flat fading channels. The general transceiver consist of converts digital data to be transmitted, into a mapping of sub-carrier and a block IFFT modulation per transmit antenna. However, is imposed by the OFDM overhead, i, e., the guard subcarriers and guard time to preserve the orthognality. The removed of the guard time at the receiver and a block of FFT demodulator per receive antenna to signal recover. Second the general principle of MIMO OFDM is explained and its signal model is introduced after. Furthermore, MIMO OFDM capacity is calculated. Third the combination of STBC and MIMO OFDM is discussed; the investigating of space time block codes for frequency selective fading channels from a capacity perspective is an important and interesting direction for future studies. The general transceiver of the hybrid scheme consists of an encoder, a space time mapper, using either space time code or space frequency code, and per transmit antenna an IFFT modulation block. The FFT block demodulation per receive antenna, after the decoding process according to each space code type. Finally, some kinds applications of MIMO OFDM in wireless communication technologies.

CHAPTER IV

Multi User Systems

4.1 Multiple Access Techniques

Multiple accesses (MA) refer to a technique that allows several users to share a common communications channel. The available domains for multiple accesses are space, time and frequency. In wireless communication, several techniques such as Time Division Multiple Access (TDMA), Frequency Division Multiple Access (FDMA) and Code Division Multiple Access (CDMA) are used for sharing the spectrum resources available for use. TDMA assigns different time slots to users while FDMA assigns a different frequency to each user. However, the CDMA technique shares the entire bandwidth by distinguishing signals with a unique signature for each user. The most traditional multiple access techniques are based on user separation using different signature waveforms. The oldest multiple access technique is frequency division multiple access (FDMA) where different signature waveforms use different frequency. The user separation is then performed simply by bandpass filtering.

The introduction of digital modulations enabled the appearance of time division multiple access (TDMA) where each user's signature waveform is limited to a predetermined time interval. Source separation is analogous to extracting the streams corresponding to each antenna in the transmit array. However, the transmit diversity detection problem is simpler, since the sources are discrete rather than continuous random variables. Another superset of transmit diversity detection is the class of problems known as multiuser Detection (MUD)[75]. In this case, the receive antenna observes K signals coming not only from different antennas, but also from different users. Detecting the signals of the individual users is also analogous to extracting the streams transmitted by each antenna in a transmit diversity system. The user separation is then performed by synchronizing and correlating with the corresponding user's signature waveform.

The appearance of spread spectrum techniques for anti-jamming and low probability of interception capabilities has led to the development of code division multiple accesses (CDMA). CDMA can be implemented using frequency hopping (FH), time hopping (TH), direct sequence (DS) spread spectrum (SS) as well as multi-carrier (MC) techniques. In FH-CDMA users' signature waveforms are located at different center frequencies at different time intervals. The hopping from one frequency to another is controlled by user specific hopping sequences. In DS CDMA, different users' signature waveforms are allowed to overlap both in time and in frequency, but they are orthogonal in the code domain. This can be achieved by allocating each user a unique spreading sequence, whereby the signal redundancy is achieved

in time domain [76]. On the contrary, in MC-CDMA the redundancy of each user's data is achieved in frequency domain [77].

The simplest way to achieve spatial multiple access is to simply separate multiple users far apart in order to allow for sufficient attenuation of the signals. More advanced techniques include space division multiple access (SDMA) [7], or beamforming, which is based on the use of closely spaced antennas to spatially isolate the users or spatial multiplexing which relies on antennas spaced far apart and the rich scattering environment to perform user separation [78,79].

Unlike in the former case, where it was necessary for different users to be placed in different spatial directions, this is not necessary for the latter one. The difference between SDM and SDMA is that the latter allows different users to transmit simultaneously on a single antenna each, whereas in SDM a single user transmits simultaneously on multiple antennas [7].

This can be justified by the fact that, similarly to the conventional SDMA case, it is essentially the spatial position of different users that allows for their separation at the receiver.

The use of multiple receive antennas theoretically enables multiple access using only a single carrier frequency. In wideband system, however, the frequency selectivity of the channel becomes one of the factors that dominate receiver performance. MC techniques are an effective way to mitigate this problem by converting a frequency selective channel into a set of frequency flat fading channels. By doing so, the channel frequency selectivity can be exploited to achieve additional diversity gains.

4.2 Multi User Detection

The receiver performance in the presence of interference is dominated by the knowledge it has about the interference structure. Depending on this knowledge, appropriate algorithms can be applied to use the receiver's DOF(Degree of Freedom) to mitigate the degrading effects of interference. Spread spectrum is a signal processing technique that distinguishes CDMA, where a data symbol is modulated with a noise like wideband signal called a pseudo noise (PN) sequence. Otherwise, the performance of wireless communications is also primarily limited by MAI in multiuser applications.

This process is known as spreading, and is intended to suppress MAI due to interference from other users in the same cell (intra cell interference), and possibly users from adjacent cells (inter cell interference).

In many situations, interference can be modeled as AWGN that has structure neither in space nor in time/frequency domains. The matched filter [80] is well known to be the optimal receiver for that scenario, if the pulse shape of the signal of interest is known at the receiver, it depends on the cross-correlation properties between the PN sequences from all active users and the spreading factor, which is defined as the ratio in bandwidth between the information bearing signal and the PN sequence. The matched filter is optimal in a white Gaussian noise environment, but suffers from the near far effect when MAI is present; the performance of the matched filter deteriorates when the received powers from interfering users are greater than that of the desired user. In case that the interference possesses any kind of structure in space and/or time, the matched filter designed for AWGN noise is not capable of exploiting it.

Signal correlation is another property which resulted in a variety of wide band and narrow band interference (WBI and NBI, respectively) suppression techniques that exploit interference correlation in time, frequency and spatial domains [76].

In the multiuser case, several works have proposed for development of advanced algorithms that can improve the receiver's performance by exploiting this structure. The optimal receiver for MAI is known to be the MUD, where all the interfering signals are detected jointly with the signal of interest (SOI), providing for the receiver in the process of eliminating the MAI and ISI, the considered receivers detect the information bearing bits of the desired user while suppressing interference.

For ISI the optimal detector is the maximum likelihood sequence estimator (MLSE) [7, 81]. The ML multiuser receiver encompasses a bank of matched filters that produces a set of sufficient statistics, followed by a Viterbi decoder. The complexity of the ML receiver is exponential in the number of users, rendering it impractical.

The combinations of detection methods that simultaneously make use of several signal properties and perform processing in several domains have attracted considerable attention. The examples are space time interference suppression [82], time frequency interference suppression [83] and joint MUD of SOI and interference for NBI and WBI interference suppression [84, 85]. Note that these methods require knowledge of channel state information (CSI) at the receiver side. In case that the CSI is not available but the signals are still of interest, one could resort to the rich literature on blind de-convolution with blind source separation, blind equalization and blind multiuser detection as special cases [76].

In channel coded systems, the complexity of an optimal receiver that jointly performs signal and interference detection with channel decoding is prohibitively complex [86, 87, 88]. However, the complexity can be significantly reduced by means of the suboptimal iterative receiver structures. In most of the cases the performance of the suboptimal iterative receivers is close to that of the globally optimal receiver due to the very reliable signal estimates obtained after channel decoding. An iterative multiuser detection and decoding [89], iterative equalization and decoding [90], and iterative channel estimation, equalization and decoding [91].

Suboptimum linear receivers such as the de-correlating and the minimum mean squared error (MMSE) receivers have been proposed [19, 83] to trade off complexity and performance among the conventional and optimal receivers, however, they still require computationally intensive matrix inversion. More practical and simple approaches include multistage decision-feedback receivers such as the V-BLAST parallel interference cancellation (PIC) detector [92, 93], as well as the serial interference cancellation (SIC) detector [93, 94]. Although both receivers have linear complexity in the number of users, the SIC causes longer delay, while the PIC demands more hardware.

The received signals are then combined using optimal weights, forming a signal with better quality than each individual one. Three common diversity schemes are maximum ratio combining (MRC), equal gain combining (ECG) and selection combining (SC) [44].

4.3 Multi User Systems

While traditional wireless communications (SISO) exploit time or frequency domain pre-processing and decoding of the transmitted and received data respectively, the use of additional antenna elements at either the base station (BS) or user equipment (UE) side (on the downlink and/or uplink) opens an extra spatial dimension to signal pre-coding and detection [95]. So called space time processing methods exploit this dimension with the aim of improving the link's performance in terms of one or more possible metrics, such as the error rate, communication data rate, coverage area and spectral efficiency (bits/sec/Hz/cell).

Depending on the availability of multiple antennas at the transmitter and or the receiver, such techniques are classified as (SIMO), (MISO) or MIMO. Thus in the scenario of a multi-antenna enabled base station communicating with a single antenna UE, the uplink and downlink are referred to as SIMO and MISO respectively [96].

When a (high-end) multi-antenna terminal is involved, a full MIMO link may be obtained, although the term MIMO is sometimes also used in its widest sense, thus including SIMO and MISO as special cases. While a point-to-point multiple antenna link between a base station and one UE is referred to as Single user MIMO (SU-MIMO), multiuser MIMO (MU-MIMO) features several UEs communicating simultaneously with a common base station using the same frequency and time domain resources.

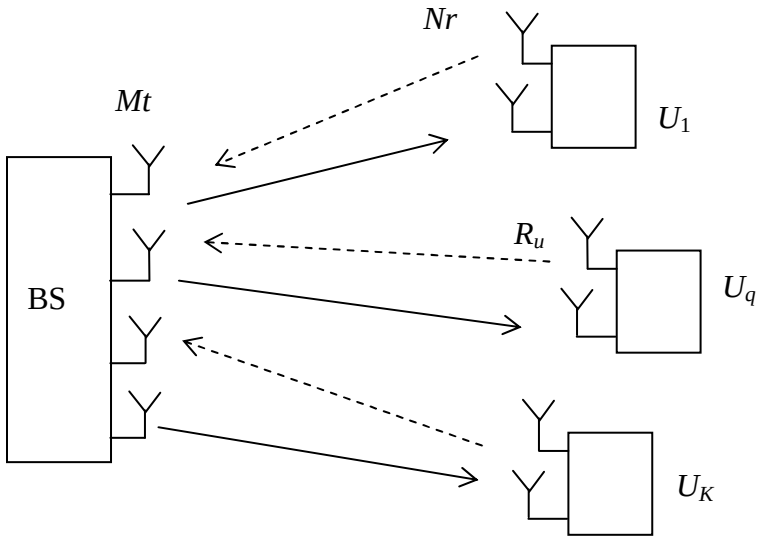

Figure 4.1**:** Block diagram of Single Cell Multi User MIMO.

Figure 4.1, Illustrates the block diagram of a single cell multiuser MIMO with Mt transmits antennas and Nr receives antennas for all selected users. By extension, considering a multi-cell context, neighboring base stations sharing their antennas in virtual MIMO fashion to communicate with the same set of UEs in different cells will be termed multi cell multiuser MIMO.

4.3.1 Comparing Single User and Multi User MIMO

The set of MIMO techniques featuring data streams being communicated to (or from) antennas located on distinct UEs in the model is referred to as Multi User MIMO (MU-MIMO). The MU-MIMO scenario differs in a number of crucial ways from its single user counterpart. In MU-MIMO, *K* UEs are selected for simultaneous communication over the same time frequency resource, from a set of *U* active UEs in the cell. Typically *K* is much smaller than *U*. Each UE is assumed to be equipped with R_u antennas, so the selected UEs together form a set of $Nr = KR_u$ UE side antennas. Since the number of streams that may be communicated over an Mt to Nr MIMO channel is limited to $min\,(Nr, Mt)$ (if complete interference suppression is intended using linear combining of the antennas), the upper bound on the number of streams in MU-MIMO is typically dictated by the number of base station antennas Mt. The number of streams which may be allocated to each UE is limited by the number of antennas R_u at that UE. For instance, with single antenna UEs, up to Mt streams can be multiplexed, with a distinct stream being allocated to each UE. This is in contrast to SU-MIMO, where the transmission of Mt streams necessitates that the UE be equipped with at least Mt antennas. Therefore a great advantage of MU-MIMO over SU-MIMO is that the MIMO multiplexing benefits are preserved even in the case of low cost UEs with a small number of antennas. As a result, it is generally assumed that in MU-MIMO it is the base station which bears the burden of spatially separating the UEs, be it on the uplink or the downlink. Thus the base station performs receive beamforming from several UEs on the uplink and transmit beamforming towards several UEs on the downlink. Another fundamental contrast between SU-MIMO and MU-MIMO comes from the difference in the underlying channel model. While in SU-MIMO the de-correlation between the spatial signatures of the antennas requires rich multi-path propagation or the use of orthogonal polarizations, in MU-MIMO the de-correlation between the signatures of the different UEs occurs naturally due to fact that the separation between such UEs is typically large relative to the wavelength [96].

4.3.2 Comparing techniques for Single and Multiple antenna UEs

In the case of MU-MIMO for single antenna UEs, it is worth noting that the number of antennas available to a UE for transmission is typically less than the number available for reception. Note that no more than Mt users can be served (i.e. $K \leq Mt$) if inter-user interference is to be suppressed fully.

In theory, essentially two ways, of exploiting the additional antennas at the UE side. In the first approach**,** the multiple antennas are simply treated as multiple virtual UEs, allowing high capability terminals to receive or transmit more than one stream, while at the same time spatially sharing the channel with other UEs. For instance, a four antenna base station could theoretically communicate in a MU-MIMO fashion with two UEs equipped with two antennas each, allowing two streams per UE, resulting in a total multiplexing gain of four. Another example would be that of two single antenna UEs, receiving one stream each, and sharing access with another two antenna UE, the latter receiving two streams. Again the overall multiplexing factor remains limited to the number of base station antennas.

The second approach for making use of additional UE antennas is to treat them as extra DOF for the purpose of strengthening the link between the UE and the base station. Multiple antennas at the UE may then be combined in MRC fashion in the case of the downlink, or in the case of the uplink STC could be used. Antenna selection is another way of extracting more diversity out of the channel.

4.4 MU MIMO Schemes

In the case of transmit beamforming and MIMO SVD based pre-coding [20, 21, 32, 33], the transmitter then has to acquire this channel knowledge (or directly the pre-coder knowledge) from the receiver usually through a limited feedback link, which causes further degradation to the available Channel State Information at the Transmitter (CSIT). When it comes to MU-MIMO, the principle advantages over SU-MIMO are clear, robustness with respect to the propagation environment, and spatial multiplexing gain preserved even in the case of UEs with small numbers of antennas.

However, such advantages come at a price. In the downlink, MU-MIMO relies on the ability of the base station to compute the required transmit beamformer, which in turn requires CSIT. The fundamental role of CSIT in the MU-MIMO downlink can be emphasized as follows:

In the extreme case of no CSIT being available and identical fading statistics for all the UEs, the MU-MIMO gains totally disappear and the SU-MIMO strategy becomes optimal.

As a consequence, one of the most difficult challenges in making MU-MIMO practical for cellular applications, and particularly for an Frequency Division Duplex (FDD) system, is devising mechanisms that allow for accurate CSI to be delivered by the UE to the base station in a resource efficient manner. This requires the use of appropriate codebooks for quantization [97, 98].

Another issue which arises for practical implementations of MIMO schemes is the interaction between the physical layer and the scheduling protocol. In both uplink and downlink cases the number of UEs which can be served in a MU-MIMO fashion is typically limited to $K = Mt$, assuming linear combining structures. Often one may even decide to limit K to a value strictly less than Mt to preserve some DOF for per user diversity. As the number of active users U will typically exceed K, a selection algorithm must be implemented to identify which set of users will be scheduled for simultaneous transmission over a particular time frequency slot.

A combination of rate maximization and QoS constraints will typically be considered. It is important to note that the choice of UEs that will maximize the sum rate (the sum over the K individual rates for a given sub-frame) is one that favors UEs exhibiting not only good instantaneous SNR but also spatial separability among their signatures.

Note that in the case of closed loop spatial multiplexing, a UE feeds back to the BS the most desirable entry from a predefined codebook. The preferred pre-coder is the matrix which would maximize the capacity based on the receiver capabilities [31, 32, 33]. In a single cell, interference free environment the UE will typically indicate the pre-coder that would result in a transmission with an effective SNR following most closely the largest singular values of its estimated channel matrix.

4.5 Multi-user Detection with V-BLAST on MIMO

4.5.1 Introduction

A multilayered space time block coded OFDM system, which is a combination of the vertical layered space time architecture, known as V-BLAST, and the space time block coded OFDM system, which use the frequency or time coding, respectively [67, 71]. This system is designed to provide reliable as well as very high data rate communications over frequency selective fading channels with low decoding complexity. OFDM is used to transform the frequency selective fading channel into multiple flat fading sub-channels.

In this section, we propose a hybrid MU multilayered space time block coded OFDM system, denoted by MU V-BLAST STBC-OFDM, which provides high data rates over frequency selective fading channel with reliable transmission. For the sake of comparison, we will mention the MU multilayered space frequency block coded OFDM systems, denoted by MU V-BLAST SFBC-OFDM.

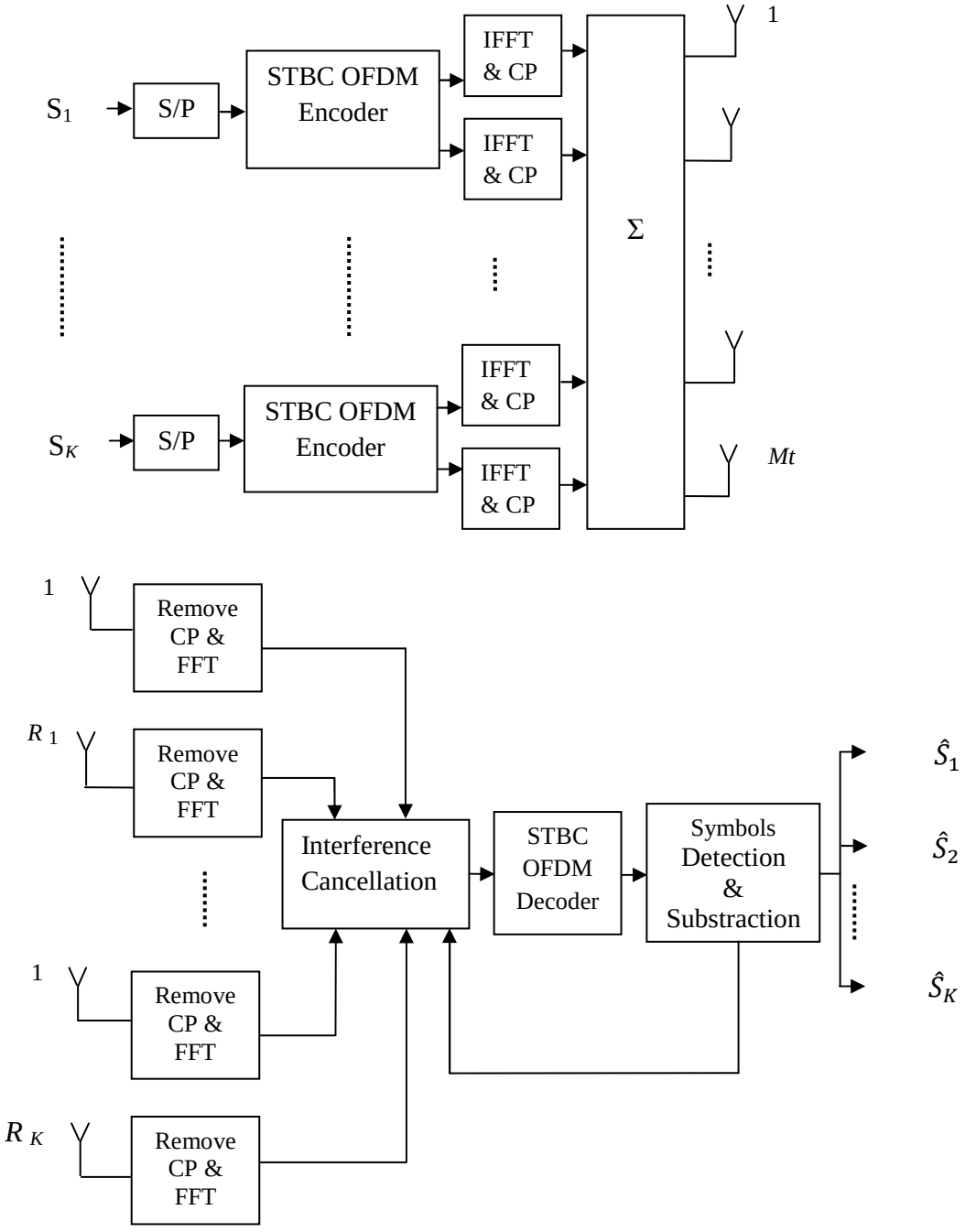

Figure 4.2: Block diagram of the multilayered MU system for downlink system

The hybrid multilayered space time or frequency block coded OFDM scheme partitions antennas at the transmitter into small groups, and uses individual space time or frequency block coded OFDM encoders to transmit information from each group of antennas as shown in Figure 4.2. At the receiver, each individual group is decoded by a non-linear processing technique that suppresses signals transmitted by other groups of antennas by treating them as interferers. The ordered successive detection strategies as shown in section 2.3.4 is considered in the formulation of the receivers is referred as ZF-OSIC.

4.5.2 System model

Frequency selective fading channels can be modeled by a tapped delay line. For a multi-path fading channel with L different paths, the fading channel between the i-th transmit antenna and j-th receive antenna has discrete time baseband equivalent finite impulse response (FIR) coefficients collected in the $L \times 1$ vector.

$$h_{ji} = \left[h_{ji}^{0}, h_{ji}^{1}, \ldots., h_{ji}^{L-1}\right]^{T} \tag{4.1}$$

For $1 \leq j \leq Nr$, $1 \leq i \leq Mt$ were h_{ji}^{l} $'s$, $l = 0,1, \ldots, L-1$ are independent and identically distributed (i.i.d.), zero-mean, complex Gaussian random variables with variance $1/2L$ per dimension. We assume that the MIMO frequency selective Rayleigh fading channel is constant during each OFDM block, and vary from block to another.

Assuming there are Nr receiving antennas for all K user, the received vector can be expressed as:

$$y = HS + w \tag{4.2}$$

Where H represents the channel matrix of size $Nr \times Mt$ and w represents AWGN noise.

The channel matrix is given by:

$$H = \begin{bmatrix} h_{11}^{k} & h_{12}^{k} & \cdots & h_{1Mt}^{k} \\ h_{21}^{k} & h_{22} & \cdots & h_{2Mt}^{k} \\ \vdots & \vdots & \ddots & \vdots \\ h_{Nr1}^{k} & h_{Nr2}^{k} & \cdots & h_{NrMt}^{k} \end{bmatrix} \tag{4.3}$$

Where h_{ji}^{k} are frequency responses at sub-carrier k, between the j-th receive antenna and the i-th transmit antenna in the case of OFDM. By apply the STBC OFDM encoding and decoding as introduced in section 3.4, for STC and SFC respectively, as shown in Figure 4.2.

4.5.3 MU STC Encoding and Decoding

The received signal of each user r_q at receive antennas R_{q1} , R_{q2} , at different time slots, after the FFT and the CP removal, the *q*-th user received signal can be represented by:

$$y_q = H_{q,STC}S + w_q \tag{4.4}$$

Where $H_{q,STC}$ channel response of each user in STC coding, and w_q is the AWGN.

4.5.3.1 User with Single receive antenna

We consider R_{q1}, the receive antenna for each user, the received signals is given by the following equations:

$$r_{q1}{}^{t1} = H_{R_{q1}1}\ S_{11} + \ H_{R_{q1}2}\ S_{12} + \cdots + H_{R_{q1}1}\quad S_{q1}\quad + \ H_{R_{q1}2}\ \ S_{q2} + w1 \tag{4.5}$$

$$r_{q1}{}^{*t2} = -H_{R_{q1}1}{}^{*}\ S_{12} + H_{R_{q1}2}{}^{*}\ \ S_{11} + \cdots - H_{R_{q1}1}{}^{*}\ S_{q2} + H_{R_{q1}2}{}^{*}\ \ S_{q1} + w'^{*}1 \tag{4.6}$$

Where $w1$, $w'^{*}1$, represent AWGN, and $H_{R_{q1}1}$, $H_{R_{q1}2}$ and $H_{R_{q1}1}{}^{*}$, $H_{R_{q1}2}{}^{*}$ are frequency responses and there conjugate, at a given sub-carrier *k*, as depicted in Figure 4.2.

Equations (4.5) and (4.6) can also be written as:

$$\begin{bmatrix} r_{q1}{}^{t1} \\ r_{q1}{}^{*t2} \end{bmatrix} = \begin{bmatrix} H_{R_{q1}1} & H_{R_{q1}2} \\ H_{R_{q1}2}{}^{*} & -H_{R_{q1}1}{}^{*} \end{bmatrix} \begin{bmatrix} S_{11} \\ S_{12} \end{bmatrix} + \cdots$$

$$+ \begin{bmatrix} H_{R_{q1}1} & H_{R_{q1}2} \\ H_{R_{q1}2}{}^{*} & -H_{R_{q1}1}{}^{*} \end{bmatrix} \begin{bmatrix} S_{q1} \\ S_{q2} \end{bmatrix} + \begin{bmatrix} w1 \\ w'^{*}1 \end{bmatrix} \tag{4.7}$$

The received signal by the *q-th* user is summation of transmitted signal from all *K* transmit stream and can be represented by equation (4.8).

$$\begin{bmatrix} r_{q1}{}^{t1} \\ r_{q1}{}^{*t2} \end{bmatrix} = \sum_{q=1}^{K} \begin{bmatrix} H_{R_{q1}1} & H_{R_{q1}2} \\ H_{R_{q1}2}{}^{*} & -H_{R_{q1}1}{}^{*} \end{bmatrix} \begin{bmatrix} S_{q1} \\ S_{q2} \end{bmatrix} + \begin{bmatrix} w_{q1} \\ w'^{*}{}_{q1} \end{bmatrix}, \quad q = 1, \dots, K \tag{4.8}$$

Equation (4.8) can be rewritten as:

$$y_q = \begin{bmatrix} r_{q1}{}^{t1} \\ r_{q1}{}^{*t2} \end{bmatrix} = H_{q1,e} \begin{bmatrix} S(1) \\ S(2) \\ \vdots \\ S(K) \end{bmatrix} + \begin{bmatrix} w(1) \\ w(2) \\ \vdots \\ w(K) \end{bmatrix} \tag{4.9}$$

Where $H_{q1,e}$ the equivalent matrix for channel user with single receive antenna is given by:

$$H_{H_{q1,e}} = \begin{bmatrix} H_{R_{q1}1} & H_{R_{q1}2} & H_{R_{q1}3} & H_{R_{q1}4} & \dots & H_{R_{q1}Mt-1} & H_{R_{q1}Mt} \\ H^{*}_{R_{q1}2} & -H^{*}_{R_{q1}1} & H^{*}_{R_{q1}4} & -H^{*}_{R_{q1}3} & \cdots & -H^{*}_{R_{q1}Mt} & -H^{*}_{R_{q1}Mt-1} \end{bmatrix} \tag{4.10}$$

$$\begin{bmatrix} {r_{q1}}^{t1} \\ {r_{q1}}^{*t2} \end{bmatrix} = \begin{bmatrix} H_{R_{q1}1} & H_{R_{q1}2} \\ {H_{R_{q1}2}}^{*} & -{H_{R_{q1}1}}^{*} \end{bmatrix} \begin{bmatrix} S_{q1} \\ S_{q2} \end{bmatrix} + \sum_{j \neq q}^{K} \begin{bmatrix} H_{R_{q1}1} & H_{R_{q1}2} \\ {H_{R_{q1}2}}^{*} & -{H_{R_{q1}1}}^{*} \end{bmatrix} \begin{bmatrix} S_{j1} \\ S_{j2} \end{bmatrix} + \begin{bmatrix} w_{q1} \\ {w'}^{*}{}_{q1} \end{bmatrix} \quad (4.11)$$

Received signal in frequency domain can be represented by equation (4.12).

$$y_q = H_{q1,e}\ S_q + \sum_{j=1, j \neq q}^{K} H_{q1,e}\ S_j + w_q$$

$$y_q = H_{q1,e}\ S_q + Z_q + w_q \quad (4.12)$$

We can see from (4.12), that the received DL signal at the MS's experience MUI component on the *q*-th user is represented as Z_q.

4.5.3.2 User with Two receive antenna

We consider R_{q1} , R_{q2}, the receive antennas for each user, the received signal r_q is given by the following equation :

$${r_{q1}}^{t1} = H_{R_{q1}1}\ S_{11} + H_{R_{q1}2}\ S_{12} + \cdots + H_{R_{q1}1}\ S_{q1} + H_{R_{q1}2}\ S_{q2} + w_{q1} \quad (4.13)$$

$${r_{q2}}^{t1} = H_{R_{q2}1}\ S_{11} + H_{R_{q2}2}\ S_{12} + \cdots + H_{R_{q2}1}\ S_{q1} + H_{R_{q2}2}\ S_{q2} + w_{q2} \quad (4.14)$$

$${r_{q1}}^{*t2} = -{H_{R_{q1}1}}^{*}\ S_{12} + {H_{R_{q1}2}}^{*}\ S_{11} + \cdots - {H_{R_{q1}1}}^{*} S_{q2} + {H_{R_{q1}2}}^{*}\ S_{q1} + {w'}^{*}{}_{q1} \quad (4.15)$$

$${r_{q2}}^{*t2} = -{H_{R_{q2}1}}^{*}\ S_{12} + {H_{R_{q2}2}}^{*}\ S_{11} + \cdots$$
$$-{H_{R_{q2}1}}^{*} S_{q2} + {H_{R_{q2}2}}^{*}\ S_{q1} + {w'}^{*}{}_{q2} \quad (4.16)$$

where w_{q1}, w_{q2}, ${w'}^{*}{}_{q1}$, ${w'}^{*}{}_{q2}$, represent AWGN and $H_{R_{q1}1}$, $H_{R_{q1}2}$, $H_{R_{q2}1}$, $H_{R_{q2}2}$ and ${H_{R_{q1}1}}^{*}$, ${H_{R_{q1}2}}^{*}$, ${H_{R_{q2}1}}^{*}$, ${H_{R_{q2}2}}^{*}$, are the frequency responses and there conjugate, at a given sub-carrier *k.* Equations (4.13),(4.14),(4.15),(4.16) can also be written as

$$\begin{bmatrix} {r_{q1}}^{t1} \\ {r_{q1}}^{*t2} \\ {r_{q2}}^{t1} \\ {r_{q2}}^{*t2} \end{bmatrix} = \begin{bmatrix} H_{R_{q1}1} & H_{R_{q1}2} \\ {H_{R_{q1}2}}^{*} & -{H_{R_{q1}1}}^{*} \\ H_{R_{q2}1} & H_{R_{q2}2} \\ {H_{R_{q2}2}}^{*} & -{H_{R_{q2}1}}^{*} \end{bmatrix} \begin{bmatrix} S_{11} \\ S_{12} \end{bmatrix} + \cdots$$
$$+ \begin{bmatrix} H_{R_{q1}1} & H_{R_{q1}2} \\ {H_{R_{q1}2}}^{*} & -{H_{R_{q1}1}}^{*} \\ H_{R_{q2}1} & H_{R_{q2}2} \\ {H_{R_{q2}2}}^{*} & -{H_{R_{q2}1}}^{*} \end{bmatrix} \begin{bmatrix} S_{q1} \\ S_{q2} \end{bmatrix} + \begin{bmatrix} w_{q1} \\ {w'}^{*}{}_{q1} \\ w_{q2} \\ {w'}^{*}{}_{q2} \end{bmatrix} \quad (4.17)$$

The received signal by the *q-th* user is summation of transmitted signal from all *K* transmit stream and can be represented by equation (4.18).

$$\begin{bmatrix} {r_{q1}}^{o} \\ {r_{q1}}^{*e} \\ {r_{q2}}^{o} \\ {r_{q2}}^{*e} \end{bmatrix} = \sum_{q=1}^{K} \begin{bmatrix} H_{R_{q1}1} & H_{R_{q1}2} \\ {H_{R_{q1}2}}^{*} & -{H_{R_{q1}1}}^{*} \\ H_{R_{q2}1} & H_{R_{q2}2} \\ {H_{R_{q2}2}}^{*} & -{H_{R_{q2}1}}^{*} \end{bmatrix} \begin{bmatrix} S_{q1} \\ S_{q2} \end{bmatrix} + \begin{bmatrix} w_{q1} \\ {w'^{*}}_{q1} \\ w_{q2} \\ {w'^{*}}_{q2} \end{bmatrix} \qquad q = 1, \dots, K \qquad (4.18)$$

Equation (4.18) can be rewritten as:

$$y_q = \begin{bmatrix} {r_{q1}}^{t1} \\ {r_{q1}}^{*t2} \\ {r_{q2}}^{t1} \\ {r_{q2}}^{*t2} \end{bmatrix} = H_{q2,e} \begin{bmatrix} S(1) \\ S(2) \\ \vdots \\ S(K) \end{bmatrix} + \begin{bmatrix} w_{q1} \\ {w'^{*}}_{q1} \\ w_{q2} \\ {w'^{*}}_{q2} \end{bmatrix} \qquad (4.19)$$

$$\begin{bmatrix} {r_{q1}}^{o} \\ {r_{q1}}^{*e} \\ {r_{q2}}^{o} \\ {r_{q2}}^{*e} \end{bmatrix} = \begin{bmatrix} H_{R_{q1}1} & H_{R_{q1}2} \\ {H_{R_{q1}2}}^{*} & -{H_{R_{q1}1}}^{*} \\ H_{R_{q2}1} & H_{R_{q2}2} \\ {H_{R_{q2}2}}^{*} & -{H_{R_{q2}1}}^{*} \end{bmatrix} \begin{bmatrix} S_{q1} \\ S_{q2} \end{bmatrix} + \sum_{j \neq q}^{K} \begin{bmatrix} H_{R_{q1}1} & H_{R_{q1}2} \\ {H_{R_{q1}2}}^{*} & -{H_{R_{q1}1}}^{*} \\ H_{R_{q2}1} & H_{R_{q2}2} \\ {H_{R_{q2}2}}^{*} & -{H_{R_{q2}1}}^{*} \end{bmatrix} \begin{bmatrix} S_{j1} \\ S_{j2} \end{bmatrix} + \begin{bmatrix} w_{q1} \\ {w'^{*}}_{q1} \\ w_{q2} \\ {w'^{*}}_{q2} \end{bmatrix} \qquad (4.20)$$

$$y_q = H_{q2,e}\ S_q + \sum_{j=1, j \neq q}^{K} H_{q2,e}\ S_j + w_q$$

$$y_q = H_{q2,e}\ S_q + Z_q + w_q \qquad (4.21)$$

We can see from (4.21), that the received DL signal at the MS's experience MUI component on the q-th user is represented as Z_q.

$$H_{q2,e} = \begin{bmatrix} H_{R_{q1}1} & H_{R_{q1}2} & H_{R_{q1}3} & H_{R_{q1}4} & \dots & H_{R_{q1}Mt-1} & H_{R_{q1}Mt} \\ H^{*}_{R_{q1}2} & -H^{*}_{R_{q1}1} & -H^{*}_{R_{q1}4} & -H^{*}_{R_{q1}3} & \dots & -H^{*}_{R_{q1}Mt} & -H^{*}_{R_{q1}Mt-1} \\ H_{R_{q2}1} & H_{R_{q2}2} & H_{R_{q2}3} & H_{R_{q2}4} & \cdots & H_{R_{q2}Mt-1} & H_{R_{q2}Mt} \\ H^{*}_{R_{q2}2} & -H^{*}_{R_{q2}2} & H^{*}_{R_{q2}4} & -H^{*}_{R_{q2}3} & \cdots & H^{*}_{R_{q2}Mt} & -H^{*}_{R_{q2}Mt-1} \end{bmatrix} \qquad (4.22)$$

We can rewrite the q-th equivalent channel user for STBC OFDM matrix as follows:

$$\widetilde{H}_{q,STBC} = \begin{bmatrix} h^{(q)}_{11} & h^{(q)}_{12} & \dots & h^{(q)}_{1Mt-1} & h^{(q)}_{1Mt} \\ h^{(q)}_{12} & -h^{(q)}_{11} & \cdots & h^{(q)}_{1Mt} & -h^{(q)}_{1Mt-1} \\ h^{(q)}_{21} & h^{(q)}_{22} & \vdots & h^{(q)}_{R_qMt-1} & h^{(q)}_{2Mt} \\ h^{(q)}_{22} & -h^{(q)}_{21} & \dots & h^{(q)}_{2Mt} & -h^{(q)}_{2Mt-1} \\ \vdots & \vdots & \vdots & \vdots & \vdots \\ \vdots & \vdots & \dots & \vdots & \vdots \\ h^{(q)}_{R_q1} & h^{(q)}_{R_q2} & \dots & h^{(q)}_{R_qMt-1} & h^{(q)}_{R_qMt} \\ h^{(q)}_{R_q2} & -h^{(q)}_{R_q1} & \dots & h^{(q)}_{R_qM} & -h^{(q)}_{R_qMt-1} \end{bmatrix} \qquad (4.23)$$

Finally the entire multiuser MIMO channel may be characterized by the super-matrix H , which may be constructed by concatenating the corresponding channel matrices $\{\widetilde{H}_q\}_{q=1}^{K}$ associated with each of the MS's, and the composite channel matrix is denote as:

$$\widetilde{H}_{STBC} = \left[\widetilde{H}_{STBC}^{(1)}, \widetilde{H}_{STBC}^{(2)}, \widetilde{H}_{STBC}^{(3)}, \ldots\ldots, \widetilde{H}_{STBC}^{(K)}\right] \tag{4.24}$$

The overall user received signal can be rewritten as:

$$\begin{bmatrix} y(1) \\ y(2) \\ \vdots \\ y(K) \end{bmatrix} = \widetilde{H}_{STBC} \begin{bmatrix} S(1) \\ S(2) \\ \vdots \\ S(K) \end{bmatrix} + \begin{bmatrix} w(1) \\ w(2) \\ \vdots \\ w(K) \end{bmatrix} \tag{4.25}$$

We can detect the desired signal vectors, $S(q)$, $q = 1,..,K$ from equation (4.25), using V-BLAST (OSIC) based on ZF solution referred to ZF-OSIC and hence remove the interference between the *K* transmitted streams and subsequently implemented the STBC decoding.

4.5.4 MU SFC Encoding and Decoding

In this section we present MU SFBC, as shown in Figure 4.2, where the user stream are coded in SFC as described in section 3.4, where the user receiver is equipped with R_{q1}, or R_{q1} and R_{q2}, the received signal r_q of each user at different time slots can be represented by:

$$y_q = H_{q,SFC} S + w_q \tag{4.26}$$

Where $H_{q,SFC}$ channel response of each user in SFC coding, and w_q is the AWGN.

4.5.4.1 User with Single receive antenna

We consider R_{q1}, the receive antennas for each user, the received signal r_q for the *q*-th user can be represented by the following equation:

$$\begin{aligned} {r_{q1}}^{o} &= {H^{o}}_{R_{q1}1}\ {S^{o}}_{11} + {H^{o}}_{R_{q1}2}\, S_{11}^{e}\ + \cdots \\ &\quad + {H^{o}}_{R_{q1}1}\, S_{q1}^{o} + {H^{o}}_{R_{q1}2}\, S_{q1}^{e} + w_{q1} \end{aligned} \tag{4.27}$$

$$\begin{aligned} {r_{q1}}^{*e} &= -{H^{*e}}_{R_{q1}1}\, S_{11}^{e} + {H^{*e}}_{R_{q1}2}\, S_{11}^{o} + \cdots \\ &\quad - {H^{*e}}_{R_{q1}1}\ S_{q1}^{e} + {H^{*e}}_{R_{q1}2}\, S_{q1}^{o} + w_{q1}^{'*} \end{aligned} \tag{4.28}$$

where w_{q1}, ${w'}_{q1}$, represent AWGN and ${H^{o}}_{R_{q1}1}$, ${H^{o}}_{R_{q1}2}$, and ${H^{e}}_{R_{q1}1}$, ${H^{e}}_{R_{q1}2}$, ${H^{*e}}_{R_{q1}1}$, ${H^{*e}}_{R_{q1}2}$, are the odd and even component frequency responses and there conjugate

respectively, at a given sub-carrier *k*, as depicted in Figure 4.2. Equations (4.27), (4.28) can also be written as:

$$\begin{bmatrix} {r_{q1}}^{t1} \\ {r_{q1}}^{*t2} \end{bmatrix} = \begin{bmatrix} {H^o}_{R_{q1}1} & {H^o}_{R_{q1}2} \\ {H^{*e}}_{R_{q1}2} & -{H^{*e}}_{R_{q1}1} \end{bmatrix} \begin{bmatrix} S_{11}^o \\ S_{11}^e \end{bmatrix} + \cdots$$
$$+ \begin{bmatrix} {H^o}_{R_{q1}1} & {H^o}_{R_{q1}2} \\ {H^{*e}}_{R_{q1}2} & -{H^{*e}}_{R_{q1}1} \end{bmatrix} \begin{bmatrix} S_{q1}^o \\ S_{q1}^e \end{bmatrix} + \begin{bmatrix} w_{q1} \\ {w^*}_{q1} \end{bmatrix} \quad (4.29)$$

The received signal by the *q-th* user is summation of transmitted signal from all *K* transmit stream and can be represented by equation (4.30).

$$\begin{bmatrix} {r_{q1}}^{o} \\ {r_{q1}}^{*e} \end{bmatrix} = \sum_{q=1}^{K} \begin{bmatrix} {H^o}_{R_{q1}1} & {H^o}_{R_{q1}2} \\ {H^{*e}}_{R_{q1}2} & -{H^{*e}}_{R_{q1}1} \end{bmatrix} \begin{bmatrix} S_{q1}^o \\ S_{q1}^e \end{bmatrix} + \begin{bmatrix} w_{q1} \\ {w^*}_{q1} \end{bmatrix} \quad (4.30)$$

Equation (4.30) can be rewritten as:

$$y_q = \begin{bmatrix} {r_{q1}}^{o} \\ {r_{q1}}^{*e} \end{bmatrix} = H_{q1,e} \begin{bmatrix} S(1) \\ S(2) \\ \vdots \\ S(K) \end{bmatrix} + \begin{bmatrix} w_{q1} \\ {w^*}_{q1} \end{bmatrix} \quad (4.31)$$

Where $H_{q1,e}$ the equivalent matrix for channel user with single receive antenna

$$H_{q1,e} = \begin{bmatrix} {H^o}_{R_{q1}1} & {H^o}_{R_{q1}2} & {H^o}_{R_{q1}3} & {H^o}_{R_{q1}4} & \dots {H^o}_{R_{q1}Mt-1} & {H^o}_{R_{q1}Mt} \\ {H^{*e}}_{R_{q1}2} & -{H^{*e}}_{R_{q1}1} & {H^{*e}}_{R_{q1}4} & -{H^{*e}}_{R_{q1}3} & \cdots {H^{*e}}_{R_{q1}Mt} & -{H^{*e}}_{R_{q1}Mt-1} \end{bmatrix} \quad (4.32)$$

$$\begin{bmatrix} {r_{q1}}^{o} \\ {r_{q1}}^{*e} \end{bmatrix} = \begin{bmatrix} {H^o}_{R_{q1}1} & {H^o}_{R_{q1}2} \\ {H^{*e}}_{R_{q1}2} & -{H^{*e}}_{R_{q1}1} \end{bmatrix} \begin{bmatrix} S_{q1}^o \\ S_{q1}^e \end{bmatrix}$$
$$+ \sum_{j \neq q}^{K} \begin{bmatrix} {H^o}_{R_{q1}1} & {H^o}_{R_{q1}2} \\ {H^{*e}}_{R_{q1}2} & -{H^{*e}}_{R_{q1}1} \end{bmatrix} \begin{bmatrix} S_{j1}^o \\ S_{j1}^e \end{bmatrix} + \begin{bmatrix} w_{q1} \\ {w^*}_{q1} \end{bmatrix} \quad (4.33)$$

From the equation we can rewrite the received signal in vector form:

$$y_q = H_{q1,e}\ S_q + \sum_{j=1, j \neq q}^{K} H_{q1,e}\ S_j + w_q$$
$$y_q = H_{q1,e}\ S_q + Z_q + w_q \quad (4.34)$$

We can see from (4.34), that the received DL signal at the MS's experience MUI component on the *k*-th user is represented as Z_q.

4.5.4.2 User with Two receive antenna

We consider R_{q1}, R_{q2}, the receive antennas for each user, the received signal of the *q*-th user can be represented by the following equation:

$$r_{q1}{}^{o} = H^{o}{}_{R_{q1}1}\ S^{o}{}_{11} + H^{o}{}_{R_{q1}2}\ S^{e}_{11}\ + \cdots$$
$$+H^{o}{}_{R_{q1}1}\ S^{o}_{q1} + H^{e}{}_{R_{q1}2}\ S^{e}_{q1} + w_{q1} \qquad (4.35)$$

$$r_{q1}{}^{*e} = -H^{*e}{}_{R_{q1}1}\ S^{e}_{11} + H^{*e}{}_{R_{q1}2}\ S^{o}_{11} + \cdots$$
$$-H^{*e}{}_{R_{q1}1}\ S^{e}_{q1} + H^{*o}{}_{R_{q1}2}\ S^{o}_{q1} + w'^{*}_{q1} \qquad (4.36)$$

$$r_{q2}{}^{o} = H^{o}{}_{R_{q2}1}\ S^{o}{}_{11} + H^{o}{}_{R_{q2}2}\ S^{e}_{11}\ + \cdots$$
$$+H^{o}{}_{R_{q2}1}\ S^{o}_{q1} + H^{e}{}_{R_{q2}2}\ S^{e}_{q1} + w_{q2} \qquad (4.37)$$

$$r_{q2}{}^{*e} = -H^{*e}{}_{R_{q2}1}\ S^{e}_{11} + H^{*e}{}_{R_{q2}2}\ S^{o}_{11} + \cdots$$
$$-H^{*e}{}_{R_{q2}1}\ S^{e}_{q1} + H^{*o}{}_{R_{q2}2}\ S^{o}_{q1} + w'^{*}_{q2} \qquad (4.38)$$

where w_{q1}, w'_{q1}, w_{q2}, w'_{q2}, represent AWGN and $H^{o}{}_{R_{q2}1}$, $H^{o}{}_{R_{q2}2}$ and $H^{e}{}_{R_{q2}1}$, $H^{e}{}_{R_{q2}2}$, $H^{*e}{}_{R_{q2}1}$, $H^{*e}{}_{R_{q2}2}$ are the odd and even component frequency responses and there conjugate, at a given subcarrier *k.*

Equations (5.35), (5.36) , (5.37) , (5.38) can also be written as:

$$\begin{bmatrix} r_{q1}{}^{o} \\ r_{q1}{}^{*e} \\ r_{q2}{}^{o} \\ r_{q2}{}^{*e} \end{bmatrix} = \begin{bmatrix} H^{o}{}_{R_{q1}1} & H^{o}{}_{R_{q1}2} \\ H^{*e}{}_{R_{q1}2} & -H^{*e}{}_{R_{q1}1} \\ H^{o}{}_{R_{q2}1} & H^{o}{}_{R_{q2}2} \\ H^{*e}{}_{R_{q2}2} & -H^{*e}{}_{R_{q2}1} \end{bmatrix} \begin{bmatrix} S^{o}_{11} \\ S^{e}_{11} \end{bmatrix} + \cdots$$
$$+ \begin{bmatrix} H^{o}{}_{R_{q1}1} & H^{o}{}_{R_{q1}2} \\ H^{*e}{}_{R_{q1}2} & -H^{*e}{}_{R_{q1}1} \\ H^{o}{}_{R_{q2}1} & H^{o}{}_{R_{q2}2} \\ H^{*e}{}_{R_{q2}2} & -H^{*e}{}_{R_{q2}1} \end{bmatrix} \begin{bmatrix} S^{o}_{q1} \\ S^{e}_{q1} \end{bmatrix} + \begin{bmatrix} w_{q1} \\ w'^{*}{}_{q1} \\ w_{q2} \\ w'^{*}{}_{q2} \end{bmatrix} \qquad (4.39)$$

The received signal by the *q-th* user is summation of transmitted signal from all *K* transmit stream and can be represented by equation (4.40)".

$$\begin{bmatrix} r_{q1}{}^{o} \\ r_{q1}{}^{*e} \\ r_{q2}{}^{o} \\ r_{q2}{}^{*e} \end{bmatrix} = \sum_{q=1}^{K} \begin{bmatrix} H^{o}{}_{R_{q1}1} & H^{o}{}_{R_{q1}2} \\ H^{*e}{}_{R_{q1}2} & -H^{*e}{}_{R_{q1}1} \\ H^{o}{}_{R_{q2}1} & H^{o}{}_{R_{q2}2} \\ H^{*e}{}_{R_{q2}2} & -H^{*e}{}_{R_{q2}1} \end{bmatrix} \begin{bmatrix} S^{o}_{q1} \\ S^{e}_{q1} \end{bmatrix} + \begin{bmatrix} w_{q1} \\ w'^{*}{}_{q1} \\ w_{q2} \\ w'^{*}{}_{q2} \end{bmatrix} \qquad (4.40)$$

Equation (4.40) can be rewritten as:

$$y_q = \begin{bmatrix} {r_{q1}}^{o} \\ {r_{q1}}^{*e} \\ {r_{q2}}^{o} \\ {r_{q2}}^{*e} \end{bmatrix} = H_{q2,e} \begin{bmatrix} S(1) \\ S(2) \\ \vdots \\ S(K) \end{bmatrix} + \begin{bmatrix} w_{q1} \\ {w^{*}}_{q1} \\ w_{q2} \\ {w^{*}}_{q2} \end{bmatrix} \tag{4.41}$$

$$\begin{bmatrix} {r_{q1}}^{o} \\ {r_{q1}}^{*e} \\ {r_{q2}}^{o} \\ {r_{q2}}^{*e} \end{bmatrix} = \begin{bmatrix} {H^{o}}_{R_{q1}1} & {H^{o}}_{R_{q1}2} \\ {H^{*e}}_{R_{q1}2} & -{H^{*e}}_{R_{q1}1} \\ {H^{o}}_{R_{q2}1} & {H^{o}}_{R_{q2}2} \\ {H^{*e}}_{R_{q2}2} & -{H^{*e}}_{R_{q2}1} \end{bmatrix} \begin{bmatrix} S_{q1}^{o} \\ S_{q1}^{e} \end{bmatrix}$$

$$+ \sum_{j \neq q}^{K} \begin{bmatrix} {H^{o}}_{R_{q1}1} & {H^{o}}_{R_{q1}2} \\ {H^{*e}}_{R_{q1}2} & -{H^{*e}}_{R_{q1}1} \\ {H^{o}}_{R_{q2}1} & {H^{o}}_{R_{q2}2} \\ {H^{*e}}_{R_{q2}2} & -{H^{*e}}_{R_{q2}1} \end{bmatrix} \begin{bmatrix} S_{j1}^{o} \\ S_{j1}^{e} \end{bmatrix} + \begin{bmatrix} w_{q1} \\ {w^{*}}_{q1} \\ w_{q2} \\ {w^{*}}_{q2} \end{bmatrix} \tag{4.42}$$

From the equation we can rewrite the received signal in vector form:

$$y_q = H_{q2,e}\ S_q + \sum_{j=1, j \neq q}^{K} H_{q2,e}\ S_j + w_q$$

$$y_q = H_{q2,e}\ S_q + Z_q + w_q \tag{4.43}$$

We can see from (5.43), that the received DL signal at the MS's experience MUI component on the q-th user is represented as Z_q.

$$H_{q2,e} = \begin{bmatrix} {H^{o}}_{R_{q1}1} & {H^{o}}_{R_{q1}2} & {H^{o}}_{R_{q1}3} & {H^{o}}_{R_{q1}4} & \cdots & {H^{o}}_{R_{q1}Mt-1} & {H^{o}}_{R_{q1}Mt} \\ {H^{*e}}_{R_{q1}2} & -{H^{*e}}_{R_{q1}1} & {H^{*e}}_{R_{q1}4} & -{H^{*e}}_{R_{q1}3} & \cdots & {H^{*e}}_{R_{q1}Mt} & -{H^{*e}}_{R_{q1}Mt-1} \\ {H^{o}}_{R_{q2}1} & {H^{o}}_{R_{q2}2} & {H^{o}}_{R_{q2}3} & {H^{o}}_{R_{q2}4} & \cdots & {H^{o}}_{R_{q2}Mt-1} & {H^{o}}_{R_{q2}Mt} \\ {H^{*e}}_{R_{q2}2} & -{H^{*e}}_{R_{q2}1} & {H^{*e}}_{R_{q2}4} & -{H^{*e}}_{R_{q2}3} & \cdots & {H^{*e}}_{R_{q2}Mt} & -{H^{*e}}_{R_{q2}Mt-1} \end{bmatrix} \tag{4.44}$$

We can rewrite the q-th equivalent channel user matrix as follows:

$$\widetilde{H}_{q,SFBC} = \begin{bmatrix} h_{11}^{o(q)} & h_{12}^{o(q)} & \cdots & h_{1Mt-1}^{o(q)} & h_{1Mt}^{o(q)} \\ h_{12}^{e^{*}(q)} & -h_{11}^{e^{*}(q)} & \cdots & h_{1Mt}^{e^{*}(q)} & -h_{1Mt-1}^{e^{*}(q)} \\ h_{21}^{o(q)} & h_{22}^{o(q)} & \cdots & h_{R_qMt-1}^{o(q)} & h_{2Mt}^{o(q)} \\ h_{22}^{e^{*}(q)} & -h_{21}^{e^{*}(q)} & \cdots & h_{2Mt}^{e^{*}(q)} & -h_{2Mt-1}^{e^{*}(q)} \\ \vdots & \vdots & \vdots & \vdots & \vdots \\ \vdots & \vdots & \cdots & \vdots & \vdots \\ h_{R_q1}^{o(q)} & h_{R_q2}^{o(q)} & \cdots & h_{R_qMt-1}^{o(q)} & h_{R_qMt}^{o(q)} \\ h_{R_q2}^{e^{*}(q)} & -h_{R_q1}^{e^{*}(q)} & \cdots & h_{R_qMt}^{e^{*}(q)} & -h_{R_qMt-1}^{e^{*}(q)} \end{bmatrix} \tag{4.45}$$

Finally the entire multiuser MIMO channel may be characterized by the super-matrix H, which may be constructed by concatenating the corresponding channel matrices $\{\widetilde{H}_q\}_{q=1}^{K}$ associated with each of the MS's, and the composite channel matrix is denote as:

$$\widetilde{H}_{SFBC} = \left[\widetilde{H}_{SFBC}^{(1)}, \widetilde{H}_{SFBC}^{(2)}, \widetilde{H}_{SFBC}^{(3)}, \ldots\ldots, \widetilde{H}_{SFBC}^{(K)}\right] \quad (4.46)$$

The overall user received signal can be rewritten as:

$$\begin{bmatrix} y(1) \\ y(2) \\ \vdots \\ y(K) \end{bmatrix} = \widetilde{H}_{SFBC} \begin{bmatrix} S(1) \\ S(2) \\ \vdots \\ S(K) \end{bmatrix} + \begin{bmatrix} w(1) \\ w(2) \\ \vdots \\ w(K) \end{bmatrix} \quad (4.47)$$

We can detect the desired signal vectors, $S(q)$, q=1,..,K from equation (4.47), using V_BLAST (OSIC) based on ZF solution referred to ZF-OSIC, and hence remove the interference between the K transmitted streams and subsequently implemented the STBC decoding.

4.6 Simulation Results

Monte Carlo simulation results are provided in this section for the multilayered space frequency and space time block coded OFDM schemes to demonstrate the performance of the proposed technique in the downlink transmission. We consider an Alamouti space time coded OFDM system with $N = 64$ (N is the FFT size). The maximum channel delay spread and the CP length are the same and equal to L=16. In other words, channel with long excess delay time, e.g. $\tau_{max} = T_G$ (T_G guard interval or CP length), exhibit a lower coherence bandwidth corresponding to higher frequency selectivity than shorter channel. The SISO channels from the transmit antenna to the receive antenna are assumed to be independent and Rayleigh distributed. The complex symbols are assumed to be quaternary phase shift keying (QPSK).

We employ Mt transmit antennas at the base station. The results are evaluated for different number of receive antennas at the MS, the bit error rate (BER) is plotted according to the signal to noise ratio (SNR). We use the notation $Mt \times Nr$ to denote a scheme with Mt Tx and Nr Rx antennas from the BTS to the all users receiver.

In simulations where the hybrid schemes STC or SFC are compared using MU V-BLAST receiver referred by ZF-OSIC, the criterion used to select the number of Tx and Rx antennas is the number of DOF available at the receiver for MUI cancellation.

4.6.1 Performance Comparison of Hybrid MU Schemes

Figure 4.3 demonstrates the performance of the proposed hybrid MU STBC-OFDM system, and show the BER under various system loads using ZF-OSIC detection. When each user has one receive antenna, three cases are investigated: a single user and 2 transmit antennas at the BTS denoted by (2x1); a 2 user system with 4 transmit antennas at BTS denoted by (4x2); and a 3 user system with 6 transmit antennas at BTS denoted by (6x3).

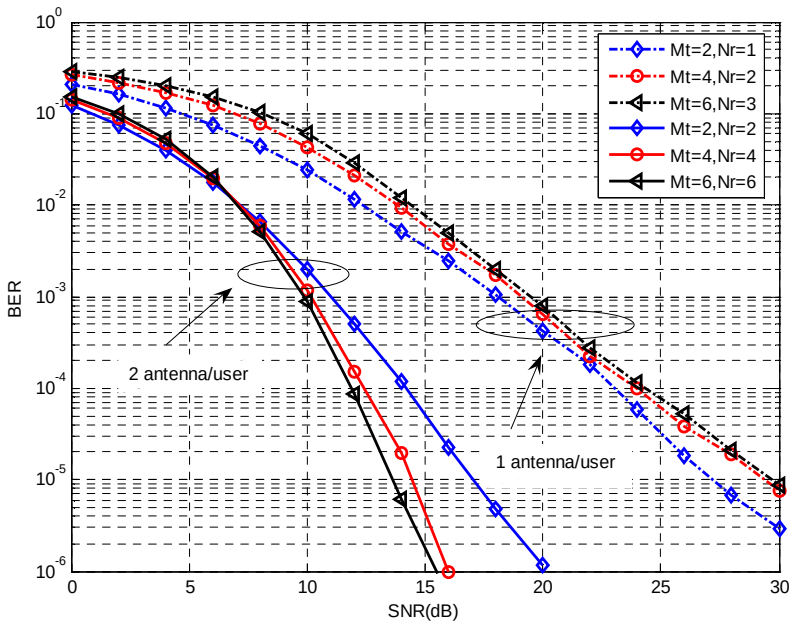

Figure 4.3: Performance comparison of single user and MU STBC-OFDM system with 1 or 2 receive antennas/user, using ZF-OSIC detection.

From Figure 4.3, it is shown that that the performances of a single user with diversity order of 2 at almost a BER=10^{-5}, performs better than 2 users and 3 users system by 2.5 dB. The performance degradation due to the imperfect cancellation of noise and MUI or (MAI from the multiple transmit antennas). Both of these factors contribute noise to the decoding process and therefore limit the STBC-OFDM performance at each user.

When each user has two receive antennas, again three cases are studied: single user and 2 transmit antennas at the BTS denoted by (2x2); a 2 user system and 4 transmit antennas at the BTS denoted by (4x4); and a 3 user system and 6 transmit antennas at the BTS denoted by (6x6). By contrast, the performance of a 3 users system at a BER=10^{-6}, performs better than 2 users by 0.5 dB and single user system by 4.5 dB, respectively. The multiuser system at high SNR, achieves better performance than a single user STBC-OFDM system, which obtained a

diversity order of 4. This higher diversity gain greatly improves the BER performance, as compared to the performance results with one receive antenna per user.

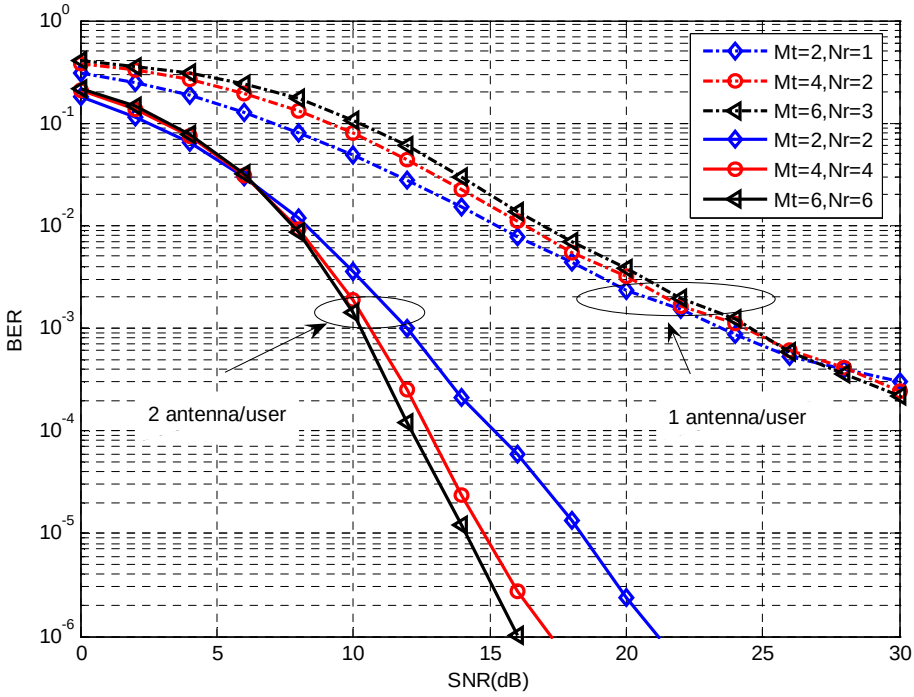

Figure 4.4: Performance comparison of single user and MU SFBC-OFDM system with 1 or 2 receive antennas/user using ZF-OSIC detection.

Figures 4.4, demonstrates the performance of the proposed hybrid MU SFBC-OFDM system, and show the BER under various system loads using ZF-OSIC detection. When each user has one receive antenna, three cases are investigated: a single user and 2 transmit antennas at the BTS denoted by (2x1); a 2 user system with 4 transmit antennas at BTS denoted by (4x2); and a 3 user system with 6 transmit antennas at BTS denoted by (6x3).

From Figure 4.4, it is shown that the hybrid MU system achieves almost the same performance with a single user SFBC coding scheme at almost a BER=10^{-4}. In this case at SNR=30 dB, some BER saturation is observed for all users system, due to some unequalized ISI residual and imperfect MUI cancellation.

When each user has two receive antennas, again three cases are studied: single user and 2 transmit antennas at the BTS denoted by (2x2); a 2 user system and 4 transmit antennas at the BTS denoted by (4x4); and a 3 user system and 6 transmit antennas at the BTS denoted by (6x6). By contrast, the performance of a 3 users system at a BER=10^{-6}, performs better than 2 users by 1 dB and single user system by 5 dB.

The multiuser system at high SNR, achieves better performance than a single user SFBC-OFDM system, which obtained a diversity order of 4. This higher diversity gain greatly improves the BER performance, as compared to the performance results with one receive antenna per user.

4.6.2 Performance Comparison between ST and SF Code

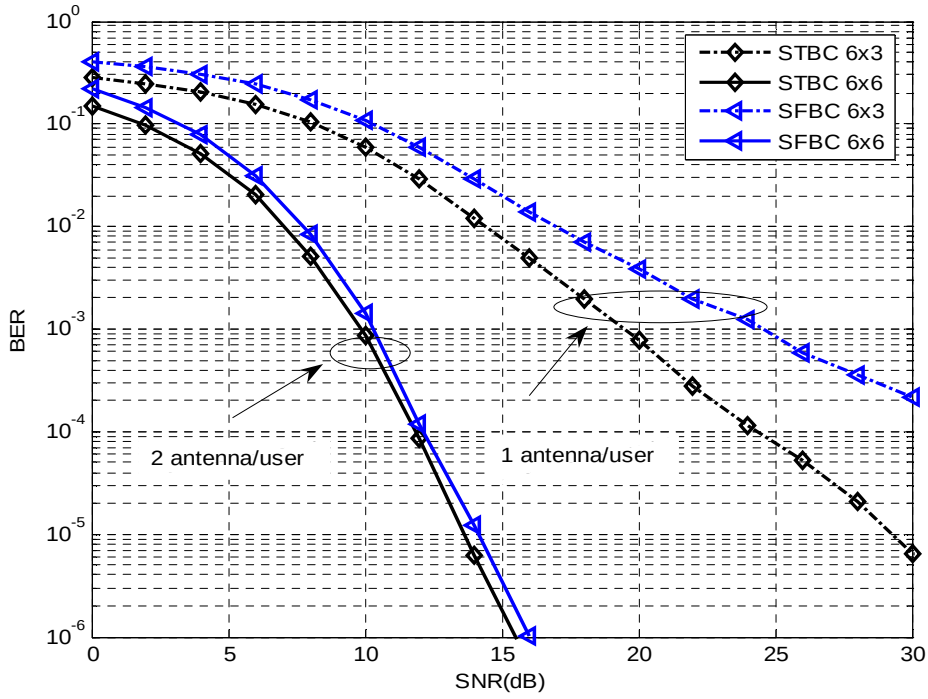

Figure 4.5: Performance comparison of 6x6 and 6x3 for hybrid MU STBC-OFDM and SFBC-OFDM with ZF-OSIC detection.

Figure 4.5, illustrate the bit error rate for a hybrid MU scheme with 6x3 and 6x6 antenna configuration, we can observe that the increase in the number of receive antenna effectively improves the performance. And show the performance comparison of hybrid MU STBC-OFDM and SFBC-OFDM in the same frequency selective fading channel. The channel is block fading but remains constant over two consecutive OFDM symbol periods as required by STBC-OFDM.

From the Figure 4.5, for the hybrid MU with 6x6 configuration scheme, it can be observed that at a BER=10^{-6}, the STBC-OFDM has a diversity gain of 0.6 dB over the SFBC-OFDM scheme. And with 6x3 configuration scheme, at almost a BER of 10^{-4}, the STBC-OFDM has a diversity gain of 7.5 dB over the SFBC-OFDM.

It was observed that increasing the *K* factor introduces more correlation between the channel paths and reduces the capacity of the channel, which results in a degradation in performance.

4.6.3 Performance of Hybrid MU STBC-OFDM under different channel taps

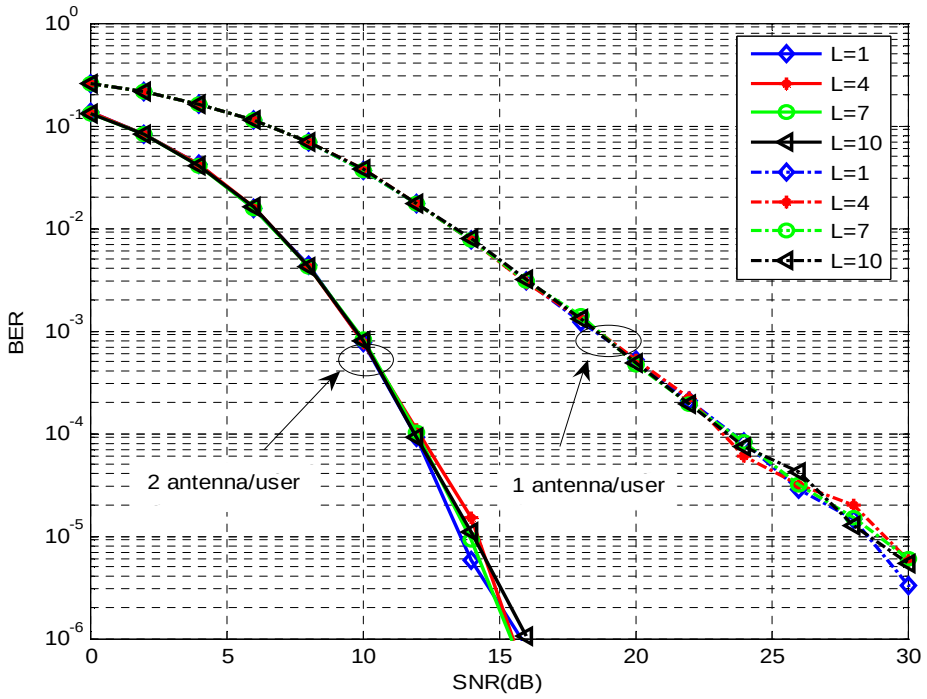

Figure 4.6: BER comparison of Hybrid MU STBC-OFDM for QPSK modulation over frequency selective fading channel with CP=10.

In this section, we examined the performance under different channel scenarios, and we compare the performance of the hybrid MU STBC-OFDM and SFBC-OFDM scheme with 2 users for Rayleigh fading channels.

Figure 4.6, illustrates the performance of multiuser detectors with 2 users for STBC-OFDM coding, and compares the performance of the 4x4 configuration of hybrid MU scheme to that of 4x2 for different *L* taps channel conditions. It can be observed that each configuration have almost the same performance with slightly difference, and the hybrid scheme perform well even in correlated channels with the increasing of *L* under the condition of $CP \geq L$. However, when adding one antenna to the user, a SNR reduction of 15 dB is achieved at a BER= 10^{-5}.

4.6.4 Performance of Hybrid MU SFBC-OFDM under different channel taps

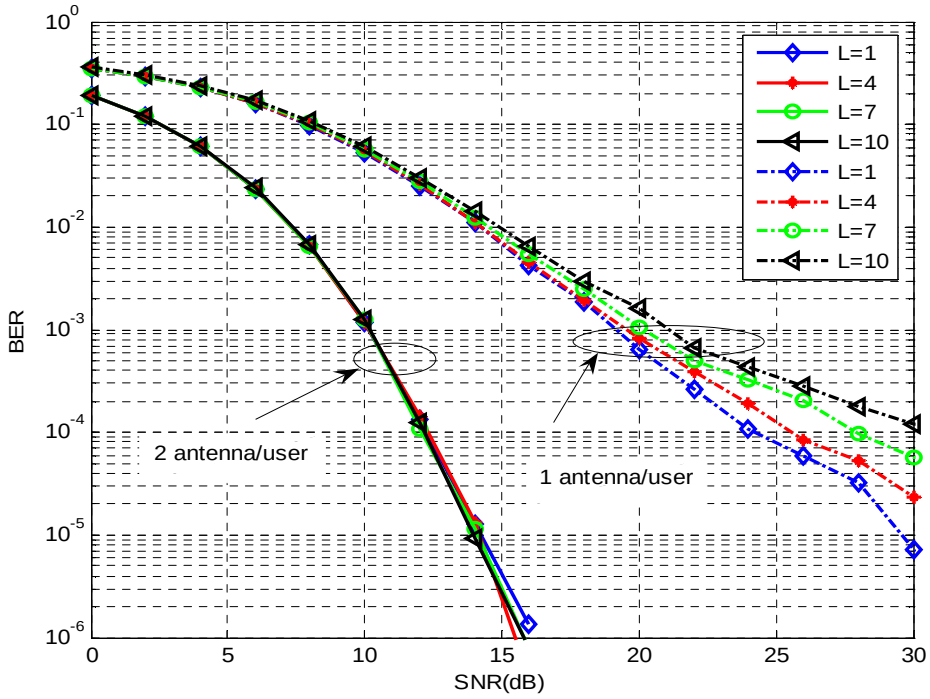

Figure 4.7**:** BER comparison of hybrid MU SFBC-OFDM for QPSK modulation over frequency selective fading channel with CP=10.

Figure 4.7, illustrates the performance of multiuser detectors with 2 users for SFBC-OFDM coding, and compares the performance of the 4x4 configuration of hybrid MU scheme to that of 4x2 for different *L* taps channel conditions. It can be observed that for 4x4 configuration has almost the same performance with slightly difference, and perform well even in correlated channels with the increasing of *L* under the condition of CP $\geq L$. By contrast, it can be observed that the performance degradation of the hybrid MU 4x2 configuration scheme with the increasing of *L* channel taps. However, when adding one antenna to the user, a SNR reduction of 15 dB is achieved at a BER= 10^{-5}, which increase with the increasing of *L*.

It was observed that increasing the *K* factor introduces more correlation between the channel paths, which results in degradation in performance. This is due to the fact that the SFBC is very sensitive to the Rayleigh fading channel, especially with high channel order.

4.7 Conclusion

In Chapter 4, the principle concept of multiuser system was presented. First part, the multiple access technique allows users to share a common communications channel. The comparison between a single and MU technique with single or multiple receive antenna, at the end of this part SDMA and beamforming technique in MIMO schemes when the channel state information (CSI) is available at the transmitter and the receiver side. Furthermore, brief discussion about multiuser detection techniques.

The second part, We have proposed the hybrid MU multilayered space frequency and space time coding schemes for OFDM systems under the frequency selective channel that provides both diversity and multiplexing gains, which achieve higher data rates with reliable transmission. The combined spatial multiplexing and space time coding architecture with orthogonal frequency division multiplexing (OFDM). The OFDM modulator transforms the frequency selective MIMO channels into parallel flat fading channels in the frequency domain.

The hybrid multilayered MU scheme was studied in downlink system using the V-BLAST, with the ZF-OSIC detection receiver, first the encoding and the decoding process for different receive antenna per user. Both space time codes (STC) and space frequency codes (SFC) are used.

The performance of the hybrid MU scheme, under various loads of *K* users for the both, with 1or 2 receive antenna per user, was compared for Rayleigh fading channel. The hybrids MU STBC-OFDM outperform and is the best choice more than hybrid MU SFBC-OFDM, and provide full receive diversity for each layer. We also, examined the effect of the delay spread of the channel, and the performance of the hybrid MU scheme was evaluated under different channel taps.

Simulations showed that space time coding is more robust than frequency coding in Rayleigh fading channel. So the hybrid MU STBC-OFDM is more robust in frequency selective channel under the condition of the CP equal at least the max of the delay spread of the channel, and the MU SFBC-OFDM is more sensitive to the delay spread of the channel. However, the main limitation of the hybrid MU scheme with ZF-OSIC detection is the increased number of receive antennas is necessary at the mobile terminal.

CHAPTER V

Combining SVD and MU MIMO-OFDM Schemes

5.1 Beamforming for Multi User Systems

Multi antenna techniques exploit multiple antennas at transmitter (T_X) and/or receiver (R_X), e. g. diversity techniques can be used to obtain reliable transmission systems or beamforming (BF) can be used to increase the signal strength towards a particular user, thus reducing interference to others. Traditionally spatial diversity is exploited involving multiple antennas in transmitter (Transmit Diversity: TD) and/or receiver (Receive Diversity: RD). Transmit diversity is a lucrative and reasonable choice for downlink (DL), i.e, BS to MS, especially for portable receivers where current drain and physical size are important constraints.

In a system with multiple transmit antennas; information can be transmitted by employing various transmission techniques. One way is to transmit a weighted version of the same information symbol from all the antennas. The weights can be adjusted to compensate for the distortion caused by the downlink channel on transmit signals. This method is called transmit beamforming and requires the receiver to estimate the downlink channel and feed back this information to the transmitter from time to time. It is shown in [21] that for the multiple access schemes, the BF always performs better in outdoor environment. Transmit and receiver beamforming for multiuser systems when each user is equipped with a single or multiple antennas have been studied [30, 33, 99]. Receiver beamforming has been shown to be effective in interference suppression in multiuser systems [31, 32, 33].

In particular, it was proven that MIMO eigen-mode (EM) transmission system is optimal [33, 83], because MIMO capacity is maximized. MIMO EM uses the left and right eigen-vectors of the channel matrix as eigen-beamformers in the receiver (Rx) and transmitter (Tx) respectively to form orthogonal spatial eigen-beams for transmission. Since channel state information (CSI) regarding the eigen-beamformers is required, a closed loop system consisting of a feedback channel from the Rx is needed if the channel is not reciprocal, such as in a FDD system. As the wireless channel is constantly changing, MIMO EM (as for all closed loop MIMO systems) is however extremely vulnerable to the presence of feedback delay which is unavoidable in a practical system [98].

In fact the advantages of MIMO are far more fundamental. The underlying mathematical nature of MIMO, where data is transmitted over a matrix rather than a vector channel, creates new and enormous opportunities beyond just the added diversity or array gain benefits. Under certain conditions, can be transmit $min\,(Nr, Mt)$ independent data streams simultaneously over the eigen-modes of a matrix channel created by Nr and Mt antennas.

The capacity grows linearly with $m = min\ (Nr, Mt)$ rather than logarithmically as shown in section 1.3. The determinant operator yields a product of m non-zero eigen-values of its matrix argument, each eigen-value characterizing the SNR over a so called channel eigen-mode. An eigen-mode corresponds to the transmission using a pair of right and left singular vectors of the channel matrix as transmit antenna and receive antenna weights respectively. Clearly, this growth is dependent on properties of the eigen-values.

In [69,100], show that use of the Singular value Decomposition (SVD) to obtain the largest eigen. In some sense, eigen beamforming is an optimal space time processing scheme [101,102]. However, it requires SVD on every subcarrier. The receiver not only needs to feedback the largest eigen, but also the corresponding eigen-vectors.

5.1.1 MIMO-OFDM EM

MIMO channel provides a multiplexing gain which results from the fact that the channel can be decomposed into a number of m parallel independent channels. By multiplexing independent data onto these independent channels, we get an m fold increase in data rate in comparison to a system with just one antenna at the transmitter and receiver. This increase data rate is called multiplexing gain or DOF gain.

The enlargement of the MIMO system capacity can be described as multiplexing data streams into parallel sub-channels (pipes) on the same frequency band. The pipes can be viewed as independent radio channels. MIMO channels can be transformed into parallel flat fading chanels through SVD. The column vectors of flat fading channel matrix H are usually non-orthogonal. However, by a SVD the channel matrix can be decomposed into diagonal matrix $D^{1/2}$ and two unitary matrices U and V.

Consider a single user MIMO-OFDM EM utilizing N sub-carriers with Mt Tx and Nr Rx antennas signaling over a MIMO frequency selective fading channel. The complex baseband representation of the received signal in the *k*-th sub-carrier, $k \in \{1, \dots, N\}$, can be denoted as

$$y_k = H_k\, x_k + w_k \qquad (5.1)$$

where $y_k \in C^{Nr\times 1}$ and $x_k \in C^{Mt\times 1}$ are the received and transmitted signal vector for the *k*-th sub-carrier respectively, $H_k \in C^{Nr\times Mt}$ is the frequency domain channel response matrix for the *k*-th subcarrier with possibly correlated coefficients $H_k^{ji} \in CN(0,1)$ where $j \in \{1, \dots, Nr\}$, $i \in \{1, \dots, Mt\}$, and $w_k \in C^{Nr\times 1}$ is the AWGN with elements $w_{k,j} \in CN(0, \sigma^2)$.

When the transmitter knows perfectly the channel state, the MIMO channel matrix of the *k*-th frequency tone H_k can be decomposed into orthogonal sub-channels using SVD. Assuming perfect CSIT, an SVD decomposition of the MIMO channel provides r_H orthogonal sub-channels where r_H is the rank of the channel matrix H_k. The MIMO channel within each sub-carrier can be decomposed into $r_H = min(Mt, Nr)$ equivalent orthogonal SISO channels (eigen-modes), as shown in section 1.3, by first performing a SVD on the channel response matrices as follows:

$$H_k = U_k D_k^{1/2} V_k^H \tag{5.2}$$

where V_k^H is the transpose conjugate of the matrix V, the $Nr \times Nr$ matrix U and the $Mt \times Mt$ matrix V are unitary matrices (i.e., $UU^H = INr$ and $V^H V = IMt$) are the Rx and Tx eigen-beamforming matrices with orthonormal columns and $D_k^{1/2} = diag(\sqrt{\lambda_{k,1}}, \dots, \sqrt{\lambda_{k,r_H}})$ is a $Nr \times Mt$ diagonal matrix whose non zero diagonal elements $\lambda_1, \lambda_2, \dots., \lambda_{r_H}$, are the real nonnegative singular values of H_k for eigen-modes, from 1 to r_H of the *k*-th sub-carrier arranged in descending order and other elements are zero.

From linear algebra the number of singular values which is also the rank of matrix H cannot exceed the number of columns or rows of the matrix. The rank of matrix is given by $r_H \leq min(Mt, Nr)$ with equality if the matrix is full rank all rows and columns are independent.

By substituting the SVD decomposition given in (5.2) into the received signal the following is obtained:

$$y_k = U_k D_k^{1/2} V_k^H \, x_k + w_k \tag{5.3}$$

Left multiplying (5.3) by U_k^H and using the unitary property of matrix *U* yields

$$U_k^H y_k = U_k^H U_k D_k^{1/2} V_k^H \, x_k + U_k^H w_k$$

$$U_k^H y_k = D_k^{1/2} V_k^H \, x_k + U_k^H w_k \tag{5.4}$$

If vectors $U_k^H y_k$, $V_k^H \, x_k$ and $U_k^H w_k$ are denoted $\tilde{y}_k$, $\tilde{x}_k$ and $\tilde{w}_k$ respectively, (5.4) simplifies to:

$$\tilde{y}_k = D_k^{1/2} \, \tilde{x}_k + \tilde{w}_k \tag{5.5}$$

In order to obtain the parallel decomposition of the channel, we define a transformation on the input and output of the channel via the unitary matrices $U$and V as follows:

$\tilde{x}_k = V_k^H\, x_k$, $\tilde{y}_k = U_k^H y_k$, and $\widetilde{w}_k = U_k^H w_k$

$UU^H = U^H U = I$, $VV^H = V^H V = I$

Note that U and V are unitary matrices so the transformation does not change neither the distribution of w not the energy content of x.

5.1.2 System Model

Let us consider a K users downlink MIMO-OFDM system equipped with Mt transmit antennas at the base station and R_q receive antennas for each user and $Nr = \sum_{q=1}^{K} R_q$. The spatial multiplexer of the q-th data branch generates a d_q dimensional vector symbol streams S_q. In this general setup, user K receives d_q data streams from the base station and $d = \sum_{q=1}^{K} d_q$. Thus we have Mt transmit antennas transmitting a total of d symbols to K users, who have a total of Nr receive antennas. The symbols of each user are collected in the data vector

$$S_q = \left[S_{q1}(1), S_{q2}(2), \dots, S_{qdq}(n)\right]^T \tag{5.6}$$

and the overall data vector is

$$S = [S^T(1), S^T(2), \dots, S^T(K)]^T \tag{5.7}$$

Where n is the number of the transmitted symbols stream for each user before encoding, in STC or in SFC respectively, defined as:

$$n = \begin{cases} STC & 1, \dots \dots, N \\ SFC & 1, \dots, N/2 \end{cases} \tag{5.8}$$

Where N is a sub-carriers OFDM number, and S_q $(q = 1,2,..,K)$ are symbols chosen from the same constellation set M. For convenience we assume no error correction coding and a uniform allocation of power across the sub streams for each user.

Every OFDM symbol has N sub-carriers. Due to the random positions and the rich scatters around the users, the users are mutual independent with each either. It is assumed that the transmitter and receiver both have perfect CSI. According to the feedback channel, the current channel condition of each user is sent to the base station correctly and timely. It is also assumed that the channel response is constant during an OFDM symbol.

The frequency selective fading channel with L multi-paths is considered. Let H_k represent The $Nr \times Mt$ MIMO channel frequency response matrix of k-th sub-carrier. Given that the total power is distributed equally on the frequency and spatial sub-channels, then the instantaneous capacity of MIMO-OFDM systems is given by [10].

$$C_{MIMO} = \frac{1}{N}\sum_{k=0}^{N-1} log_2[det(I_{Nr} + \rho\, H_k H_k^H)]$$

$$= \sum_{k=0}^{N-1} C_k \qquad (5.9)$$

Where, $\rho = \frac{P_{tot}}{Mt\ N\ \sigma_n^2}$, P_{tot} is the total transmitted power, σ_n^2 is the noise power, C_k is the capacity at the k-th subcarrier.

Assuming that the transmitted data streams are independently encoded and independently decoded, the sum rate capacity of the multiuser system is simply the summation of each user's individual channel capacity. Under the uniform power allocation, the sum rate capacity is given by

$$C_q = \sum_{q=1}^{K} log_2\left[det\left(I_{R_q} + \frac{E_{s,q}}{\sigma^2}\ H_q^H H_q\right)\right] \qquad (5.10)$$

At the BS before the STBC OFDM encoding we implement the eigen-beamforming, pre-processing spatial multiplexing requires CSI, in the case of OFDM systems the transmitter requires pre-processing knowledge for all subcarriers, the symbol vectors n for the q-th user is multiplied by a $(Mt \times d_q)$, pre-processing matrix P_q as shown in Figure 5.1.

The transmitted data symbol S_q which is pre-processed via

$$X_q = P_q S_q \qquad k = 1,2,..,K \qquad (5.11)$$

Where S_q is the transmitted symbol vector after MIMO encoding and P_q is the beamforming matrix , and assumed with the pre-processed symbol vectors from the other users to produce the composite transmitted symbol vector.

$$X = \sum_{q=1}^{K} P_q S_q \qquad (5.12)$$

The pre-processed symbol vectors are passed through the combining block STBC-OFDM encoder, by using the Alamouti schemes in time coding STBC-OFDM or in frequency coding SFBC-OFDM as introduced in section 3.4.

A block of data symbols (OFDM symbol) transmitted over each transmitter passes through an *N* point IFFT, and the CP is appended.

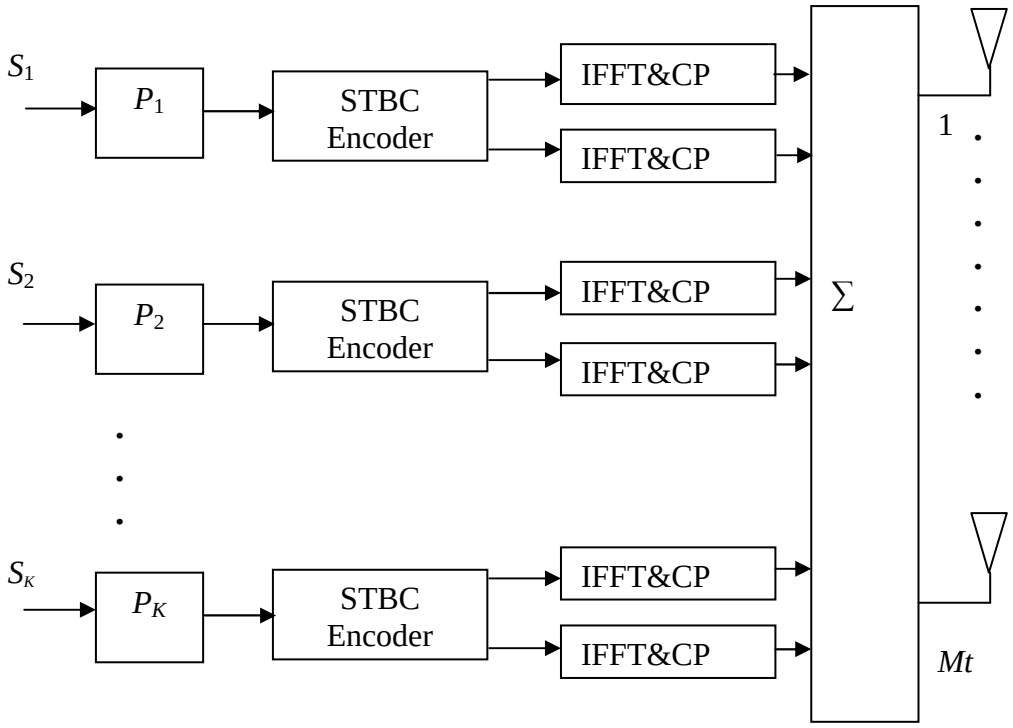

Figure 5.1: Block diagram of the SDMA DL MUT Pre-Processing

The BS transmitter broadcast the signal to multiple K users simultaneously (i,e, in the same time) over the same frequency band through the frequency selective fading channel.

At each receiver as shown in Figure 5.2 and Figure 5.8, the CP removed and the FFT is applied to revert the received signals back to frequency domain. Hence the frequency selective MIMO channel is decoupled into N parallel flat fading channels. The R_q dimensional received signal y_q at the q-th user where $R_q = 1,2$, is a super-position of the K signal branches distorted by channel fading plus AWGN.

The complex baseband representation of the received signal vectors in the *k*-th sub-carrier where $k = 1 \ldots . N$ can be expressed as:

$$y_q = \sum_{j=1}^{K} H_q C_j + w_q \tag{5.13}$$

Where *C,* is the code matrix of Alamouti scheme of the OFDM symbols.

The channel transfer matrix between the BS and the *q*-th user is denoted as:

$$H_q = \begin{bmatrix} H_{11}^{(q)} & H_{12}^{(q)} & \ldots . & H_{1Mt}^{(q)} \\ H_{21}^{(q)} & H_{22}^{(q)} & \ldots . & H_{2Mt}^{(q)} \\ \vdots & \vdots & \vdots & \vdots \\ H_{R_q 1}^{(q)} & H_{R_q 2}^{(q)} & \ldots . & H_{R_q M}^{(q)} \end{bmatrix} \tag{5.14}$$

H_q: $(R_q \times Mt)$ is the frequency domain channel response matrix for sub-carrier k, and H_{ji}^{q} is the fading coefficient modelled as a finite impulse response filter (FIR) with *L* taps, associated with the i^{th} BS antenna and *r*-th receive antenna of user q, at a given sub-carrier *k*. where $r = \{1, \ldots, R_q\}$ and $i = \{1, \ldots, Mt\}$.The elements of H_q are samples of independent and identically distributed (i,i,d) complex Gaussian random variables, circularly symmetric distributed with unit variance $CN(0,1)$.

The AWGN at the *r*-th receive antenna of user, $w_q = \left[w_1, w_2, \ldots, w_{R_q}\right]$, follows distribution $CN(0, \sigma_w^2 I)$**,** where I is the $(R_q \times R_q)$ identity matrix. Finally the entire multiuser MIMO channel may be characterized by the super-matrix H, which may be constructed by concatenating the corresponding channel matrices $\{H_q\}_{q=1}^{K}$ associated with each of the MS's, and the composite channel matrix is denote as:

$$H = \left[H^{(1)}, H^{(2)}, H^{(3)}, \ldots \ldots, H^{(K)}\right]^T \tag{5.15}$$

We rewrite the equation (5.13) by explicit the matrix coding as function with data symbol, and introducing the pre-processed data symbol, hence the signal form become as follows:

$$\tilde{y}_q = \sum_{j=1}^{K} \widetilde{H}_q X_j + w_q \tag{5.16}$$

$$\tilde{y}_q = \sum_{j=1}^{K} \widetilde{H}_q P_q S_j + w_q \tag{5.17}$$

Where $\widetilde{H}_q$ is the equivalent channel transfer matrix in STC or SFC between the BTS and the q-th user for STBC-OFDM and SFBC-OFDM respectively denoted by the following channel matrix:

$$\widetilde{H}_{q,STBC} = \begin{bmatrix} h_{11}^{(q)} & h_{12}^{(q)} & \dots & h_{1Mt-1}^{(q)} & h_{1M}^{(q)} \\ h_{12}^{(q)} & -h_{11}^{(q)} & \cdots & h_{1Mt}^{(q)} & -h_{1Mt-1}^{(q)} \\ h_{21}^{(q)} & h_{22}^{(q)} & \vdots\vdots & h_{R_qMt-1}^{(q)} & h_{2Mt}^{(q)} \\ h_{22}^{(q)} & -h_{21}^{(q)} & \dots & h_{2Mt}^{(q)} & -h_{2Mt-1}^{(q)} \\ \vdots & \vdots & \vdots & \vdots & \vdots \\ \vdots & \vdots & \dots & \vdots & \vdots \\ h_{R_q1}^{(q)} & h_{R_q2}^{(q)} & \dots & h_{R_qMt-1}^{(q)} & h_{R_qMt}^{(q)} \\ h_{R_q2}^{(q)} & -h_{R_q1}^{(q)} & \dots & h_{R_qM}^{(q)} & -h_{R_qMt-1}^{(q)} \end{bmatrix} \quad (5.18)$$

$$\widetilde{H}_{q,SFBC} = \begin{bmatrix} h_{11}^{o(q)} & h_{12}^{o(q)} & \dots & h_{1Mt-1}^{o(q)} & h_{1Mt}^{o(q)} \\ h_{12}^{e^*(q)} & -h_{11}^{e^*(q)} & \cdots & h_{1M}^{e^*(q)} & -h_{1Mt-1}^{e^*(q)} \\ h_{21}^{o(q)} & h_{22}^{o(q)} & \vdots\vdots & h_{R_qMt-1}^{o(q)} & h_{2Mt}^{o(q)} \\ h_{22}^{e^*(q)} & -h_{21}^{e^*(q)} & \dots & h_{2Mt}^{e^*(q)} & -h_{2M-1}^{e^*(q)} \\ \vdots & \vdots & \vdots & \vdots & \vdots \\ \vdots & \vdots & \dots & \vdots & \vdots \\ h_{R_q1}^{o(q)} & h_{R_q2}^{o(q)} & \dots & h_{R_qMt-1}^{o(q)} & h_{R_qMt}^{o(q)} \\ h_{R_q2}^{e^*(q)} & -h_{R_q1}^{e^*(q)} & \dots & h_{R_qMt}^{e^*(q)} & -h_{R_qMt-1}^{e^*(q)} \end{bmatrix} \quad (5.19)$$

Where h_{ji} , h_{ji}^* corresponds to the channel response and there conjugate for STBC-OFDM system, where h_{ji}^o, h_{ji}^e and $h_{ji}^{o^*}$, $h_{ji}^{e^*}$ dennoting the odd and the even component, and there conjugate channel response for SFBC-OFDM system between transmit antenna i and receive antenna j.

5.2 Zero Forcing Receiver Based On SVD

In the beamforming mode, P_q is derived from the SVD of the channel matrix known by the transmitter. The optimal eign-beamforming as presented in [83, 97], is the pre-coding matrix where $P = V$, which is derived from the channel SVD as shown in section 1.3, and from (5.2), where the decomposition of *k*-th user channel SVD yielding

$$\widetilde{H}_q = U_q D_q^{1/2} V_q^H \tag{5.20}$$

Then V_q matrix is set as P_q, the pre-coding matrix is defined as :

$$P_q = V_q \qquad q = 1,2, \dots K \tag{5.21}$$

By substituting (5.21) in (5.17) the received signal can be expressed as:

$$\begin{aligned} \tilde{y}_q &= \sum_{j=1}^{K} \widetilde{H}_q V_j S_j + w_q \\ &= \widetilde{H}_q V_q S_q + \sum_{j=1, j\neq q}^{K} \widetilde{H}_q V_j S_j + w_q \\ \tilde{y}_q &= \widetilde{H}_q V_q \, S_q + Z_q + w_q \end{aligned} \tag{5.22}$$

V_q and S_q is the pre-coding matrix and the transmitted symbol vector n corresponding to the *q*-th user.

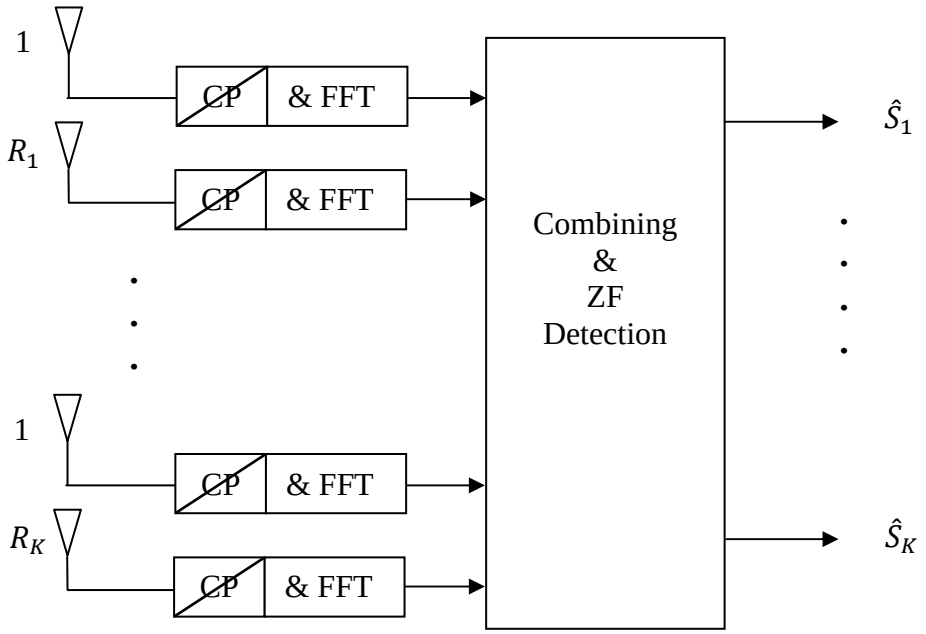

Figure 5.2: Block diagram of the SDMA DL ZF receiver

From (5.22) we see that the CCI or MUI component on the q-th user is represented as Z_q, and the equivalent effective channel can expressed by:

$$\widetilde{H}=\left[\widetilde{H}_1, \widetilde{H}_2, \widetilde{H}_3, \ldots\ldots, \widetilde{H}_K\right]^T \tag{5.23}$$

The composite multiuser received signal encountered by all receivers may be formulated as a column based super-vector constituted by the received signal vectors associated with each of the user terminal thus we have

$$\tilde{y} = \widetilde{H}V\,S + W \tag{5.24}$$

$$\begin{bmatrix} \tilde{y}^{(1)} \\ \tilde{y}^{(2)} \\ \vdots \\ \tilde{y}^{(K)} \end{bmatrix} = \widetilde{H}V \begin{bmatrix} S^{(1)} \\ S^{(2)} \\ \vdots \\ S^{(K)} \end{bmatrix} + W \tag{5.25}$$

$V = \left[V^{(1)}, V^{(2)}, V^{(3)}, \ldots\ldots, V^{(K)}\right]^T.$

$W = \left[w^{(1)}, w^{(2)}, w^{(3)}, \ldots\ldots, w^{(K)}\right]^T.$

V and W are the space time pre-processor super-matrix, as well as the AWGN noise, the super-vector constructed by concatenating the corresponding quantities associated with each user terminals. We may express the effective channel super-matrix $\widetilde{H}V$ of (5.25) as follows:

$$\widetilde{H}V = \begin{bmatrix} \widetilde{H}^{(1)}V^{(1)} & \widetilde{H}^{(1)}V^{(2)} & \ldots\ldots & \widetilde{H}^{(1)}V^{(q)} & \ldots\ldots & \widetilde{H}^{(1)}V^{(K)} \\ \widetilde{H}^{(2)}V^{(1)} & \widetilde{H}^{(2)}V^{(2)} & \ldots\ldots & \widetilde{H}^{(2)}V^{(q)} & \ldots\ldots & \widetilde{H}^{(2)}V^{(K)} \\ \vdots & \vdots & \vdots & \vdots & \vdots & \vdots \\ \widetilde{H}^{(q)}V^{(1)} & \widetilde{H}^{(q)}V^{(2)} & \vdots & \widetilde{H}^{(q)}V^{(q)} & \ldots\ldots & \widetilde{H}^{(q)}V^{(K)} \\ \vdots & \vdots & \vdots & \vdots & \ldots\ldots & \vdots \\ \widetilde{H}^{(K)}V^{(1)} & \widetilde{H}^{(K)}V^{(2)} & \ldots\ldots & \widetilde{H}^{(K)}V^{(q)} & \ldots\ldots & \widetilde{H}^{(K)}V^{(K)} \end{bmatrix} \tag{5.26}$$

The receiver sees the equivalent matrix

$$\widetilde{\widetilde{H}} = \widetilde{H}V \tag{5.27}$$

And we can detect the desired signal vector streams, S from (5.25), by the implementation of the pseudo inverse for ZF detection of the equivalent channel matrix according to [18], hence remove the interference between the transmitted user streams and subsequently implemented the STBC decoding.

We assume transmission symbol vector without pre-processing matrix and applies the pseudo inverse of classical ZF yielding to:

$$\widetilde{H}_{ZF} = (\widetilde{H}^H \widetilde{H})^{-1} \widetilde{H}^H \quad (5.28)$$

In contrast, with the pre-processing matrix and the equivalent effective channel, we can express the ZF based on SVD at the receiver solution as shown in Figure 5.2, which is referred to ZF-SVD1 as follow:

$$\widetilde{\widetilde{H}}_{ZF} = (\widetilde{\widetilde{H}}^H \widetilde{\widetilde{H}})^{-1} \widetilde{\widetilde{H}}^H \quad (5.29)$$

By setting (5.27) into (5.29) it can be easily shown that

$$\widetilde{\widetilde{H}}_{ZF} = V^H \widetilde{H}_{ZF} \quad (5.30)$$

5.3 Simulation Results

We consider the same parameter simulation as mentioned in section 4.6, but at the except we utilize the ZF-SVD1 detection for the hybrid MU STBC-OFDM and SFBC-OFDM scheme over Rayleigh fading channel, and compare the performance under various loads of *K* users for the both, with 1or 2 receive antenna per user.

5.3.1 Performance Comparison of Hybrid MU Schemes

Figure 5.3 demonstrates the performance of the proposed hybrid MU STBC-OFDM system, and show the BER under various system loads using ZF-SVD1 detection. When each user has one receive antenna, three cases are investigated: a single user and 2 transmit antennas at the BTS denoted by (2x1); a 2 user system with 4 transmit antennas at BTS denoted by (4x2); and a 3 user system with 6 transmit antennas at BTS denoted by (6x3). From Figure 5.3, it is shown that that the performances of a single user with diversity order of 2 at a BER=10^{-4}, performs better than 2 users system by 3.5 dB, and 3 users system by 4.5 dB, where MUI dominant perturbation**.** The downlink pre-coder cannot completely eliminate MUI interference at each mobile.

The performance degradation due to the imperfect cancellation of noise and MUI, where in ZF-SVD1 detection the noise term may be amplified in a way that influences the decoding output in negative way. Both of these factors contribute noise to the decoding process and therefore limit the STBC-OFDM performance at each user.

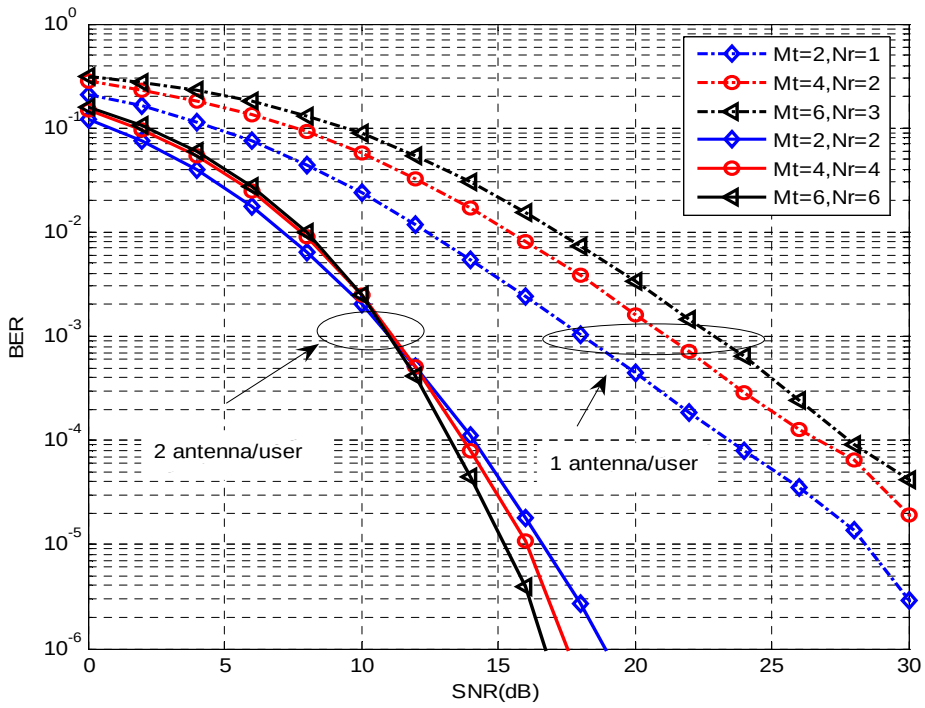

Figure 5.3: Performance comparison of single user and MU STBC-OFDM system with 1 or 2 receive antennas/user, using ZF-SVD1 detection.

When each user has two receive antennas, again three cases are studied: single user and 2 transmit antennas at the BTS denoted by (2x2); a 2 user system and 4 transmit antennas at the BTS denoted by (4x4); and a 3 user system and 6 transmit antennas at the BTS denoted by (6x6).

Similarly, at low SNR, the performance of a single user system performs slightly better than 2 and 3 users system, respectively. By contrast the multiuser system at high SNR, achieves better performance than a single user STBC-OFDM system, which obtained a diversity order of 4. The performance of 3 users at a BER=10^{-6}, performs better than 2 users by 1 dB and single user system by 2.5 dB, respectively. This higher diversity gain greatly improves the BER performance, as compared to the performance results with one receive antenna per user.

Figure 5.4 demonstrates the performance of the proposed hybrid MU SFBC-OFDM system, and show the BER under various system loads using ZF-SVD1 detection.

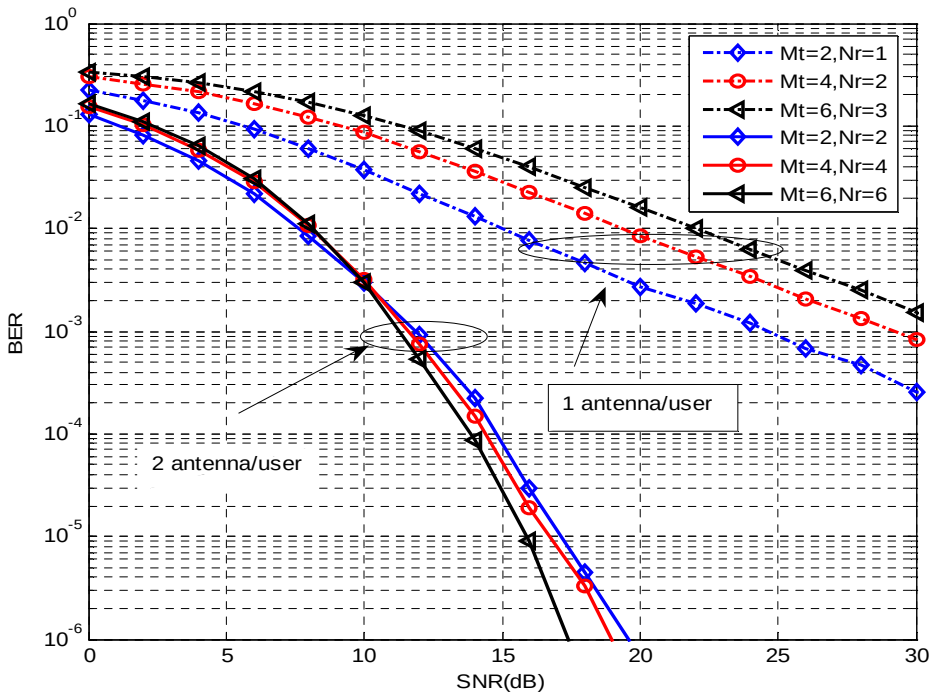

Figure 5.4: Performance comparison of single user and MU SFBC-OFDM system with 1 or 2 receive antennas/user, using ZF-SVD1 detection.

When each user has one receive antenna, three cases are investigated: a single user and 2 transmit antennas at the BTS denoted by (2x1); a 2 user system with 4 transmit antennas at BTS denoted by (4x2); and a 3 user system with 6 transmit antennas at BTS denoted by (6x3). From Figure 5.4, it is shown that the performance of a single user with diversity order of 2 at almost a BER=10^{-3}, performs better than 2 users system by 5 dB, and 3 users system by 7 dB respectively.

The performance degradation is due to the imperfect cancellations of noise and MUI. As the user number *K* increases, more MUI is observed and the BER floor is more severe. As seen before the noise enhancement influences to the decoding process and for consequences leads to performance degradation. Both of these factors contribute noise to the decoding process and therefore limit the SFBC-OFDM performance at each user.

When each user has two receive antennas, again three cases are studied: single user and 2 transmit antennas at the BTS denoted by (2x2); a 2 user system and 4 transmit antennas at the BTS denoted by (4x4); and a 3 user system and 6 transmit antennas at the BTS denoted by (6x6).

Similarly, at low SNR, the performance of a single user system performs slightly better than 2 and 3 users system, respectively. By contrast the multiuser system at high SNR, achieves better performance than a single user STBC-OFDM system, which obtained a diversity order of 4. The performance of 3 users at a BER=10^{-6}, performs better than 2 users by 1.5 dB and single user system by 2 dB, respectively. This higher diversity gain greatly improves the BER performance, as compared to the performance results with one receive antenna per user.

5.3.2 Performance Comparison between ST and SF code

Figure 5.5 compares the BER performance for hybrid MU scheme with 6x3 and 6x6 antenna configuration, we can observe that the increase in the number of receive antenna effectively improves the performance, and shows the performance comparison of hybrid MU STBC-OFDM and SFBC-OFDM in the same frequency selective fading channel. The channel is block fading but remains constant over two consecutive OFDM symbol periods as required by STBC-OFDM.

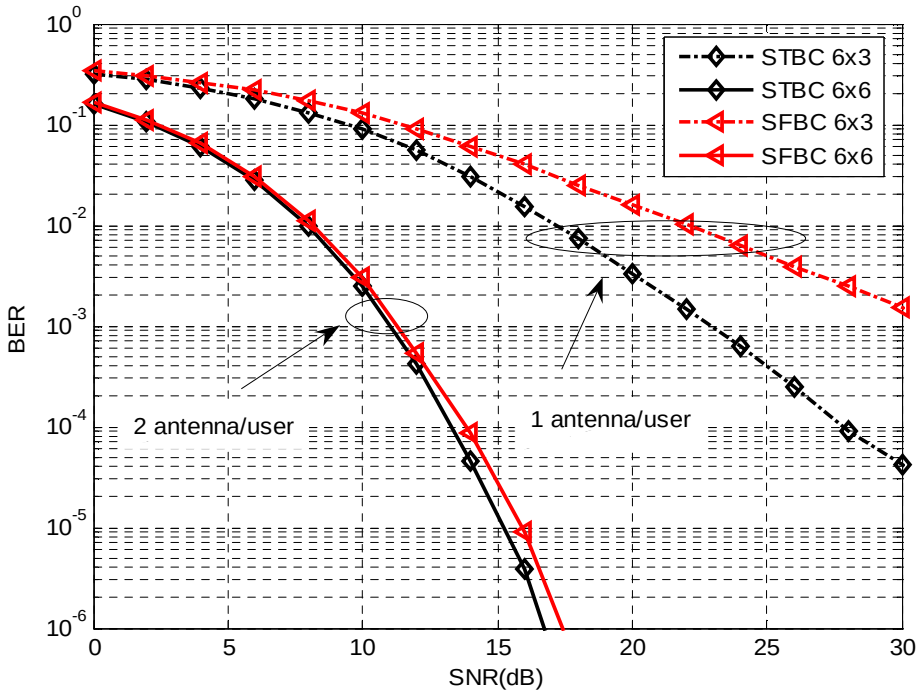

Figure 5.5: Performance comparisons over 6x6 and 6x3 for Hybrid MU STBC-OFDM and SFBC-OFDM with ZF-SVD1 detection.

From the Figure 5.5, the hybrid MU with 6x6 configuration scheme, it can be observed that at a BER=10^{-6}, the STBC-OFDM has a diversity gain of 1 dB over the SFBC-OFDM. And with 6x3 configuration scheme, at almost a BER= 10^{-3}, the STBC-OFDM has a diversity gain of about 8 dB over the SFBC-OFDM. It was observed that increasing the *K* factor introduces more correlation between the channel paths, which results in degradation in performance.

5.3.3 Performance of Hybrid MU STBC-OFDM under different channel taps

In this section, we examined the performance under different channel taps, and we compare the performance of the hybrid MU STBC-OFDM and SFBC-OFDM scheme with 2 users over Rayleigh fading channels.

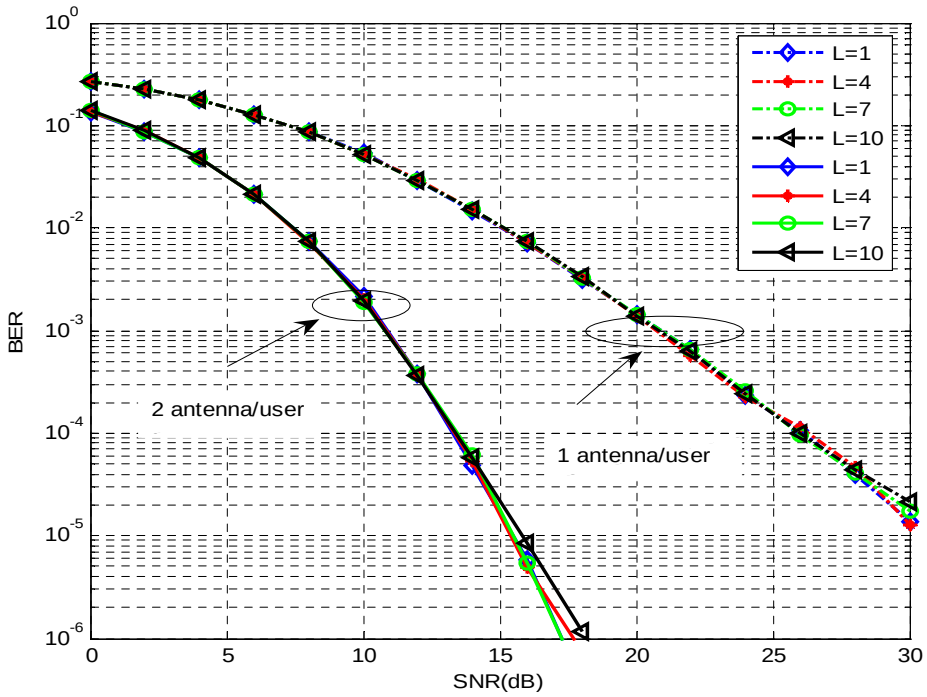

Figure 5.6: BER comparison of Hybrid MU STBC-OFDM for QPSK modulation over frequency selective fading channel with CP=10.

Figure 5.6, show the simulation results for different values of the frequency selective channel order of multiuser detectors, with 2 users for STBC-OFDM coding, and compares the performance of the 4x4 configuration hybrid MU scheme to that of 4x2 for different *L* taps channel conditions. It can be observed that for each configuration has almost the same performance with slightly difference, and the hybrid scheme perform well even in correlated channels with the increasing of *L* under the condition of $CP \geq L$. However, when adding one antenna to the user, a SNR reduction of 14 dB is achieved at almost a BER=10^{-5}.

5.3.4 Performance of Hybrid MU SFBC-OFDM under different channel taps

Figure 5.7, show the simulation results for different values of the frequency selective channel order of multiuser detectors, with 2 users for SFBC-OFDM coding, and compares the performance of the 4x4 configuration hybrid MU scheme to that of 4x2 for different *L* taps channel conditions.

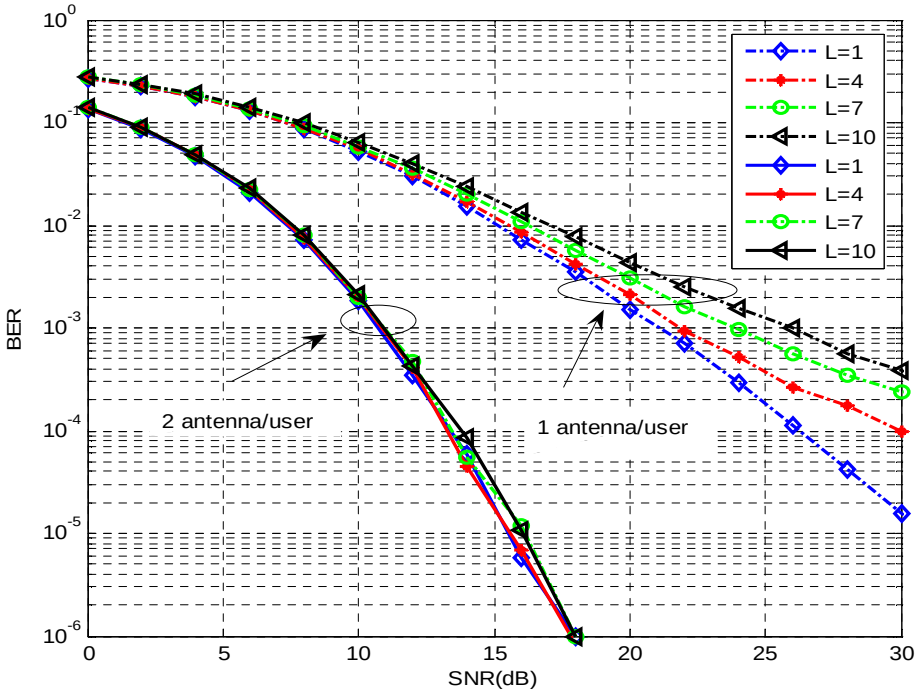

Figure 5.7: BER comparison of Hybrid MU SFBC-OFDM for QPSK modulation over frequency selective fading channel with CP=10.

It can be observed that for 4x4 configuration has almost the same performance with slightly difference, and perform well even in correlated channels with the increasing of *L* under the condition of CP $\geq$ *L*. By contrast, it can be observed that the performance degradation of the 4x2 configuration hybrid MU scheme with the increasing of *L* channel taps. However, when adding one antenna to the user, a SNR reduction of 14 dB is achieved at almost a BER=10^{-5}, which increases with the increasing of *L*.

It was observed that the increasing the *K* factor introduces more correlation between the channel paths, which results in a degradation in performance. This is due to the fact that the SFBC is very sensitive to the Rayleigh fading channel, especially with high channel order.

5.4 ZF Transmitter Based on SVD

In this section we present the SVD MU transmission and MU detector, the ZF transmitter based on SVD which is referred to ZF-SVD2. As shown in Figure 5.1, for each user the n symbol vector stream is pre-processed before using the STBC OFDM encoding by pre-multiplying it with an $(Mt \times d_q)$ component DL pre-processing matrix P_q.

$$X_q = P_q\, S_q \qquad q = 1,2, \ldots\ldots, K \tag{5.31}$$

After the DL pre-processing, the composite of the Mt component pre-processed symbol stream can be expressed as:

$$X = \sum_{q=1}^{K} X_q = P\, S \tag{5.32}$$

Where P is an $(Mt \times \sum_{q=1}^{K} d_q)$ component matrix given by

$$P = [P_1, P_2, \ldots\ldots, P_K] \tag{5.33}$$

And S is an $(\sum_{q=1}^{K} d_q \times n)$ component symbols stream containing the transmitted DL symbol information, with n is the length of symbol vectors stream which is given by:

$$S = [S_1^T, S_2^T, \ldots\ldots, S_K^T]^T \tag{5.34}$$

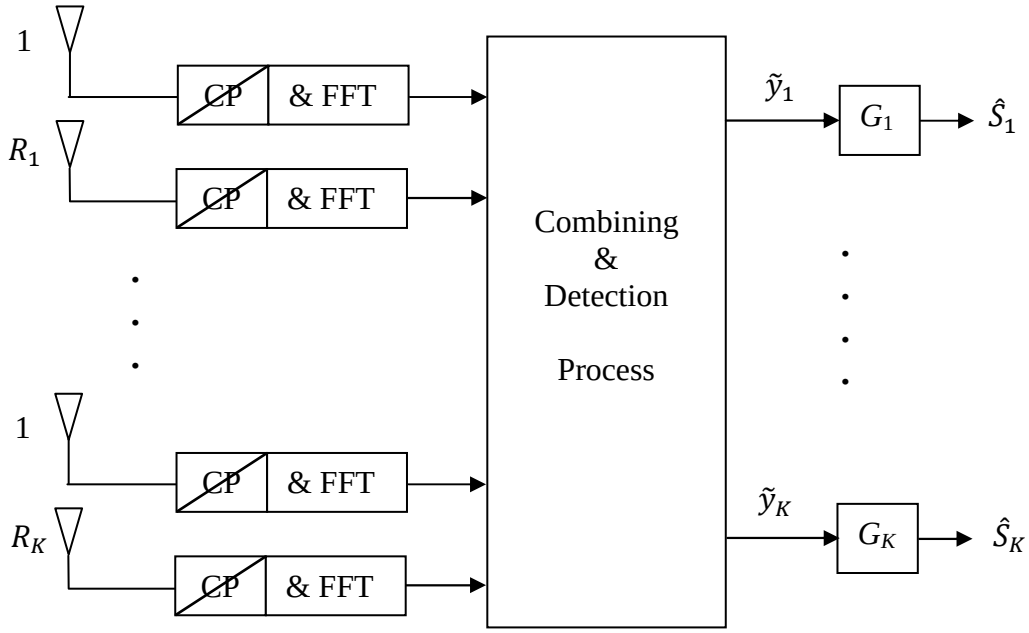

Figure 5.8: Block diagram of the SDMA DL MUD Post-Processing

As shown in Figure 5.8 the received R_q component vector symbol $\tilde{y}_q$ of the q-th MS can be expressed as:

$$\tilde{y}_q = \sum_{j=1}^{K} \tilde{H}_q X_j + w_q \tag{5.35}$$

By substituting (5.32) into (5.35) the received signal $\tilde{y}_k$may be expressed as:

$$\begin{aligned} \tilde{y}_q &= \textstyle\sum_{j=1}^{K} \tilde{H}_q P_j S_j + w_q \\ &= \tilde{H}_q P S + w_q \\ &= \tilde{H}_q P_q S_q + \textstyle\sum_{j=1, j\neq q}^{K} \tilde{H}_q P_j S_j + w_q \\ &= \tilde{H}_q P_q S_q + Z_q + w_q \qquad q = 1,2,\dots,K \end{aligned} \tag{5.36}$$

We can see from (5.36), that the received DL signal at the MS's experience MUI component as well known the CCI on the q-th user is represented as Z_q. Let us assume that the CSI is available at both the transmitter and the receiver, and then we use the SVD decomposition of the channel user $\tilde{H}_k$ from (5.2) we arrive at:

$$\begin{aligned} \tilde{H}_q &= U_q \left[D_q^{\frac{1}{2}}, 0 \right] V_q^H = U_q \left[D_q^{\frac{1}{2}}, 0 \right] \begin{bmatrix} V_{qs}^H \\ V_{qn}^H \end{bmatrix} \\ &= U_q D_q^{1/2} V_{qs}^H \end{aligned} \tag{5.37}$$

Where U_q and V_q are $(2R_q \times 2R_q)$ and $(Mt \times Mt)$ component unitary matrices, respectively, and D_q is an $(2R_q \times 2R_q)$ component diagonal matrix containing the eigenvalues of $\tilde{H}_q \tilde{H}_q^H$ i.e., we have:

$$D_q = diag\left\{\lambda_{q1}, \lambda_{q2}, \dots\dots\dots, \lambda_{q2R_q}\right\}$$

Furthermore in (5.37) U_q consist of the eigenvectors of $\tilde{H}_q \tilde{H}_q^H$ and V_{qs} is an $(Mt \times d_q)$, where $d_q = 2$, component matrix, which is constituted by eigenvectors correspond- ding to the non zero eigen-values of $\tilde{H}_q^H \tilde{H}_q$. By contrast V_{qn} is an $[Mt \times (Mt - d_q)]$ component matrix, which is constituted by the eigenvectors corresponding to the zero eigen-values of $\tilde{H}_q^H \tilde{H}_q$. Upon substituting (5.37) into the first line of (5.36) the received DL signal symbol $\tilde{y}_q$ of the q-th user may be expressed as:

$$\tilde{y}_q = U_q D_q^{1/2} V_{qs} P_q S_q + w_q \quad q = 1,2,\dots\dots,K \tag{5.38}$$

The composite of collect all the K received DL signals vector streams $\tilde{y}_q$ of (5.38) into a symbol vector stream

$\tilde{y} = [\tilde{y}_1^T(1), \tilde{y}_1^T(2), \dots\dots, \tilde{y}_K^T(n)]$

Then the overall DL received signal vector streams $\tilde{y}$ of the K M's can be expressed as:

$$\tilde{y} = U\, D^{1/2}\, V_s^H\, P\, S + W \tag{5.39}$$

Where we introduced the following definitions:

$U = diag\{U_1(1), U_2(2), \dots., U_K(n)\}$
$D = diag\{D_1(1), D_2(2), \dots., D_K(n)\}$
$W = [\, w_1^T(1), w_2^T(2), \dots\dots, w_K^T(n)]$
$V = [\, V_{1s}(1), V_{2s}(2), \dots\dots, V_{Ks}(n)]$

The DL BS transmit pre-processing matrix P is designed so that the DL MUI can efficiently be suppressed. As shown in (5.40), according to [31], the MUI can fully be removed when the DL pre-processing matrix to satisfy:

$$V_s^H P = B \tag{5.40}$$

Where the power allocation regime of

$$B = diag\left\{B_1, B_2, \dots., B_{\sum_{q=1}^{K} d_q}\right\} = diag\left\{B_{11}, .., B_{1d_q}; \dots.; B_{K1}, .., B_{Kd_q}\right\}$$

Represent the transmission power constraint.

$$P = [V_s^H]^+ B = \bar{P}\, B \tag{5.41}$$

Where $[V_s^H]^+$ denotes the pseudo inverse of the matrix V_s^H, and

$\bar{P} = V_s[V_s^H V_s]^{-1}$

When substituting the overall DL pre-processing matrix of (5.40) into (5.39) the overall received signal vector y of K Ms user can be simplified to

$$\tilde{y} = U\, D^{1/2}\, B\, S + W \tag{5.42}$$

To be more specific, the d_q length observation symbol vector of the q-th MS can be expressed as:

$$\tilde{y}_q = U_{\,q} D_q^{1/2}\, B_q\, S_q + w_q \tag{5.43}$$

Where

$B_q = diag\left\{B_{q1}, B_{q2}, \ldots, B_{qd_q}\right\}$

Explicitly, the *q*-th user endures no MUI imposed by the other users, however, there may exist IAI among the antenna specific symbols transmitted by the BS to the *q*-th MS this IAI can suppressed with the aid of the SVD based matrices $\{U_k\}$ of (5.37). By $G_q = U_q^H$ according to Figure 5.8, the user specific decision variables can individually be expressed as:

$$\hat{S}_q = D_q^{1/2} B_q S_q + U_q^H w_q \qquad q = 1,2, \ldots\ldots, K \tag{5.44}$$

or jointly as

$$\hat{S} = D^{1/2} BS + U^H w \tag{5.45}$$

From (5.46) we can observe Parallel Pipeline channels between transmit antennas and receive antennas without decreasing of channel rank.

The overall of the user decision of *n* symbol stream can be expressed as:

$$\hat{S} = \left[\hat{S}_1, \hat{S}_2, \ldots\ldots\ldots\ldots, \hat{S}_K\right] \tag{5.46}$$

A natural power allocation scheme is to allocate the same power to each symbol stream. In this case the coefficients B_i are set $B_1 = \ldots\ldots = B_{\sum_{q=1}^{K} d_q} = B$, where B is the constant, given by [31]:

$$B = \sqrt{\frac{\sum_{k=1}^{K} d_q}{trace([V_s^H V_s]^{-1})}} \tag{5.47}$$

5.5 Simulation Results

We consider the same parameter simulation as mentioned in section 4.6 , but at the except we utilize the ZF-SVD2 detection for the hybrid MU STBC-OFDM and SFBC-OFDM coding scheme, and compare the performance under various loads of *K* users for the both, with 1 or 2 receive antenna per user. We consider the same notation $Mt \times Nr$ to denote a scheme with Mt Tx and Nr Rx antennas.

5.5.1 Performance Comparison of Hybrid MU Schemes

Figure 5.9, shows the performance of the proposed hybrid MU STBC-OFDM system over Rayleigh fading channel, and compares the BER under various system loads using ZF-SVD2 detection. When each user has one receive antenna, three cases are investigated: a single user and 2 transmit antennas at the BTS denoted by (2x1); a 2 user system with 4 transmit antennas at BTS denoted by (4x2); and a 3 user system with 6 transmit antennas at BTS denoted by (6x3).

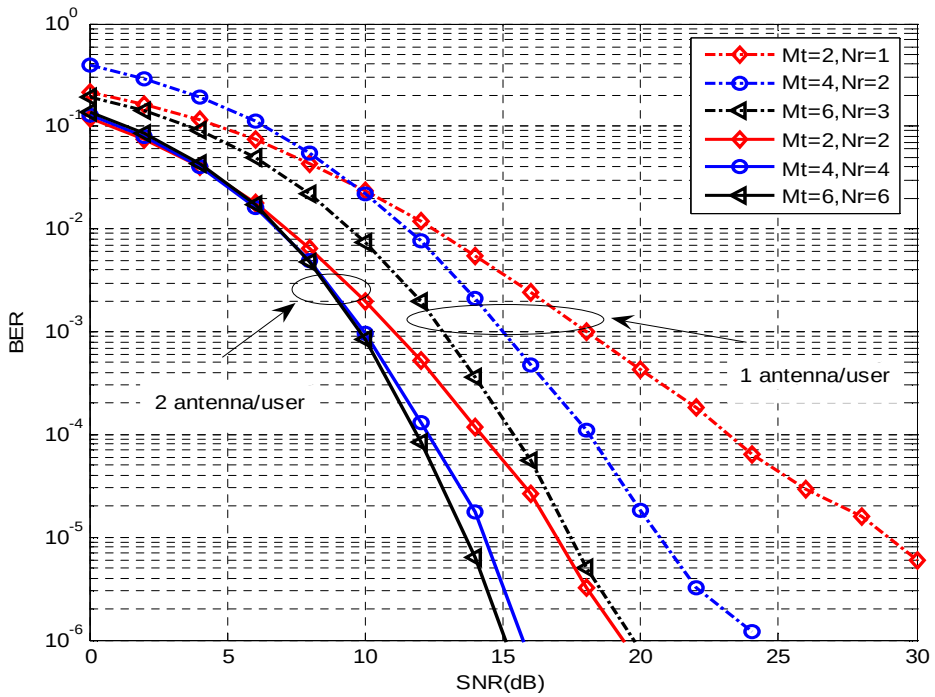

Figure 5.9: Performance comparison of single user and MU STBC-OFDM system with 1 or 2 receive antennas/user, using ZF-SVD2 detection.

It can be seen from Figure 5.9, at a BER=10^{-5}, the performance of a 3 user with diversity order of 2 outperforms the 2 users system by 3.5 dB, and single user system by 11.5 dB. The downlink pre-processing completely eliminates the MUI and IAI interference at each mobile. When each user has two receive antennas, again three cases are studied: single user and 2 transmit antennas at the BTS denoted by (2x2); a 2 user system and 4 transmit antennas at the BTS denoted by (4x4); and a 3 user system and 6 transmit antennas at the BTS denoted by (6x6).

Similarly, we can observe that at a BER=10^{-6}, the performance of a 3 user system performs better than 2 users by 1 dB and single user system by 4 dB, respectively. The system enhancements due to high diversity order. This higher diversity gain greatly improves the BER performance, as compared to the performance results with one receive antenna per user.

When using the eigen-beamforming to a tone by tone and the ZF-SVD2 detection, this yielding to form an orthogonal equivalent channel matrix, which leads to preserve the orthogonality of the code structure, consequently, significant performance BER. The system performance is highly dependent on the number of users in the system. As the user number *K* increases, more MUI is observed and completely eliminates.

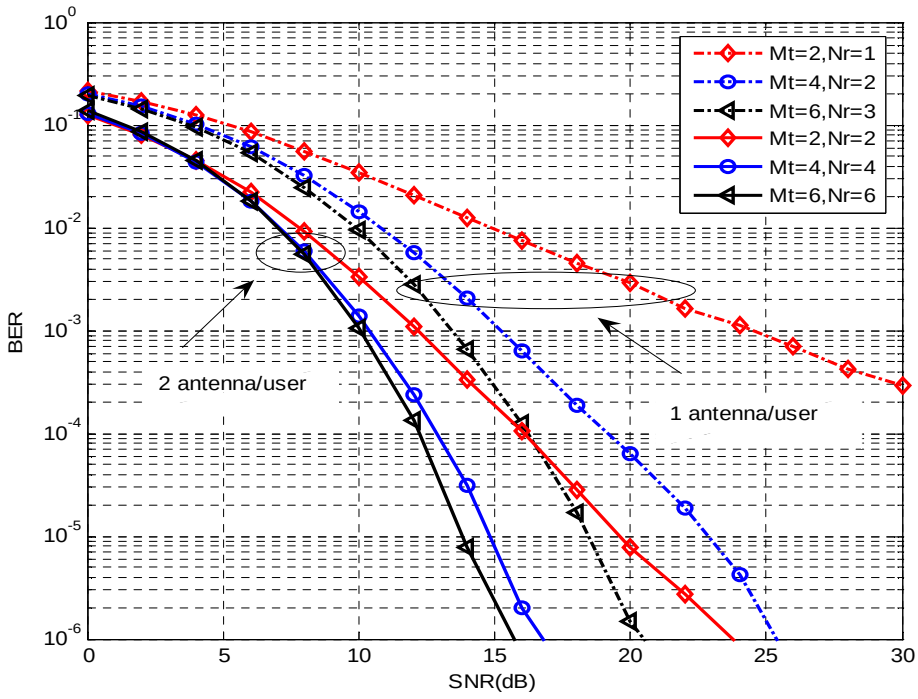

Figure 5.10: Performance comparison of single user and MU SFBC-OFDM system with 1 or 2 receive antennas/user, using ZF-SVD2 detection.

Figure 5.10, shows the performance of the proposed hybrid MU SFBC-OFDM system over Rayleigh fading channel, and compares the BER under various system loads using ZF-SVD2 detection.

When each user has one receive antenna, three cases are investigated: a single user and 2 transmit antennas at the BTS denoted by (2x1); a 2 user system with 4 transmit antennas at BTS denoted by (4x2); and a 3 user system with 6 transmit antennas at BTS denoted by (6x3). It can be seen from Figure 5.10, at almost a BER=10^{-4}, the performance of a 3 user with diversity order of 2 outperforms the 2 users system by 2.5 dB, and single user system by 15 dB. The downlink pre-processing completely eliminates the MUI and IAI interference at each mobile. When each user has two receive antennas, again three cases are studied: single user and 2 transmit antennas at the BTS denoted by (2x2); a 2 user system and 4 transmit antennas at the BTS denoted by (4x4); and a 3 user system and 6 transmit antennas at the BTS denoted by (6x6).

From Figure 5.10, we can see at a BER=10^{-6}, the performance of a 3 user system performs better than 2 users by 1 dB and single user system by 7.5 dB, respectively. The system enhancements due to high diversity order. This higher diversity gain greatly improves the BER performance, as compared to the performance results with one receive antenna per user.

Similarly, when using the eigen-beamforming to a tone by tone and the ZF-SVD2 detection, this yielding to form an orthogonal equivalent channel matrix, which leads to preserve the orthogonality of the code structure, consequently, significant performance BER. The system performance is highly dependent on the number of users in the system. As the user number *K* increases, more MUI is observed and completely eliminated.

5.5.2 Performance Comparison between ST and SF code

Figure 5.11, compares the BER performance for hybrid MU scheme with 6x3 and 6x6 antenna configuration, we can observe that the increase in the number of receive antenna effectively improves the performance, and shows the performance comparison of hybrid MU STBC-OFDM and SFBC-OFDM in the same frequency selective fading channel. The channel is block fading but remains constant over two consecutive OFDM symbol periods as required by STBC-OFDM.

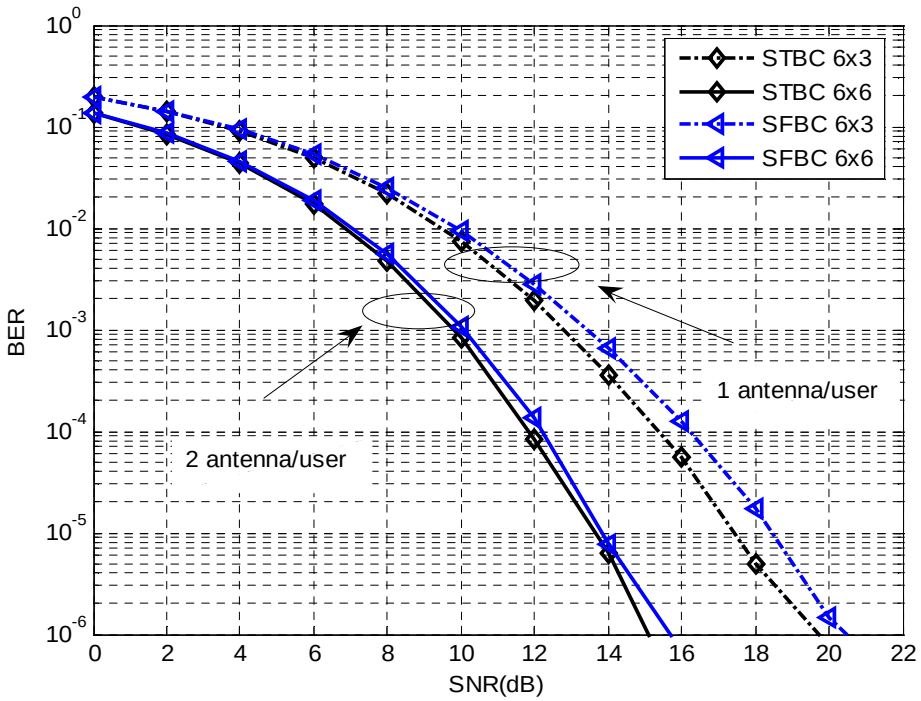

Figure 5.11: Performance comparison over 6x6 and 6x3 for Hybrid MU STBC-OFDM and SFBC-OFDM with ZF-SVD2 detection.

From the Figure 5.11, the hybrid MU scheme with 6x6 configuration antenna, it can be observed that at a BER=10^{-6}, STBC-OFDM has a diversity gain of 0.6 dB over the SFBC-OFDM scheme. And with 6x3 configuration scheme, the STBC-OFDM has a diversity gain of 0.7 dB over SFBC-OFDM.

5.5.3 Performance of Hybrid MU STBC-OFDM under different channel taps

In this section, we examined the performance of the hybrid MU STBC-OFDM scheme under different channel scenarios, and compare the performance of the hybrid MU scheme with K=2 users over Rayleigh fading channels.

Figure 5.12, show the simulation results for different values of the frequency selective channel order multiuser detectors with 2 users for STBC-OFDM coding, and compares the performance of the 4x4 configuration hybrid MU scheme to that of 4x2 for different L taps channel conditions.

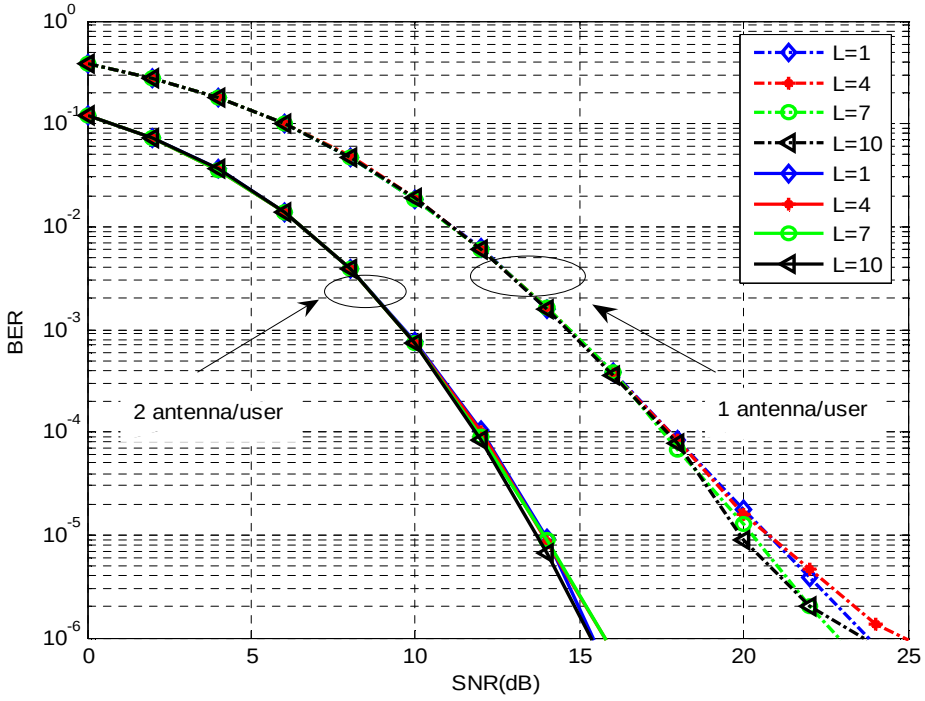

Figure 5.12: BER comparison of Hybrid MU STBC-OFDM for QPSK modulation over frequency selective fading channel with CP=10.

It can be observed that for 4x2 configuration has almost the same performance at low SNR, where at high SNR under channel order L=10 has better performance.

Similarly, with 4x4 configuration at high SNR, the performance under channel order L=10 is the best. The hybrid scheme perform well even in correlated channels with the increasing of L under the condition of $CP \geq L$. However, when adding one antenna to the user, a SNR reduction of 7.5 dB is achieved at a BER= 10^{-6} which decreases slightly with the increasing of L.

As the number of taps of the channel increases, the diversity order of MU STBC-OFDM increases as well to the maximum value of L=10. It is clearly evident that as the number of taps for the channel increases, the diversity order increases as well.

5.5.4 Performance of Hybrid MU SFBC-OFDM under different channel taps

Now, we examined the performance of the hybrid MU SFBC-OFDM scheme under different channel scenarios, and compare the performance of the hybrid MU scheme with K=2 users over Rayleigh fading channels.

Figure 5.13, show the simulation results for different values of the frequency selective channel order of multiuser detectors, with 2 users for SFBC-OFDM coding, and compares the performance of the 4x4 configuration hybrid MU scheme to that of 4x2 for different L taps channel conditions. It can be observed that for 4x2 configuration has almost the same performance at low SNR, where at high SNR with channel order L=1 (flat fading channel) has better performance.

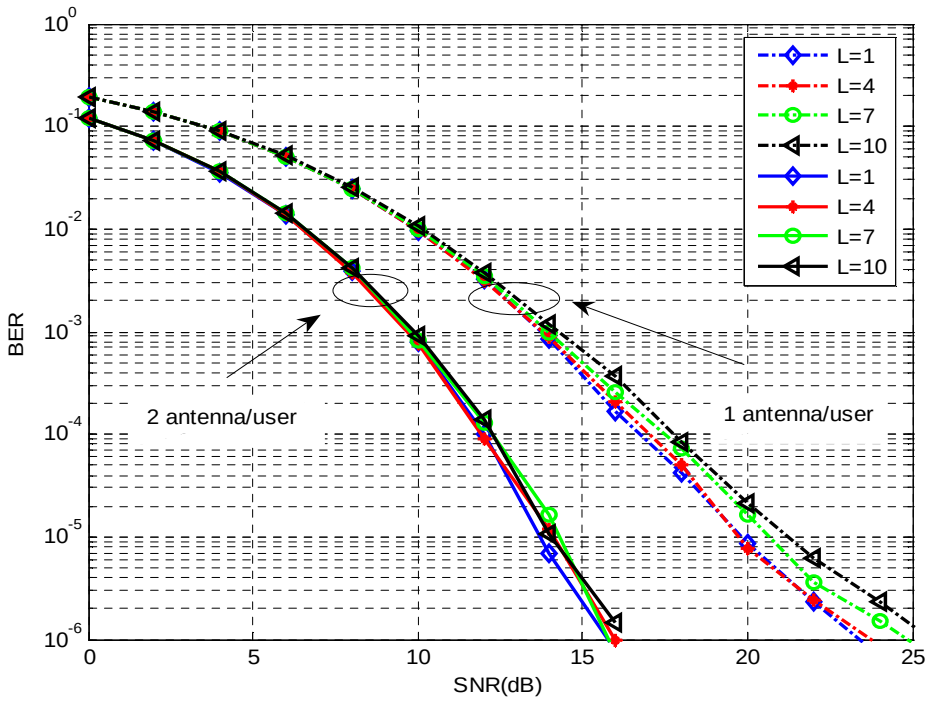

Figure 5.13: BER comparison of Hybrid MU SFBC-OFDM for QPSK modulation over frequency selective fading channel with CP=10.

Similarly, with 4x4 configuration at high SNR, the performance with channel order L=1(flat fading channel) is the best. However, when adding one antenna to the user, a SNR reduction of 7.5 dB is achieved at a BER= 10^{-6} which increases with the increasing of L.

We can say that, the MU SFBC-OFDM is sensitive to the high channel order. As the number of taps of the channel increases, the diversity order of MU SFBC-OFDM decreases as well to the maximum value of L=10 under the condition of $\mathrm{CP} \geq L$. It is clearly evident that as the number of taps for the channel increases, the diversity order decreases as well.

5.6 Conclusion

In this chapter, the combination of SVD with hybrid MU schemes is presented. First , the proposed of the pre-coding data for the downlink system, based on the SVD for hybrid MU space frequency and space time coding schemes for OFDM systems under the frequency selective channel, that provides diversity gain, Unfortunately, this suffers from induces the additional problem of noise enhancement, especially if the channel is rank deficient or ill conditioned. The performance is highly dependent on the number of users in the system and highly degraded as the number of active users increases at low SNR where the user is equipped with one receive antenna. Simulations show, that the space time coding is more robust than frequency coding over Rayleigh fading channel. However, the main limitation of the hybrid MU scheme with ZF-SVD1 detection is the increased number of receives antennas is necessary at the mobile terminal.

Second, We have proposed the pre-processing and the post-processing for the downlink system based on the SVD for hybrid MU space time and space frequency schemes for OFDM systems over the frequency selective channel, that provides diversity gain, where the MU MIMO channels were decomposed into parallel SISO channels corresponding to their singular values, efficiently the hybrid MU scheme, exploits diversity techniques. These are space, time and frequency diversity to overcome fading found in the radio channel and provides high performance.

Simulations show again, that the performance of hybrid MU space time coding and frequency coding have almost the same performance with slightly difference. The both system are robust in frequency selective channel. The system performance is highly dependent on the number of users in the system. As the number of active users K increases, leads to the increasing of the system performance.

CHAPTER VI

Performances Comparison of all Detection Technique

6.1 Performances Comparison of all Detection Techniques

Figure 6.1, 6.2 and 6.3, 6.4, shows the performance comparison of the hybrid MU schemes, STBC-OFDM or SFBC-OFDM with ZF-OSIC, ZF-SVD1, and ZF-SVD2 detection technique, Performance is determined over frequency selective, time variant fading channels, under various system loads *K* with single or two receive antenna. Perfect channel estimation is assumed at the transmitter and receiver end.

In the case where the number of users in the system is $K = 2$, we compare the performance of the 4x4 configuration scheme of hybrid MU system with that of the 4x2 configuration scheme. Where in the case of number of users in the system is $K=3$, we compare the performance of the 6x6 configuration scheme of hybrid MU system with that of the 6x3 configuration scheme.

6.1.1 Performance Comparison of Hybrid MU STBC-OFDM over 4x4 and 4x2

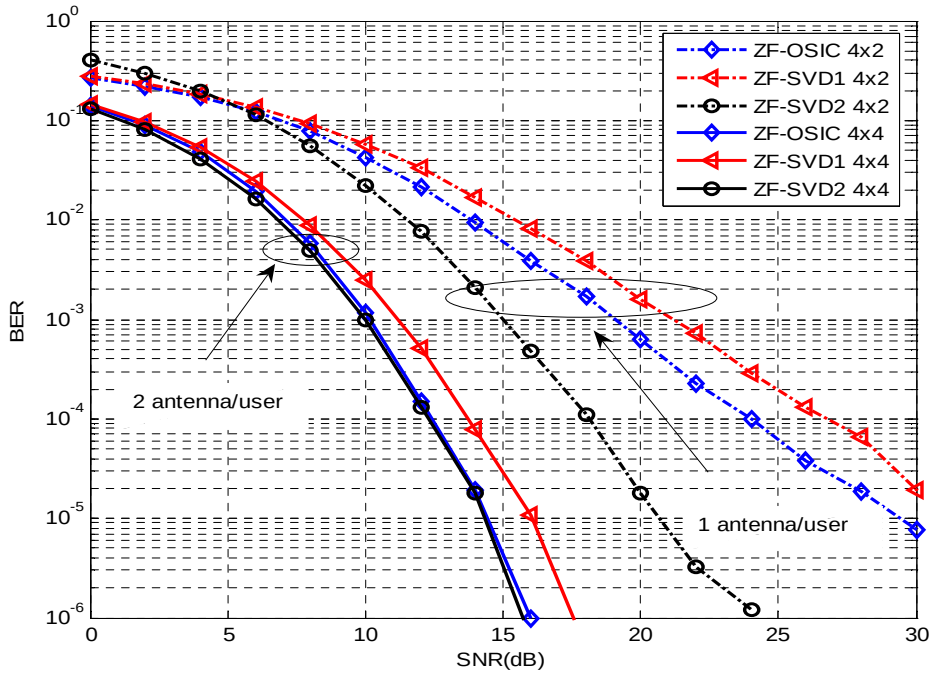

Figure 6.1: BER performance over 4x4 and 4x2 STBC-OFDM system using ZF-OSIC, ZF-SVD1 and ZF-SVD2 detection technique.

From the Figure 6.1, in the case of 4x4 hybrid configuration STBC-OFDM, it can be seen that at a BER=10^{-6} the ZF-SVD2 outperforms the ZF-SVD1 by 1.6 dB, and performs slightly better than the ZF-OSIC. Where In the case of 4x2 configuration hybrid STBC-OFDM, at almost a BER=10^{-5} the SVD2 outperforms the ZF-SVD1 by 10 dB, and outperforms the ZF-OSIC by 8 dB.

6.1.2 Performance Comparison of hybrid MU STBC-OFDM over 6x6 and 6x3

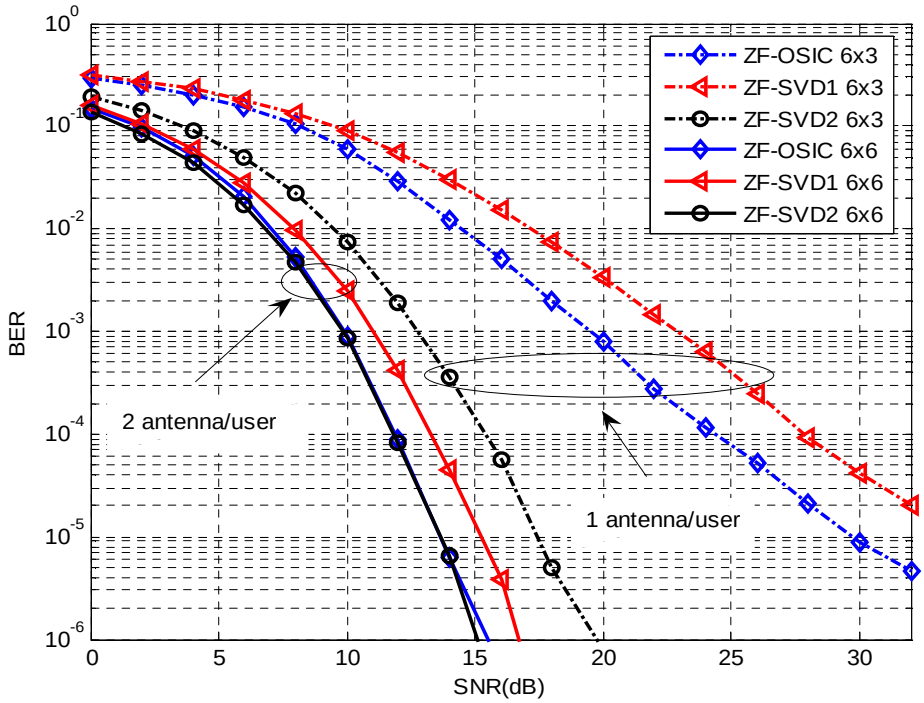

Figure 6.2: BER performance over 6x6 and 6x3 STBC-OFDM system using ZF-OSIC, ZF-SVD1 and ZF-SVD2 detection technique

From Figure 6.2, in the case of 6x6 configuration hybrid STBC-OFDM, it can be seen that at a BER=10^{-6} the ZF-SVD2 outperforms the ZF-SVD1 by 2 dB, and performs slightly better than the ZF-OSIC at high SNR.

Where In the case of 6x3 hybrid STBC-OFDM, at almost a BER=10^{-5} the SVD2 outperforms the ZF-SVD1 by 15 dB, and outperforms the ZF-OSIC by 11 dB.

6.1.3 Performance Comparison of hybrid MU SFBC-OFDM over 4x4 and 4x2

In the case where the number of users in the system is $K = 2$, we compare the performance of hybrid MU SFBC-OFDM over 4x4 with that of the 4x2 configuration system.

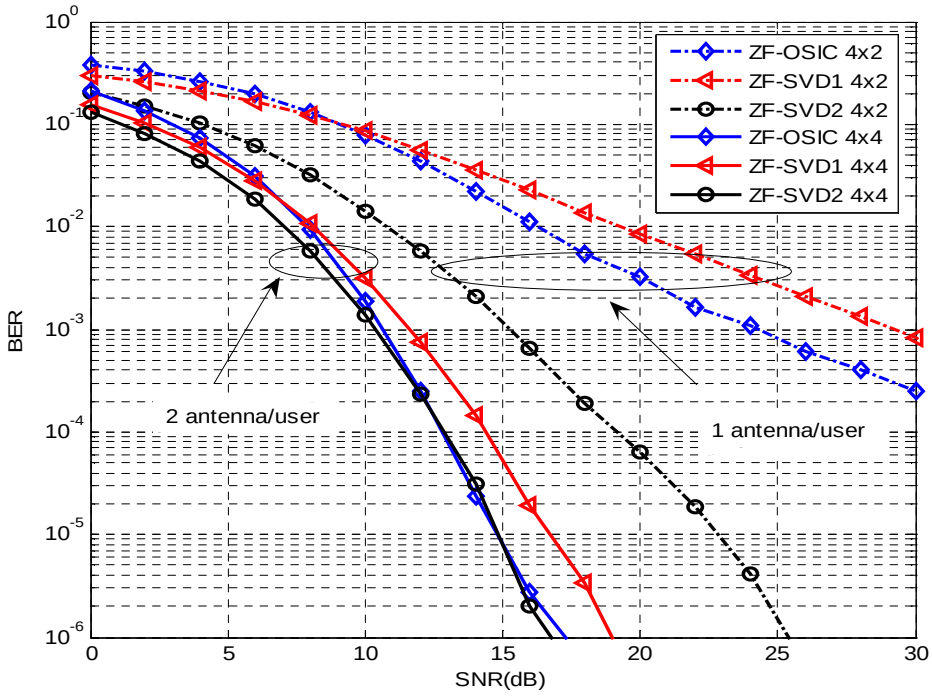

Figure 6.3: BER performance of 4x4 and 4x2 SFBC-OFDM system using ZF-OSIC, ZF-SVD1 and ZF-SVD2 detection technique

From Figure 6.3, in the case of 4x4 hybrid MU SFBC-OFDM, it can be seen that at a BER=10^{-6} the ZF-SVD2 outperforms the ZF-SVD1 by 2 dB, and performs slightly better than the ZF-OSIC. Where In the case of 4x2 hybrid STBC-OFDM, at a BER=10^{-3} the SVD2 outperforms the ZF-SVD1 by 15 dB, and outperforms the ZF-OSIC by 10 dB.

6.1.4 Performance Comparison of hybrid MU SFBC-OFDM over 6x6 and 6x3

In the case where the number of users in the system is $K = 3$, we compare the performance of hybrid MU SFBC-OFDM over 6x6 with that of the 6x3 configuration system.

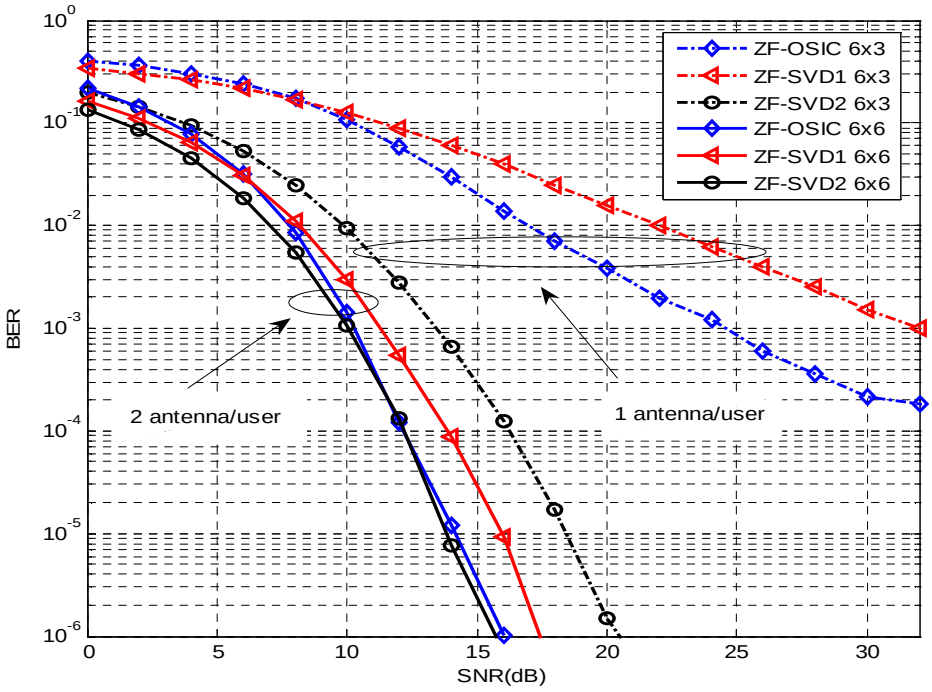

Figure 6.4: BER performance over 6x6 and 6x3 SFBC-OFDM system using ZF-OSIC, ZF-SVD1 and ZF-SVD2 detection technique

From Figure 6.4, in the case of 6x6 hybrid SFBC-OFDM, it can be seen that at a BER=10^{-6} the ZF-SVD2 outperforms the ZF-SVD1 by 2 dB, and performs slightly better than the ZF-OSIC.

Where In the case of 6x3 hybrid SFBC-OFDM, at a BER=10^{-3} the SVD2 outperforms the ZF-SVD1 by 18.5 dB, and outperforms the ZF-OSIC by 11 dB.

6.2 Summary of Results and conclusion

First, the performance of the hybrid multi user space time code and space frequency code with ZF-OSIC receiver for the downlink system was compared for an AWGN channel and a frequency selective fading channel under different channel order, with the assumption of perfect knowledge of the channel estimation at the receiver side. The non linear successive interference cancellation (SIC) based receiver e, g V-BLAST, its decodes the sub-streams, substracts its interference and then decodes the later sub-streams. However, V-BLAST was not designed for exploiting transmits diversity and need more receive antenna diversity.

The performance of V-BLAST receiver is mainly dependent on the first sub-streams, which has the lowest diversity gain and limited by error propagation. The performance of ZF-OSIC receiver was highly degraded according to the *K* system loading since the multiple antenna interference led to a strong impact on the performance degradation of a multistage interference cancellation receiver.

The hybrid multi user STBC-OFDM outperforms the SFBC-OFDB system. Furthermore, the MU STBC-OFDM is more robust than MU SFBC-OFDM over the frequency selective channel. However, decrease the delay time in decoding.

Second, the combination of the hybrid MU space time and space frequency coding, with the SVD decomposition of the user channels for the pre-coding downlink with ZF-SVD1 receiver, with the assumption of perfect knowledge of the channel estimation at the transmitter and the receiver side. Unfortunately, the ZF-SVD1 may suffer from noise enhancement, especially if the channel is rank deficient or ill conditioned. Again, the hybrid multi user STBC-OFDM outperforms the SFBC-OFDM system. Furthermore, the MU STBC-OFDM is more robust than MU SFBC-OFDM over the frequency selective channel.

Third, the performance combination of the hybrid MU space time and space frequency schemes for OFDM systems with SVD assisted MU transmitter and MU detector, using the pre-processing and the post-processing for the downlink system based on the SVD of the channel user ZF-SVD2, with the assumption of perfect knowledge of the channel estimation at the transmitter and the receiver side, under the frequency selective channel, that provides diversity gain. The hybrid multi user STBC-OFDM performs slightly better than the SFBC-OFDM system. However, decrease the delay time in decoding process for SFBC-OFDM.

Furthermore, the performance of the hybrid MU schemes is highly dependent on the number of users in the system. As the number of active users K increases, leads to the increasing of the system performance.

Finally, the ZF-SVD2 outperforms the ZF-OSIC and ZF-SVD1, respectively, and is more robust in frequency selective channel, and provides more diversity gain, by exploiting space, time and frequency diversity.

Conclusion and Future works

7. Conclusion and Future Works

7.1 **Conclusion**

The goal of this thesis was to study the hybrid approach to combine the advantages of MIMO wireless systems, the Space Time block code and spatial Multiplexing to design wireless receivers. We summarize the most important aspects and results of our work, present some conclusions, and provide suggestions for future work.

The reliability of the wireless link (downlink, uplink) can be improved using MIMO-STBC system. Increasing the number of antenna at both ends can enhance the reliability of the system proportionaly with diversity gain. This result can be achieved with no increase in transmitted power and with no cost of extra bandwidth. The robustness of this system in fading channel environment made it as a possible candidate technology for new generation of wireless system. The performance of MIMO system is highly depending on channel estimation algorithms.

Therefore the application of high performance and efficient channel estimation in order to increase the performance of MIMO or MIMO-OFDM system is essential. The challenge in MIMO-OFDM channel estimation is reducing the computational complexity. The capacity of MIMO channels was studied. Moreover the results of MIMO capacity shows that capacity increases linearly with increasing in number of antennas at the both sides. Figure1.8, shows that, when *Mt*=4 and *Nr*=4 we achieve the highest capacity as compared with *Mt*=2 and *Nr*=3 and *Mt*=3 and *Nr*=2 respectively in MIMO system. The results of *Mt* =2 and *Nr =3* is the same as *Mt =3* and *Nr =2*. Increasing the number of antennas at either side of MIMO system will have the same effect of raising the capacity, it is implied that this capacity is optimally achieved if the number of transmit and receive antennas are equal. We also showed the theoretical basis for the Alamouti code and the spatial multiplexing in MIMO systems. Finally, it can be concluded that SVD decomposition can be as an ultimate solution for reduction computational complexity.

This thesis focused on three advances in MIMO communication systems. The first studied a combined spatial multiplexing and space time coding architecture and MIMO-OFDM systems in order to bridge the gap between these two MIMO systems (diversity gain, high data rate**)**. The OFDM modulator transforms the frequency selective MIMO channels into parallel flat fading channels in the frequency domain. The receiver structures for hybrid multiuser V-BLAST detector for the downlink system for a MIMO channel were illustrated. The

performance of the receiver for a hybrid MU V-BLAST system was evaluated with assumption of perfect channel estimation at the receiver.

In this system, the information is divided into layers and each layer is encoded by a space time code. This is known as multi-layered space time coded system. Space time block codes (STBC) is used as the layer codes. Due to the short code length of STBC, the number of receive antennas should be at least equal to the number of layers. This multi-layered architecture is a spatial multiplexing scheme with spatial and time or frequency diversity at each layer.

First, we compared and evaluated the performance of multi-layered space time of serial detection algorithms for the hybrid MU V-BLAST schemes over frequency selective MIMO channels under different load of the downlink systems *K*. We also consider the design of bandwidth efficient space frequency time codes for MIMO-OFDM systems. Second, we compared and evaluated the performance of the hybrid MU schemes under different scenarios of the channel. The degradation of the performance with the increasing of the downlink system load when the user is equipped with single receive antenna. The main results of this study show that the performance of STBC-OFDM is more robust than SFBC-OFDM encoding in frequency selective channel.

The second part, the performance of the hybrid multi-user schemes in the downlink system was compared and evaluated for fading selective channel with the assumption of perfect knowledge of the channel, the combining of the singular value decomposition with the MU schemes, when the CSI is available at the transmitter and the receiver sides, then using the SVD MU assisted transmitter and MU detector. The use of the beamforming, the pre-processing and the post-processing at the transmitter (‘Base station’) and the receiver (‘ mobile station’), respectively. Two proposed schemes based on the SVD, the ZF receiver, and the ZF transmitter. Simulation results show that the later outperforms the ZF receiver. However, the performance of ZF receiver was highly degraded according to the system loading, when the user is equipped with one receive antenna. Furthermore, the additional term of noise amplification.

Finally, the performance of the three hybrid MU detection was compared and evaluated, according to the simulation results, the ZF transmitter with reduction complexity outperforms, the V-BLAST detection with successive interference canceller and the ZF receiver, respectively. For the all proposed schemes the STBC-OFDM is more robust than the SFBC-OFDM encoding in frequency selective channel. Our hybrid approach provides more diversity gain, by exploiting space, time and frequency diversity.

7.2 Future Works

This project was partially about the performance investigation of the hybrid Multi User schemes. The future work can be defined as the performance investigation of the hybrid schemes with the high mobility environment. In overall, there is a lot of open field in MIMO systems which are attractive to research. As an example, receiver design or designing the detection algorithm with low computational complexity for different MIMO structure. Different transmission environments can be examined, and compared.

Other extensions include:

1- Using higher order constellation and higher FFT size of OFDM sub-carrier.
2- Investigating the use of the coded modulation techniques, such as (bit interleaved coded Modulation BICM, trellis modulation) when used in conjunction with space time coding.
3- The impact of the carrier offset (CFO).
4- Channel environment scenario when the *L* tapas of the channel is longer than the CP length.

Publication :

A. Boudaa, M. Bouziani, ‘’ Combining SFBC_OFDM Systems with SVD Assisted Multiuser Transmitter and Multiuser Detector,’’ in IOSR Journal of Electronic and Communication Engineering. Vol.6, Jul-Aug 2013.

IOSR Journal of Electronics and Communication Engineering (IOSR-JECE)
e-ISSN: 2278-2834,p- ISSN: 2278-8735.Volume 6, Issue 6 (Jul. - Aug. 2013), PP 24-28
www.iosrjournals.org

Combining SFBC_OFDM Systems with SVD Assisted Multiuser Transmitter and Multi user Detector

Ahmed. Boudaa[1], Merahi. Bouziani[2]
[1]*(Departement of Electronic / University of Djillali Liabes , Algeria)*
[2]*(Departement of Electronic / University of Djillali Liabes , Algeria)*

Abstract: *In this work, we exploit the SVD assisted multiuser transmitter (MUT) and multiuser detector (MUD) technique, using downlink (DL) preprocessing transmitter and DL postprocessing receiver matrice .In combination with space frequency block coding (SFBC). And also propose the precoded DL transmission scheme, were the both proposed schemes take advantage of the channel state information (CSI) of all users at the base station (BS), but only of the mobile station (MS)'s own CSI, to decompose the MU MIMO channels into parallel single input single output (SISO), these two proposed schemes are compared to the vertical layered space time (V_BLAST) combined with SFBC (SFBC_VBLAST). Our Simulation results show that the performance of the proposed scheme with DL Zero Forcing (ZF) transmitter for interference canceller outperforms the SFBC_VBLAST and the precoded DL schemes with ZF receiver in frequency selective fading channels.*

Keywords – *Post processing, Preprocessing,, SFBC, SVD, ZF.*

I. INTRODUCTION

Multiple Input Multiple Output (MIMO) is a new technology that can dramatically increase the spectral efficiency by using antenna arrays at both transmitter and receiver. An effective and practical way to approaching the capacity of MIMO wireless channels is to employ space time coding (STC). There are various approaches in coding structures including space time trellis codes (STTC) [1], space time block codes (STBC) [2], space time turbo trellis codes and layered space time (LST) codes. The pure example of LST is vertical Bell laboratories space time (VBLAST) [3]**.**

STBC is a simple and attractive space time coding scheme that was proposed by Alamouti [4**]**. It requires only a small degree of additional complexity. In particular, the Alamouti code offers very simple encoding, decoding and is particularly suitable for future wireless systems. Increasing demand for higher data rate requires transmission over broadband channel which is frequency selective. As a result, inter symbol interference (ISI) is introduced, which severely degrades the system performance. Using orthogonal frequency division multiplexing (OFDM) can turn frequency selective MIMO channel into a set of parallel frequency flat MIMO channels. In practice, combination OFDM and STBC is very popular and robust technique to mitigate ISI and improve the performance of the communication in terms of taking advantage of the spatial diversity in MIMO transmitting systems [5-6**].** Alamouti is remarkable orthogonal transmission structure can be applied in space time or space frequency domain in OFDM systems. The orthogonal designs can be applied as space time block coded (STBC_OFDM) [7], or frequency block coded (SFBC_OFDM) [8**].** The efficient design of the DL transmitter is of paramount importance for the sake of achieving a high throughput (high data rates), to obtain this, it is important to find schemes that to reduce the effects of fading and explore new type of diversity, as well as to reduce the effect of multiuser interference (MUI), also referred to as multiple access interference (MAI), and inter antenna interference (IAI). Otherwise, the performance of such STBC MIMO OFDM systems may also seriously degrade in the presence of MAI due to multiuser applications. The effect of MUI can be mitigated by employing spatio temporal preprocessing at the transmitter. Consequently, the DL receiver complexity may be reduced at the advent of transmit preprocessing at the base station (BS), a technique which is also often referred as Multiuser transmission (MUT) [9]. Employing the singular value decomposition (SVD). More specifically, the spatio temporal preprocessing technique of decomposes a MIMO channel into a set of parallel single user MIMO channels [10], which facilitates the employments of well known MIMO processing technique. If the CSI associated to different mobile station (MS) is available at the BS, the use of preprocessing scheme at the transmitter BS, allows simpler MS receiver implementation and eventually better performance.

In this paper, we propose two schemes based on SVD the zero forcing transmit scheme denoted (ZF_Tx_svd) and ZF receive scheme denoted (ZF_Rx_svd) combined with the MU SFBC OFDM system. This paper is organized as follows, in section II we present the MIMO OFDM eigenmode, section III the system overview, section IV the multi user detector, describing the ZF interference canceller at the receiver and at the

transmitter based on SVD, section V the simulation results are provided, finally in section VI we give our conclusions.

II. MIMO OFDM EIGENMODE

The DL of multiuser spatial multiplexing (MUSM) communication system is investigated where antenna arrays are used at both the base transceiver station (BTS) and at K mobile users. Due to the low complexity realisation at the mobile units, and the large diversity gain, linear processing Maintaining the Integrity of the specifications for MIMO system also referred to as Closed loop MIMO , where CSI is known at the transmitter, is used to multiple user and pre-cancel inter user interference. In particular, it was proven that MIMO eigenmode (EM) transmission system is optimal because MIMO capacity is maximized. MIMO EM uses the left and right eigenvectors of the channel matrix as eigenbeamformers in the receiver and the transmitter respectively to form the orthogonal spatial eigenbeams for transmission. We utilize SVD to obtain the largest eigen. In some sense, eigenbeamforming is an optimal space time processing scheme. However, it requires SVD on every subcarrier. It has been well known that SVD technique is an appropriate way to diagonalize the MIMO channel matrix.

MIMO OFDM system utilizing N subcarriers with M_t Transmit and M_r receive antennas signalling over MIMO frequency selective fading channel, $H_f: (M_r \times M_t)$ is the frequency domain channel response matrix for the fth subcarrier with possibly correlated coefficient, ${h_{ij}}^f$: *CN(0,1)* where $i = 1,..M_r$, and $j = 1,..M_t$. The columns vectors of flat fading channel matrix H_f are usually non orthogonal. However by SVD the channel matrix, H_f can be decomposed into diagonal matrix $D^{1/2}$ and two unitary matrices U and V. Assuming perfect CSI an SVD decomposition of the MIMO channels, H_f can be written as $H_f = U_f D_f {V_f}^H$. where , ${V_f}^H$ is the transpose conjugate of the matrix V_f, the $(M_r \times M_r)$ matrix U_f and the $(M_t \times M_t)$ matrix V_f are unitary matrices (i.e. $U_f {U_f}^H = IM_r$ and $V_f {V_f}^H = IM_t$), and D is a $(M_r \times M_t)$ diagonal matrixes whose non zero diagonal elements $\{\lambda_1, \lambda_2, ... \lambda_{R_{Hf}}\}$ are the real non negative singular values of H_f. We have $R_{Hf} = min(M_t \times M_r)$ is the rank of the channel matrix H_f. Therefore, the channel matrix H_f can be decomposed into orthogonal sub channel, the closed loop MIMO OFDM system can use eigenbeamforming on a tone by tone basis to transform a frequency selecting MIMO channel into a collection of $R_H N$ parallel subchannels.

III. SYSTEM OVERVIEW

We consider a downlink multiuser environment with a BS communication supporting K user mobile station (MS's) as shown in Figure. 1, the base station employs M transmit antennas and the kth users MS could be equipped with R_k receive antennas as shown in Figure. 2.a and Figure. 2.b, where $= 1,2, ..., K$ is the spatial multiplexer of the kth data branch generates a T_k dimensional vector symbol streams $S_k = [x_{k1}(1), x_{k2}(2), ... x_{kT_k}(n)]^T$, where T_k =2, is the transmit Alamouti matrix and n is the number of the transmitted symbols stream for each user before encoding, in space frequency coding (SFC), where *n=1..N/2*, (N= number of OFDM subcarrier). Where symbols $S_{k,d}$ $(k = 1,2, ..., K; d = 1,2)$ are chosen from the same constellation set S . For convenience we assume no error correction coding and a uniform allocation of power across the substreams for each user. At the BS before the SFBC encoding we implement the eigenbeamforming, preprocessing spatial multiplexing units requires CSI, and in the case of OFDM systems the transmitter requires preprocessing knowledge for all subcarriers, the symbol vectors n for the kth user is multiplied by a ($M \times T_k$) preprocessing matrix P_k as shown in Figure. 1, yielding:

$$X_k = P_k S_k \quad = 1,2, ..., K \tag{1}$$

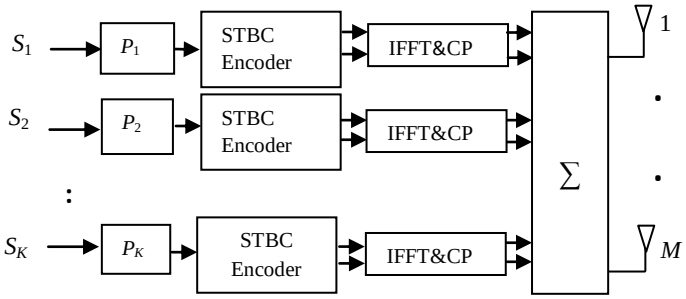

Figure. 1. Block diagram of the DL MUT Preprocessing

We assumed with the preprocessing symbol vectors from the other users to produce the composite transmitted symbol vector.

$$X_k = \sum_{k=1}^{K} P_k S_k \quad (2)$$

The preprocessed symbol vectors are passed through the combining block SFBC_OFDM encoder, by using the Alamouti schemes in frequency coding. A block of data symbols (OFDM symbol) transmitted over each transmitter passes through an *N* point inverse fast Fourier transform (IFFT), and the cyclic prefix (CP) is appended. The BS transmitter broadcast the signal to multiple *K* users simultaneously over the same frequency band through the frequency selective fading channel. At each receiver as shown in Figure. 2.a and Figure. 2.b, the CP removed and the fast Fourier transform (FFT) is applied to revert the received signals back to frequency domain. Hence the frequency selective MIMO channel is decoupled into *N* parallel flat fading channels. The R_k dimensional received signal y_k at the *k*th user where R_k=1,2 is a superposition of the *K* signal branches distorted by channel fading plus additive white Gaussian noise (AWGN).

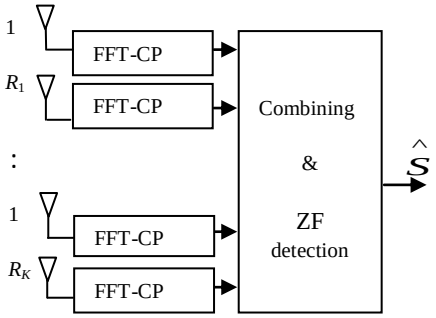

Figure. 2.a. Block diagram of the DL ZF receiver

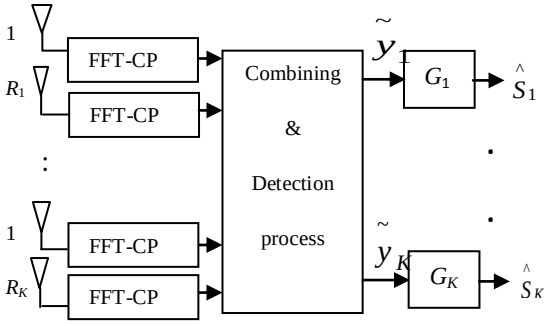

Figure. 2.b. Block diagram of the DL MUD

The complex baseband representation of the received signal vectors in the *f*th subcarrier where *f*=1… *N* can be expressed as:

$$y_k = \sum_{j=1}^{K} H_k C_j + w_k \quad (3)$$

The component *C* is the code matrix of Alamouti scheme of the OFDM symbols. The channel transfer matrix between the BS and the *k*th user H_k:(R_kx*M)* is the frequency domain channel response matrix for subcarrier *f*, and $h_{r,m}^{k}$ is the fading coefficient modelled as a finite impulse response filter (FIR) with *L* taps, associated with the *m*th BS antenna and *r*th receive antenna of user *k*, at a given subcarrier *f* .

Let $h_{rm}^{k} = [h_{rm}^{k}(0), h_{rm}^{k}(1), \ldots . h_{rm}^{k}(L-1)]$ (4)

Where *r*= {1,…,R_k} and *m*={1,…..*M*}. The elements of H_k are samples of independent and identically distributed (i,i,d) complex Gaussian random variables, circularly symmetric distributed with unit variance *CN*(0,1). The additive white Gaussian noise (AWGN) at the *r*th receive antenna of user *k*, $w = [w_1, w_1, \ldots, w_{R_k}]$ follows distribution $CN(0, {\sigma_w}^2 I)$**,** where *I* is the (R_k×R_k) identity matrix. Finally the entire multiuser MIMO channel may be characterized by the supermatrix *H*, which may be constructed by concatenating the corresponding channel matrices $\{H_k\}_{k=1}^{K}$ associated with each of the MS's, and the composite channel matrix is denote as:

$$H = \left[H^{(1)}, H^{(2)}, \ldots . H^{(K)}\right]^T \quad (5)$$

We can write the equation (3), hence the signal form become as follows:

$$\tilde{y}_k = \tilde{H}_k PS + w_k = \tilde{H}_k P_k S_k + \sum_{j=1, j\neq k}^{K} \tilde{H}_k P_j S_j + w_k$$
$$= \tilde{H}_k P_k S_k + Z_k + w_k \qquad k= 1,2,\ldots,K \quad (6)$$

P_k and S_k is the preproceesing matrix and the transmitted symbols vector *n* corresponding to the *k*th user. From (6) we see that the MUI component on the *k*th user is represented as Z_k, and $\tilde{H}_k$ is the equivalent channel transfer matrix between the BS and the *k*th user .If we have CSI available at both the transmitter and the receiver, and then we use the SVD decomposition of the channel user $\tilde{H}_k$ [11] .

$$\tilde{H}_k = U_k \left[D_k^{\frac{1}{2}}, 0\right] V_k = U_k \left[D_k^{\frac{1}{2}}, 0\right] \begin{bmatrix} {V_{ks}}^H \\ {V_{kn}}^H \end{bmatrix} \quad (7)$$

Where U_k and V_k are ($2R_k$×$2R_k$) and (*M*×*M*) component unitary matrices, respectively, and D_k is an ($2R_k$×$2R_k$) component diagonal matrix containing the eigenvalues of $\tilde{H}_k {\tilde{H}_k}^H$.

IV. Multi User Detector

4.1 ZF Receive Scheme Based On SVD

The optimal eignbeamforming as shown in [12-13], is the precoding matrix where P=V, which is derived from (7) and consequently the precoding matrix is defined as:

$$P_k = V_k \qquad k = 1,2,\dots,K \tag{8}$$

By substituting (8) in (6) the received signal can be expressed as:

$$\tilde{y}_k = \tilde{H}_k V_k S_k + Z_k + w_k \tag{9}$$

V_k and S_k is the precoding matrix and the transmitted symbols vector n corresponding to the kth user, and the equivalent effective channel can be expressed by:

$$\tilde{H} = [\tilde{H}_1, \tilde{H}_2, \dots, \tilde{H}_K]^T \tag{10}$$

The composite multiuser received signal may be express as:

$$\tilde{y}_k = \tilde{H} V S + w \tag{11}$$

$$V = [V^{(1)}, V^{(2)}, \dots V^{(K)}], w = [w^{(1)}, w^{(2)}, \dots, w^{(K)}]$$

V and w are the space time precoding supermatrix, as well as the AWGN noise. The receiver sees the equivalent channel matrix.

$$\tilde{\tilde{H}} = \tilde{H} V \tag{12}$$

And according to Figure. 2.a we can detect the desired signal vector streams S by the implementation of the ZF detection of equivalent channel matrix, hence remove the interference between the transmitted user streams and subsequently implemented the SFBC decoding. With the precoding matrix and the equivalent effective channel, we can express the ZF receiver based on SVD solution which is referred to ZF_Rx_svd as follow:

$$\tilde{\tilde{H}}_{ZF} = V^H \tilde{H}_{ZF} \quad \text{, where } \tilde{H}_{ZF} = (\tilde{H}^H \tilde{H})^{-1} \tilde{H}^H \tag{13}$$

4.1. ZF Transmit Scheme Based On SVD

In this section we present the ZF transmit scheme to pre-cancel the MUI interference based on the SVD, at the BS station, from (6) and (7) the received signal of the kth user $\tilde{y}_k$ may be expressed as:

$$\tilde{y}_k = U_k D^{1/2} {V_{ks}}^H P S + w_k \qquad k = 1,2,\dots,K \tag{14}$$

Then the overall DL received signal vector streams $\tilde{y}_k$ of the K M's can be expressed as:

$$\tilde{y}_k = U D^{1/2} {V_s}^H P S + w \tag{15}$$

According to [11], The DL BS transmit preprocessing matrix P is designed, that the DL MUI can efficiently be suppressed. The MUI can fully be removed when the DL preprocessing matrix to satisfy:

$$P = [{V_s}^H]^+ B = \bar{P} B \tag{16}$$

Where the power allocation regime of $B = diag\{B_{11}, B_{1T_k}; \dots.; B_{K1}, \dots, B_{KT_k}\}$ and $[{V_s}^H]^+$ denotes the pseudo inverse of the matrix ${V_s}^H$, which is referred to ZF_Tx_svd**,** and $\bar{P} = V_s[{V_s}^H V_s]$.

When substituting the overall DL preprocessing matrix of (16) into (15) the overall received signal vector y of K MS user can be simplified to

$$\tilde{y}_k = U D^{1/2} B S + w \tag{17}$$

The symbol vector of the kth MS can be expressed as:

$$\tilde{y}_k = U_k {D_k}^{1/2} B_k S_k + w_k \tag{18}$$

The IAI can be suppressed with the SVD based matrices $\{U_k\}$ of (7). By $\{G_k = {U_k}^H\}$ according to Figure. 2.b the user specific decision variables can individually be expressed as:

$$\hat{S}_k = {D_k}^{1/2} B_k S_k + {U_k}^H w_k \qquad k = 1,2,\dots,K \tag{19}$$

And the overall decision variables can expressed as:

$$\hat{S} = D^{1/2} B S + U^H w \tag{20}$$

The overall of the user decision symbol stream can be expressed as: $\hat{S} = [\hat{S}_1, \hat{S}_2, \dots.., \hat{S}_K]^T$

V. Simulation Results

In this section, we consider SFBC system with N = 64 (N: number of subcarrier OFDM). Combined with the SVD MUT and MUD by applying the ZF receiver and ZF transmitter scheme and compared them with ZF_VBLAST. The maximum channel delay spread and the CP length are the same and equal to L=16. In other words, channel with long excess delay time, exhibit a lower coherence bandwidth corresponding to higher frequency selectivity than shorter channel. The SISO channels from the transmit antennas to the receive antennas are assumed to be independent and Rayleigh distributed. The complex symbols are assumed to be quaternary phase shift keying (QPSK).

Figure.3. Shows the BER performance comparison of two users SFBC_OFDM system. When each user has one receive antenna and 4 BTS transmit antennas (4×2 users/1Rx). It is shown that the ZF_Tx_sdv scheme's outperforms the ZF_VBLAST by 16 dB, and the ZF_Rx_svd by 20 db at BER=10^{-4} . VBLAST, decodes the substreams, subtracts its interference and then decodes the later substreams. However, was not

designed for exploiting transmits diversity. The performance of VBLAST receiver is mainly dependent on the first substreams, which has the lowest diversity gain and limited by error propagation. Where in ZF_Rx_svd, the noise term may be amplified in a way that influences the decoding output in negative way.

Figure.4. Shows the BER performance comparison of two users SFBC_OFDM system. When each user has two receive antenna and 4 BTS transmit antennas (4×2 users/2Rx).

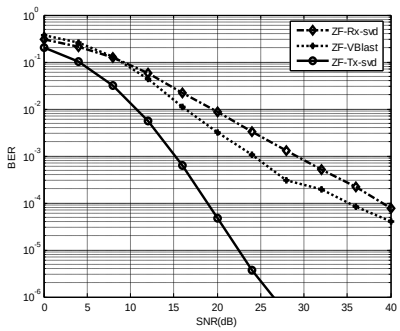

Figure.3. BER performance comparison of 2 users SFBC_OFDM System, with 4 BTS transmit antenna and 1 receive antenna per user, using ZF_Tx_svd

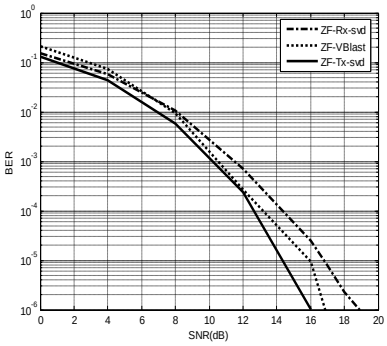

Figure.4. BER performance comparison of 2 users SFBC_OFDM System, with 4 BTS transmit antenna and 2 receive antenna per user, using ZF_Tx_svd

It is shown that the ZF_Tx_svd scheme's outperforms the ZF_VBLAST by 1dB, and the ZF_Rx_svd by 3 db at BER=10^{-6}. By adding one antenna at each receiver, however, a significant SNR reduction of 10 dB is achieved at BER=10^{-6} for ZF_Tx_svd scheme. The eigenmode selection achieves a higher diversity order than simple spatial multiplexing and increase the diversity gain.

VI. CONCLUSION

Multiuser SFBC_OFDM system combined with SVD assisted MUT and MUD is studied in the frequency selecting fading channel, from the results the ZF transmit scheme based on SVD for MUI precanceller outperforms the ZF_VBLAST and ZF receiver based on SVD. It can be concluded that the space frequency coded system coupled with SVD assisted MUT and MUD with ZF transmit scheme efficiently exploits diversity techniques. These are, space and frequency diversity to overcome fading found in the radio channel, and provides high performance.

References

[1] V. Tarokh, N. Seshadri, and A. R. Calderbank, *Space-time codes for high data rate wireless communication, Performance criterion and code construction*, IEEE Trans. Inform. Theory, vol.44, no.2, 744-765, Mar.1998.

[2] V. Tarokh, H. Jafarkhani and A .R. Calderbank, *Space-time block codes from orthogonal design*, IEEE Trans. Info. Th., vol. 45, no. 5, 1456-1467, Jul. 1999.

[3] Thuong Le-Tien, Tuan Ly-Huu, *V BLAST Detection in Space Time Coding Wireless system and implementation on FPGA*, International Symposium on Electrical Electronics Engineering 2007-Oct 24, 25 2007-HCM City, Vietnam .

[4] S.M. Alamouti. *A simple transmit diversity technique for wireless communications.* IEEE J.Select. Areas Common, vol.16, 1451-1458.1998.

[5] A.Doufexi, E.Tameh, A.Nix, A.Pal, M.Beach, C.Williams, *Throughput and Coverage of WLANs Employing STBC under Different Channel Conditions*, ISWCS 2004, Mauritius, September 2004.

[6] Muhammad Imadur Rahman, Nicola Marchetti, Suvra Sekhar Das, Frank H.P. Fitzek, Ramjee Prasad, *Combining Orthogonal Space Frequency Block Coding and Spatial Multiplexing in MIMO-OFDM System,"*(is available at http:// www.kom.aau.dk/ ff/document/ InOWo 2005).

[7] K. F. Lee and D. B. Williams, *A space-time coded transmitter diversity technique for frequency selective fading channels*, in Proc. IEEE Sensor Array and Multichannel Signal Processing Workshop, Cambridge, MA, 149-152. March 2000.

[8] K. F. Lee and D. B. Williams, *A Space-frequency transmitter diversity technique for OFDM systems,* in Proc. IEEE GLOBECOM, San Francisco, CA, 1473-1477,Nov. 2000.

[9] R.Irmer, *Multiuser transmission in code division multiple access mobile Communications systems*, Ph.D. dissertation, Technische Universitat Dresden, 2005.

[10] Gordon L. Stuber, John Barry, Steve W. Mc Laughlin,Ye (Geoffrey) Li, Mary Ann Ingram, Thomas G. *Broadband MIMO OFDM Wireless Communications,"*(is available at http:// www.ece.gatech.edu/ users/stuber/nsf3/ pubs/./proc-ieee.).

[11] W.Liu, L. L.Yang, and L. Hanzo, *SVD assisted multiuser transmitter and multiuser detector design for MIMO system*, IEEE Transactions on Vehicular Technology, Vol. 58, No. 2, February 2009.

[12] Daniel Schneider, Joachim Speidel othar Stadelmeier, Dietmar Schill, *Precoded Spatial Multiplexing MIMO for Inhome Power Line communications* , in Global Telecommunications Conference (IEEE GLOBECOM 2008), New Orleans, 2008.

[13] Runhua Chen, Robert W. Heath, Jeffrey G. Andrews, *Transmit Selection Diversity for Unitary Precoded Multiuser Spatial Multiplexing Systems With Linear Receivers*, proc of IEEE Global Telecommunications Conference, Nov. 29-Dec. 3, 2004, Dallas, TX, USA. (is available at http:// www.users. ece.utexas.edu/ rheath/ papers/ 2005/.

Appendix

Appendix A :

SDM :

$$S = [\, s_1 \quad s_2 \,] \tag{A.1}$$

The Alamouti Code Matrix:

$$G_{STBC} = \begin{bmatrix} s_1 & -s_2{}^* \\ s_2 & s_1{}^* \end{bmatrix} \tag{A.2}$$

Alamouti 2×1 Schemes :

$$r_1 = h_1 s_1 + h_2 s_2 + n_1 \tag{A.3}$$

$$r_2 = -h_1 s_2^* + h_2 s_1^* + n_2 \tag{A.4}$$

$$\begin{bmatrix} r_1 \\ r_2 \end{bmatrix} = \begin{bmatrix} s_1 & -s_2^* \\ s_2 & s_1^* \end{bmatrix} \begin{bmatrix} h_1 \\ h_2 \end{bmatrix} + \begin{bmatrix} n_1 \\ n_2 \end{bmatrix} \tag{A.5}$$

$$\begin{bmatrix} r_1 \\ r_2^* \end{bmatrix} = \begin{bmatrix} h_1 & h_2 \\ h_2^* & -h_1^* \end{bmatrix} \begin{bmatrix} s_1 \\ s_2 \end{bmatrix} + \begin{bmatrix} n_1 \\ n_2^* \end{bmatrix} \tag{A.6}$$

The equation (A.6) can be written as:

$$\boldsymbol{r = H\,S + n} \tag{A.7}$$

Then, the equivalent matrix channel model of Alamouti 2×1 schemes can be represented as

$$\boldsymbol{H} = \begin{bmatrix} h_1 & h_2 \\ h_2^* & -h_1^* \end{bmatrix} \tag{A.8}$$

Alamouti 2×2 Schemes :

$$r_1(t) = h_{11} s_1 + h_{12} s_2 + n_{11} \tag{A.9}$$

$$r_2(t) = h_{21} s_1 + h_{22} s_2 + n_{21} \tag{A.10}$$

$$r_1(t+T) = -h_{11} s_2^* + h_{12} s_1^* + n_{12} \tag{A.11}$$

$$r_2(t+T) = -h_{21} s_2^* + h_{22} s_1^* + n_{22} \tag{A.12}$$

$$r_1^*(t+T) = -h_{11}^* s_2 + h_{12}^* s_1 + n_{12}^* \tag{A.13}$$

$$r_2^*(t+T) = -h_{21}^* s_2 + h_{22}^* s_1 + n_{22}^* \tag{A.14}$$

$$\begin{bmatrix} r_1(0) \\ r_2(0) \\ r_1^*(T) \\ r_2^*(T) \end{bmatrix} = \begin{bmatrix} h_{11} & h_{12} \\ h_{21} & h_{22} \\ h_{12}^* & -h_{11}^* \\ h_{22}^* & -h_{21}^* \end{bmatrix} \begin{bmatrix} s_1 \\ s_2 \end{bmatrix} + \begin{bmatrix} n_1(0) \\ n_2(0) \\ n_1^*(T) \\ n_2^*(T) \end{bmatrix} \tag{A.15}$$

The equation (A.15) can be written as:

$$\boldsymbol{r = H\,S + n} \tag{A.16}$$

Then, the equivalent matrix channel model of Alamouti 2×2 schemes can be represented as

$$\boldsymbol{H} = \begin{bmatrix} h_{11} & h_{12} \\ h_{21} & h_{22} \\ h_{12}^* & -h_{11}^* \\ h_{22}^* & -h_{21}^* \end{bmatrix} \tag{A.17}$$

4 × 2 Stacked STBCs:

In this case, two data streams can be sent using a double space time transmit diversity (DSTTD) scheme that essentially consists of operating two 2×1 Alamouti code systems in parallel . DSTTD, also called "Stacked STBCs", combines transmit diversity and maximum ratio combining techniques along with a form of spatial multiplexing.

The received signals at times 0 and T on antennas 1 and 2 can be represented with the equivalent channel model as:

$$\begin{bmatrix} r_1(0) \\ r_1^*(T) \\ r_2(0) \\ r_2^*(T) \end{bmatrix} = \begin{bmatrix} h_{11} & h_{12} & h_{13} & h_{14} \\ h_{12}^* & -h_{11}^* & h_{13}^* & -h_{13}^* \\ h_{21} & h_{22} & h_{23} & h_{24} \\ h_{22}^* & -h_{21}^* & h_{24}^* & -h_{23}^* \end{bmatrix} \begin{bmatrix} s_1 \\ s_2 \\ s_3 \\ s_4 \end{bmatrix} + \begin{bmatrix} n_1(0) \\ n_1^*(T) \\ n_2(0) \\ n_2^*(T) \end{bmatrix} \tag{A.18}$$

Then, the equivalent matrix channel model of 4 × 2 DSTTD can be represented as

$$\begin{bmatrix} \boldsymbol{r_1} \\ \boldsymbol{r_2} \end{bmatrix} = \begin{bmatrix} H_{11} & H_{12} \\ H_{21} & H_{22} \end{bmatrix} \begin{bmatrix} \boldsymbol{s_1} \\ \boldsymbol{s_2} \end{bmatrix} + \begin{bmatrix} \boldsymbol{n_1} \\ \boldsymbol{n_2} \end{bmatrix} \tag{A.19}$$

$$H_{11} = \begin{bmatrix} h_{11} & h_{12} \\ h_{12}^* & -h_{11}^* \end{bmatrix} \tag{A.20}$$

$$H_{21} = \begin{bmatrix} h_{21} & h_{22} \\ h_{22}^* & -h_{21}^* \end{bmatrix} \tag{A.21}$$

$$H_{12} = \begin{bmatrix} h_{13} & h_{14} \\ h_{13}^* & -h_{13}^* \end{bmatrix} \tag{A.22}$$

$$H_{22} = \begin{bmatrix} h_{23} & h_{24} \\ h_{24}^* & -h_{23}^* \end{bmatrix} \tag{A.23}$$

Thus, DSTTD can achieve a diversity order of $Nd = 2Nr$ (ML detection) or $Nd = 2$ (ZF detection) due to the 2 × 1 Alamouti code while also transmitting 2 data streams (spatial multiplexing order of 2).

If the same linear combining scheme is used as in the 2 × 1 STBC case, then the following decision statistics can be obtained.

$$\tilde{s}_1 = (|h_{11}|^2 + |h_{12}|^2 + |h_{21}|^2 + |h_{22}|^2)s_1 + I_3 + I_4 + 2\ noise\ terms \quad (A.24)$$

$$\tilde{s}_2 = (|h_{11}|^2 + |h_{12}|^2 + |h_{21}|^2 + |h_{22}|^2)s_2 + I_3 + I_4 + 2\ noise\ terms \quad (A.25)$$

$$\tilde{s}_3 = (|h_{13}|^2 + |h_{14}|^2 + |h_{23}|^2 + |h_{24}|^2)s_3 + I_1 + I_2 + 2\ noise\ terms \quad (A.26)$$

$$\tilde{s}_4 = (|h_{13}|^2 + |h_{14}|^2 + |h_{23}|^2 + |h_{24}|^2)s_4 + I_1 + I_2 + 2\ noise\ terms \quad (A.27)$$

Where I_i is the interference from the *i*-th transmit antenna, due to transmitting 2 simultaneous data streams. The detection process of DSTTD should attempt to suppress the interference between the two STBC encoders, and for this purpose can turn to any the spatial multiplexing receivers, such as ZF, MMSE, and BLAST. In contrast to OSTBCs (Alamouti codes), the ML receiver for stacked STBCs is not linear.

4×4 Stacked STBC:

$$\begin{bmatrix} r_1(0) \\ r_1^*(T) \\ r_2(0) \\ r_2^*(T) \end{bmatrix} = \begin{bmatrix} h_{11} & h_{12} & h_{13} & h_{14} \\ h_{12}^* & -h_{11}^* & h_{14}^* & -h_{13}^* \\ h_{21} & h_{22} & h_{23} & h_{24} \\ h_{22}^* & -h_{21}^* & h_{24}^* & -h_{23}^* \\ h_{31} & h_{32} & h_{33} & h_{34} \\ h_{32}^* & -h_{31}^* & h_{34}^* & -h_{33}^* \\ h_{41} & h_{42} & h_{43} & h_{44} \\ h_{42}^* & -h_{41}^* & h_{44}^* & -h_{43}^* \end{bmatrix} \begin{bmatrix} s_1 \\ s_2 \\ s_3 \\ s_4 \end{bmatrix} + \begin{bmatrix} n_1(0) \\ n_1^*(T) \\ n_2(0) \\ n_2^*(T) \end{bmatrix} \quad (A.28)$$

Then, the equivalent matrix channel model of 4 × 4 DSTTD can be represented as

$$\begin{bmatrix} \boldsymbol{r_1} \\ \boldsymbol{r_2} \end{bmatrix} = \begin{bmatrix} H_{11} & H_{12} \\ H_{21} & H_{22} \end{bmatrix} \begin{bmatrix} \boldsymbol{s_1} \\ \boldsymbol{s_2} \end{bmatrix} + \begin{bmatrix} \boldsymbol{n_1} \\ \boldsymbol{n_2} \end{bmatrix} \quad (A.29)$$

$$H_{11} = \begin{bmatrix} h_{11} & h_{12} \\ h_{12}^* & -h_{11}^* \\ h_{21} & h_{22} \\ h_{22}^* & -h_{21}^* \end{bmatrix} \quad (A.30)$$

$$H_{21} = \begin{bmatrix} h_{31} & h_{32} \\ h_{32}^* & -h_{31}^* \\ h_{41} & h_{42} \\ h_{42}^* & -h_{41}^* \end{bmatrix} \quad (A.31)$$

$$H_{12} = \begin{bmatrix} h_{13} & h_{14} \\ h_{14}^* & -h_{13}^* \\ h_{23} & h_{24} \\ h_{24}^* & -h_{23}^* \end{bmatrix} \quad (A.32)$$

$$H_{22} = \begin{bmatrix} h_{33} & h_{34} \\ h_{34}^* & -h_{33}^* \\ h_{43} & h_{44} \\ h_{44}^* & -h_{43}^* \end{bmatrix} \quad (A.33)$$

If the same linear combining scheme is used as in the 2 × 2 STBC case, then the following decision statistics can be obtained.

$$\tilde{s}_1 = (|h_{11}|^2 + |h_{12}|^2 + |h_{21}|^2 + |h_{22}|^2)s_1 + I'_3 + I'_4 + 4\,noise\ terms \quad (A.34)$$

$$\tilde{s}_2 = (|h_{11}|^2 + |h_{12}|^2 + |h_{21}|^2 + |h_{22}|^2)s_2 + I'_3 + I'_4 + 4\,noise\ terms \quad (A.35)$$

$$\tilde{s}_3 = (|h_{13}|^2 + |h_{14}|^2 + |h_{23}|^2 + |h_{24}|^2)s_3 + I'_1 + I'_2 + 4\,noise\ terms \quad (A.36)$$

$$\tilde{s}_4 = (|h_{13}|^2 + |h_{14}|^2 + |h_{23}|^2 + |h_{24}|^2)s_4 + I'_1 + I'_2 + 4\,noise\ terms \quad (A.37)$$

Appendix B:

Space Time Block Code OFDM:

For each pair of two successive data symbol vectors, if $S1$ is the first block data symbol vector and $S2$ is the second block vector, which are the frequency domain symbols, they are defined as:

$$S1 = [S(1)\ S(2)\ S(3) \dots \dots \dots \dots S(N)] \qquad (B.1)$$

$$S2 = [S(N+1)\ \ S(N+2) \dots S(2N)] \qquad (B.2)$$

The equivalent space time block code transmission matrix is given by

$$G_{STBC} = \begin{bmatrix} S1 & -S2^* \\ S2 & S1^* \end{bmatrix} \qquad (B.3)$$

Therefore, entries of the transmission matrix are the OFDM symbol vectors $S1$, $S2$, and their complex conjugates.

STBC User 2x1:

Let $r^1(k)$ and $r^2(k)$ represent the demodulated symbols, $r^1(k)$ and $r^2(k)$, ,can be represented as

$$r^1(k) \ = H_{11}(k)\ S1(k) + H_{12}(k)\ S2(k) + n^1(k) \qquad (B.4)$$

$$r^2(k) = -H_{11}(k)\ S2^*(k) + H_{12}(k)\ S1^*(k) + n^2(k) \qquad (B.5)$$

$$r^{2^*}(k) = -H_{11}{}^*(k)\ S2(k) + H_{12}{}^*(k)\ S1(k) + n^{2^*}(k) \qquad (B.6)$$

The decision variables are constructed by combining $r^1(k)$, $r^2(k)$, and are calculated by the following equations:

$$\hat{S}1(k) = H_{11}{}^*(k)\ r^1(k) + H_{12}(k)\ r^{2^*}(k) \qquad (B.7)$$

$$\hat{S}2(k) = H_{12}{}^*(k) r^1(k) - H_{11}(k) r^{2^*}(k) \qquad (B.8)$$

Substituting equations (B.4) and (B.6) into equations (B.7) and (B.8), we get

$$\hat{S}1(k) = H_{11}{}^*(k)\ \big(\ H_{11}(k)\ S1(k) + H_{12}(k)\ S2(k) + n^1(k)\big) + H_{12}(k)\ \ \Big(-H_{11}{}^*(k)\ S2(k) + H_{12}{}^*(k)\ S1(k) + n^{2^*}(k)\Big) \qquad (B.9)$$

$$\hat{S}2(k) = H_{12}{}^*(k)\big(H_{11}(k)\ S1(k) + H_{12}(k)\ S2(k) + n^1(k)\big) - H_{11}(k)\Big(-H_{11}{}^*(k)\ S2(k) + H_{12}{}^*(k)\ S1(k) + n^{2^*}(k)\Big) \qquad (B.10)$$

$$\hat{S}1(k) = (|H_{11}|^2 + |H_{12}|^2\ )\,S1(k) + (\ {H_{11}}^*(k)H_{12}(k) - {H_{11}}^*(k)H_{12}(k)\ )S2(k)) + \left(\ {H_{11}}^*(k)\,n^1(k) + H_{12}(k)n^{2^*}(k)\right) \quad (B.11)$$

$$\hat{S}2(k) = (|H_{11}|^2 + |H_{12}|^2\ )\,S2(k) + (H_{12}{}^*(k)\left(H_{11}(k) - H_{11}(k)(H_{12}{}^*(k)\ )S1(k) + H_{12}{}^*(k)n^1(k) - H_{11}(k)n^{2^*}(k)\right) \quad (B.12)$$

$$\hat{S}1(k) = (|H_{11}|^2 + |H_{12}|^2\ )\,S1(k) + {H_{11}}^*(k)\,n^1(k) + H_{12}(k)n^{2^*}(k) \quad (B.13)$$

$$\hat{S}2(k) = (|H_{11}|^2 + |H_{12}|^2\ )\,S2(k) + {H_{12}}^*(k)\,n^1(k) - H_{11}(k)\,n^{2^*}(k)) \quad (B.14)$$

STBC User 2×2:

We assume that the channel responses are constant during the two time slots. Let $r_1^1(k), r_1^2(k)$ and $r_2^1(k), r_2^2(k)$, represent the demodulated symbols, after the OFDM demodulator, on the *k*-th sub-carrier at the first and second time slot, respectively, at receive antenna 1 and 2 .The received signal $r_1^1(k), r_1^2(k)$ and $r_2^1(k)$, $r_2^2(k)$, $k = 1,2,\dots,N$,can be represented as

First receiver:

$$r_1^1(k) = H_{11}(k)\,S1(k) + H_{12}(k)\,S2(k) + n_1^1(k) \quad (B.15)$$

$$r_1^2(k) = -H_{11}(k)\,S2^*(k) + H_{12}(k)\,S1^*(k) + n_1^2(k) \quad (B.16)$$

$${r_1^2}^*(k) = -{H_{11}}^*(k)\,S2(k) + {H_{12}}^*(k)\,S1(k) + {n_1^2}^*(k) \quad (B.17)$$

Second receiver:

$$r_2^1(k) = H_{21}(k)\,S1(k) + H_{22}(k)\,S2(k) + n_2^1(k) \quad (B.18)$$

$$r_2^2(k) = -H_{21}(k)\,S2^*(k) + H_{22}(k)\,S1^*(k) + n_2^2(k) \quad (B.19)$$

$${r_2^2}^*(k) = -{H_{21}}^*(k)\,S2(k) + H_{22}(k)\,S1(k) + {n_2^2}^*(k) \quad (B.20)$$

The decision variables are constructed by combining $r_1^1(k), r_1^2(k)$, $r_2^1(k), r_2^2(k)$, and the channel frequency response. And are calculated by the following equations

$$\hat{S}1(k) = {H_{11}}^*(k)\,r_1^1(k) + H_{12}(k)\,{r_1^2}^*(k) + H_{21}(k)\,r_2^1(k) + H_{22}(k){r_2^2}^*(k) \quad (B.21)$$

$$\hat{S}2(k) = H_{12}(k)\,r_1^1(k) - H_{11}(k){r_1^2}^*(k) + H_{22}(k)\,r_2^1(k) - H_{21}(k)\,{r_2^2}^*(k) \quad (B.22)$$

Substituting equations (B.18) and (B.20) into equations (B.21) and (B.22), we get

$$\hat{S}1(k) = H_{11}{}^{*}(k)(H_{11}(k)\,S1(k) + H_{12}(k)\,S2(k) + n_1^1(k)\,)$$
$$+ H_{12}(k)(-H_{11}{}^{*}(k)\,S2(k) + H_{12}{}^{*}(k)\,S1(k) + n_1^{2^*}(k))$$
$$+H_{21}(k)(H_{21}(k)\,S1(k) + H_{22}(k)\,S2(k) + n_2^1(k))$$
$$+H_{22}(k)\left(-H_{21}{}^{*}(k)\,S2(k) + H_{22}(k)\,S1(k) + n_2^{2^*}(k)\right) \qquad (B.23)$$

$$\hat{S}2(k) = H_{12}(k)(H_{11}(k)\,S1(k) + H_{12}(k)\,S2(k)$$
$$+ n_1^1(k)\,) - H_{11}(k)\left(-H_{11}{}^{*}(k)\,S2(k) + H_{12}{}^{*}(k)\,S1(k) + n_1^{2^*}(k)\right)$$
$$+\ H_{22}(k)\left(H_{21}(k)\,S1(k) + H_{22}(k)\,S2(k) + n_2^1(k)\right)$$
$$- H_{21}(k)\left(-H_{21}{}^{*}(k)\,S2(k) + H_{22}(k)\,S1(k) + n_2^{2^*}(k)\right) \qquad (B.24)$$

$$\hat{S}1(k) = (|H_{11}|^2 + |H_{12}|^2 + |H_{21}|^2 + |H_{22}|^2\,)S1(k) +$$
$$+ (H_{11}{}^{*}(k)H_{12}(k) - H_{11}{}^{*}(k)\,H_{12}(k) - H_{21}{}^{*}(k)\,H_{22}(k) + H_{21}(k)H_{22}(k))S2(k)$$
$$+\left(H_{11}{}^{*}(k)n_1^1(k) + H_{21}(k)n_2^1(k) + H_{12}(k)n_1^{2^*}(k) + H_{22}(k)n_2^{2^*}(k)\right) \qquad (B.25)$$

$$\hat{S}2(k) = (|H_{11}|^2 + |H_{12}|^2 + |H_{21}|^2 + |H_{22}|^2\,)S2(k)$$
$$+\left(H_{11}(k)H_{12}(k) - H_{11}(k)H_{12}{}^{*}(k) + H_{21}(k)\,H_{22}(k) - H_{21}(k)H_{22}(k)\right)S1(k)$$
$$-H_{11}(k)\,n_1^{2^*}(k) + H_{12}(k)\,n_1^1(k) - H_{21}(k)\,n_2^{2^*}(k) + H_{22}(k)\,n_2^1(k) \qquad (B.26)$$

$$\hat{S}1(k) = (|H_{11}|^2 + |H_{12}|^2 + |H_{21}|^2 + |H_{22}|^2)S1(k)$$
$$+\left(H_{11}{}^{*}(k)n_1^1(k) + H_{21}(k)n_2^1(k) + H_{12}(k)n_1^{2^*}(k) + H_{22}(k)n_2^{2^*}(k)\right) \qquad (B.27)$$

$$\hat{S}2(k) = (|H_{11}|^2 + |H_{12}|^2 + |H_{21}|^2 + |H_{22}|^2\,)S2(k)$$
$$+H_{12}(k)\,n_1^1(k) - H_{11}(k)\,n_1^{2^*}(k) - H_{21}(k)\,n_2^{2^*}(k) + H_{22}(k)\,n_2^1(k) \qquad (B.28)$$

Space Frequency Block Code OFDM:

In SFBC-OFDM, the data symbol vector for q-th user is defined as $S^q = [S(1)S(2) \dots S(N)]$, where N is the number of OFDM sub-carrier. The symbol vector is coded into two length $1 \times N$ vectors, S_1 and S_2 by the space frequency encoder block as:

$$S_1 = [S(1) \ -S^*(2) \dots \dots S(N-1) \ -S^*(N)] \qquad (B.29)$$

$$S_2 = [S(2) \quad S^*(1) \dots . . S(N) \quad S^*(N-1)] \qquad (B.30)$$

S_1 is transmitted from the first antenna transmitter, while S_2 is transmitted simultaneously from the second antenna transmitter. Let S^e and S^o be two length $N/2$ vectors denoting the even and odd component vectors of S. Therefore,

$$S^o = [S(1) \ S(3) \dots \ S(N-3) \ S(N-1)] \qquad (B.31)$$

$$S^e = [S(2) \ S(4) \dots \dots \dots \ S(N-2) \ S(N)] \qquad (B.32)$$

Equations (31),(32) can then be expressed in terms of the even and odd component vectors as

$$S_1{}^e = -S^{e*} \qquad S_1{}^o = S^o$$

$$S_2{}^e = S^{o*} \qquad S_2{}^o = S^e \qquad (B.33)$$

SFBC User 2×1:

Let $r(k)$ represents the demodulated symbol, after the OFDM demodulator, on the k-th sub-carrier, $k = 1,2, \dots . , N$

$$r(k) = H_{11}(k) \ S_1(k) + H_{12}(k) \, S_2(k) + n(k) \qquad (B.34)$$

Where $H_{ji}(k)$ is the channel frequency response from transmit antenna i to receive antenna j, on the k-th sub-carrier. Let $r^e(k)$ and $r^o(k)$, $k = 1,2, \dots . , N/2$, represent the even and odd components of $r(k)$. Thus, $r^e(k)$ and $r^o(k)$, can be represented as:

$$r^e(k) = H_{11}^e(k) \, S_1^e(k) + H_{12}^e(k) \, S_2^e(k) + n^e(k) \qquad (B.35)$$

$$r^o(k) = H_{11}^o(k) \, S_1^o(k) + H_{12}^o(k) \, S_2^o(k) + n^o(k) \qquad (B.36)$$

Where $n^e(k)$ and $n^o(k)$ represent the even and odd components, respectively, of the demodulated noise vector. Substituting equation (B.33) into equations (B.35) and (B.36), we get

$$r^o(k) = H_{11}^o(k) \, S^o(k) + H_{12}^o(k) \ S^e(k) + n^o(k) \qquad (B.37)$$

$$r^e(k) = -H_{11}^e(k) \, S^{e*}(k) + H_{12}^e(k) \, S^{o*}(k) + n^e(k) \qquad (B.38)$$

From equations (B.37) and (B.38), we conclude that SFBC-OFDM can be represented by the transmission matrix for adjacent OFDM sub-carrier.

$$G_{SFBC} = \begin{bmatrix} S^o & -S^{e*} \\ S^e & S^{o*} \end{bmatrix} \qquad (B.39)$$

The decision variables are constructed by combining $r^e(k)$, $r^o(k)$ and the channel frequency response. $\hat{S}^e(k)$ and $\hat{S}^o(k)$, $k = 1,2, \ldots, N/2$ are calculated by the following equations:

$$r^o(k) = H_{11}^o(k)\, S^o(k) + H_{12}^o(k)\ S^e(k) + n^o(k) \qquad (B.40)$$

$$r^e(k) = -H_{11}^e(k)\, S^{e*}(k) + H_{12}^e(k)\, S^{o*}(k) + n^e(k) \qquad (B.41)$$

$$r^{e*}(k) = -H_{11}^{e\ *}(k)\, S^e(k) + H_{12}^{e\ *}(k)\, S^o(k) + n^{e*}(k) \qquad (B.42)$$

Assuming the complex channel gains between adjacent sub-carriers are approximately constant, such as

$H_{11}^o(k) = H_{11}^e(k) = H_{11} \qquad H_{12}^o(k) = H_{12}^e(k) = H_{12}$

Therefore,

$$\hat{S}^o(k) = H_{12}^e(k)\, r^{e*}(k) + H_{11}^{o\ *}(k)\ r^o(k) \qquad (B.43)$$

$$\hat{S}^e(k) = -H_{11}^e(k)\, r^{e*}(k) + H_{12}^{o\ *}(k)\ r^o(k) \qquad (B.44)$$

$$\begin{aligned} \hat{S}^o(k) = {} & H_{12}^e(k)\ \left(-H_{11}^{o\ *}(k)\, S^e(k) + H_{12}^{o\ *}(k)\, S^o(k) + n^{e*}(k) \right) \\ & + H_{11}^{o\ *}(k)\left(H_{11}^o(k)\, S^o(k) + H_{12}^o(k)\ S^e(k) + n^o(k) \right) \end{aligned} \qquad (B.45)$$

$$\begin{aligned} \hat{S}^e(k) = {} & -H_{11}^e(k)\ (-H_{11}^{o\ *}(k)\, S^e(k) + H_{12}^{o\ *}(k)\, S^o(k) + n^{e*}(k)\ ) \\ & + H_{12}^{o\ *}(k)\left(H_{11}^o(k)\, S^o(k) + H_{12}^o(k)\ S^e(k) + n^o(k) \right) \end{aligned} \qquad (B.46)$$

$$\begin{aligned} \hat{S}^o(k) = {} & (|H_{11}^o|^2 + |H_{12}^e|^2\ )S^o(k) + H_{12}^e(k)\ (-H_{11}^{o\ *}(k)\, S^e(k) + n^{e*}(k)) \\ & + H_{11}^{o\ *}(k)\ (H_{12}^o(k)\ S^e(k) + n^o(k)) \end{aligned} \qquad (B.47)$$

$$\begin{aligned} \hat{S}^e(k) = {} & (|H_{11}^o|^2 + |H_{12}^o|^2)\, S^e(k) - H_{11}^e(k)\ \left(H_{12}^{o\ *}(k)\, S^o(k) + n^{e*}(k) \right) \\ & + H_{12}^{o\ *}(k)\left(H_{11}^o(k)\, S^o(k) + n^o(k) \right) \end{aligned} \qquad (B.48)$$

$$\begin{aligned} \hat{S}^o(k) = {} & (|H_{11}^o|^2 + |H_{12}^e|^2\ )S^o(k) + (-H_{11}^{o\ *}(k)H_{12}^e(k) + H_{11}^{o\ *}(k)H_{12}^o(k)\ )\, S^e(k) \\ & + H_{11}^{o\ *}(k)n^o(k) + H_{12}^e(k)\, n^{e*}(k) \end{aligned} \qquad (B.49)$$

$$\begin{aligned} \hat{S}^e(k) = {} & (|H_{11}^o|^2 + |H_{12}^o|^2)\, S^e(k) + (H_{12}^{o\ *}(k)\, H_{11}^o(k) - H_{11}^e(k)\ H_{12}^{o\ *}(k)\ )S^o(k) \\ & + H_{12}^{o\ *}(k)n^o(k) - H_{11}^e(k)n^{e*}(k) \end{aligned} \qquad (B.50)$$

Therfore,

$$\hat{S}^o(k) = (|H_{11}^o|^2 + |H_{12}^e|^2)S^o(k) + H_{11}^{o\,*}(k)n^o(k) + H_{12}^e(k)\,n^{e*}(k) \quad (B.51)$$

$$\hat{S}^e(k) = (|H_{11}^o|^2 + |H_{12}^o|^2)\,S^e(k) + H_{12}^{o\,*}(k)n^o(k) - H_{11}^e(k)n^{e*}(k) \quad (B.52)$$

$$\hat{S}^o(k) = (|H_{11}^o|^2 + |H_{12}^e|^2)\,S^o(k) + 2\ terme\ noise \quad (B.53)$$

$$\hat{S}^e(k) = (|H_{11}^o|^2 + |H_{12}^o|^2)\,S^e(k) + 2\ terme\ noise \quad (B.54)$$

$$\hat{S}^o(k) = (|H_{11}|^2 + |H_{12}|^2)\,S^o(k) + 2\ terme\ noise \quad (B.55)$$

$$\hat{S}^e(k) = (|H_{11}|^2 + |H_{12}|^2)\,S^e(k) + 2\ terme\ noise \quad (B.56)$$

Where $\hat{S}^e(k)$ and $\hat{S}^o(k)$, $k = 1,2,\dots,N/2$ are combined together to construct $\hat{S}(k)$, $k = 1,2,\dots,N$. $\hat{S}(k)$, is sent to the maximum likelihood decoder, to decide the most probable sent vectors S.

SFBC User 2×2:

Let $r_1(k)$, $r_2(k)$ represents the demodulated symbol, after the OFDM demodulator, on the *k*-th sub-carrier, $k = 1,2,\dots,N$ at receive antenna 1 and 2.

$$r_1(k) = H_{11}(k)\ S_1(k) + H_{12}(k)\,S_2(k) + n_1(k) \quad (B.57)$$

$$r_2(k) = H_{21}(k)\ S_1(k) + H_{22}(k)\,S_2(k) + n_2(k) \quad (B.58)$$

Where $H_{ji}(k)$) is the channel frequency response from transmit antenna j to receive antenna i, on the *k*-th sub-carrier. Let $r_1^e(k)$, $r_1^o(k)$ and $r_2^e(k)$, $r_2^o(k)$, $k = 1,2,\dots,N/2$, represent the even and odd components of $r_1(k)$, $r_2(k)$ respectively. Thus, $r_1^e(k)$, $r_1^o(k)$ and $r_2^e(k)$ $r_2^o(k)$, can be represented as:

$$r_1^e(k) = H_{11}^e(k)\,S_1^e(k) + H_{12}^e(k)\,S_2^e(k) + n_1^e(k) \quad (B.69)$$

$$r_1^o(k) = H_{11}^o(k)\,S_1^o(k) + H_{12}^o(k)\,S_2^o(k) + n_1^o(k) \quad (B.70)$$

$$r_2^e(k) = H_{21}^e(k)\,S_1^e(k) + H_{22}^e(k)\,S_2^e(k) + n_2^e(k) \quad (B.71)$$

$$r_2^o(k) = H_{21}^o(k)\,S_1^o(k) + H_{22}^o(k)\,S_2^o(k) + n_2^o(k) \quad (B.72)$$

Where $n_1^e(k)$, $n_1^o(k)$ and $n_2^e(k)$, $n_2^o(k)$ represent the even and odd components, respectively, of the demodulated noise vector. Substituting equation (B.33) into equations (B.69), (B.70) and (B.71), (B.72) we get

$$r_1^e(k) = -H_{11}^e(k)\,S^{e*}(k) + H_{12}^e(k)\,S^{o*}(k) + n_1^e(k) \quad (B.73)$$

$$r_1^o(k) = H_{11}^o(k)\,S^o(k) + H_{12}^o(k)\ S^e(k) + n_1^o(k) \quad (B.74)$$

$$r_2^e(k) = -H_{21}^e(k)\,S^{e*}(k) + H_{22}^e(k)\,S^{o*}(k) + n_2^e(k) \quad (B.75)$$

$$r_2^o(k) = H_{21}^o(k)\,S^o(k) + H_{22}^o(k)\ S^e(k) + n_2^o(k) \quad (B.76)$$

$$r_1^{e^*}(k) = -H_{11}^{e}{}^*(k)\, S^e(k) + H_{12}^{e}{}^*(k)\, S^o(k) + n_1^{e^*}(k) \qquad (B.77)$$

$$r_2^{e^*}(k) = -H_{21}^{e}{}^*(k)\, S^e(k) + H_{22}^{e}{}^*(k)\, S^o(k) + n_2^{e^*}(k) \qquad (B.78)$$

The decision variables are constructed by combining $r_1^e(k), r_1^o(k), r_2^e(k), r_2^o(k)$, $\hat{S}^e(k)$ and $\hat{S}^o(k)$ are calculated by the following equations:

$$\hat{S}^o(k) = H_{12}^e(k)\, r_1^e(k) + H_{11}^{o}{}^*(k) r_1^o(k) + H_{22}^e(k) r_2^e(k) + H_{21}^{o}{}^*(k)\, r_2^o(k) \qquad (B.79)$$

$$\hat{S}^e(k) = -H_{11}^e(k)\, r_1^{e^*}(k) + H_{12}^{o}{}^*(k)\, r_1^o(k) - H_{21}^e(k)\, r_2^{e^*}(k) + H_{22}^{o}{}^*(k) r_2^o(k) \qquad (B.80)$$

$$\begin{aligned}\hat{S}^o(k) = {} & H_{12}^e(k)\,(-H_{11}^{e}{}^*(k)\, S^e(k) + H_{12}^{e}{}^*(k)\, S^o(k) + n_1^{e^*}(k)\,) \\ & + H_{11}^{o}{}^*(k)(H_{11}^o(k)\, S^o(k) + H_{12}^o(k)\; S^e(k) + n_1^o(k)) \\ & + H_{22}^e(k)\left(-H_{21}^{e}{}^*(k)\, S^e(k) + H_{22}^{e}{}^*(k)\, S^o(k) + n_2^{e^*}(k)\right) \\ & + H_{21}^{o}{}^*(k)\,(H_{21}^o(k)\, S^o(k) + H_{22}^o(k)\; S^e(k) + n_2^o(k))\,)\end{aligned} \qquad (B.81)$$

$$\begin{aligned}\hat{S}^e(k) = {} & -H_{11}^e(k)\,(-H_{11}^{e}{}^*(k)\, S^e(k) + H_{12}^{e}{}^*(k)\, S^o(k) + n_1^{e^*}(k)\,) \\ & + H_{12}^{o}{}^*(k)\,(H_{11}^o(k)\, S^o(k) + H_{12}^o(k)\; S^e(k) + n_1^o(k)\;) \\ & - H_{21}^e(k)\,(-H_{21}^{e}{}^*(k)\, S^e(k) + H_{22}^{e}{}^*(k)\, S^o(k) + n_2^{e^*}(k)) \\ & + H_{22}^{o}{}^*(k)\left(H_{21}^o(k)\, S^o(k) + H_{22}^o(k)\; S^e(k) + n_2^o(k)\right)\end{aligned} \qquad (B.82)$$

$$\begin{aligned}\hat{S}^o(k) = {} & (|H_{11}^o|^2 + |H_{12}^e|^2 + |H_{21}^o|^2 + |H_{22}^e|^2\,)\, S^o(k) \\ & + H_{12}^e(k)(-H_{11}^{e}{}^*(k)\, S^e(k) + n_1^{e^*}(k)\,) \\ & + H_{11}^{o}{}^*(k)(\, H_{12}^o(k)\; S^e(k) + n_1^o(k)) \\ & + H_{22}^e(k)\left(-H_{21}^{e}{}^*(k)\, S^e(k) + n_2^{e^*}(k)\right) \\ & + H_{21}^{o}{}^*(k)(H_{22}^o(k)\, S^e(k) + n_2^o(k)\,)\end{aligned} \qquad (B.83)$$

$$\begin{aligned}\hat{S}^e(k) = {} & (\,|H_{11}^e|^2 + |H_{12}^o|^2 + |H_{21}^e|^2 + |H_{22}^o|^2\,)\, S^e(k) \\ & - H_{11}^e(k)\,(H_{12}^{e}{}^*(k)\, S^o(k) + n_1^{e^*}(k)\,) \\ & + H_{12}^{o}{}^*(k)(H_{11}^o(k)\, S^o(k) + n_1^o(k)) \\ & - H_{21}^e(k)\,\left(H_{22}^{e}{}^*(k)\, S^o(k) + n_2^{e^*}(k)\right) \\ & + H_{22}^{o}{}^*(k)\left(H_{21}^o(k)\, S^o(k) + n_2^o(k)\right)\end{aligned} \qquad (B.84)$$

$$\begin{aligned}\hat{S}^o(k) = {} & (|H_{11}^o|^2 + |H_{12}^e|^2 + |H_{21}^o|^2 + |H_{22}^e|^2\,)\, S^o(k) \\ & + (-H_{11}^{e}{}^*(k) H_{12}^e(k)\, S^e(k) + H_{12}^e(k)\, n_1^{e^*}(k)\,) \\ & + (\, H_{12}^o(k)\, H_{11}^{o}{}^*(k)\, S^e(k) + H_{11}^{o}{}^*(k)\, n_1^o(k)) \\ & + \left(-H_{21}^{e}{}^*(k)\, H_{22}^e(k) S^e(k) + H_{22}^e(k) n_2^{e^*}(k)\right) \\ & + (H_{21}^{o}{}^*(k) H_{22}^o(k)\; S^e(k) + H_{21}^{o}{}^*(k) n_2^o(k)\,)\end{aligned} \qquad (B.85)$$

$$\hat{S}^e(k) = (\,|H_{11}^e|^2 + |H_{12}^o|^2 + |H_{21}^e|^2 + |H_{22}^o|^2\,)S^e(k) + (-H_{11}^e(k)\,{H_{12}^e}^*(k)\,S^o(k) - H_{11}^e(k)\,n_1^{e*}(k)) + ({H_{12}^o}^*(k)H_{11}^o(k)\,S^o(k) + {H_{12}^o}^*(k)n_1^o(k)) + \left(-H_{21}^e(k){H_{22}^e}^*(k)\,S^o(k) - H_{21}^e(k)\,n_2^{e*}(k)\right) + \left({H_{22}^o}^*(k)H_{21}^o(k)\,S^o(k) + {H_{22}^o}^*(k)\,n_2^o(k)\right) \quad (B.86)$$

$$\hat{S}^o(k) = (|H_{11}^o|^2 + |H_{12}^e|^2 + |H_{21}^o|^2 + |H_{22}^e|^2\,)\,S^o(k) + (H_{12}^o(k)\,{H_{11}^o}^*(k) - {H_{11}^e}^*(k)H_{12}^e(k) - ({H_{21}^e}^*(k)\,H_{22}^e(k)) + ({H_{21}^o}^*(k)H_{22}^o(k)))\,S^e(k) + H_{12}^e(k)\,n_1^{e*}(k) + {H_{11}^o}^*(k)\,n_1^o(k) + H_{22}^e(k)\,n_2^{e*}(k) + {H_{21}^o}^*(k)n_2^o(k) \quad (B.87)$$

$$\hat{S}^e(k) = (\,|H_{11}^e|^2 + |H_{12}^o|^2 + |H_{21}^e|^2 + |H_{22}^o|^2\,)S^e(k) + ({H_{12}^o}^*(k)H_{11}^o(k) - H_{11}^e(k)\,{H_{12}^e}^*(k) - H_{21}^e(k){H_{22}^e}^*(k) + {H_{22}^o}^*(k)H_{21}^o(k)\,)S^o(k) - H_{11}^e(k)\,n_1^{e*}(k) - H_{21}^e(k)n_2^{e*}(k) + {H_{12}^o}^*(k)n_1^o(k) + {H_{22}^o}^*(k)n_2^o(k) \quad (B.88)$$

Assuming the complex channel gains between adjacent sub-carriers are approximately constant, such as

$H_{11}^e(k) = H_{11}^o(k)$, $H_{12}^e(k) = H_{12}^o(k)$, $H_{21}^e(k) = H_{21}^o(k)$, $H_{22}^e(k) = H_{22}^o(k)$

$$\hat{S}^o(k) = (|H_{11}^o|^2 + |H_{12}^e|^2 + |H_{21}^o|^2 + |H_{22}^e|^2\,)\,S^o(k) + \left(H_{12}^o(k)\,{H_{11}^o}^*(k) - {H_{11}^e}^*(k)H_{12}^e(k) - ({H_{21}^e}^*(k)\,H_{22}^e(k)) + ({H_{21}^o}^*(k)H_{22}^o(k))\right)\,S^e(k) + H_{12}^e(k)\,n_1^{e*}(k) + {H_{11}^o}^*(k)\,n_1^o(k) + H_{22}^e(k)\,n_2^{e*}(k) + {H_{21}^o}^*(k)n_2^o(k) \quad (B.89)$$

$$\hat{S}^e(k) = (\,|H_{11}^e|^2 + |H_{12}^o|^2 + |H_{21}^e|^2 + |H_{22}^o|^2\,)\,S^e(k) + ({H_{12}^o}^*(k)H_{11}^o(k) - H_{11}^e(k)\,{H_{12}^e}^*(k) - H_{21}^e(k){H_{22}^e}^*(k) + {H_{22}^o}^*(k)H_{21}^o(k)\,)S^o(k) - H_{11}^e(k)\,n_1^{e*}(k) - H_{21}^e(k)n_2^{e*}(k) + {H_{12}^o}^*(k)n_1^o(k) + {H_{22}^o}^*(k)n_2^o(k) \quad (B.90)$$

$$\hat{S}^o(k) = (|H_{11}^o|^2 + |H_{12}^e|^2 + |H_{21}^o|^2 + |H_{22}^e|^2\,)\,S^o(k) + H_{12}^e(k)\,n_1^{e*}(k) + {H_{11}^o}^*(k)\,n_1^o(k) + H_{22}^e(k)\,n_2^{e*}(k) + {H_{21}^o}^*(k)n_2^o(k) \quad (B.91)$$

$$\hat{S}^e(k) = (\,|H_{11}^e|^2 + |H_{12}^o|^2 + |H_{21}^e|^2 + |H_{22}^o|^2\,)S^e(k) - H_{11}^e(k)\,n_1^{e*}(k) - H_{21}^e(k)n_2^{e*}(k) + {H_{12}^o}^*(k)n_1^o(k) + {H_{22}^o}^*(k)n_2^o(k) \quad (B.92)$$

Were $\hat{S}^e(k)$ and $\hat{S}^o(k)$, $k = 1,2,\dots,N/2$ are combined together to construct $\hat{S}(k), k = 1,2,\dots,N$. $\hat{S}(k)$, is sent to the maximum likelihood decoder, to decide the most probable sent vectors S.

References

References

[1] Lei shao and surnit Roy, "Downlink Multi cell MIMO_OFDM: An architecture for next generation Wireless networks," *in wireless communications and networking conference,Vol.2, pp.1120-1125. 2005. Available at http://www.ieeexplore.ieee. Org /iel5/ 9744/30729/01424666.pdf .*

[2] Loch Lomond. "OFDM for Advanced Wireless Communications,"*25-27. October 2006, Munich, DE 30.October.01. November, 2006, UK. Available at http://www.hueggenberg.com and http://www.steepestascent.com.*

[3] Albert Van zelst. "MIMO OFDM system for wireless LANs," *Eindhoven technical University, 14 April. 2004. Available at alexandria.tue.nl/extra2/200411059.pdf.*

[4] Wolniansky, G. J. Foschini, G. D. Golden, and R. A. Valenzuela, "VBLAST: An architecture for realizing very high data rates over the rich scattering wireless Channel," *in Proc IEEE-URSI International Symposium on Signals, Systems and Electronics, Pisa, Italy, May 1998.*

[5] V. Tarokh, H. Jafarkhani, A.R. Calderbank, " Space-Time Block Coding for Wireless Communication : Performance Results," *IEEE SAC, Vol. 17, No. 3, pp.451-460, Mar. 1999.*

[6] Markus Rupp, Christoph Mecklenbrauker, Gerhard Gritsch, "High Diversity with Simple Space Time Block Codes and Linear Receivers," *in the Proceeding IEEE of Globecom 03, San Francisco, December 2003.*

[7] A.van Zelst, "Space Division Multiplexing Algorithms," *in Electro technical conference, MELECON 2000, 10th Mediteranean, pp.1218-1221. Available at www. avzelst.nl / melecon2000_a_van_ zelst.pdf.*

[8] Fawaz S. Al-Qahtani and Zahir M. Hussein, "Performance of Space Time Block Coded OFDM in Time-Selective Macro cell Channel Environments," *Available at researchbank. rmit.edu.au/esrv/rmit:15893/A_Qahtani.pdf.*

[9] Kun Fang, Geert Leus and Luca Rugini, "Alamouti Space-Time Coded OFDM systems in Time and Frequency Selective Channels," *IEEE Conference on Global Telecommunications, pp. 1-5, 27. San Francisco, CA. November. 2006.*

[10] Muhammad Imadur Rahman, Nicola Marchetti, Suvra Sekhar Das, Frank H.P. Fitzek, Ramjee Prasad, " Combining Orthogonal Space Frequency Block Coding and Spatial Multiplexing in MIMO-OFDM System," *Center for Teleinformatique (CTIF), Aalborg university Denmark, 2005. Available at http:// www.kom.aau.dk/ ff/document/ InOWo 2005.*

[11] Ho-Chul Jung, Chang-Ju Kim, Jong-Ho Kim, and Hyung-Rae Park, " A Comparative Performance Analysis of STBC-OFDM systems under Rayleigh Fading Environments," *School of Avionics and Telecommunications Engineering Hankuk Aviation university, 2000. Available at www.eurasip.org/proceding/Ext/IST05/ Publication /372.pdf.*

[12] Vahid Tarokh, Hamid Jafarkhani, and A. R. Calderbank, "Space Time Block Codes from Orthogonal Designs," *IEEE Transactions information theory, Vol. 45, No. 5, July. 1999.*

[13] S.M. Alamouti. "A simple transmit diversity technique for wireless communications." *IEEE J. Select. Areas Communications, Vol.16, 1998, pp. 1451-1458.*

[14] K. F. Lee and D. B. Williams, "A space-time coded transmitter diversity technique for frequency selective fading channels," *in Proc. IEEE Sensor Array and Multichannel Signal Processing Workshop, Cambridge, MA, March 2000, pp. 149-152.*

[15] K. F. Lee and D. B. Williams, "A Space-frequency transmitter diversity technique for OFDM systems," *in Proc. IEEE Globecom, San Francisco, CA, Nov. 2000. pp. 1473- 1477.*

[16] G. Bauch, "Space-time block codes versus space-frequency block codes," *VTC 2003-Spring, Vol.1, pp.567-571. 2003.*

[17] Zhang, Min and Abhayapala, T. D. and Jayalath, Dhammika and Smith, David and Athaudage, C. R. N, "Multi-rate Space-Time-Frequency Linear block coding," *In Proceedings IEEE International Conference on Communications, 2008. ICC '08, Beijing, China. pp. 4084-4089. Available at users.cecs.anu.edu.au/~thush/publications/p08_121.pdf*

[18] Angela Doufexi, Andrew Nix, Mark Beach, "Combined Spatial Multiplexing and STBC to Provide Throughput Enhancements to Next Generation WLANs," *in: IST Mobile and wireless Communications Sumit, 2005. Aavailable at http://www.rose.bristol.ac.uk /dspace/ bitstream/.../doufexi_IST_2005.pdf.*

[19] Tim C.W. Schenk, Guido Dolmans and Isabella Modonesi, "Throughput of a MIMO OFDM based WLAN system," *Proc. Symposium IEEE Benelux Chapter on Communications and Vehicular Technology, 2004 (SCVT2004), Gent, Belgium, Nov. 2004.*

[20] Zhuo chen, Branka vucetic, jinhong yuan, "Comparison of three closed loop transmit diversity schemes," *in Proc. of IEEE VTC'03, Jeju Island, Korea, Apr. 2003. Available at http://www. ee.usyd.edu.au/~zhuochen/VTC03Spr.pdf.*

[21] Daniel V.P. Figueiredo, Muhammad Imadur Rahman, Nicola Marchetti, Frank H.P. Fitzek, Marcos D. Katz, Youngkwon Cho, Ramjee Prasad, "Transmit Diversity Vs Beamforming for Multi-User OFDM Systems," *Wireless personnel mobile communications, 2004. Available at kom.aau.dk/~ff/documents/wpmc2004dvpf.pdf.*

[22] Cheng-Zhou Zhan, Kai-Yuan Jheng, Yen-Lian Chen, Ting-Jhun Jheng, and An-Yeu Wu, "High-Convergence-Speed Low-Computation-Complexity SVD Algorithm for MIMO-OFDM Systems," *in international symposium on VLSI Deign , Automation and test. DAT'09, pp.195-198.2009. Available at access.ee.ntu.edu.tw/Publications/CA89_ 2009.pdf.*

[23] Ove Edfors, Magus Sagnus Sandell, Jan-Jaap van de Beek, Sarah Kate Wilson and Per Ola Borjesson, "An application of the Singular Value Decomposition to OFDM Channel Estimation," *in proceeding, radioveten. Konf .pp.678-686. Available at lup.lub.lu.se/record /1056136/file/10568.pdf.*

[24] Tiziano Bianchi and Fabrizio Argenti, "SVD-Based Equalisation for Zero Padded Multi carrier systems in Time variant Fading channels," *IEEE Transactions on Signal processing, Vol.55, No.2, pp.594-604. Available at www.eurasip.org/ proceedings/eusipco/ eusipco2006 /.../1568981822.pdf.*

[25] T. Yoo and A. Goldsmith, "On the Optimality of Multi antenna Broadcast Scheduling using Zero-Forcing Beamforming", *IEEE Journal on Sel. Areas in Comm, Vol. 24, No. 3, pp. 528-541, March. 2006.*

[26] R. Irmer, "Multiuser transmission in code division multiple access mobile Communications systems," *Ph.D. dissertation, Technische Universitat Dresden, 2005.*

[27] H. Jafarkhani, "A quasi-orthogonal space-time block code," *IEEE Transactions on Communications," Vol. COM-49, pp. 1-4, January. 2001.*

[28] N. Sharma, C. B. Papadias, "Improved quasi-orthogonal codes through constellation rotation," *IEEE Transactions on Communications, Vol. COM-51, pp. 332–335, March. 2003.*

[29] Quentin H. Spencer, A. Lee Swindlehurst, and Martin Haardt, " Zero-Forcing Methods for Downlink Spatial Multiplexing in Multiuser MIMO Channels," *IEEE Transactions on signal Processing, Vol. 52, No. 2, pp. 461–471. February. 2004.*

[30] Runhua Chen, Robert W. Heath, Jeffrey G. Andrews, "Transmit Selection Diversity for Unitary Precoded Multiuser Spatial Multiplexing Systems With Linear Receivers," *proc of IEEE Global Telecommunications Conference, Nov.29-Dec. 3,Dallas, TX,USA. 2004. Available at http:// www.users. ece.utexas.edu/ rheath/ papers/ 2005/.*

[31] W. Liu, L. L. Yang, and L. Hanzo, "SVD assisted multiuser transmitter and multiuser detector design for MIMO system," *IEEE Transactions on Vehicular Technology, Vol. 58, No. 2, February. 2009.*

[32] Mirette Sadek, Alireza Tarighat, and Ali H. Sayed, "A Leakage-Based Precoding Scheme for Downlink Multi-User MIMO Channels," *IEEE Transactions on wireless communications, Vol. 6, No. 5, May. 2007.*

[33] Runhua Chen, Jeffrey G. Andrews, and Robert W. Heath, Jr, "Multiuser Space Time Block Coded MIMO System with Unitary Downlink Precoding," *in IEEE conference on communications,pp.2689-2693. Available at http://www.ece. utexas.edu/~jandrews/.../ CheAnd_ ICC04.pdf.*

[34] Herve Boeglen, "Transmissions numériques avancées, " *Available at. http:// www.herve.boeglen.free.fr/Files_IUT/Cours_trc6.ppt.*

[35] Xavier Wautelet, "Turbo Equalization and Turbo Estimation for Multiple-Input Multiple-Output Wireless Systems," *Universite catholique de Louvain. September 2006. Belgique. Available at http:// www.dial.academielouvain.be/vital/ access/ services/ Download /boreal.../PDF_01.*

[36] Alamgir Mohammed, "On the Performance of different MIMO systems using Adaptive modulation," *in Proc of 2nd ATcrc Telecom and Networking Conference and Workshop, 16-18 October, 2002, Freemantle, Perth, Australia. Available at http:// www.scribd. com/doc/28492479/02-Whole.*

[37] Karen Su, "Space Time Coding: From Fundamentals to the future," *First year PhD, report. Available at http:// www. cl.cam.ac.uk/research/dtg/publications/ public/ks349/ Su03Z .pdf.*

[38] Xinying Yu, "Space Time Coding for Large Antenna Arrays," *North Carolina State University. Electrical engineering, PhD. 14 March. 2006. Available at http://www. repository.lib.ncsu.edu/ir/bitstream/1840.16/.../etd. pdf .*

[39] Zelalem Fikre, "Performance Comparison of Spatial Multiplexing and Spatial Diversity in Rate Adaptive Wireless MIMO Systems," *June 2007. Addis Ababa university. Available at http://www.etd.aau.edu.et/dspace/.../1497/.../Zelalem%20Fikre.pdf.*

[40] Yousaf Ali Shah, "Performance Analysis of Multiple Antenna Techniques in WiMAX," *Blekinge Institute of Technology, July 2010. Available at www.bth.se/fou/ cuppsats. nsf/ FINAL_VERSION.pdf.*

[41] Reihaneh Malekafzaliardakani, "Transmit Adaptation Scheme for MIMO-OFDM Systems," 2006-11-17. Stockholm, Sweden. *Available at https://eeweb01.ee.kth.se/upload/ publications/.../XR-EE-KT_2006_010.pdf.*

[42] Jan Vcelak, Tomaz Javornik, Jan Sykora, Gorazd Kandus, Sreco Plevel, "Multiple Input Multiple Output Wireless Systems," *Electrotechnical, Slovenija Review, Ljubljana,Vol.70,No.4,pp.234–239,2003. Available at http://feld.cvut.cz/~sykora/papers/ publications /Vcelak-javornik-sykora-kandus-Plevel_2003_EIRev.pdf.*

[43] Anou Abderrahmane, Mehdi Merouane, Bensebti Messaoud, "Diversity Techniques to combat fading in WiMAX," *WSEAS Transactions on Communications Issue 2, Vol.7, February. 2008. Available at www.wseas.us/e-library/conferences/.../EHAC-35.pdf.*

[44] Lam chi Thuang, "Analysis of antenna diversity techniques used in MIMO system," *International symposium on electrical and Electronics. Oct. 11,12. HCM City, Vietnam. 2005.*

[45] B. Vucetic and J. Yuan, "Space-time coding," *West Sussex, England; Hoboken, NJ : Wiley, c2003. TK5102.92.V82, 2003.*

[46] Bing Hui and Kyung Hi Chang**,** "A Linear Precoding Technique for OFDM Systems with Cyclic Delay Diversity," *KSII Transactions on Internet and Information systems. Vol. 2, No. 5, October. 2008.*

[47] Ravikiran Nory, "Performance Analysis of Space-Time Coded Modulation Techniques using GBSB-MIMO Channel Models," *June 04, 2002. Blacksburg, Virginia Polytechnic Institute and State University. Available scholar.lib.vt.edu/theses/.../etd.../ vravi_thesis.pdf*

[48] V. Tarokh, N. Seshadri, and A. R. Calderbank, "Space-time codes for high data rate wireless communication: Performance criterion and code construction", *IEEE Trans. Inform. Theory, Vol.44, No.2, pp.744-765, Mar.1998.*

[49] R. .Knopp, P. Humblet, "Information capacity and power control in single cell multiuser communications," *in IEEE proceeding international conference on communications ICC'95,'Gateway to Globalization', Vol.1, Seattle. 1995. pp.331-335.*

[50] Markus Rupp and Christoph F, Mecklenbrauker, " Improving Transmission by MIMO Channel Structuring," *in the IEEE Proceeding of the ICC'03 Conference, May 11-15, Anchorage, Alaska, USA. 2003.*

[51] Nasir D. Gohar, Zimran Rafique, "V-BLAST: A Space Division Multiplexing technique providing a spectral efficiency necessary for high data rate wireless networks," *2nd International Bhuran conference of Applied sciences and technology, June 16-21, Bhuran, Pakistan. 2003.*

[52] G.J.Foschini, "Layered space-time architecture for wireless communication in a fading environment when using multi element antennas," *Bell Labs Technical Journal, Vol.1, No.2, pp.41-59, Autumn. 1996.*

[53] Jaime Adeane and Ian J. Wassell Wasim Q. Malik, "Error Performance of Ultrawideband MIMO Spatial Multiplexing Systems," *IET microwaves antennas and propagation, Vol.3, No.3, pp.363-371. Available at www.mit.edu/~wqm/Papers/ Malik_ ietuwb07_ mult.pdf.*

[54] Thuong Le-Tien, Tuan Ly-Huu," V BLAST Detection in Space Time Coding Wireless system and implementation on FPGA," *International Symposium on Electrical Electronics Engineering, 24 October 2007, HCM City, Vietnam.*

[55] Fenghua Li, "Performance Analysis of V-BLAST Detectors for the MIMO channel," *Stockholm, Sweden, 21 June 2007. Available at https://eeweb01.ee.kth.se/upload/.../ IR-SB-XR-EE-KT%202007:004.pdf.*

[56] Samir Al-Ghadhban, "Multi-layered Space Frequency Time Codes," *The Virginia Polytechnic Institute and State University. Nov. 4. 2005. Blacksburg, Virginia. Available at phdtree.org/.../25752816-multi-layered-space- frequency-time-codes.pdf.*

[57] A. J. Paulraj, R. Nabar, and D. Gore, "Introduction to Space-Time Wireless Communications."*Cambridge University Press, 2000.*

[58] Jia Liu, Erik Bergenudd, Vinod Patmanathan, Romain Masson, "OFDM Project," *Project Course in Signal Processing and Digital Communication KTH, Stockholm, 30th May 2005. Available at www.s3.kth.se/signal/project_course/.../final_report.pdf.*

[59] Kazuaki Takeda, Takeshi Itagaki, and Fumiyuki Adachi, "Space-Time Transmit Diversity Combined with Frequency-domain Equalization for Single-carrier Transmission," *IEEE communications letters, Vol.5, No.7, pp.304-306.*

[60] Geert Leus, Imad Barhumi, and Marc Moonen, "Per-Tone Equalization for MIMO-OFDM Systems," *IEEE transactions on signal processing,Vol.51, No.11, pp.2965-2975.2003.*

Available at ieeexplore.ieee.org/iel5/78/27749/01237428.pdf?arnumber=1237428.

[61] Reza Abdolee, "Performance of MIMO Space-Time Coded system and Training Based Channel Estimation for MIMO-OFDM system," *University of Technology. November 2006. Malaysia.*

[62] Amal Alameh, Emad Azzam, Anis Tabboush, "An FPGA-based Implementation of an LMMSE Detector for MIMO OFDM Communication Systems," *Final year project, American University of Beirut. May 23. 2006.*

[63] Gordon L. Stuber, John Barry, Steve W. McLaughlin, Ye (Geoffrey) Li, Mary Ann Ingram, Thomas G, " Broadband MIMO-OFDM Wireless Communications,'' *proceeding of the IEEE,Vol.92, No.2.2004. pp.271-294. Available at www.ece.gatech.edu/users/stuber /nsf3/ pubs/.../proc-ieee.pdf.*

[64] Ho Chin Keong, "Overview on OFDM Design," *Communication Systems & Signal Processing Centre for Wireless communications National University of Singapore November 9, 2001. Available at www1.i2r.a-star.edu.sg/~hock/presentation_basics_ ofdm.pdf.*

[65] Eric Phillip LAWREY, "Adaptive Techniques for Multiuser OFDM," *Degree of Doctor of philosophy, School of Engineering James Cook University in December 2001.*

[66] Jianxuan Du, "Layered Space Time Structure for MIMO-OFDM Systems," *School of Electrical and Computer Engineering Georgia Institute of Technology. July. 12, 2005. Available at https://smartech.gatech.edu/bitstream/handle/1853/7204/Du_Jianxuan_ 200508_ phd.pdf.*

[67] Ahmed S. Ibrahim Mohamed M. Khairy A. F. Hussein, "Multilayered Space-Frequency Block Coded OFDM Systems," *Available at www.cspl.umd.edu/asibrahim/ Ibrahim_ gspx04.pdf.*

[68] Stefan Kaiser, "Space Frequency Block Codes and Code Division Multiplexing in OFDM Systems,'' *Available at http:// www.kn .dlr.de/People/.../Globecom2003_Kaiser. Pdf.*

[69] Nana Leng, Shouyi Yang, and Yanhui Lu. '' On the performance of Alamouti-based OFDM system with multiuser resource allocation and scheduling,'' *IEEE Communication system, pp*: *426-430. Nov 2008. Availabl at http://www. 202.194.20.8/proc/ ICCS2008/ papers/ 088.pdf.*

[70] Jaekwon Kim, Robert W. Heath, Jr., and Edward J. Powers. "Receiver Designs for Alamouti Coded OFDM Systems in Fast Fading Channels," *IEEE Transactions on wireless Communications, Vol. 4, NO. 2, March. 2005. Available at ieeexplore.ieee.org/iel5/7693/ 30621/ 01413221.pdf.*

[71] Ahmed S. Ibrahim, Mohamed M. Khairy, and A. F. Hussein, "Multi layerd space Time Block Codes for OFDM systems," *Available at www.cspl.umd.edu/asibrahim/ Ibrahim_ ICEE04.pdf.*

[72] Weifeng Su, Zoltan Safar1 and K. J. Ray Liu, "Diversity Analysis of Space-Time-Frequency Coded Broadband OFDM Systems," *Available at sig_umd.edu/%2F publication %2F/ su_diversity_STFC_OFDM_ewc_200402.pdf.*

[73] Andreas A. Hutter, Selim Mekrazi, Beza N. Getu, Fanny Platbrood, ''Alamouti-based space-frequency coding for OFDM,'' *in IEEE wireless communications and networking conference, WCNC. Vol.1, pp.1-6. Available at http://www.eurecom.fr/util/ publidownload. fr.htm.*

[74] ROHDE & SCHWARZ GmbH & Co. KG . Mühldorfstrabe, "Introduction to MIMO Systems," *Available at. http://www.rohde-schwarz.com.*

[75] S. Verd_u, "Multiuser Detection," *Cambridge University Press, New York, 1998.*

[76] OULUN YLIOPISTO, "Iterative Receiver for Interference Cancellation and Suppression In Wireless Communcations," *University of Oulu, December 9th, 2004, OULU. Acta universitatis Ouluensis. Series c.Technica (215)-0355-3313. Available at Hercules.oulu.fi/ isbn9514275977/isbn9514275977.pdf* .

[77] L. Hanzo, M. Munster, B.J. Choi and T. Keller, "OFDM and MC-CDMA for Broadband Multi-user Communications, WLANs and Broadcasting," *John Wiley and Sons, pp.619-714.2007. Available at www-mobile.ecs.soton.ac.uk/.../Samp%20Chaps%201, %2017, %2019-OFDM. Pdf.*

[78] Zhengang Pan, Kai-Kit Wong and Tung-Sang Ng, "Generalized Multiuser Orthogonal Space-Division Multiplexing," *IEEE Transactions on wireless Communications, Vol. 3, No. 6, November. 2004.*

[79] Diego Piazza and Umberto Spagnolini, "Random Beamforming for Spatial Multiplexing in Downlink Multiuser MIMO Systems," *in Personnel, 16th IEEE International symposium on Indoor and Mobile Ratio Communications, PIMRC, Vol. 4, pp. 2161-2165, 2005.*

[80] Chockalingam, "Low-Complexity Multiuser/MIMO Detection," *Department of Electrical Communication Engineering. In Indian institute of science, Bangalore, workshop on recent Trends in wireless communications. 10 April. 2008.*

[81] Jos Akhtman, Chun-Yi Wei and Lajos Hanzo, "Reduced-Complexity Maximum-Likelihood Detection in Downlink SDMA Systems," *In: 64th IEEE vehicular Technology conference, VTC, pp.1-5. 2006.*

[82] W. C. Freitas Jr., A. L. F. de Almeida and F. R. P. Cavalcanti, "Interference Cancellation Receiver for Space-Time Block-Coded systems Over Frequency selective channels," *in IEEE international telecommunications symposium, pp.555-559. Available at http://www.reserchgate.net/publcation/239565531-interference_...._channels.*

[83] Yuichi Kakishima, Haidoan Le, See Ho Ting, Kei Sakaguchi and Kiyomichi Araki, " Experimental Analysis of MIMO-OFDM Eignmode Transmission with Interference Canceller," *the 17th Annual IEEE International Symposium on Personal, Indoor and Mobile Radio Communications (PIMRC'06),11-14 September, Helsinki. 2006. Available at www.mcrg.ee.titech.ac.jp/seminar/061102_kakishima.pdf.*

[84] Laura Cottatellucci, Ralf R. Muller, and Merouane Debbah, " Linear Detectors for Multi User MIMO systems with Correlated Spatial Diversity," *14 th European signal processing Conference EUSIPCO,September 4-8, Florance, Italy. 2008.*

[85] Mario Marques da Silva, Americo M. C. Correia and Rui Dinis, "Wireless Systems On transmission techniques for multi-antenna W-CDMA systems," *European transactions on Telecommunications,Vol. 20, No.1, pp.107-121.Available at online library-wiley.com/doi/10. 1002/elt.12552/pdf.*

[86] Min Zhang and Thushara D. Abhayapala David Smith, "Multi-rate Space-Time-Frequency Linear Block Coding," *IEEE Transactions on communications,Vol.54.No.12. Dec2009. Available at newport.eecs.uci.edu/~ayanogh/trans_bicm_and_stbc_ofdm.pdf.*

[87] Zih-Yin Ding, Chi-Yun Chen and Tzi-Dar Chiueh, "Design of a MIMO-OFDM Baseband Receiver for Next-Generation Wireless LAN," *in Proceeding IEEE international symposium on circuits and systems, ISCAS , 2006. Available at http://www. gra103.aca.ntu. edu.tw/gdoc/95/ F93943006a.pdf.*

[88] Jianming Wu, "Design and Performance Analysis for LDPC Coded Modulation in Multi user MIMO systems," *B.E., Nanjing University of Aeronautics and Astronautics, University of Pittsburgh 2006.*

[89] Li Zhang Mathini Sellathurai Jonathon Chambers, "An Iterative Multiuser Receiver for Space-Time Coded MIMO-OFDM System," *Available at http://ima.org.uk/_dB/_ documents/ L._Zhang.pdf.*

[90] Robert F.H. Fischer, "Lattice-Reduction-Aided Equalization and Generalized Partial-Response Signaling for Point-to-Point Transmission over Flat-Fading MIMO Channels," *Turbo Codes&Related Topics; 6th International ITG-Conference on Source and Channel Coding (TURBOCODING), 2006 4th International Symposium on 3-7 April. 2006.*

[91] Giuseppe Caire, Nihar Jindal, Niranjay Ravindran, "Multiuser MIMO Downlink Made Practical: Achievable Rates with Simple Channel State Estimation and Feedback Schemes," *IEEE Transactions Information Theory. May, 2009. Available at www.ee.princeton.edu/ seminars/iss/.../ Jindal.Paper.pdf*

[92] F. -C. Zheng and A. G. Burr, "Signal Detection for Orthogonal Space-Time Block Coding Over Time-Selective Fading Channels: A PIC Approach for the $\mathcal{G}_i$ Systems," *IEEE transactions on Communications, Vol. 53, No. 6, June. 2005.*

[93] Mincheol Park, "Performance Evaluation of Multiuser Detectors with V-BLAST to MIMO Channel," *Doctoral dissertation, Virginia Polytechnic Institute and state university. May 2003. Blacksburg, Virginia.*

[94] Xuan Nam Tran, Anh Tuan Le and Tadashi Fujino, "Performance Comparison of MMSE-SIC and MMSE-ML Multiuser Detectors in a STBC-OFDM System," *in personal, Indoor and Mobile Radio Communications, pp.1050-1054, 2005.*

[95] Ali M. Khachan, Adam J. Tenenbaum and Raviraj S. Adve, "Linear Processing for the Downlink in Multiuser MIMO Systems with Multiple Data Streams," *in IEEE International conference on communications ICC'06,pp.4113-4118.2006. Available at www.comm. utoronto.ca/.../ AliAdamPrecoding_ICC2006.pdf.*

[96] David Gesbert, Cornelius van Rensburg, Filippo Tosato, and Florian Kaltenberger, " Multiple antenna techniques," *UMTS Long Term Evolution: from Theory to Practice. pp. 243-283.2009. Available www. aldraji. Com/downlaod/2LTE-the UMTS Long Term Evolution.pdf.*

[97] Daniel Schneider, Joachim Speidel othar Stadelmeier, Dietmar Schill, " Precoded Spatial Multiplexing MIMO for Inhome Power Line communications," *in Global Telecommunications Conference (IEEE GLOBECOM 2008), New Orleans, 2008. pp.1-5.*

[98] Tarkesh Pande, David J. Love, and James V. Krogmeier, "Reduced Feedback MIMO-OFDM Precoding and Antenna Selection," *IEEE transactions on Signal processing, Vol. 55, No. 5, pp. 2284-2293. June 18. 2006.*

[99] Christoph Windpassinger, Robert F.H. Fischer, Tomas Vencel, Johannes B. Huber, "Precoding in Multi-Antenna and Multi-User Communications," *IEEE Transactions on wireless communications, Vol. 3, No.4, pp.1305-1316. 2004.*

[100] G. H. Golub and C. F. Van Loan, "Matrix Computations," Baltimore: *Johns Hopkins University Press, third ed., 1996.*

[101] Taesang Yoo and Andrea Goldsmith, "Optimality of Zero-Forcing Beamforming with Multiuser Diversity," *IEEE international on Communications, Vol.1.16, No.20, Seoul, Korea, May. 2005, pp. 542-546.*

[102] T. Yoo and A. Goldsmith, "On the Optimality of Multi antenna Broadcast Scheduling using Zero-Forcing Beamforming," *IEEE Journal on Sel. Areas in Comm, Vol. 24, No. 3, pp. 528-541, March. 2006.*

Abstract

In this work, we exploit the SVD assisted Multiuser Transmitter (MUT) and Multiuser Detector (MUD) techniques, using the Downlink (DL) pre-processing transmitter and DL post-processing receiver matrices with the combination of the MIMO OFDM space Time block code (STBC). And also propose the pre-coded DL transmission scheme, were both proposed schemes take advantage of the channel state information (CSI) of all users at the base station (BS), but only of the mobile station (MS) owns CSI, to decompose the MU MIMO channels into parallel single input single output (SISO), these two proposed schemes are compared to the vertical Bell layered space time (V-BLAST) detector combined with STBC OFDM (V-BLAST STBC OFDM). Our simulation results on hybrid approach show that the performance of the proposed scheme with DL Zero Forcing (ZF) transmitter outperforms the V-BLAST STBC OFDM and the pre-coded DL schemes with ZF receiver, respectively, in frequency selective fading channels. So this hybrid approach, exploit the time, space and frequency diversity.

ملخص

محتوى هذه الرسالة يقوم على استخدام تقنية التجزئة الأحادية للمصفوفة في نظام متعدد المستخدمين للإرسال و الاستقبال و الرصد واستعمال مصفوفة معالجة المعلومة ما قبل الإرسال و ما بعد الاستقبال في نظام البث ألمهبطي للهواتف النقالة. بالإضافة إلي ذلك يتم استعمال نظام الشيفرة الزمكاني بإدماجه مع نظام تعدد الموجات الحاملة التعامدية حيث نقوم كذلك باقتراح نظام التشفير على مستوي قاعدة البث والإرسال. هاتان التقنيتان تقومان بالأساس على توفر معلومة تقنية حول قنوات البث لجميع مستخدمي شبكة الهاتف النقال على مستوي قاعدة البث و الإرسال لكن يتم تجزئة قناة كل مستخدم على حدى و التي تتمثل في قناة متعددة الإرسال و الاستقبال لجميع المستخدمين إلى قنوات فرعية متوازية و مستقلة. بعد ذلك تتم مقارنة التقنيتان الهجينتان مع تقنية التشفير الزمكاني العمودي الطبقي .نتائج المحاكاة أظهرت أن معالجة المعلومة ما قبل الإرسال بتقنية الإجبار الصفري أفضل من تقنية الرصد بنظام الشيفرة الزمكاني العمودي و تقنية التشفير عند البث و الإجبار الصفري عند الاستقبال في قنوات الانتقاء الترددي. إذن هذه التقنية تقوم باستغلال التعدد الزمني و المكاني والترددي للإرسال.